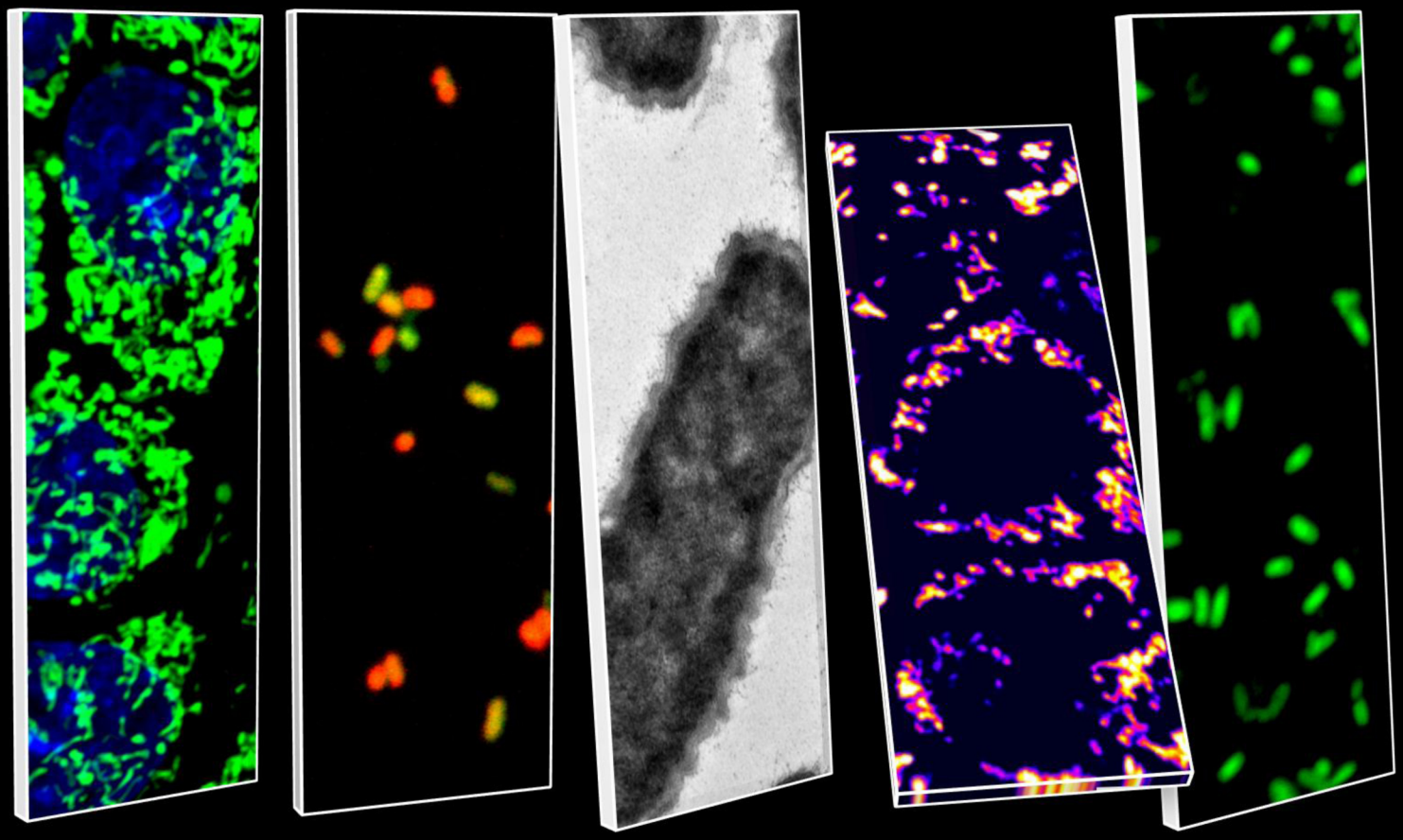

Ângela Rosalina Sanches Inácio

A systematic investigation of the potential use of surfactants as microbicides:
implications for surfactant use in the prophylaxis of sexually transmitted infections

2012

· U C ·

Universidade de Coimbra

Ângela Rosalina Sanches Inácio

A systematic investigation of the potential use of surfactants as microbicides:

implications for surfactant use in the prophylaxis of sexually transmitted infections

2012

· U C ·

UNIVERSIDADE DE COIMBRA

Cover: panel composed of different microscopy images. From left to right each frame corresponds to: confocal image of MDCK II cells stained with Hoechst 33342 (blue) and Rh123 probe (green); *Escherichia coli* with damaged membrane visualized with propidium iodide (red) and SYTO 9 (green); transmission electron microscopy of *E. coli* cells; pseudo-colored image of MDCK II cells stained with Rh123 probe; viable *E. coli* cells stained with SYTO 9 (green).

A systematic investigation of the potential use of surfactants as microbicides: implications for surfactant use in the prophylaxis of sexually transmitted infections

Estudo sistemático sobre a potencial utilização de surfactantes como agentes microbicidas: implicações para o seu uso na profilaxia de infecções sexualmente transmissíveis

Ângela Rosalina Sanches Inácio

2012

UNIVERSIDADE DE COIMBRA

Dissertation presented to the Faculty of Sciences and Technology of the University of Coimbra in partial fulfillment of the requirements for a Doctoral degree in Biosciences.

Dissertação apresentada à Faculdade de Ciências e Tecnologia da Universidade de Coimbra para prestação de provas de Doutoramento em Biociências.

This work was performed at the Center for Neuroscienece and Cell Biology (CNBC), University of Coimbra, under the supervision of Doctor Otília Vieira (CNBC, University of Coimbra) and co-supervision of Professor Doctor Winchil Vaz (Department of Chemistry, University of Coimbra) and Professor Doctor Emília Duarte (CNBC and Department of Life Sciences, University of Coimbra). Its execution was supported by a PhD fellowship from the Portuguese Foundation for Science and Technology (SFHR/BD/3897/2007).

Este trabalho foi realizado no Centro de Neurociências e Biologia Celular (CNBC) da Universidade de Coimbra, sob a supervisão da Doutora Otília Vieira (CNBC, Universidade de Coimbra) e co-supervisão do Professor Doutor Winchil Vaz (Departamento de Química, Universidade de Coimbra) e da Professora Doutora Emília Duarte (CNBC e Departamento de Ciências da Vida, Universidade de Coimbra), ao abrigo de uma bolsa de Doutoramento financiada pela Fundação para a Ciência e a Tecnologia (SFHR/BD/38397/2007).

FCT
Fundação para a Ciência e a Tecnologia
MINISTÉRIO DA CIÊNCIA, TECNOLOGIA E ENSINO SUPERIOR

Financiamento no âmbito do QREN – POPH – Tipologia 4.1, comparticipado pelo Fundo Social Europeu e por fundos nacionais do MCTES.

POPH
PROGRAMA OPERACIONAL POTENCIAL HUMANO

QREN
QUADRO DE REFERÊNCIA ESTRATÉGICO NACIONAL

UNIÃO EUROPEIA
Fundo Social Europeu

Agradecimentos

À Doutora Otília Vieira, minha orientadora, agradeço por me ter recebido como aluna em circunstâncias incomuns, por todo o apoio ao longo destes anos e pela confiança depositada no meu trabalho. Obrigada pela orientação, apoio e incentivos sem os quais este trabalho não teria sido possível.

Ao Professor Doutor Winchil Vaz, meu co-orientador, pelas muitas discussões científicas e críticas construtivas que em muito contribuíram não só para o avanço deste projecto como para o enriquecimento do meu conhecimento científico.

Á Professora Doutora Emília Duarte por todo o apoio e incentivo durante os meus anos académicos e por ter aceitado tão prontamente co-supervisionar o meu trabalho.

Ao Professor Doutor António Moreno e à Doutora Maria Sancha Santos por todo o conhecimento científico que prontamente me transmitiram, pelas produtivas discussões científicas e pelo incansável apoio no trabalho experimental.

A todos os colegas do grupo "Infection and Pathogens", Michelle, Luís, Elda, João, Faraj e todos os outros que por lá passaram ao longo destes anos, pela amizade, companheirismo, conselhos e apoio. Foi um prazer fazer esta caminhada na vossa companhia. Em especial queria agradecer à Katia, ao Faraj e à Luísa pela contribuição directa na realização de algumas experiências e ao Luís pelas muitas discussões e ajuda na análise dos resultados.

À Professora Doutora Caetana Carvalho e à Professora Doutora Cláudia Cavadas por terem acreditado nas minhas capacidades e me terem incentivado a continuar a minha formação académica e não desistir.

A todos os colegas do Centro de Neurociências com quem me cruzei e trabalhei durante este tempo e que de alguma forma contribuíram para a minha aprendizagem e amadurecimento científico.

Às técnicas do CNC, por tanto terem facilitado o meu trabalho e estarem sempre disponíveis.

À FCT por ter financiado a minha bolsa.

Aos meus pais, por sempre acreditarem em mim, pela liberdade que me deram para fazer as minhas escolhas e por sempre terem feito o que lhes era possível para ajudar na minha formação e crescimento. Sem o apoio deles não teria chegado até aqui.

À minha irmã pela boa disposição e pelo ânimo que sempre deu nos piores momentos.

Ao Gabriel, pelo apoio incondicional nos bons e maus momentos, pelo companheirismo e por toda a ajuda. Sem isso esta tese não teria chegado a bom termo.

Ao João, que não está mais aqui mas que será sempre lembrado por todos os bons momentos partilhados dentro e fora do laboratório.

"But, however many ways there may be of being alive, it is certain that there are vastly more ways of being dead, or rather not alive."
(Richard Dawkins)

"Discovery consists of seeing what everybody has seen and thinking what nobody has thought."

(Albert Szent-Györgyi, 1893-1986)

Table of contents

Abbreviations and acronyms

ADP	adenosine 5'-diphosphate
ADP/O	ADP-to-oxygen ratio
AIDS	acquired immunodeficiency syndrome
ANOVA	analysis of variance
API	analytical profile index
ATP	adenosine 5'-triphosphate
BCA	bicinchoninic acid
Bodipy	boron-dipyrromethene
BSA	bovine serum albumin
C_{10}TAB	decyltrimethylammonium bromide
C_{12}BZK	dodecyl-N-benzyl-N,N-dimethylammonium bromide (benzalkonium)
C_{12}PB	N-dodecylpyridinium bromide
C_{12}PC	N-dodecylpyridinium chloride
C_{12}TAB	dodecyltrimethylammonium bromide
C_{14}TAB	tetradecyltrimethylammonium bromide
C_{16}TAB	hexadecyltrimethylammonium bromide
Caco-2	human colorectal adenocarcinoma cell line
CCCP	carbonyl cyanide m-chlorophenylhydrazone
CFU	colony forming units
CI	confidence interval
CMC	critical micelle concentration
C_nTAB	*n*-alkyl-N,N,N-trimethylammonium bromides
CoQ	coenzyme Q_{10}, also known as ubiquinone
Cyt c	cytocrome c
DDPS	N-dodecyl-N,N-dimethylammonium-propanesulfonate
DIC	differential interference contrast
DMEM	Dulbecco's modified Eagle medium
DMSO	dimethyl sulfoxide
DNA	deoxyribonucleic acid

E. coli	*Escherichia coli*
EC_{50}	stimulatory concentration 50
EDTA	ethylenediamine tetraacetic acid
EGTA	ethylene glycol tetraacetic acid
FAD	flavin adenine dinucleotide
$FADH_2$	reduced form of flavin adenine dinucleotide (hydroquinone form)
FCCP	carbonyl cyanide 4-(trifluoromethoxy)phenylhydrazone
FCS	fetal calf serum
FSDC	fetal skin dendritic cell line
HBV	hepatitis B virus
HeLa	human cervical adenocarcinoma cell line
HEPES	4-(2-hydroxyethyl)-1-piperazineethanesulfonic acid
HIV	human immunodeficiency virus
HPVs	human papillomaviruses
HSV-2	herpes simplex virus type 2
IC_{50}	inhibitory concentration 50
ID	Identification
IM	mitochondrial inner membrane
IMDM	Iscove's modified Dulbecco's media
INT	2-p-(iodophenyl)-3-(p-nitrophenyl)-5-phenyltetrazolium chloride
LB	Luria-Bertani broth
LD	lethal dose
LD_{10}	lethal dose 10
LD_{50}	lethal dose 50
LD_{90}	lethal dose 90
LDH	lactate dehydrogenase
MDCK II	Madin-Darby canine kidney II cell line
MEM	minimum essential medium
MIC	minimal inhibitory concentration
Monolaurin	*rac*-1-lauroylglycerol
MTT	3-(4,5-dimethylthiazol-2-yl)-2,5-diphenyltetrazolium bromide

MW	multiwell
n	number of carbons in the surfactant hydrophobic chain
N-9	Nonoxynol-9
NAD^+	nicotinamide adenine dinucleotide
NADH	reduced form of nicotinamide adenine dinucleotide
ND	not determined
NPN	N-phenyl-l-naphthylamine
OM	mitochondrial outer membrane
Opti-MEM	improved minimal essential medium
PBS	phosphate-buffered saline
PI	propidium iodide
PS	phosphatidylserine
QACs	quaternary ammonium compounds
RCR	respiratory control ratio
Rh123	rhodamin 123
RNA	ribonucleic acid
ROS	reactive oxygen species
rpm	revolutions per minute
SD	standard deviation
SDS	sodium dodecyl sulfate
STIs	sexually transmitted infections
TX-100	Triton X-100
UNAIDS	Joint United Nations Programme on HIV/AIDS
VBNC	viable but non-culturable
WHO	World Health Organization

Abstract

Sexually transmitted infections (STIs) are a major public-health problem worldwide. According to the World Health Organization there are 340 million new cases of bacterial and protozoal STIs (Gonorrhea, Syphilis, Chlamydia and Trichomoniasis) per year, a number that does not include the millions of new STIs of fungal (Candidiasis) and viral etiology (Herpes Simplex type 2, Hepatitis B, HPVs and HIV). The direct treatment costs and the serious perinatal collateral damage caused by STIs represent hefty financial and social burdens, particularly in developing countries. Thus, the urgent need for cheap, safe, effective, easy-to-use and easy-to-store woman-controlled topical applications for prophylaxis against STIs makes surfactant-containing formulations an interesting option that requires a more fundamental knowledge concerning surfactant toxicology and structure-activity relationship.

In the present work, the *in vitro* effects of surfactant concentration, exposure time and structure on the viability of mammalian cell types typically encountered in the vaginal mucosa, namely, fully polarized and confluent epithelial cells, confluent non-polarized epithelial-like cells and dendritic cells are reported. Representatives of the different families of commercially available surfactants – nonionic (Triton X-100 and Monolaurin), zwitterionic (DDPS), anionic (SDS), and cationic (C_nTAB (*n* = 10 to 16), C_{12}PB and C_{12}BZK) – were examined. Since the most common and most prevalent in co-infections with HIV bacterial STIs are caused by *Chlamydia trachomatis* and *Neisseria gonorrhoeae*, both Gram-negative bacteria, the microbicidal effect of cationic surfactants, the most promising ones among the compounds studied, was evaluated using *Escherichia coli* as Gram-negative bacteria cell model.

Triton X-100, DDPS and SDS were toxic to all cell types at concentrations around their critical micelle concentration (CMC) suggesting a non-selective mode of action involving cell membrane destabilization and/or destruction. Up to a concentration of 10 times CMC Monolaurin was not toxic to all cell types. All cationic surfactants were toxic at concentrations far below their CMC and showed significant differences in their toxicity towards polarized as compared with non-polarized cells. Cationic amphiphiles of the C_nTAB family, differing in the number of carbons constituting their hydrophobic chain, exhibit a non-linear dependence of their toxicity on the alkyl chain length. Surfactant toxicity was also dependent on the chemical structure of the polar head group, being surfactants with larger polar head groups (C_{12}BZK and C_{12}PB) and more delocalized positive charge (C_{12}PB) the most toxic. The results also show that surfactant concentrations close to the critical micelle concentration cause acute toxicity whereas lower concentrations can lead to a persistent post-exposure toxicity, suggesting an intracellular locus of action.

Although, among surfactants, quaternary ammonium compounds (QACs) have been proven to be the most useful antiseptic and disinfectants, the results from the toxicological study performed show that these are also the most toxic for mammalian cells. Understanding the toxicity mechanisms, particularly at concentrations below surfactant CMC, and the sequence of events underlying surfactant-mediated epithelial cell death is crucial for the design and development of more effective and safer molecules. To this end, the mechanisms mediating surfactant-induced polarized epithelial cell toxicity were studied. The results show that mitochondrial dysfunction is an early event in cationic surfactant-induced toxicity, already starting at sub-lethal concentrations, and characterized by mitochondrial fragmentation accompanied by decreased cellular energy charge at higher concentrations. Moreover, the results obtained on isolated mitochondrial fractions demonstrate that all the compounds tested acted by a common mechanism that involves the inhibition of the NADH-ubiquinone oxidoreductase (Complex I) and by hampering the mitochondrial phosphorylative system. For low concentrations, QACs-induced mitochondrial dysfunction culminates in apoptosis, while the exposure of epithelial cells to high surfactant concentration induces a shift from apoptosis to necrosis. These results highlight the importance of including a rigorous assessment of mitochondrial function and cytotoxicity when evaluating new microbicide candidates.

Concerning the antimicrobial efficacy of cationic amphiphiles against *Escherichia coli*, it was found to be greatly dependent on the length of their alkyl chain and to exponentially decrease with the increase in surfactant alkyl chain length. Moreover, distinct from what was observed in the case of mammalian cells, the dose-response toxicity curves were biphasic. These two phases of the toxicity curve were found to correspond to two discrete effects of cationic surfactants which occur at different threshold concentrations: a bacteriostatic action at low concentrations and a bactericidal activity at higher concentrations. With the increase in the alkyl chain length, the fractional contribution of the bacteriostatic effect to the global antimicrobial activity of QACs also decreases, giving rise to a predominant bactericidal action. Furthermore, as in the case of mammalian cells, the antimicrobial efficiency of QACs was also dependent on the chemical structure of the polar head group, with surfactants possessing larger polar head groups (C_{12}BZK and C_{12}PB) and more delocalized positive charge (C_{12}PB) being the most toxic. It was also observed that bacterial cells exposed to low concentrations of C_{10}TAB, C_{12}TAB and C_{12}PB, presented significant morphological alterations, such as anomalies in the inner membrane structure and in the septum formation, emergence of elongated bacterial cells and in some cases, detachment of the outer membrane.

The major concern in the development of clinically useful microbicides for STIs prophylaxis is their selective toxicity against the pathogenic agents. With this in mind, the specificity of cationic

surfactants toxic effects was also addressed by comparing the toxicity curves obtained for both *E. coli* and mammalian polarized epithelial cells. With the exception of C_{16}TAB, bacteria were more susceptible to cationic surfactants than mammalian cells, a selectivity that probably results from differences in the lipid composition as well as in the membrane potential between the target pathogen and host cell membranes. Cationic surfactants with short hydrophobic chains (10 or 12 carbons), larger polar head groups and more delocalized charge, presented the highest therapeutic indices, being the best candidates to be used for the prevention of bacterial STIs. Although the therapeutic indices obtained may be considered narrow, in view of the limitations of the *in vitro* mammalian cell models used, namely the lack of mucus production which might limit surfactants absorption, it is expected that *in vivo* the toxicity of cationic surfactants towards vaginal mucosa cells will be lower than reported here.

In conclusion, the results presented in this thesis not only contribute to the understanding of the mechanisms involved in surfactant toxicity and microbicidal action, but also offer predictive power with regard to their safety, which may be useful in designing more effective and less harmful surfactants for use in topical applications for STI prophylaxis.

Resumo

As infecções sexualmente transmissíveis (ISTs) representam um grave problema de saúde pública em todo o mundo. Segundo a Organização Mundial de Saúde, por ano surgem 340 milhões de novos casos de ISTs causadas por bactérias e protozoários (Gonorréia, Sífilis, Clamídia e Tricomoníase), um número que não inclui os milhões de novos casos de ISTs com origem em fungos (Candidíase) e vírus (Herpes Simplex tipo 2, Hepatite B, VPHs e VIH). Os custos directos do tratamento e os danos colaterais perinatais graves provocados pelas ISTs representam pesados encargos financeiros e sociais, particularmente nos países em desenvolvimento. Assim sendo, a necessidade urgente de microbicidas para uso tópico, baratos, seguros, eficazes, fáceis de usar e de armazenar e cuja utilização na profilaxia de ISTs possa ser controlada pela mulher, fazem das formulações contendo surfactantes uma opção interessante, que requer um conhecimento mais fundamental sobre os efeitos toxicológicos dos surfactantes e a relação entre a sua estrutura e actividade microbicida.

No presente estudo, foram avaliados os efeitos *in vitro* da concentração de surfactante, do tempo de exposição e da estrutura dos compostos na viabilidade de diferentes tipos de células de mamífero comumente encontradas na mucosa vaginal, nomeadamente, células epiteliais confluentes e completamente polarizadas, células com origem epitelial confluentes mas não polarizadas e células dendríticas. Compostos representativos das diferentes famílias de surfactantes comercialmente disponíveis – não iónicos (Triton X-100 e Monolauril), zwiteriónicos (DDPS), aniónicos (SDS) e catiónicos (C_nTAB (*n* = 10 to 16), C_{12}PB, e C_{12}BZK) – foram estudados. Uma vez que as ISTs bacterianas mais comuns e prevalentes em co-infecções com VIH são causadas por *Chlamydia trachomatis* e *Neisseria gonorrhoe*, ambas bactérias Gram-negativas, o efeito microbicida dos surfactantes catiónicos, os mais promissores de entre os compostos estudados, foi avaliada utilizando *Escherichia coli* como modelo experimental de uma bactéria Gram-negativa.

Os surfactantes Trinton X-100, DDPS e SDS exerceram efeitos tóxicos em todos os tipos de células apenas a concentrações próximas da concentração micelar crítica (CMC), o que sugere um modo de acção não selectivo, envolvendo a desestabilização e/ou destruição da membrana celular. Até uma concentração máxima 10 vezes superior à CMC, o Monolauril não se mostrou tóxico para nenhum dos tipos de células estudados. Todos os surfactantes catiónicos se mostraram tóxicos a concentrações muito inferiores à respectiva CMC, apresentando diferenças significativas quanto a sua toxicidade em células polarizadas e não polarizadas. Anfifilas catiónicas pertencentes à família dos C_nTAB, mas diferindo no número de carbonos que constituem a sua cadeia hidrofóbica, mostram uma dependência não linear da sua toxicidade em relação ao tamanho da cadeia alquílica. A toxicidade dos surfactantes também se mostrou dependente da estrutura

química do grupo da cabeça polar, sendo que os surfactantes com cabeças polares constituídas por grupos maiores (C_{12}BZK e C_{12}PB) e com carga mais deslocalizada (C_{12}PB) os mais tóxicos. Os resultados também mostram que concentrações de surfactantes próximas da concentração micelar crítica causam toxicidade aguda, enquanto concentrações mais baixas podem conduzir a uma toxicidade persistente pós-exposição, o que sugere um local de acção intracelular.

Embora de entre os surfactantes os compostos quaternários de amónio (CQAs) se tenham mostrado como os mais úteis e eficazes enquanto anti-sépticos e desinfectantes, os resultados do estudo toxicológico realizado mostram que estes são também os mais tóxicos para as células de mamíferos. O entendimento dos mecanismos de toxicidade, em particular, a concentrações abaixo da CMC, bem como da sequência de eventos subjacente à morte de células epiteliais induzida pelos surfactantes, é essencial para o desenvolvimento de moléculas mais eficazes e seguras. Neste sentido, os mecanismos responsáveis pela toxicidade induzida pelos surfactantes em células epiteliais polarizadas foram estudados. Os resultados mostram que a disfunção mitocondrial é um evento precoce na toxicidade induzida por surfactantes catiónicos, manifestando-se a concentrações sub-letais, caracterizando-se pela fragmentação das mitocôndrias acompanhada por um decréscimo no estado energético das células a concentrações mais elevadas. Para além disso, os resultados obtidos em fracções mitocondriais isoladas demonstram que todos os compostos testados actuam através de um mecanismo comum que envolve a inibição da NADH-ubiquinona oxidoreductase (Complexo I) e o comprometimento do sistema fosforilativo mitocondrial. A baixas concentrações, as disfunções induzidas por CAQs culminam na apoptose das células, enquanto a exposição das células epiteliais a altas concentrações de surfactantes induz uma mudança da apoptose em favor da necrose. Estes resultados ilustram a importância de incluir uma avaliação rigorosa da função mitocondrial e da citotoxicidade aquando da avaliação de novos compostos candidatos a microbicidas.

No que respeita à eficácia antimicrobiana das anfifilas catiónicas contra a *Escherichia coli*, observou-se que esse efeito é largamente dependente do tamanho da cadeia alquílica, sendo que a a actividade antimicrobiana diminui de forma exponencial com o aumento do tamanho da cadeia alquílica do surfactante. Além disso, contrastando com o que foi observado no caso das células de mamífero, as curvas dose-resposta da toxicidade obtidas apresentam uma forma bifásica. Essas duas fases da curva de toxicidade foram identificadas como dois efeitos distintos dos surfactantes catiónicos, que ocorrem quando diferentes concentrações são atingidas: um efeito bacteriostático a baixas concentrações e um efeito bactericida a concentrações mais altas. Com o aumento da cadeia alquílica, a fracção da contribuição do efeito bacteriostático para a acção antimicrobiana dos CAQs também diminui, danda origem a uma predominância da acção bactericida. Além do mais, tal como no caso das células de mamífero, a eficiência antimicrobiana dos CAQs mostrou-se

dependente da estrutura química da cabeça polar, sendo os surfactantes com maiores grupos polares (C_{12}BZK e C_{12}PB) e com a carga positiva mais deslocalizada (C_{12}PB) os mais tóxicos. Foi também observado que as bactérias expostas a baixas concentrações de C_{10}TAB, C_{12}TAB e C_{12}PB, apresentavam alterações morfológicas significativas, tais como anomalias na estrutura da membrana interna e na formação do septo, surgimento de bactérias alongadas e, em alguns casos, descolamento da membrana externa.

A maior preocupação no desenvolvimento de microbicidas úteis para o uso clínico na profilaxia das ISTs é a selectividade dos mesmos contra agentes patogénicos. Tendo isto em conta, a especificidade dos efeitos tóxicos dos surfactantes catiónicos foi também analisada através da comparação das curvas de toxicidade obtidas para a *E. coli* e para as células epiteliais polarizadas de mamífero. Com a excepção do C_{16}TAB, as bactérias revelaram-se mais susceptíveis aos efeitos tóxicos dos surfactantes quando comparadas com as células de mamífero, susceptibilidade essa que provavelmente resulta das diferenças entre a composição lipídica e o potencial de membrana existentes entre as células do agente patogénico e das células do hospedeiro. Os surfactantes catiónicos com cadeias hidrofóbicas curtas (10 ou 12 carbonos), com maiores grupos polares e carga mais deslocalizada apresentaram os índices terapêuticos mais altos, sendo os melhores candidatos para serem utilizados na prevenção de ISTs bacterianas. Ainda que os índices terapêuticos possam ser considerados baixos, tendo em conta as limitações do modelo *in vitro* usado no caso das células de mamífero, em particular a ausência da produção de muco que pode limitar a absorção dos detergentes, é de esperar que *in vivo* a toxicidade induzida pelos surfactantes catiónicos nas células da mucosa vaginal seja menor do que aquela aqui descrita.

Em conclusão, os resultados apresentados nesta tese contribuem não só para a melhor compreensão dos mecanismos envolvidos nos efeitos tóxicos e na actividade microbicida dos surfactantes, como também oferecem uma maior capacidade de prever a segurança de tais compostos, o que pode ser útil para o desenvolvimento de surfactantes mais eficazes e seguros para o uso em aplicações tópicas na profilaxia de ISTs.

Chapter 1

Introduction

Summary

Introduction

1.1. Sexually transmitted infections (STIs)

Sexually transmitted infections are a group of communicable diseases transferred mainly through sexual intercourse, which have occupied a central place in the public health for at least the past 500 years (Oriel, 1994; Hawkes, 2008). Some STIs can also be transmitted via the re-use of needles after utilization by an infected person, as well as through childbirth or breastfeeding. Until the early 1990s, STIs were commonly referred to as venereal diseases (*veneris* is the Latin genitive form of the name Venus, the Roman goddess of love). Prejudice and blame related to these maladies led, in the 19th century, to the enactment in the United Kingdom of the "Contagious Diseases Act" which legislated the arrest and confinement of infected prostitutes at the London Lock Hospital, an institution created in 1746 to deal with venereal disease patients (Oriel, 1994; Ruiz, 2010). At that time the most frequent maladies assailing the European population were syphilis and gonorrhea (Oriel, 1994; Rothschild, 2005). For a long period, venereal diseases were generally incurable, being the treatment limited to ameliorating the disease's symptoms. The first effective treatment for an STI was an organoarsenic compound whose therapeutic utility was discovered in 1909, sold under the trade name of "Salvarsan" (Hoechst, Germany), which was effective in the treatment of syphilis (Hartman, 1915; Abraham, 1948; Williams, 2009). With the discovery of penicillin by Alexander Fleming in 1928 and the subsequent discovery of several other antibiotics, a large number of STIs became easily curable. The discovery of an effective treatment together with the intensive public campaigns against STIs led to the erroneous perception, during the 1960s and 1970s, that STIs had ceased to be a serious public-health threat (Oriel, 1994). It was in that context that, in 1981, the first patients with the acquired immunodeficiency syndrome (AIDS) were diagnosed in the United States (reviewed in Gallo & Montagnier, 2003). In 1984 it was accepted by the medical and scientific community that the human immunodeficiency virus (HIV) was the causative agent of AIDS (reviewed in Gallo & Montagnier, 2003). By the time it emerged into the public consciousness that AIDS was an STI that could not be cured, HIV had already started to spread and already in 1989 HIV was declared as a pandemic (Hymes *et al.*, 1989). A major factor complicating the control of STIs spread, even to the present day, is that frequently these infections have asymptomatic periods during which the

disease can be transmitted to others. In the particular case of HIV, the asymptomatic period can last for years.

Despite the advances in modern medical care, STIs are still one of the major global causes of illness, infertility, long term disability and death (World Health Organization, 2007). The combined efforts to develop an effective HIV vaccine, although producing promising results, have yet to meet its goal (Flynn *et al.*, 2005; Pitisuttithum *et al.*, 2006; Buchbinder *et al.*, 2008; Rerks-Ngarm *et al.*, 2009; Gray *et al.*, 2011). In fact, the only STI vaccine available nowadays is for high-risk types of human papillomavirus. Although at the present date there is no cure for the acquired immunodeficiency syndrome (AIDS), antiretroviral therapy in patients infected with HIV greatly reduces morbidity and mortality (Palella *et al.*, 1998; Murphy *et al.*, 2001), often accompanied by a considerable recovery of the immunologic function (Autran *et al.*, 1997; Lederman *et al.*, 1998). Oral pre-exposure prophylaxis with antiretroviral drugs has also recently been proven effective in preventing HIV transmission (Abdool Karim *et al.*, 2010; Grant *et al.*, 2010; Cohen *et al.*, 2011). Still, the evidence supporting these results is limited and further studies are needed to confirm the beneficial effects of prophylactic antiretroviral therapy (Obiero *et al.*, 2012). Besides, it cannot be ignored that HIV is a highly mutable virus that often develops resistance to antiretroviral drugs, a phenomenon that is becoming increasingly more frequent (Miller *et al.*, 1998; Wainberg & Friedland, 1998; Little *et al.*, 2002; Wilson *et al.*, 2008; Perez Bercoff *et al.*, 2010). The emergence of multi-drug resistant pathogens has also been extensively reported among pathogens that cause otherwise curable STIs, such as *Neisseria gonorrhoeae*, *Chlamydia trachomatis*, *Treponema pallidum* and *Trichomonas vaginalis* (Belland *et al.*, 1994; West *et al.*, 1995; Knapp, 1998; Somani *et al.*, 2000; Schwebke & Vermund, 2001; Shafir *et al.*, 2009; Sandoz & Rockey, 2010; Stamm, 2010; Lewis & Lukehart, 2011; Unemo & Shafer, 2011). As expected, the increasing prevalence of multi-drug resistant pathogens has large repercussions in the prevention and treatment strategies presently used, making the prevention of STIs a serious challenge.

1.2. Epidemiology of STIs

STIs are caused by more than 20 different pathogens, including bacteria, viruses, protozoans, fungi and ectoparasites (World Health Organization, 2007). Some of these pathogens can be sexually transmissible even when nonsexual routes of transmission predominate, and others, such as HIV and syphilis, can also be transmitted through blood transfusion, tissue transplant and from mother to child during pregnancy and childbirth. A list of common sexually transmitted pathogens and the diseases associated with them is presented in Table 1.1. Many of

Table 1.1. Common sexually transmitted pathogens and associated diseases and sequelae (adapted from Perine *et al.*, 1985, and modified according to the current state of the literature and the latest reports from the WHO).

Pathogens		Disease or syndrome
Bacterial agents	*Neisseria gonorrhoeae*	gonorrhoea or gonococcal infection; urethritis; epididymitis; cervicitis; proctitis; pharyngitis; conjunctivitis; endometritis; perihepatitis; bartholinitis; amniotic infection syndrome; premature delivery and premature rupture of membranes; salpingitis and related sequelae (infertility, ectopic pregnancy, recurrent salpingitis)
	Chlamydia trachomatis	chlamydial infections; urethritis; epididymitis; cervicitis; proctitis; salpingitis; inclusion conjunctivitis; infant pneumonia; otitis media; trachoma; lymphogranuloma venereum; perihepatitis; bartholinitis; Reiter's disease; fetal and neonatal mortality
	Treponema pallidum	syphilis
	Hemophilus ducreyi	chancroid
	Klebsiella granulomatis	granuloma inguinale or donovanosis
	Gardnerella hemophilus vaginalis	vaginitis
	Mycoplasma hominis	postpartum fever; salpingitis
	Ureaplasma urealyticum	urethritis; chorioamnioitis; low birth-weight
	Group B β-hemolytic streptococcus	neonatal sepsis; neonatal meningites
Viral agents	Human immunodeficiency virus (HIV types 1 and 2)	acquired immune deficiency syndrome (AIDS)
	Herpes simplex virus type 2 (HSV-2)	primary and recurrent genital herpes; aseptic meningitis; neonatal herpes with associated mortality or neurologic sequelae; carcinoma of the uterine cervix; spontaneous abortion and premature delivery
	Human papillomavirus (HPVs)	certain subtypes lead to cervical cancer in women; condyloma acuminate (genital warts); laryngeal papilloma in infants
	Hepatitis B virus (HBV)	hepatitis; chronic cases may lead to cancer of the liver
	Cytomegalovirus	causes inflammation in a number of organs including the brain, the eye, and the bowel; heterophile-negative infectious mononucleosis; protean manifestations in the immunosuppressed host; cervicitis; congenital infection induce gross birth defects, cognitive impairment (e.g. mental retardation, sensorineural deafness) and infant mortality
Protozoan agents	*Trichomonas vaginalis*	vaginal trichomoniasis; vaginites; urethritis; balanitis
Fungal agents[1]	*Candida albicans*	vulvovaginitis in women; inflammation of the glans penis and foreskin (balano-posthitis) in men
Ectoparasites	*Phthirus pubis*	pubic louse infestation ("crabs")
	Sarcoptes scabiei	scabies

[1] Although sexual intercourse is not the major route for the propagation of *Candida albicans* infections, candidiasis in commonly mentioned in the WHO reports alongside with STIs.

these diseases are curable by treatment with appropriate antibiotics and chemotherapeutic agents. However, in spite of this, STIs remain a major public health problem, comprising hefty financial and social burdens in industrialized and, more so, in developing countries. STIs are not only a cause of acute morbidity but many result in complications with sequelae such as infertility in men and women, ectopic pregnancy, cervical cancer, premature mortality, congenital syphilis and fetal wastage, low birth weight, premature births and opthalmia neonatorum (World Health Organization, 2007). The annual number of new infections and their global distribution for the most common and prevalent sexually transmitted pathogens is illustrated in Figure 1.1.

Regarding the AIDS epidemic, although the latest UNAIDS report confirms that worldwide HIV incidence is falling, several countries continue to experience a rise in the number of HIV infections, most notably in eastern Europe and central Asia (UNAIDS, 2010). In terms of absolute number of people carrying HIV, the largest epidemics still remains in sub-Saharan Africa (22.5 million people), south and south-east Asia (4.1 million people). All over the world, there are still 33.3 million people living with HIV. More than half of all people living with HIV are women and girls, a result of their greater biological and social vulnerability (Ackermann & de Klerk, 2002; World Health Organization, 2002; Hladik & Hope, 2009), and the majority of new infections are acquired through heterosexual intercourse (UNAIDS, 2010). Besides HIV, other viral infections, such as HSV-2 and HPVs have also become of great concern. In 2003, the number of people infected with HSV-2 was estimated at 536 million and the number of new infections ascended to 23.6 million per year (Looker *et al.*, 2008). Moreover, the World Health Organization estimates that 340 million new cases of the four main curable STIs (Gonorrhea, Syphilis, Chlamydia and Trichomoniasis) occur every year, 75-85% of which in developing countries (World Health Organization, 2007). Similar to the case of HIV infections, Sub-Saharan Africa is the most affected region, accounting for 20% of the global STI estimates. The overall yearly incidence rate of curable STIs in Africa is estimated at 254 per 1000 people in reproductive ages (15–49 years), but is only 77–91 per 1000 in industrialized countries (Gerbase *et al.*, 1998; World Health Organization, 2007).

Bacterial and viral (HSV-2 and HPVs) STIs impose an enormous onus of morbidity and mortality, particularly in poorer countries, either through a direct impact on reproductive and child health, or by facilitating the sexual transmission of HIV by breaking the organism's first line of defense - a consequence of the inflammatory related damage, resulting from other infections, inflicted in the vaginal epithelium (Fleming & Wasserheit, 1999; Mayaud & McCormick, 2001; Wald & Link, 2002; Corey *et al.*, 2004; Galvin & Cohen, 2004; Pao *et al.*, 2005; Abu-Raddad *et al.*, 2008; van de Wijgert *et al.*, 2008; Van Der Pol *et al.*, 2008; Smith-McCune *et al.*, 2010). Particularly in the case of HSV-2, there is very strong evidence supporting a synergistic relationship between the two

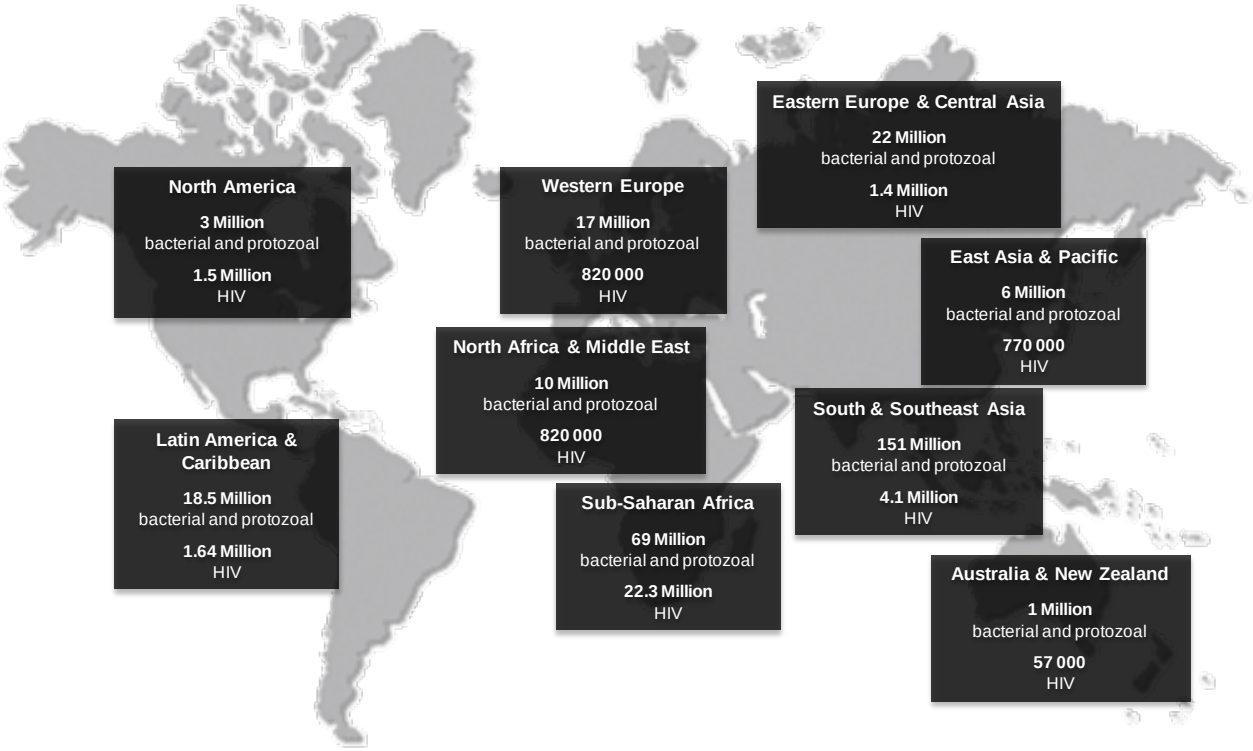

Figure 1.1. Global estimates and geographical distribution of the annual number of curable STIs new cases (among adults) and HIV infections. In the case of curable STIs the numbers correspond to Trichomoniasis (173 million), Chlamydia (92 million), Gonorrhea (62 million) and Syphilis (12 million), which are the more prevelent curable STIs. The global total for curable STIs is 340 million, whereas in the case of HIV infection is 33.3 million (Source: WHO (2007) and UNAIDS (2010)).

viral infections, being HSV-2 reactivation responsible for an increased HIV susceptibility and infectiousness, and also by accelerating AIDS progression (reviewed in Celum, 2010). Conversely, HIV infections may also contribute to the increase of other STIs caused by viruses, such as HSV-2, responsible for herpes, and HPVs, of which several strains are the cause of genital warts and cervical, vaginal, vulvar, anal and penile cancers (Corey *et al.*, 2004; Mayaud & Mabey, 2004; Rebbapragada *et al.*, 2007; Celum, 2010). In all these scenarios women and children are the ones most affected. For example, gonococcal and chlamydial infections in women often result in pelvic inflammatory disease, which in one fourth of the cases results in infertility (World Health Organization, 2007). Moreover, untreated STIs are intimately associated with congenital and perinatal infections in neonates. According to the World Health Organization (2007), in pregnant women with untreated early syphilis, 25% of pregnancies result in stillbirth and 14% in neonatal death, while in the case of gonococal infections, up to 35% of the pregnancies result in abortions and premature deliveries. Furthermore, worldwide up to 4000 newborn babies become blind every year because of eye infections attributable to untreated maternal gonococcal and chlamydial infections. In view of these facts, women have a particular need for STIs prevention methods. Currently available and effective options for prevention of STIs, including HIV, are essentially

restricted to condoms (Davis & Weller, 1999; Weller & Davis, 2002). However, limited economic resources and gender inequality, particularly in developing countries, may narrow women's ability to negotiate consistent condom use with their sexual partners, leaving them vulnerable to unwanted pregnancy and STIs (Heise & Elias, 1995; Ackermann & de Klerk, 2002). As such, there is an urgent need for STIs prevention methods that can be used by women without requiring the partner's consent. Safe and effective topical microbicides, such as vaginal gels, represent one of the most promising prevention strategies (reviewed in Hoffer & Robles, 2002; Stone, 2002; Lederman *et al.*, 2006; McGowan, 2006; Rosenberg *et al.*, 2006; Nuttall, 2010).

1.3. Mechanisms of infection and microbicide development strategies

At present, most of the global HIV epidemic is driven by heterosexual transmission, accounting for 80% of the new HIV infections (UNAIDS, 2010). The probability of heterosexual HIV transmission has been estimated to be around 0.01% to 0.4% in each sexual act (Padian *et al.*, 1997; Gray *et al.*, 2001), increasing to 0.03% to 0.5% at "high-risk" exposures (i.e. individuals already infected with another STI) (reviewed in Galvin & Cohen, 2004). However, HIV sexual transmission is not uniformly efficient and depends on the route of transmission. The probability of transmission per coital act is 1/10-1/1600 in cases of male-to-male transmission, 1/200-1/2000 in male-to-female transmission and 1/200-1/1000 in female-to-male transmission (Peterman & Curran, 1986; DeGruttola *et al.*, 1989; Padian *et al.*, 1997; Vittinghoff *et al.*, 1999; Gray *et al.*, 2001). Although in most of the cases this "per-act" estimates for HIV transmission risk are not particularly high, several risk factors can influence the infectiousness and susceptibility of HIV infection, such as: long HIV asymptomatic period, frequent sexual contact and cumulative risk of exposure during an extended period of time, inflammation or ulcerative lesions of the genital tract and having sex during an acute infection period (Wald & Link, 2002; Galvin & Cohen, 2004; Pilcher *et al.*, 2004; Cutler & Justman, 2008; Powers *et al.*, 2008; Smith-McCune *et al.*, 2010).

The risk of HIV infection, as of other sexually transmitted diseases, is higher for women, with an estimate of more than 50% of annual infections worldwide occurring through HIV invasion of the female genital tract via exposure to virus-containing semen (World Health Organization, 2002; UNAIDS, 2010). The anatomical differences between men and women are believed to play a critical role in women's increased susceptibility. During sexual intercourse, women are exposed to a larger amount of infectious fluids (semen) than men. Moreover, the mucous membrane area exposed during sexual intercourse is larger, providing extra sites for the viral infection to occur

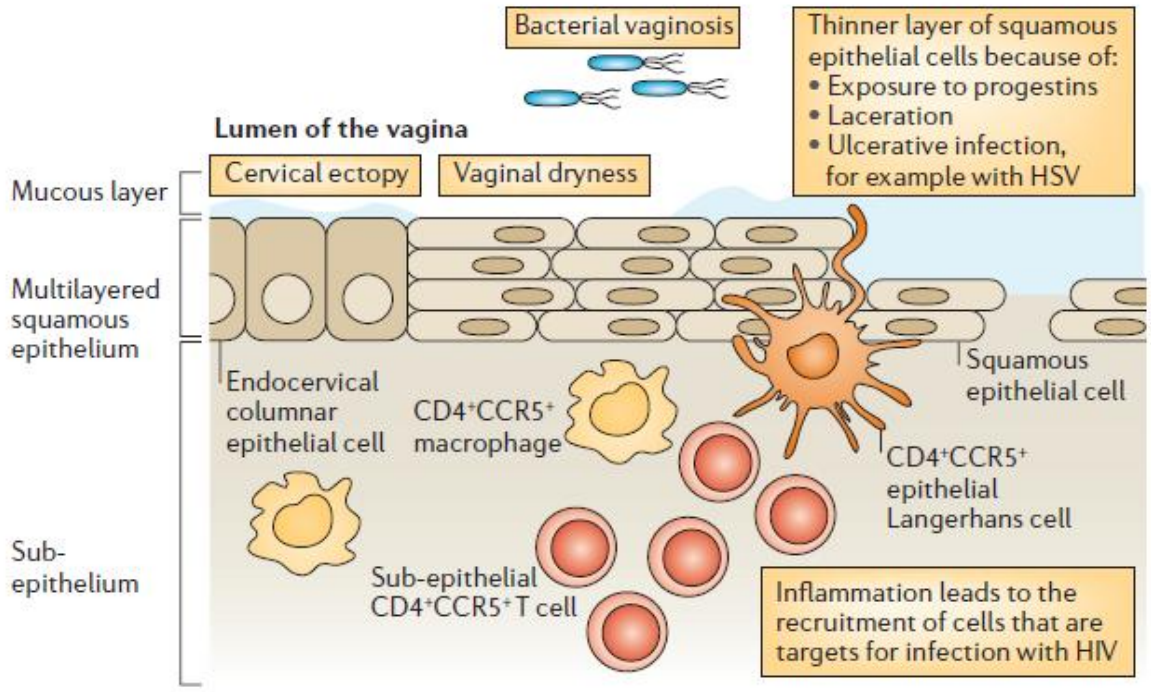

Figure 1.2. Risk-factors for vaginal HIV infection. The factors that can increase the risk of HIV infection include: ectopic protrusion of endocervical columnar epithelium into the ectocervix; thinning of the squamous epithelial layer; bacterial vaginosis; vaginal drying; inflammation, which leads to an increase in the number of target cells in the submucosa; trauma; ulcerative infections that might allow more ready access of virus to sub-epithelial dendritic cells (DCs) expressing C-type lectins, such as DC-specific intercellular adhesion molecule 3 (ICAM3)-grabbing non-integrin (DC-SIGN), and $CD4^+$ T-cells (adapted from Lederman *et al.*, 2006).

(World Health Organization, 2002; Hladik & Hope, 2009). Although vaginal epithelial tissues have limited permeability to particles greater than 30 nm (HIV size is 80–100 nm) (Shattock *et al.*, 2000), it has been shown that HIV can penetrate the superficial layers of the vaginal squamous epithelium and sequesters itself in the surface of the epithelial cells until it can infect CD4+ T-helper and Langerhans cells, both present in the mucosal epithelium (Miller & Shattock, 2003; Cutler & Justman, 2008; Hladik & Doncel, 2010). As a result of friction during sexual intercourse, microabrasions can occur, opening breaches in the epithelium and facilitating HIV access to the basal epithelial cells that are susceptible to viral binding or even to subepithelial targets like T-cells and dendritic cells (reviwed in Shattock & Moore, 2003; Hladik & Doncel, 2010). As already mentioned, pre-existing inflammation resulting from lower genital infections also facilitates infection by thinning and disrupting the squamous vaginal epithelium, recruiting HIV target cells to the site of infection, and interfering with innate immunity against infectious pathogens (Thurman & Doncel, 2011). Several of the risk-factors that increase the susceptibility of women to HIV infection are also shared with other STI pathogens (i.e. anatomical features; physical abrasion; impairment of the immune system functioning). Taking into consideration the whole process from the initial contact to the establishment of HIV infection, the mechanisms involved provide several

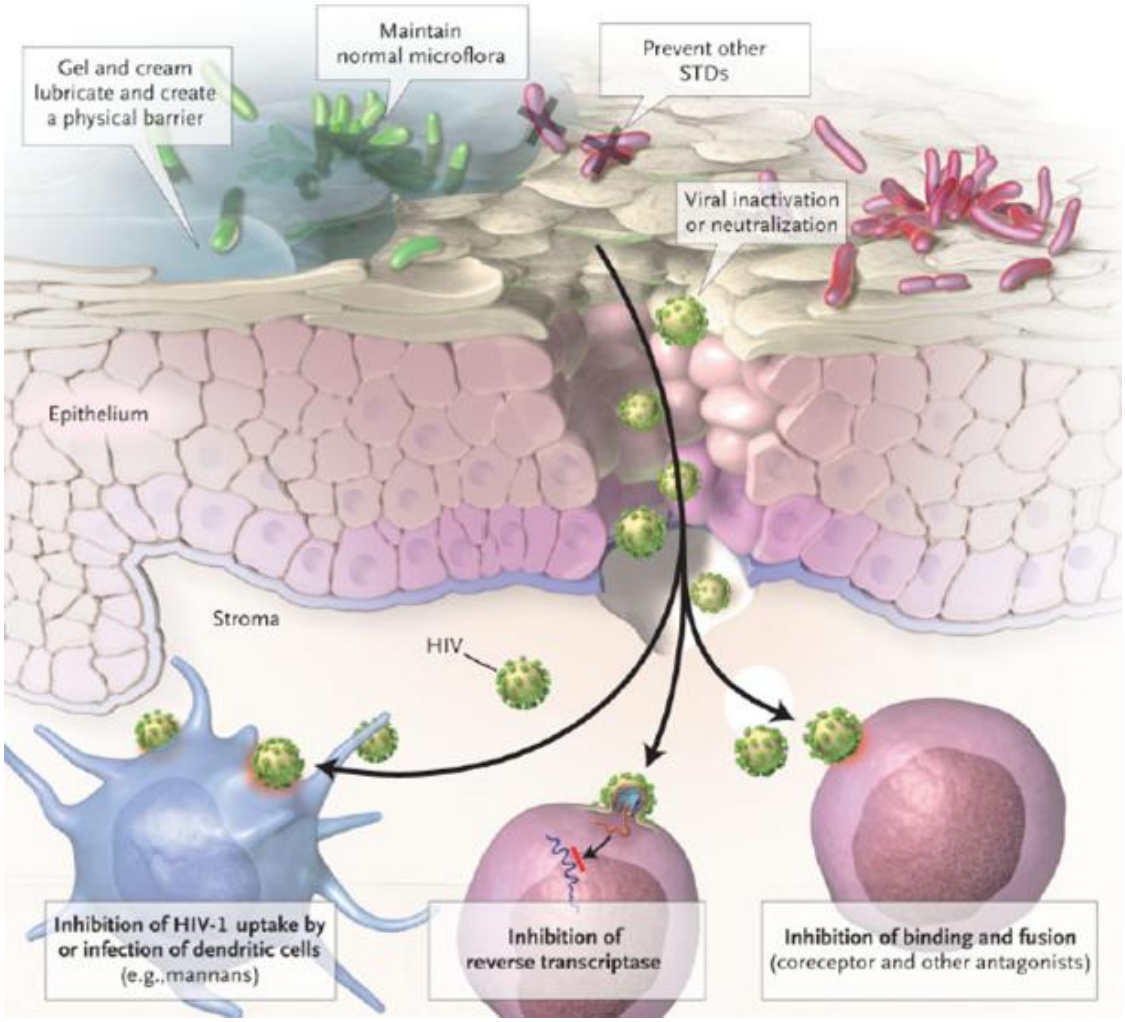

Figure 1.3. Potential targets for microbicide compounds. Possible actions of vaginally administered topical microbicides may include: prevention (or treatment) of STIs in order to reduce epithelial inflammation and ulceration; working as lubricant coat at the epithelium surface in order to reduce the risk of trauma and provide a physical barrier against viral infection; maintaining the normal vaginal flora, which sustains an acidic pH that reduces viral and bacterial capacity to elicit infection; destruction of viral membranes; inhibition of HIV uptake by dendritic cells; blockade of HIV adsorption and fusion to the host cells; and inhibition of reverse transcriptase activity and integration into the host cell genome (adapted from Moore, 2005).

niches that could be explored as target sites for surfactants (Fig. 1.2). In this context, three broad classes of microbicides have been under study: membrane disrupters; vaginal milieu protectors; and viral entry inhibitors (Fig 1.3).

Topical microbicides are prophylactic agents designed to reduce HIV and/or other STIs when applied to the vagina or rectum. Microbicides are conceived to be discrete, self administered, women-controlled prophylactic products, which could be available as gels, creams, films, suppositories or vaginal rings. Ideally, microbicides should be safe, effective, discrete, easy-to-use, should have long shelf lives and, particularly important in the case of developing countries, be cheap and without specific demands concerning product storage.

Research targeting the development of a chemical product for vaginal use that prevents HIV infection began in earnest in the early 1990s, in a publication authored by Dr Zena Stein (1990) calling attention for the urgent need of woman-controlled prophylactic methods capable of preventing STIs spread, particularly HIV. Since that time a roster of sixteen candidate microbicides have entered the clinical phase of development, and a much higher number are currently under development throughout several research centers spread around several countries (Cutler & Justman, 2008; for a comprehensive review see Hendrix *et al.*, 2009). Tables 1.2 and 1.3 show the most recent information regarding the current status of several microbicide candidates under development or undergoing clinical trials.

The first generation of topical microbicides was mainly focused on compounds with a broad-range of antimicrobial activity combined with spermicidal action, particularly, surface active agents or surfactants (Fig 1.4). The first clinical trial to assess the effectiveness of a microbicide was a trial of the Nonoxynol-9 (N-9) sponge (Martin *et al.*, 1997). However, instead of conferring protection against HIV infections, N-9 increased the incidence of genital tract lesions. Subsequent trials with N-9 and another surfactant-based product, SAVVY® (C31G) vaginal gel, also failed to prevent HIV transmission (Stephenson, 2000; Fichorova *et al.*, 2001; Peterson *et al.*, 2007; Feldblum *et al.*, 2008) and doubt was cast over their utility as general microbicides. In view of these results the further development of this generation of microbicides rapidly fell into disfavor, giving rise to a second generation of compounds in the late 1990s (reviewed in Karim, 2006). Anionic polimeres used as inhibitors of viral entry, such as Carraguard® and PRO2000®, also did not demonstrate efficacy (Skoler-Karpoff *et al.*, 2008; McCormack *et al.*, 2010). The initial discouraging results of microbicide clinical trials turned the main focus of current research to the development of formulations containing specific antiretroviral drugs (reviewed in Nuttall, 2010). Currently, two new generations of microbicides, which comprise several antiretroviral drugs and co-receptor blockers, are being explored (Fig. 1.4). However the development of an effective microbide product is challenging and, to the present date, there are no microbicide products approved.

1.4. Surfactants in the prevention of STIs

Surfactants are amphiphilic molecules consisting of at least two parts: an apolar hydrophobic tail and a polar hydrophobic head. They are often classified on the basis of the charge of the polar head group. According to this, they are divided into non-ionic (without net charge), zwiterionic (having both positive and negative charge), anionic (negative charge) and cationic

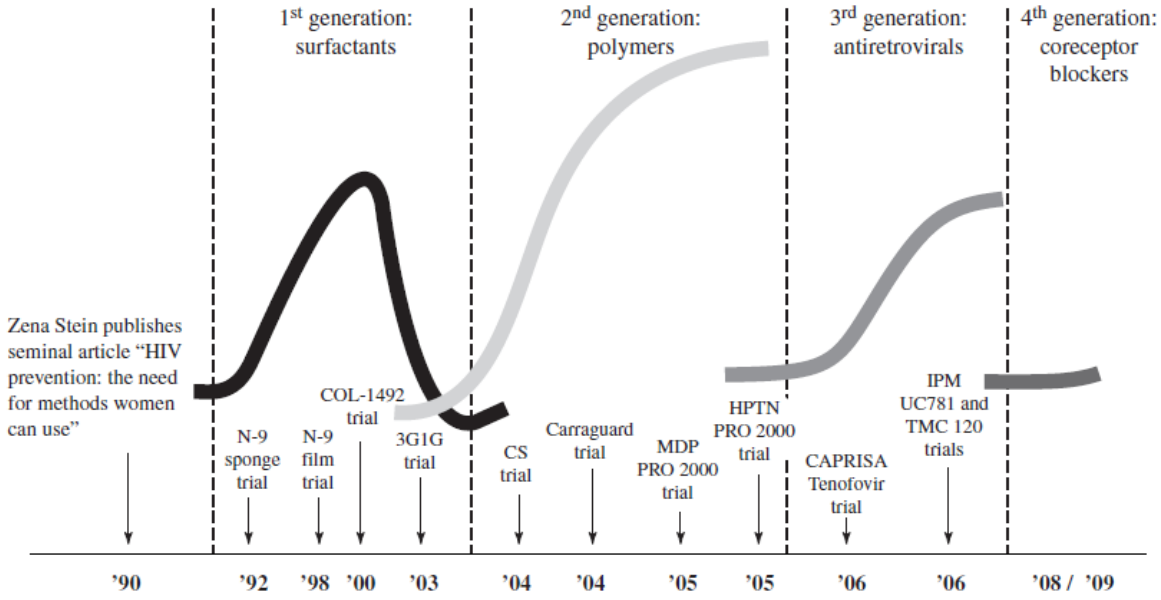

Figure 1.4. Evolution of microbicide research and development. Since the early 90's, three generations of microbicides have been studied in clinical trials. The number of undergoing clinical tests for each class of microbicides is represented by the height of the respective curve (adapted from Karim, 2006).

(positive charge) (Holmberg *et al.*, 2003). Disinfectant properties of surfactant solutions have been known for several decades (Domagk, 1935) and they have been marketed as contraceptive agents for over 30 years (Hitchcock, 2000; Ayotte & Colin, 2002; Stone, 2002; Wilkinson *et al.*, 2002). In the last twenty years there have been an increasing number of reports on the use of surfactants as disinfectants in vaginal hygiene products for the prevention of sexually transmitted diseases, in particular HIV (Hicks *et al.*, 1985; Malkovsky *et al.*, 1988). This has provided the initial incentive for the search among surfactants of compounds that by compromising the HIV virus and/or hampering its mechanisms of infection would be valuable as microbicides agents for topical use. Moreover, this class of compounds combines other characteristics that are essential in a good microbicide: they are stable and have relative long shelf lives, their synthesis is not expensive and, although they have been in use for a long time, the number of reports concerning bacterial resistance is reduced (Gilbert & Moore, 2005).

The disappointing results of the clinical trials using surfactants has raised the urgency to study in detail the biological mechanisms responsible for microbicides toxicity and to provide new *in vitro* models and safety biomarkers, in order to improve the prediction of clinical outcomes in large-scale efficacy trials. In fact, posterior *in vitro* and *in vivo* studies have demonstrated that N-9, even when applied at the minimal concentration needed for a brief partial protection against HSV-2 infection in a mouse model, caused a subsequent increase in infection susceptibility without signs of toxic effects being detected by colposcopy. N-9 increased infection susceptibility was

Table 1.2. Selected non-specific microbicide candidates in clinical phases of development (adapted from Cutler & Justman, 2008).

	Advantages	Disanvantages	Examples	Clinical trials status
Membrane disrupters				
non-specific disruption of cellular and microbial membranes	active against wide range of pathogens; often spermicidal	potentially toxic to host cells	Nonoxinol-9	No current clinical trials for HIV prevention. Two phase III efficacy trials completed in 1996 and 2000, one of which showed increased HIV-1 seroincidence with N-9 when used more than three times per day.
			C31G (SAVVY)	Two phase III trials in Ghana (n=2142) and Nigeria (n=1800) halted in November, 2005, and August, 2006, because of low HIV seroincidence rate in the study population.
			Sodium lauryl sulfate (Invisible Condom)	Phase II safety trial in Cameroon completed. Results pending (clinicaltrials.gov identifier NCT00136643).
				Phase II/III trial assessing efficacy in high-risk women planned.
Vaginal milieu protectors/acidifying agents				
restores protective acidic pH of vagina by buffering semen	spermicidal; activity against HIV, HSV, *Chlamydia trachomatis*	none known	Carbopol 974P (BufferGel)	Phase II/IIb trial (HPTN 035) ongoing: 3101 women in five countries (Malawi, South Africa, USA, Zambia, and Zimbabwe; clinicaltrials.gov NCT00074425).
			Acidform (Amphora)	Phase III trial in Madagascar testing diaphragm with Acidform for prevention of *N gonorrhoeae* and *C trachomatis* is planned.
Entry inhibitors: anionic polymers				
negative charge causes interaction with HIV's viral envelope proteins and interferes with attachment of HIV to CD4+ cells	many have activity against other STI pathogens (including *Chlamydia trachomatis*, *Neisseria gonorrhoeae*, and HSV)	not all virus types respond equally well to negative charge properties of these compounds	Naphthalene sulfonate (PRO2000)	Phase II/IIb trial (HPTN 035) ongoing: 3101 women in five countries (Malawi, South Africa, USA, Zambia, and Zimbabwe; clinicaltrials.gov NCT00074425)
				Phase III (MDP-301, UK Medical Research Council): PRO2000 originally in two concentrations (0.5% *vs* 2.0%) *vs* placebo gel. 2.0% arm stopped in February, 2008. Enrolment of 9395 women completed in July, 2008, and trial to be completed in late 2009 (clinicaltrials.gov NCT00262106).
			Carrageenan (Carraguard/PC515)	Phase III trial completed in South Africa (n=6202). Results released in February, 2008, show gel to be safe with no difference in HIV incidence between study and placebo groups.
			Cellulose sulfate (Ushercell)	Two phase III trials in Africa and India halted in January, 2007, for increased HIV seroincidence during interim analysis of one trial.
			Cellulose acetate phthalate (CAP)	Phase I trial of 13% gel halted because of heavy vaginal discharge in multiple participants.
			Dendrimers: SPL7013 (Vivagel)	Showed protection from HIV in a macaque model and from HSV in two animal models. Completed phase I male tolerance study. Phase I safety trial completed in Kenya with results pending (clinicaltrials.gov NCT00331032).
				Phase I trial ongoing in the USA (clinicaltrials.gov NCT00442910).

Table 1.3. Selected specific microbicide candidates in clinical phases of development (adapted from Cutler & Justman, 2008).

	Advantages	Disanvantages	Examples	Clinical trials status
Entry inhibitors: CCR5 blockers				
block CCR5 co-receptor and interfere with attachment of HIV to host cells	targets specific ligand	no activity against other STI pathogens	PSC-RANTES	Protected macaques from SHIV (SF162) with no evidence of systemic absorption or toxicity.
			CMPD167	Full protection of macaques from SHIV (162P4) not achieved alone, but only with addition of BMS-378806 and C52-L, two peptides that block the viral–host cell interaction at different loci (gp120 and gp41, respectively).
Reverse transcriptase inhibitors				
interfere with HIV reverse transcriptase enzyme	Tenofovir: active in multiple cell types TMC-120 and UC781 (NNRTIs):delayed development of resistance compared with first-generation NNRTIs	no activity against other STI pathogens	Tenofovir (PMPA; nucleotide analogue)	Phase I safety trial testing 0·3% and 1% gel formulations in HIV-positive and HIV-negative sexually active and sexually abstinent women found gel to be safe and well tolerated. Two phase I pharmacokinetic trials and a third phase I trial evaluating the effect of tenofovir gel on mediators of mucosal immunity are ongoing (clinicaltrials.gov identifiers NCT00561496, NCT00540605, and NCT00594373). Phase II expanded safety trial in India and USA completed in 2007; results pending (clinicaltrials.gov NCT00111943). Phase IIb trial in South Africa ongoing (CAPRISA 004; clinicaltrials.gov NCT00441298). Phase II/IIb trial (MTN 003) in South Africa comparing two oral antiretroviral drugs (tenofovir and emtricitabine) *vs* 1% tenofovir gel is planned (clinicaltrials.gov NCT00705679).
			TMC120 (NNRTI)	Phase III efficacy study (IPM 009) and at least eight phase I/II safety trials planned. Phase I study completed, indicating safety after 6 days of daily dosing.
			UC781 (NNRTI)	Three phase I trials assessing safety and acceptability of 0.1% or 0.25% formulation applied vaginally are ongoing (clinicaltrials.gov NCT00441909, NCT00132444, and NCT00385554) Phase I trial assessing safety and acceptability with rectal use in HIV-negatives adults ongoing (clinicaltrials.gov NCT00408538) Male tolerance study ongoing (A06-104; clinicaltrials.gov NCT00385554)

SHIV - chimeric simian/human immunodeficiency virus; NNRTI - non-nucleoside reverse transcriptase inhibitor

accompanied by a rapid exfoliation and re-growth of epithelial cell layer (Cone *et al.*, 2006), macrophage infiltration into the vaginal lumen and inflammation (Fichorova *et al.*, 2001; Catalone *et al.*, 2005; Cone *et al.*, 2006). The disruption of the epithelial barrier either by exfoliation (Cone *et al.*, 2006) or by disruption of tight junctions (as in the case of cellulose sulfate) (Mesquita *et al.*, 2009), accompanied by a pro-inflammatory response (Fichorova *et al.*, 2001; Catalone *et al.*, 2005; Cone *et al.*, 2006; Mesquita *et al.*, 2009), provides a direct access of the HIV to the *lamina propria* where virus target cells are more abundant, increasing the risk of HIV infection. Thus, spermicide/microbicide clinical safety testing based on pelvic examinations and colposcopy should be complemented with the analysis of other safety biomarkers in order to guarantee the security of these products before entering the market.

1.5. Objectives of the present work

In the light of the discouraging results obtained in surfactant-based microbicides clinical trials, research on the field turned its main focus into the development of formulations containing specific antiretroviral drugs (reviewed in Nuttall, 2010). However, several disadvantages are associated with the use of such drugs, namely: high risk of propelling the development of HIV resistant strains; high production costs; and effectiveness limited to viral infections. In view of these drawbacks alternative strategies are desired, if not in fact needed. Although the clinical trials with N-9 and SAVVY® (C31G) may seem to have sealed the fate of surfactant-based formulations as such an alternative, a more basic, bottom-up focused study may reveal ways of avoiding surfactants side effects and overcoming the toxicity issues that hamper their therapeutic use. This can be achieved through a systematic screening of different surfactant families concerning both their microbicide activity and its toxic effects towards the host cells. One important aspect, previously overlooked in pre-clinical and clinical studies, is that at concentration close or above surfactant CMC, its effects are scarcely selective and results in the undesired indiscriminate membrane disruption. A report by Vieira and colleagues (2008) illustrates the importance of dosing the surfactants relative to their CMC, and demonstrated that even though surfactants were not effective in preventing viral infection, cationic surfactants exhibited a selective toxicity towards bacterial cells, acting as antimicrobial agents at sub-toxic concentrations for mammalian polarized epithelial cells. The results from that work raise the question whether cationic surfactants may turn out to be reliable microbicide agents for bacterial STIs. Following this line of evidence, the present study was devised in order to evaluate how surfactant structure can affect its antimicrobial activity and whether surfactants structural properties can be exploited for the design of new more

effective compounds. To this end, a step-by-step, systematic investigation of the toxicity of different types of surfactants towards mammalian and bacterial cells was performed. Furthermore, the mechanisms involved in surfactant toxicity regarding both mammalian and bacterial cells were also explored. In both cases, the results were analysed taking into account surfactant physico-chemical properties (i.e. alkyl-chain size, polar head charge and structure, CMC) as these are known to condition the effect of surfactants on lipid bilayer membranes (Aranzazu Partearroyo *et al.*, 1990; Schnitzer *et al.*, 2005; Ahyayauch *et al.*, 2006; Vieira *et al.*, 2008).

Chapter II

Material and methods

Summary

Material and methods

2.1. Reagents

All mammalian cell culture reagents were purchased from Gibco® Life Technologies S.A. (Paisley, Scotland, UK), the Luria broth base (Miller's LB broth base) was supplied by Invitrogen™ Life Technologies S.A. (Carlsbad, CA, USA) and the agar-agar was obtained from Merck (Darmstadt, Germany). Cell culture flasks (Nunclon™Δ Surface) and the Pierce® BCA Protein Assay Kit were acquired from Thermo Scientific (Waltham, USA). 90 mm diameter plastic petri dishes (Gosselin) and 24- and 96-well multiwell plates were purchased from Corning Costar (Corning, NY, USA). The ibiTreat surface µ-Slides with 8 wells were supplied by ibidi GmbH (München, Germany). The Cytotoxicity Detection Kit^{PLUS} (LDH assay) and the ATP Bioluminescence Assay Kit CLS II were obtained from Roche Applied Science (Mannheim, Germany). The ADP/ATP Ratio Assay Kit (Bioluminescent) was supplied by abcam (Cambridge, UK) and the ApoLive-Glo™ Multiplex Assay by Promega (Madison, WI, USA). Hoechst 33342, Propidium Iodide (PI), Rhodamine 123, Bodipy 493/503 and the Live/Dead® BacLight™ Bacterial Viability kit were purchased from Molecular Probes® Invitrogen Corporation (Paisley, Scotland, UK). FITC Annexin V was obtained from BD Biosciences Pharmingen (San Diego, CA, USA). Glutaraldehyde, sodium cacodylate buffer and osmium tetroxide were purchased from Electron Microscopy Sciences (Hatfield, PA, USA). Glutamate, malate, succinate, adenosine 5′-diphosphate (ADP) sodium salt, adenosine 5′-triphosphate (ATP) magnesium salt, rotenone, oligomycin, carbonyl cyanide 4-(trifluoromethoxy)phenylhydrazone (FCCP), 3-(4,5-dimethylthiazol-2-yl)-2,5-diphenyltetrazolium bromide (MTT), staurosporine, the nonionic surfactants Triton X-100 (TX-100) and rac-1-lauroylglycerol (Monolaurin), the anionic surfactant sodium dodecyl sulfate (SDS), the zwitterionic surfactant N-dodecyl-N,N-dimethylammonium-propanesulfonate (DDPS) and the cationic surfactants dodecyltrimethylammonium bromide (C_{12}TAB), tetradecyltrimethylammonium bromide (C_{14}TAB), hexadecyltrimethylammonium bromide (C_{16}TAB), N-dodecylpyridinium bromide (C_{12}PB), N-dodecylpyridium chloride (C_{12}PC) and dodecyl-N-benzyl-N,N-dimethylammonium bromide (C_{12}BZK) were purchased from Sigma-Aldrich (St. Louis, MO, USA). Decyltrimethylammonium bromide (C_{10}TAB) was purchased from Fluka (St. Louis, MO, USA). All other chemicals used were supplied by Sigma-Aldrich

(St. Louis, MO, USA) or Merck (Darmstadt, Germany). All chemicals were of the highest commercially available purity grade and were used as received.

2.2. Biological materials

Caco-2, a colorectal adenocarcinoma human cell line, and HeLa, a human cervical adenocarcinoma cell line, were purchased from ATCC (Manassas, VA, USA). The MDCK II immortalized canine columnar kidney epithelial cell line was a gift of Professor Kai Simons (Max Planck Institute of Molecular Cell Biology and Genetics, Dresden, Germany) and the fetal mouse skin-derived dendritic cell line was kindly supplied by Dr. G. Girolomoni (Laboratory of Immunology, Instituto Dermopatico dell'Imacolata, IRCCS, Rome, Italy). *Escherichia coli* (5144572) isolated from human necropsies was kindly supplied by Dr. Célia Nogueira (Microbiology Institute of the Faculty of Medicine from the University of Coimbra, Coimbra, Portugal). Bacterial identity and biotype code were determined by the API 20E system (see Appendix B for a detailed description of the biochemical characterization and antibiotic resistance profile of the bacteria). Male Wistar rats (8 weeks old) were purchased from Charles Rivers Laboratories (Paris, France).

2.3. Methods I – Surfactant toxicity towards mammalian cell lines

2.3.1. Determination of the Critical Micelle Concentration (CMC)

In the present study, representatives of all families of commercially available surfactants, namely non-ionic, zwitterionic, anionic and cationic surfactants were tested (Table 2.1). CMC was measured as previously described by Brito and Vaz (1986). Briefly, 1 mM working solution of the fluorescent probe N-phenyl-I-naphthylamine (NPN) was prepared in 99% ethanol shortly before use. Serial dilutions of surfactants were prepared in a saline buffer with similar pH and saline composition as the OptiMEM media used in cell incubation. The buffer composition was 1.8 mM $CaCl_2$, 0.8 mM $MgSO_4$, 5.3 mM KCl, 26.2 mM $NaHCO_3$, 117.2 mM NaCl, and 1.0 mM $NaH_2PO_4.H_2O$, pH 7.3. For the determination of the CMCs, NPN was added to each tube to a final concentration of 10 μM (final ethanol concentration ≤ 0.1%) and samples were kept at room temperature for 30 minutes prior to measuring the emission spectra. Fluorescence spectra were acquired at 25°C on a SpectraMax Gemini EM spectrofluorometer (Molecular Devices Inc., Sunnyvale, CA, USA). Samples were excited at 356 nm and the emission intensity was recorded between 400 and 450 nm. The maximum emission peak was observed at approximately 420 nm.

Table 2.1. Surfactants chemical structure.

Family	Surfactant	Abbreviation	Molecular formula	Chemical structure
Non-ionic	Triton X-100	TX-100	$C_{16}H_{26}O_2$	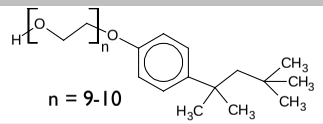
	1-lauroyl-*rac*-glycerol	Monolaurin	$C_{15}H_{30}O_4$	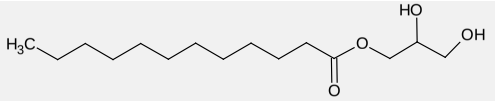
Zwiterionic	N-dodecyl-N,N-dimethylammonium-propanesulfonate	DDPS	$C_{17}H_{37}NO_3S$	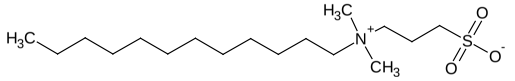
Anionic	sodium dodecyl sulfate	SDS	$C_{12}H_{25}NaO_4S$	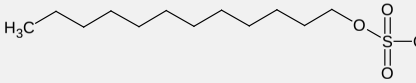
Cationic	decyltrimethylammonium bromide	C_{10}TAB	$C_{13}H_{30}BrN$	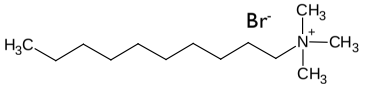
	dodecyltrimethylammonium bromide	C_{12}TAB	$C_{15}H_{34}BrN$	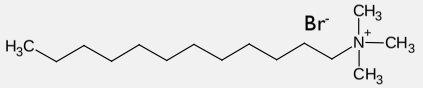
	tetradecyltrimethylammonium bromide	C_{14}TAB	$C_{17}H_{38}BrN$	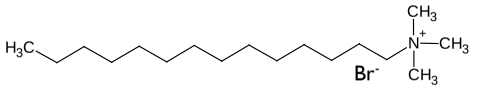
	hexadecyltrimethylammonium bromide	C_{16}TAB	$C_{19}H_{42}BrN$	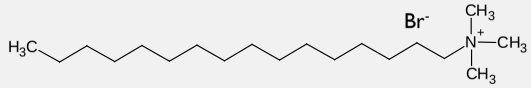
	N-dodecylpyridinium bromide	C_{12}PB	$C_{17}H_{30}BrN$	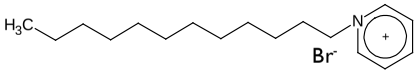
	N-dodecylpyridinium chloride	C_{12}PC	$C_{17}H_{30}ClN$	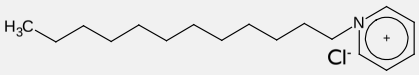
	dodecyl-N-benzyl-N,N-dimethylammonium bromide	C_{12}BZK	$C_{21}H_{38}BrN$	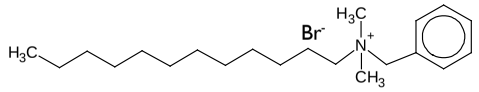

Measurement of the CMC of C_{12}PB was carried out using a similar protocol but replacing the NPN fluorescent probe by boron-dipyrromethene (Bodipy 493/503) at a final concentration of 0.9 µM (in 99% ethanol). In this case excitation was at 483 nm and emission intensity was recorded at 510 nm. As a control, the CMC of C_{12}BZK was measured with both Bodipy and NPN with essentially identical results.

2.3.2. Cell culture and experimental treatment

MDCK II cells were grown at an initial density of 56 250 cells/cm^2 on 96-MW plates for 3 days in MEM with GlutaMAX™, supplemented with 10% FCS, 100 units/mL of penicillin and 100 µg/mL streptomycin. Caco-2 cells were plated at an initial density of 100 000 cells/cm^2 in 96-MW plates and kept for 10 days in D-MEM with GlutaMAX™, supplemented with 10% FCS, 100 units/mL of penicillin, 100 µg/mL streptomycin, 1% sodium pyruvate and 1% of non-essential amino acids. After that time, both cell lines were confluent and polarized. HeLa cells were seeded in 96-MW plates at an initial density of 62 500 cells/cm^2 and grown in D-MEM with GlutaMAX™ with 10% FCS and 100 units/mL of penicillin, 100 µg/mL streptomycin for 24 hours, when they reached confluence. The dendritic FSDC cells were grown at an initial density of 68 750 cells/cm^2 in 96-MW plates for 24 hours, until they were 80% confluent, in IMDM with 10% FCS, 100 units/mL of penicillin and 100 µg/mL streptomycin (Girolomoni *et al.*, 1995; Neves *et al.*, 2008). The cells were then exposed to different concentrations of surfactants for 20, 60, 180 and 540 minutes. Stock solutions of surfactants were prepared in OptiMEM cell culture medium, without serum and antibiotics, as multiples of the respective CMC. At the end of the incubation with surfactants the cell culture medium was collected and replaced by fresh complete medium without phenol red. The cells were cultured for a further 24 hours.

2.3.3. Evaluation of *in vitro* surfactant toxicity towards mammalian cells

Cell viability was assessed 24h after the cells had been exposed to different concentrations of surfactants for 20, 60, 180 and 540 minutes. Viable cells were measured by their ability to reduce the yellow tetrazolium salt 3-(4,5-dimethylthiazole-2-y)-2,5-diphenyltetrasodiumbromide (MTT), to an insoluble purple formazan salt detectable by spectrophotometric analysis (Mosmann, 1983). Briefly, cells were incubated with the MTT dye (1 mg/mL) in cell culture medium without phenol red for 2 hours at 37°C and 5% CO_2. The precipitated dye was then dissolved by addition of 100 µL of a 16% SDS in 50% DMSO solubilisation solution to each well (final volume 225 µL/well), overnight. The samples were quantified colorimetrically at 570 nm wavelength

(background wavelength correction at 620 nm) on a SpectraMax Plus384 microplate spectrophotometer (Molecular Devices Inc., Sunnyvale, CA, USA). The background absorbance (culture medium plus MTT without cells) was subtracted from the absorbance of each sample and data are shown as percentage of control.

The activity of the lactate dehydrogenase enzyme (LDH) in the extracellular medium was determined in HeLa cells, in order to evaluate plasma membrane integrity. This protein is a soluble cytoplasmatic enzyme and can be found in the cell culture medium as a result of extensive plasma membrane damage. After treatment with $C_{10\text{-}16}$TAB for 540 minutes, the incubation medium was collected and replaced by fresh medium without phenol red and the cells were kept in culture for a further 24 hours. At the end of the experiment the culture media was collected and the cells were lysed. The LDH activity of the incubation media, cell culture media and cell lysates (intracellular content) was determined with a commercial colorimetric kit (Cytotoxicity Detection Kit^{PLUS}), according to the standard protocol provide by the supplier. This assay is based on a coupled two-step reaction: first, NAD^+ is reduced to NADH, with the release of H^+, by the LDH-catalyzed conversion of lactate to pyruvate; second, diaphorase uses the newly-formed NADH and H^+ to catalyze the reduction of a tetrazolium salt (2-p-(iodophenyl)-3-(p-nitrophenyl)-5-phenyltetrazolium chloride, INT) to formazan. The quantity of formazan formed is proportional to the amount of LDH released into the cell culture medium. Absorbance was measured at a wavelength of 490 nm (background wavelength correction at 600 nm) on a SpectraMax Plus384 microplate spectrophotometer. The background absorbance (cell culture medium without cells) was subtracted from the absorbance of each sample. Data are presented as percentage of the total activity for each condition (cell lysates activity plus incubation media and 24 hours post-incubation cell culture media activity). In the case where the intracellular LDH activity was compared between conditions, results are also expressed as percentage of control.

2.3.4. Statistical analysis

Results are expressed as Means ± Standard Deviations (SD). The cell viability dose-response curves were fitted with a four-parameter logistic equation (Seefeldt *et al.*, 1995; Knezevic *et al.*, 2007) through computer-assisted curve fitting (SigmaPlot® 11.0, SPSS Science Inc., Chicago, IL). The fitted equation was:

$$y = y_0 + \frac{(y_{\max} - y_0)}{1 + 10^{(\log(x) - \log(IC_{50}))b}}$$

Where x is the surfactant concentration; y_{max} is the maximal percentage of cell viability, y_0 is the basal cell viability; b is the Hill coefficient, the slope of the curve between its maximum and minimum thresholds; IC_{50} is the inhibitory concentration 50 (for further details see Appendix A). From these data, it was possible to calculate the lethal dose (LD) 10, 50 and 90 concentrations for each individual data set. The LD concentrations were plotted against time of exposure to the surfactants and a mono-exponential decay equation was adjusted to the data, using SigmaPlot® 11.0. The fitted equation was:

$$y = y_0 + ae^{-bt}$$

Where t is time; y_0 is the LD concentration at an exposure time of 0 minutes; a is the difference between y_0 and the asymptotic LD concentration at "infinite" exposure time; b is the decay constant. Statistical analysis was carried out in GraphPad PRISM® software version 5.0 (GraphPad Software Inc, LaJolla, CA). Comparison between groups was performed using the two-way ANOVA parametric test. The Bonferroni's post hoc test was used for multiple comparisons and statistical significance was considered for $p < 0.05$.

2.4. Methods II – Assessment of apoptosis in polarized epithelial cells exposed to cationic surfactants

2.4.1. Cell viability and caspase 3/7 activity assay

MDCK II cells were grown as described in Section 2.3.2. After achieving complete polarization, the cells were exposed to different concentrations of C_{10}TAB for 3 hours. At the end of incubation the OptiMEM media containing surfactant was replaced by fresh cell culture media without phenol red and viability and caspase 3/7 activity were assayed using the ApoLive-Glo™ Multiplex Assay, according to the manufacturer's instructions. As a positive control for apoptosis, cells were incubated with 1 µM staurosporine for 6 hours (Araki, 2002). In the first part of the assay, cell viability was assessed with a cell-permeant fluorogenic viability reagent that is cleaved by live-cell proteases into a fluorescent product. This reaction can only take place within cells with intact membrane. The fluorescence signal is proportional to the number of live cells and can be detected using a spectrofluorometer. The viability reagent was added to each well and mixed briefly by orbital shaking (300 rpm, 30 seconds). Cells were further incubated at 37°C with 5% CO_2 air for 1 hour. At the end of incubation fluorescence was measured on a SpectraMax Gemini EM spectrofluorometer. Samples were excited at 400 nm and the emission intensity was recorded

at 505 nm. The second part of the assay was performed by adding the Caspase-Glo® 3/7 reagent to each well. This reagent is a luminogenic substrate for caspase 3/7 which emits light when cleaved. Samples were incubated at room temperature for 1 hour and then transferred into black opaque 96 MW plates. Luminescence was read on LMax II 384 luminometer (Molecular Devices Inc., Sunnyvale, CA, USA), using an integration time of 5 seconds. Data are presented as percentage of control for both, cell viability and caspase 3/7 activity.

2.4.2. LDH cytotoxicity assay

The cytotoxic effect of C_{10}TAB towards fully polarized MDCK II cells grown in 96 MW plates was evaluated by the LDH assay, after 3 hours of exposure. At the end of incubation, the activity of the LDH released to the culture media was measured using the Cytotoxicity Detection Kit^{PLUS}, as described in Section 2.3.3. The percentage of cytotoxicity was calculated according to the manufacturer's instructions, using the following equation:

$$Cytotoxicity(\%) = \frac{exp.value - low\,control}{high\,control - low\,control} \times 100$$

Where $exp.value$ is the experimental value obtained for each sample; $low\,control$ is the LDH activity in the culture media of mock-treated cells; $high\,control$ is the maximum releasable LDH activity in the cells obtained after cell lysis.

2.4.3. Evaluation of apoptotic and necrotic cell death by annexin V and propidium iodide (PI) staining

One of the earliest hallmarks of apoptotic cell death is the translocation of phosphatidylserine (PS) from the inner to the outer leaflet of the plasma membrane (Martin *et al.*, 1995). FITC labeled annexin V, a Ca^{2+} dependent phospholipid-binding protein with high affinity for PS (Andree *et al.*, 1990), can be used to detect exposed PS on the membrane of apoptotic cells. Using annexin V in combination with PI staining, a dye that only enters membrane-damaged injured cells (Macklis & Madison, 1990; Vitale *et al.*, 1993), allows the identification of viable cells (annexin V and PI negative), early apoptotic cells (annexin V positive, PI negative) and late apoptotic and/or necrotic cells (annexin V and PI positive). MDCK II cells were seeded (56 250 cells/cm^2) on optically transparent sterile ibiTreat surface µ-Slides with 8 wells and grown for 3 days as described in Section 2.3.2. After that time, complete polarization was achieved and cells were treated with different concentrations of C_{10}TAB for 3 hours. At the end of incubation

surfactant-containing media was removed and replaced by fresh media with 5 µg/mL PI. Cells were incubated at 37°C and 5% CO_2 for 5 minutes, after which they were washed twice in phosphate-buffered saline (PBS) (137 mM NaCl, 2.7 mM KCl, 1.8 mM KH_2PO_4, 10 mM $NaHPO_4.2H_2O$, pH 7.4) followed by 15 minutes incubation at room temperature with 2 µg/mL Hoechst 33342, for nuclei staining, and annexin V diluted 1:10 in annexin V binding buffer. Lastly, cells were washed and kept in annexin V binding buffer for immediate visualization in a Carl Zeiss Laser Scanning Confocal Microscope LSM 510 (Carl Zeiss Inc., Oberkochen, Germany).

2.4.4. Quantification of intracellular ATP and ADP levels

Intracellular ATP levels were determined by the luciferin-luciferase bioluminescent assay after cells were incubated for 3 hours with different concentrations of C_{10}TAB. This technique allows the detection of very low ATP amounts by measuring the light emitted during the ATP-dependent luciferin oxidation catalyzed by luciferase enzyme. MDCK II were seeded in 24 MW plates (56 250 cells/cm^2) and grown until reaching complete polarization, as described in Section 2.3.2. After the treatment, cells were washed with cold PBS and disrupted with 500 µL of ice-cold lysis buffer (50 mM Tris-HCl, 4 mM EDTA, pH 7.5), for intracellular ATP extraction. An aliquot of the sample was taken out for protein quantification by the bicinchoninic acid (BCA) method (Pierce® BCA Protein Assay Kit), using bovine serum albumin (BSA) as standard. The remaining sample was further incubated at 90°C for 90 seconds, to precipitate the protein, followed by centrifugation at 16 000 g for 10 minutes (Santos *et al.*, 1999). The supernatant was then collected and the ATP content determined using the ATP Bioluminescence Assay Kit CLS II, according to the standard protocol provide by the supplier. In order to determine the exact ATP content in each sample, an ATP calibration curve was prepared using the ATP standard stock provided with the kit. Luminescence was read on LMax II 384 luminometer, using an integration time of 5 seconds. Results were normalized to protein content and expressed as percentage of mock-treated control cells. The ATP/ADP ratio of the samples was determined with the same method using the ADP/ATP Ratio Assay Kit. This kit contains an ADP converting enzyme which catalyses the conversion of the ADP contained in the sample into ATP, allowing the subsequent detection by the luciferin-luciferase reaction.

2.4.5. Evaluation of mitochondrial morphology and membrane potential ($\Delta\psi_m$) by laser-scanning confocal microscopy

Analysis of mitochondrial morphology and mitochondrial membrane potential was performed using the mitochondrial membrane potential-sensitive probe Rhodamine 123 (Rh123),

as described elsewhere (Johnson *et al.*, 1981; Bereiter-Hahn & Voth, 1994; Baracca *et al.*, 2003; Koopman *et al.*, 2005; Koopman *et al.*, 2006; Solaini *et al.*, 2007). This probe is a membrane-permeant lipophilic cation that accumulates into the mitochondria matrix in response to the electrical potential across the mitochondrial inner membrane, as a consequence of its charge and solubility in both membrane lipids and aqueous phase (Johnson *et al.*, 1981; Emaus *et al.*, 1986; Smith, 1990). Stock solutions of Rh123 were prepared in ethanol and stored at -20°C until use. MDCK II cells were grown as described in Section 2.4.3 and incubated with different concentrations of C_{10}TAB for 1 or 3 hours. At the end of the treatment, cells were labeled with 10 µg/mL Rh 123 and 2 µg/mL Hoechst 33342 in DMEM without phenol red buffered with 20 mM HEPES, for 30 minutes at 37°C, as previously described (Lachowiez *et al.*, 1989). The final ethanol concentration in each well was lower than 0.1%. As a positive control, 10 µM FCCP was added to Rh123 labelled mock-treated cells in order to completely dissipate the $\Delta\psi_{m.}$ When the evaluation of membrane integrity was carried out in tandem, cells were previously stained with PI as described in Section 2.4.3. Samples were examined in a Carl Zeiss Laser Scanning Confocal Microscope LSM 510.

2.4.6. Image acquisition and analysis

Mitochondrial morphometric analysis was carried out in confocal optical sections of cells probed with Rh 123. Image acquisitions were made in a confocal microscope with a Plan-Apochromat 63x oil immersion objective (NA = 1.40) using the Carl Zeiss Laser Scaning System LSM 510 software. The experimental approach used follows the basic outlines described by Frezza and colleagues (Frezza *et al.*, 2007). Surface rendering was carried out in 10-20 µm z-stack images composed of 0.43 µm optical slices using Imaris (Bitplane AG, Switzerland). From this volumetric reconstruction the number, area and volume of distinct mitochondrial particles were calculated.

2.4.7. Mitochondria isolation

Liver mitochondria were isolated from 8 weeks old male Wistar rats using a well established protocol (Pereira *et al.*, 2007; Silva & Oliveira, 2012). Rats were sacrificed by cervical dislocation (1 animal per preparation) and the liver quickly excised and placed in ice-cold isolation buffer (250 mM sucrose, 10 mM HEPES, 0.5 mM EGTA, 1 mg/mL BSA fatty acid free, pH 7.4). The liver was chopped into small pieces and washed several times to remove contaminating blood. The tissue was then homogenized in 60 mL of ice-cold isolation buffer using a Potter-Elvejehm

homogenizer with an electrically driven Teflon pestle, followed by a 2 000 g centrifugation at 4°C for 10 minutes. The supernatant was collected and centrifuged again at 12 000 g, 4°C, for 10 minutes. At the end of centrifugation the mitochondrial pellet was resuspended and rinsed twice in ice-cold washing buffer (250 mM sucrose, 10 mM HEPES, pH 7.4). Finally, the pellet was resuspended again in washing buffer and kept on ice until used for oxygen consumption or ATPase activity assays. Mitochondrial protein content was determined by the Biuret method (Gornall *et al.*, 1949), using BSA as standard.

2.4.8. Evaluation of mitochondrial respiration

Mitochondrial oxygen consumption was measured polarographically with a Clark-type oxygen electrode (Yellow Springs Instrument Inc., Ohio, USA) (Estabrook, 1967) connected to a flatbed Perkin-Elmer recorder, in a 1-mL thermostated water-jacketed closed chamber with magnetic stirring, at 30°C. The experiments were performed using 1 mg of protein in 1 mL respiration medium (135 mM sucrose, 65 mM KCl, 2.5 mM $MgCl_2$, 5 mM KH_2PO_4, 5 mM HEPES, pH 7.4). Different concentrations of the tested cationic surfactants (0-8 µL of a CMC/3 stock solution in distilled water) were added to the liver mitochondrial isolates and incubated for 5 minutes prior to mitochondrial energization (State 2 respiration) with 5 mM glutamate plus 2.5 mM malate (which generates Complex I substrate, NADH, in the mitochondrial matrix) or with 5 mM succinate (Complex II substrate) in the presence of 2 µM rotenone to inhibit Complex I. State 3 respiration was elicited by addition of 125 nmol/mL of ADP and State 4 respiration was achieved after complete phosphorylation of the ADP added. Approximately 1 minute after the beginning of State 4 respiration, 1 µg/mL oligomycin was added to the system, in order to inhibit proton passive flux through the ATP synthase. After that, Uncoupled State respiration was driven by addition of 1 µM FCCP. Respiration rates were calculated assuming that the oxygen concentration in the respiration medium was 236 nmol O_2/mL at 30°C. The respiratory control ratio (RCR), an indicator of mitochondrial membrane integrity and energy-conserving capacity, was determined as the ration between State 3 and State 4 respiration rates (Chance & Williams, 1956). As a measure of the oxidative phosphorylation efficiency, the ADP-to-oxygen ratio (ADP/O) was calculated as the ratio between the total amount of ADP added to elicit Sate 3 (in nmol) and the amount of atomic oxygen consumed (in nmol) during State 3 respiration to phosphorylate all the ADP added to the system (Chance & Williams, 1956; Estabrook, 1967). Table 2.2 summarizes the main features that define each of the mitochondrial respiratory states.

Table 2.2. Characterization of mitochondrial respiratory states (adapted from Nicholls & Ferguson, 2002).

Respiratory state		[O_2]	Substrate level	ADP level	Respiration rate	Rate-limiting substance
1	mitochondria alone (in the presence of Pi)	> 0	low	low	very slow	substrate
2	substrate addition	> 0	high	low	slow	ADP
3	addition of a limited amount of ADP	> 0	high	high	fast	respiratory chain
4	all ADP converted to ATP	> 0	high	low	slow	ADP
5	anoxia	0	high	low	0	oxygen

2.4.9. Assessment of mitochondrial F_0F_1-ATPase activity

The effect of cationic surfactants on mitochondrial ATP hydrolase activity was evaluated by monitoring the pH changes of the respiration medium occurring during ATP hydrolysis, as previously described (Madeira *et al.*, 1974; Moreno & Madeira, 1991; Pereira *et al.*, 2007). The pH changes were measured using a pH meter connected to a flatbed Perkin-Elmer recorder. Freshly isolated mitochondria (1 mg of protein) were incubated during 5 minutes with different concentrations of the tested cationic surfactants (0-8 µL of a CMC/3 stock solution in distilled water) at 30°C in 1 mL respiration media (135 mM sucrose, 65 mM KCl, 2.5 mM $MgCl_2$, 2.5 mM KH_2PO_4, 0.5 mM HEPES, pH 7.0), supplemented with 2 µM rotenone. Reactions were initiated by addition of Mg-ATP to a final concentration of 1 mM. Oligomycin (2 µg/mL), a selective inhibitor of the F_0-ATP synthase complex, was added to the system in order to abolish proton consumption, avoiding further pH changes. A control assay was performed in the presence of 1 µM FCCP to induce membrane permeabilization to protons. The system was calibrated using known concentrations of KOH and proton production was calculated 1.5 minutes after Mg-ATP addition. The same procedure was performed using disrupted mitochondria, which were previously frozen and thawed three times, in order to evaluate the direct effect of cationic surfactants on the catalytic activity of the F_1-ATPase.

2.4.10. Statistical analysis

Results are expressed as Means ± SD, unless otherwise stated. The cell dose-response curves were fitted using a four-parameter logistic equation (Seefeldt *et al.*, 1995; Knezevic *et al.*, 2007), as described in Section 2.3.4, through computer-assisted curve fitting (SigmaPlot® 11.0). When required, data were adjusted to different mathematical models obtained from modifications

of the logistic equation, as detailed in Appendix A. Statistical analysis was carried out in GraphPad PRISM® software version 5.0. Comparison between groups was performed using the one-way ANOVA parametric test. The Dunnet's post hoc test was used for multiple comparisons and statistical significance was considered for $p < 0.05$.

2.5. Methods III – Microbicidal activity of cationic surfactants

2.5.1. Bacterial cell growth

E. coli was used as an experimental model of Gram-negative bacteria to test the bacteriostatic and bactericidal activities of cationic surfactants. *E. coli* was isolated from human necropsies and identified by API 20E test strips (bioMérieux, Inc., Montreal, Quebec). Frozen stock cultures (in 15% glycerol) were prepared and stored at -80°C for further use. Before each experiment, bacteria from frozen stocks were inoculated in 10 mL of Miller's Luria broth (LB) and grown overnight in an orbital shaker (200 rpm) at 37°C. The bacterial culture was then diluted 1:100 (v/v) in 10 mL of fresh LB and grown until reaching the late logarithmic growth phase (approximately 4.5 hours). After that, bacteria were diluted in LB medium to reach the desired number of colony forming units (CFU) per milliliter, in presence or absence of cationic surfactants.

2.5.2. Minimal inhibitory concentration (MIC) of cationic surfactants

The MIC for each cationic surfactant assayed was determined by the broth macrodilution method (Wiegand *et al.*, 2008; CLSI, 2009). A series of surfactants dilutions were prepared as multiples of the respective CMC, using LB medium, and placed in 6 MW plates. An inoculum prepared from a late logarithmic phase growing bacteria (see Section 2.5.1) was added to each well to reach a final number of 1.5×10^8 CFU/mL (the equivalent to 0.5 McFarland) or 1.5×10^5 CFU/mL. A control without surfactant was also prepared. Bacterial cultures were incubated overnight in an orbital shaker (200 rpm) at 37°C. The minimal inhibitory concentration was determined as the lowest surfactant concentration at which no visible growth was observed. The experiment was repeated at least 3 times.

2.5.3. Effect of cationic surfactants on *Escherichia coli* viability

E. coli cell suspensions (1.5×10^8 CFU/mL) prepared from a late logarithmic phase growing bacteria, as described in Section 2.5.1, were exposed for 10, 20, 60 and 120 minutes to different

concentrations of cationic surfactants prepared in LB medium, at 37°C in an orbital shaker (200 rpm). At the end of incubation an aliquot of each sample was serially diluted in LB medium and spread in LB-agar plates using the drop method as described by Miles and Misra (1938). The plates were incubated at 37°C for 8-10 hours and the number of visible colonies per plate was counted and expressed as percentage of mock-treated bacteria, in order to determine the percentage of survival of culturable bacteria (Campanha *et al.*, 1999; Liu *et al.*, 2004; Andres & Fierro, 2010).

2.5.4. C_{10}TAB bactericidal activity

The bactericidal effect of C_{10}TAB was evaluated after 1 hour of exposure (as described in the previous Section), using a commercial bacterial viability kit (Live/Dead® BacLight™ Bacterial Viability kit) to directly evaluate the number of viable and total bacteria (Boulos *et al.*, 1999; Bar *et al.*, 2009). The kit comprises two different fluorescent probes: SYTO 9, a green-fluorescent dye that stains the nucleic acids of both healthy and dead bacteria, and PI, a red-fluorescent nucleic acid probe that only penetrates in bacteria with damaged membranes, causing a reduction in SYTO 9 fluorescence in double labeled cells. At the end of incubation, bacteria were centrifuged at 10 000 g for 15 minutes and resuspended in PBS. The two fluorescent dyes, SYTO 9 and PI, were mixed in a 1:1 proportion and 3 µL were added to 1mL of each sample, followed by 15 minutes incubation in the dark at room temperature. The fluorescence emission spectrum were acquired at room temperature on a SpectraMax Gemini EM spectrofluorometer, according to the manufacturer's instructions (excitation at 470 nm and emission between 490 and 700 nm). Bacterial viability was determined by the ratio between integrated green fluorescence (510-540 nm) and integrated red fluorescence (620-650 nm) for each sample. Data are expressed as percentage of control bacterial cells. For fluorescence microscopy analysis, stained bacterial suspensions were mounted in a glass slide for immediate visualization in a Carl Zeiss Laser Scanning Confocal Microscope LSM 510. Viable bacteria only displayed green fluorescent whereas dead bacteria were also red fluorescent.

2.5.5. Transmission electron microscopy

For electron microscopy, *Escherichia coli* was grown and treated with different surfactant concentrations for 1 hour, as described in Section 2.5.3. At the end of incubation, bacterial cells were washed twice with 0.1 M sodium cacodylate (pH 7.2), pre-fixed overnight with 1.25% glutaraldehyde plus 4% paraformaldehyde at 4°C, washed again with sodium cacodylate and

fixed with 2% osmium tetroxide in veronal-acetate buffer (pH 6.2) for 2 hours at room temperature. Bacterial suspensions were then washed in distilled water and post-fixed with 1% uranil acetate for 30 minutes at room temperature (Silva *et al.*, 1987). Next, samples were dehydrated in a graded series of ethanol and propylene oxide as follows: 70% ethanol for 10 minutes, 90% ethanol for 10 minutes, 100% ethanol during 30 minutes repeated four times followed by 10 minutes immersion in propylene oxide. Lastly, samples were embedded in Epon resin. Ultrathin sections were stained with uranyl acetate/lead citrate and examined in a Zeiss EM 902A transmission electron microscope (Carl Zeiss Inc., Oberkochen, Germany).

2.5.6. Statistical analysis

Results are expressed as Means ± SD. The toxicity dose-response curves were fitted with a four-parameter logistic equation (Seefeldt *et al.*, 1995; Knezevic *et al.*, 2007), as described in Section 2.3.4, through computer-assisted curve fitting (SigmaPlot® 11.0). When the dose-response curves exhibited a biphasic sigmoid shape instead of a monotonic sigmoid profile, the following equation was used to fit the experimental data:

$$y = C + \frac{(D-C)\times Frac.}{1+10^{\left(\left(\log(x)-\log(IC_{50}1)\right)\times b1\right)}} + \frac{(D-C)\times(1-Frac.)}{1+10^{\left(\left(\log(x)-\log(IC_{50}2)\right)\times b2\right)}}$$

Where C and D are the minimal (lower limit) and maximal (upper limit) responses, respectively; $IC_{50}1$ is the inhibitory concentration 50 of the first curve; $IC_{50}2$ is the inhibitory concentration 50 of the second curve; $b1$ and $b2$ are is the Hill coefficients of each equation; $Frac.$ is the fraction of the curve corresponding to the first equation; x is the drug concentration (for further details see Appendix A). From these data, it was possible to calculate the lethal dose (LD) 10, 50 and 90 concentrations for each surfactant (Campanha *et al.*, 1999; Liu *et al.*, 2004). The LD concentrations were plotted against time of exposure to the surfactants and fitted using a mono-exponential decay equation, using SigmaPlot® 11.0, as described in Section 2.3.4.

Chapter III

In vitro surfactant structure-toxicity relationship: implications for surfactant use in prophylaxis of sexually transmitted infections

The work presented in this chapter was published in:

Inácio ÂS, Mesquita KA, Baptista M, Ramalho-Santos J, Vaz WLC, and Vieira OV (2011) *In Vitro* Surfactant Structure-Toxicity Relationships: Implications for Surfactant Use in Sexually Transmitted Infection Prophylaxis and Contraception. PLoS ONE 6(5): e19850. doi:10.1371/journal.pone.0019850

Summary

***In vitro* surfactant structure-toxicity relationship:** implications for surfactant use in prophylaxis of sexually transmitted infections

3.1. Introduction

Sexually transmitted infections (STIs) are a major public-health problem worldwide. Direct treatment costs and serious perinatal collateral damage caused by STIs represent hefty financial and social burdens, particularly in developing countries (Terris-Prestholt et al., 2006). The World Health Organization estimates 340 million new cases of bacterial and protozoan STIs per year (World Health Organization, 2007), a number that does not include the millions of new STIs with fungal and viral etiology. In recent years, HIV infections in women constitute more than half of the new infections, a result of their greater biological (reviewed in Hladik & Hope, 2009) and social vulnerability (reviewed in Ackermann & de Klerk, 2002). The correct and persistent use of condoms provides a high level of protection against all STIs, but many women lack the social and/or economic power to persuade their partners to use them. Consequently, there is an urgent need for new woman-controlled prevention methods. Topical applications (e.g. vaginal gels) with microbicidal and spermicidal activity, that can be used by women without the need for consent of a male partner are one possible answer to the problem (see Stone & Jiang, 2006).

The bacteriostatic and bactericidal actions of surfactants have been recognized for many years. Surfactant-based devices for purposes of contraception have been in use for decades and the first microbicidal vaginal gels to be tested in clinical trials were surfactant-based (Nonoxynol-9 and SAVVY® (C31G) vaginal gel). However, all the surfactant-based microbicide candidates that completed Phase III clinical trials failed to prevent HIV infection (Stephenson, 2000; Fichorova *et al.*, 2001; Peterson *et al.*, 2007; Feldblum *et al.*, 2008) and their utility as general microbicides was also questionable. More recent Phase III studies, with nonspecific microbicide gels that did not include surfactants (Carraguard® and PRO2000®) also did not demonstrate efficacy (Skoler-Karpoff *et al.*, 2008; McCormack *et al.*, 2010). These disappointing results stress the urgency in understanding the detailed biological mechanisms responsible for microbicides toxicity and the necessity to develop new *in vitro* models and safety biomarkers, in order to improve the prediction of clinical outcomes in large-scale efficacy trials in the future.

The initial discouraging results of microbicide clinical trials turned the main focus of current research to the development of formulations containing specific antiretroviral drugs (reviewed in Nuttall, 2010). However, it cannot be ignored that HIV is a highly mutable virus and is known to develop resistance to antiretroviral drugs (Miller et al., 1998; Wilson et al., 2008; Perez Bercoff et al., 2010). Although at present, and from the perspective of richer societies, prophylaxis against HIV infection steals the limelight, the targeting of STIs with bacterial and protozoan etiologies are of major importance because the inflammation caused by these infections not only has a direct impact on human health but also facilitates and increases HIV transmission (reviewed in Fleming & Wasserheit, 1999; Mayaud & McCormick, 2001; Galvin & Cohen, 2004).

Previous *in vitro* studies showed that cationic surfactants may work as bactericides at concentrations that are not harmful to polarized mammalian epithelial cells (Vieira et al., 2008). Thus, despite the negative results of the clinical trials referred above, a step-by-step, systematic investigation of the toxicity of different types of surfactants towards mammalian cells (particularly polarized epithelial cells and other cell types encountered in the vaginal mucosa) seems to be warranted. With this objective in mind the effects of concentration, exposure time and surfactant structure on the *in vitro* viability of mammalian cells that model the most vulnerable cell types that exist in the human cervicovaginal mucosa, namely, fully polarized columnar epithelial cells (MDCK II and Caco-2), human cervical non-polarized epithelial cells (HeLa) and dendritic cells (FSDC) were evaluated. Representatives of all families of commercially available surfactants were tested: nonionic – Triton X-100 (TX-100) and rac-1-lauroylglycerol (Monolaurin); zwitterionic – N-dodecyl-N,N-dimethylammonium-propanesulfonate (DDPS); anionic – sodium dodecyl sulfate (SDS); and cationic – a homologous series of *n*-alkyl-N,N,N-trimethylammonium bromides (C_nTAB with *n* from 10 through 16), N-dodecylpyridinium bromide (C_{12}PB), and dodecyl-N-benzyl-N,N-dimethylammonium (better known as Benzalkonium) bromide (C_{12}BZK). All these surfactants are commercially available and were chosen because their action as microbicides is well documented in the literature. As previously described (Vieira et al., 2008), the surfactant effects were compared taking into account their respective critical micelle concentrations (CMC).

3.2. Results

3.2.1. Surfactant critical micelle concentrations

The formation of surfactant micelles in aqueous media may be considered, under certain conditions, to be similar to a phase separation between an aqueous solution of surfactant monomers and a micellar phase. The surfactant concentration at which this phase separation

occurs is the CMC. Within a given homologous series of surfactants the CMC is linearly proportional to the free energy of partitioning of the apolar part of the surfactant between an apolar environment, such as a micelle or the lipid bilayer of a cell membrane, and the aqueous phase (Tanford, 1991). Surfactant, at all concentrations, partitions into the membrane and at concentrations below the surfactant CMC an equilibrium is established between surfactant monomers in the aqueous phase and surfactant in the membrane. At concentrations above the surfactant CMC, surfactant micelles co-exist with the surfactant-containing membranes and phospholipids are transferred from the membrane to the micelles. At a high enough concentration of micelles the equilibrium state is a solution of mixed surfactant/phospholipids micelles and the membrane is dissolved. However, long before membrane dissolution occurs, non-ideal miscibility of surfactant and phospholipids in membranes may lead to perturbation of the properties (lateral packing and pressure, permeability, etc.) of the membrane. These perturbations will affect physiologically important processes that occur at the membrane level (reviewed in Balgavy & Devinsky, 1996; Heerklotz, 2008). Thus, since CMC may be considered to be an approximate measure of the partition coefficient of the surfactant between the aqueous and apolar (membrane/micellar) phases, it is important to use the CMC as a reference concentration when comparing the toxic effects of any surfactant homologous series. In the present study the stock solutions of surfactants used to treat the cells were prepared as fractions (or multiples) of their CMC in Opti-MEM serum-free cell culture media. Since the CMC can be dependent on the ionic strength and pH, the CMC of each surfactant was measured under the same experimental conditions and the results are listed in Table 3.1.

Table 3.1. Critical Micelle Concentrations (CMC) of the surfactants used calculated in a saline buffer (1.8 mM $CaCl_2$, 0.8 mM $MgSO_4$, 5.3 mM KCl, 26.2 mM $NaHCO_3$, 117.2 mM NaCl and 1.0 mM $NaH_2PO_4.H_2O$, pH 7.3).

Surfactant		**CMC** (M)		
Family	**Name**	**Experimental**	**Literature**	**Reference**
Non-ionic	TX-100	$(2.0 \pm 0.1) \times 10^{-4}$	2.0×10^{-4}	(Brito & Vaz, 1986)
	Monolaurin	$(4.2 \pm 0.5) \times 10^{-5}$	4.4×10^{-5}	(Piao *et al.*, 2006)
Zwiterionic	DDPS	$(2.0 \pm 0.1) \times 10^{-3}$	2.0×10^{-3}	(Brito & Vaz, 1986)
Anionic	SDS	$(2.6 \pm 0.3) \times 10^{-4}$	2.6×10^{-3}	(Brito & Vaz, 1986)
Cationic	C_{10}TAB	$(4.0 \pm 0.1) \times 10^{-2}$	4.0×10^{-2}	(Brito & Vaz, 1986)
	C_{12}TAB	$(3.5 \pm 0.3) \times 10^{-3}$	3.5×10^{-3}	(Brito & Vaz, 1986)
	C_{14}TAB	$(2.9 \pm 0.1) \times 10^{-4}$	2.8×10^{-4}	(Brito & Vaz, 1986)
	C_{16}TAB	$(2.6 \pm 0.2) \times 10^{-5}$	2.6×10^{-5}	(Brito & Vaz, 1986)
	C_{12}PB	$(3.9 \pm 0.1) \times 10^{-3}$	1.0×10^{-2}	(Skerjanc *et al.*, 1999)
	C_{12}PC	$(4.7 \pm 0.2) \times 10^{-3}$	5.0×10^{-3}	(Simoncic & Span, 1998)
	C_{12}BZK	$(1.7 \pm 0.9) \times 10^{-3}$	5.0×10^{-3}	(Kopecky, 1996)

Data are shown as Mean ± SD of at least 3 independent experiments.

Note: The literature values cited are not for the saline buffer in which the present results were obtained but for an aqueous phase with ionic strength most closely resembling the buffer solution here used. The literature value reported for C_{12}PC was measured in water.

3.2.2. Effect of surfactant type, concentration and exposure time on the viability of polarized columnar epithelial cells

The primary target for bacterial and viral sexually transmitted infections, in women, is the non-keratinized squamous epithelium of the vagina and ectocervix, as well as the single-layer columnar epithelium of the endocervix. It has been shown that the vaginal columnar epithelium is the primary site of damage in the use of surfactants (Fichorova *et al.*, 2001; Catalone *et al.*, 2005). Therefore, the effect of four classes of commercially available surfactants towards the viability of MDCK II and Caco-2 columnar epithelial cell lines was tested. These two cell lines, although not of vaginal origin, are derived from mammalian columnar epithelia and can be grown to a completely confluent and polarized state, with relatively non-leaky tight junctions, closely resembling the characteristics of the vaginal columnar epithelium. There is a vast literature on the nature and properties of these polarized epithelial cell lines in culture and they have been widely used in similar conditions as reported here (Irvine *et al.*, 1999; Velarde *et al.*, 1999; Ekelund *et al.*, 2005; Vieira *et al.*, 2008).

MDCK II and Caco-2 cells were exposed to different concentrations of surfactants during 20, 60, 180 and 540 minutes. The surfactants studied were: the nonionic TX-100 and Monolaurin, the zwitterionic DDPS, the anionic SDS and the cationic C_{10}TAB. Cell toxicity was measured by the MTT assay 24 hours post-exposure to surfactants. The MTT assay is one of the most used cytotoxicity assays and is based on the reduction of the yellow tetrazolium salt, 3-(4,5-dimethylthiazole-2-y)-2,5-diphenyltetrasodiumbromide (MTT) to purple formazan crystals by mitochondrial and/or cytoplasmic dehydrogenases. Cell viability is expressed as percentage of the viability of mock-treated control cells. A four parameter logistic equation (Seefeldt *et al.*, 1995; Knezevic *et al.*, 2007) was fitted to the data of each independent experiment and the lethal dose 90 (LD_{90}), lethal dose 50 (LD_{50}) and lethal dose 10 (LD_{10}), surfactant concentrations at which cell viability was, respectively, 10%, 50% and 90% of the control were determined for each exposure time (the LD_{10}, LD_{50} and LD_{90} values for all the surfactants and all cells types reported on in this chapter are listed in more detail in the Appendix A, Tables A.1-A.4). The LD *vs.* exposure-time curves for each surfactant tested could be fitted using a mono-exponential decay equation (Fig. 3.1) and the decay constants obtained for the LD_{90}, LD_{50} and LD_{10} curves were similar (Table 3.2), which indicates that the mechanism(s) that cause(s) the death of 10% of the cells is the same as that responsible for killing 50 and 90% of the cells. All surfactants used in this study revealed concentration and time-dependent toxic effects. The results also showed that surfactants exhibited different degrees of toxicity depending on the nature of the polar head. For TX-100, DDPS and SDS, cytotoxicity was not observed up to concentrations close to the CMC (Fig. 3.1A-F), whereas the toxicity of C_{10}TAB was evident at concentrations much lower than its

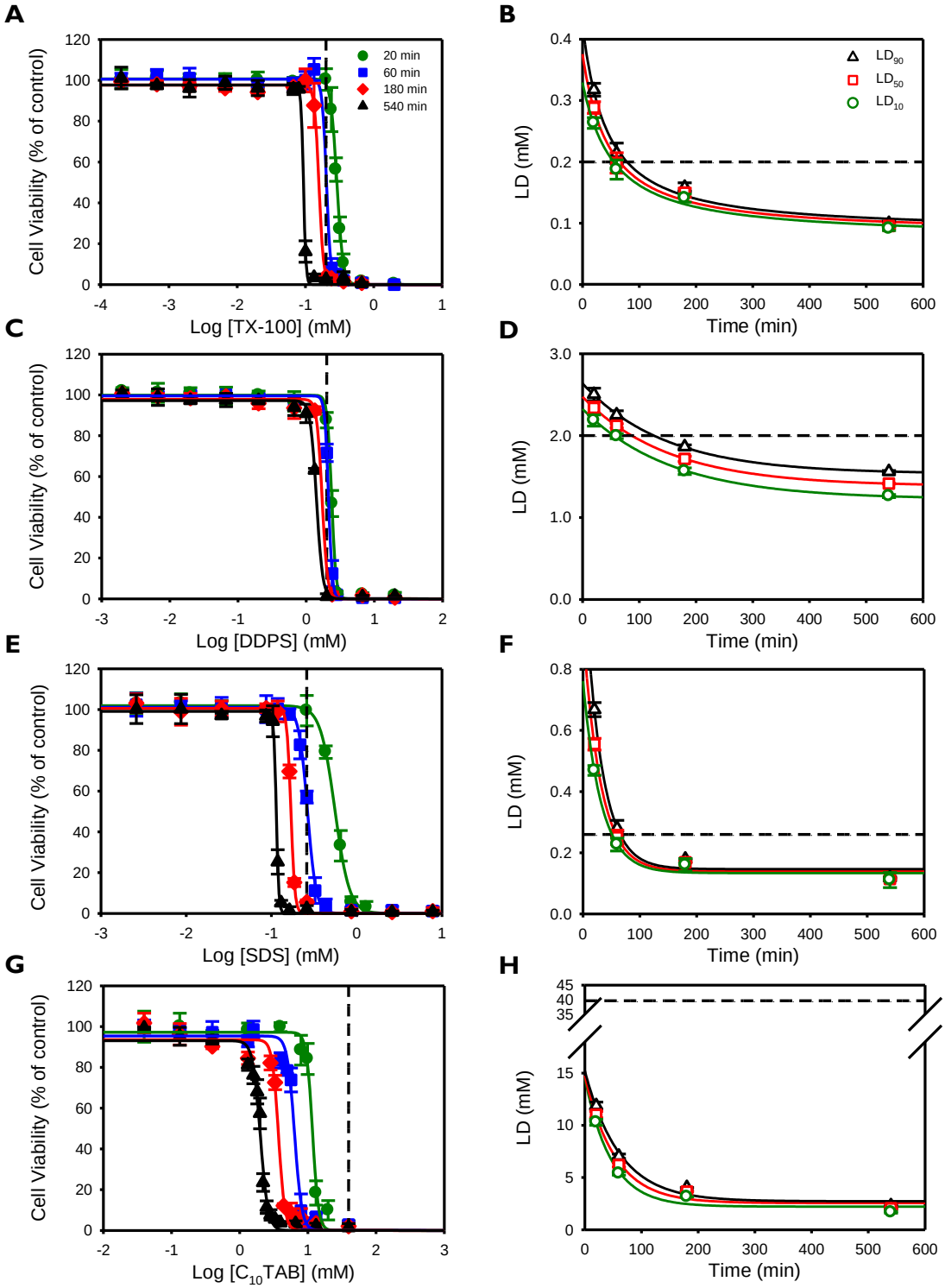

Figure 3.1. Effect of different surfactant classes on polarized and confluent MDCK II cells viability. Four surfactant classes were evaluated: nonionic TX-100 (**A**, **B**), zwitterionic DDPS (**C**, **D**), anionic SDS (**E**, **F**) and cationic C_{10}TAB (**G**, **H**). Cell viability was assessed by the MTT assay 24 hours after the cells had been exposed to different concentrations of surfactants for 20 (green closed circles), 60 (blue closed squares), 180 (red closed diamonds) and 540 (black closed triangles) minutes (left panels). Cell viability is expressed as percentage of the viability of control cells. The data of each independent experiment was fitted with a four parameter logistic equation and the LD_{10} (green open circles), LD_{50} (red open squares) and LD_{90} (black open triangles) concentrations determined for each time point (right panels). A mono-exponential decay equation was fitted to the LD *vs.* exposure-time curves and for each surfactant tested the decay constants calculated for the LD_{90}, LD_{50} and LD_{10} curves were similar. The CMC of each surfactant is represented by the black dashed line. Data are presented as Mean ± SD of at least 3 independent experiments, each one done in triplicate.

Table 3.2. Decay constants (min^{-1}) calculated for the exposure-time-dependence of the LD_{90}, LD_{50} and LD_{10} concentrations.

Surfactant		Decay constant (min^{-1})				
Family	**Name**		**MDCK II**	**Caco-2**	**HeLa**	**FSDC**
Non-ionic	TX-100	LD_{90}	$(1.37 \pm 0.85) \times 10^{-2}$	$(4.33 \pm 0.80) \times 10^{-2}$	$(2.07 \pm 0.76) \times 10^{-2}$	$(10.0 \pm 1.00) \times 10^{-3}$
		LD_{50}	$(1.25 \pm 0.82) \times 10^{-2}$	$(3.87 \pm 0.78) \times 10^{-2}$	$(2.07 \pm 0.67) \times 10^{-2}$	$(8.67 \pm 0.58) \times 10^{-3}$
		LD_{10}	$(1.15 \pm 0.74) \times 10^{-2}$	$(3.70 \pm 1.01) \times 10^{-2}$	$(2.00 \pm 1.01) \times 10^{-2}$	$(8.00 \pm 1.00) \times 10^{-3}$
Zwiterionic	DDPS	LD_{90}	$(7.33 \pm 0.58) \times 10^{-3}$	$(7.18 \pm 5.88) \times 10^{-3}$	$(8.33 \pm 2.52) \times 10^{-3}$	$(7.00 \pm 2.83) \times 10^{-3}$
		LD_{50}	$(7.00 \pm 1.00) \times 10^{-3}$	$(6.91 \pm 3.59) \times 10^{-3}$	$(9.00 \pm 4.36) \times 10^{-3}$	$(5.06 \pm 3.35) \times 10^{-3}$
		LD_{10}	$(7.00 \pm 1.00) \times 10^{-3}$	$(7.99 \pm 1.88) \times 10^{-3}$	$(9.33 \pm 4.93) \times 10^{-3}$	$(5.00 \pm 1.00) \times 10^{-3}$
Anionic	SDS	LD_{90}	$(3.40 \pm 0.62) \times 10^{-2}$	$(1.57 \pm 0.15) \times 10^{-2}$	$(1.87 \pm 0.32) \times 10^{-2}$	$(8.00 \pm 2.00) \times 10^{-3}$
		LD_{50}	$(3.28 \pm 0.69) \times 10^{-2}$	$(2.03 \pm 0.40) \times 10^{-2}$	$(1.73 \pm 0.59) \times 10^{-2}$	$(8.67 \pm 3.79) \times 10^{-3}$
		LD_{10}	$(3.22 \pm 0.79) \times 10^{-2}$	$(2.50 \pm 0.46) \times 10^{-2}$	$(1.77 \pm 0.93) \times 10^{-2}$	$(9.33 \pm 2.31) \times 10^{-3}$
Cationic	$C_{10}TAB$	LD_{90}	$(1.70 \pm 0.30) \times 10^{-2}$	$(2.10 \pm 0.89) \times 10^{-2}$	$(9.33 \pm 0.58) \times 10^{-3}$	$(1.20 \pm 0.27) \times 10^{-2}$
		LD_{50}	$(1.97 \pm 0.25) \times 10^{-2}$	$(2.40 \pm 0.36) \times 10^{-2}$	$(8.67 \pm 1.53) \times 10^{-3}$	$(1.53 \pm 0.32) \times 10^{-2}$
		LD_{10}	$(2.23 \pm 0.31) \times 10^{-2}$	$(2.60 \pm 0.44) \times 10^{-2}$	$(7.67 \pm 1.15) \times 10^{-3}$	$(1.90 \pm 0.79) \times 10^{-2}$

Data are shown as Mean ± SD of at least 3 independent experiments.

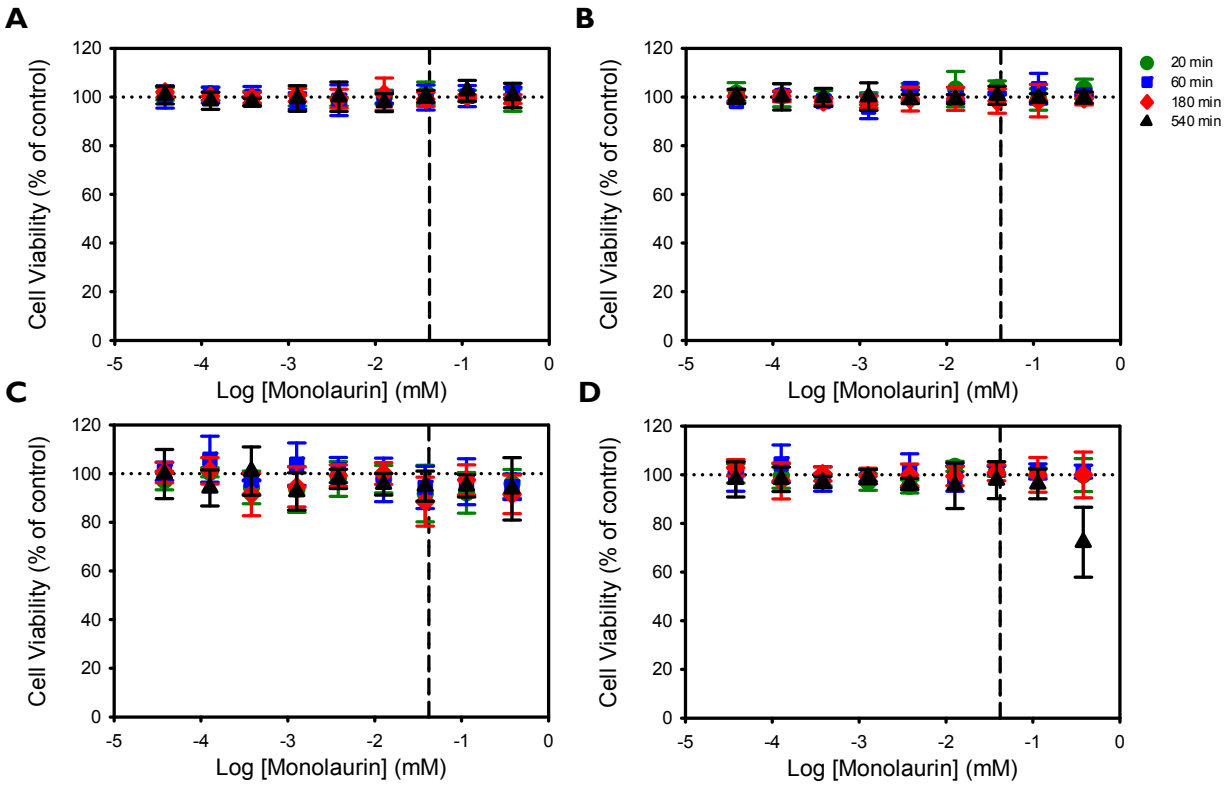

Figure 3.2. Effect of Monolaurin upon cell viability. MDCK II (**A**), Caco-2 (**B**), HeLa (**C**) and FSDC (**D**) cells were exposed to different concentrations of Monolaurin for 20 (green closed circles), 60 (blue closed squares), 180 (red closed diamonds) and 540 (black closed triangles) minutes. Cell viability was assessed by the MTT assay 24 hours after the cells had been exposed to the surfactant and cell viability is expressed as percentage of the viability of control cells. The CMC of Monolaurin is represented by the black dashed line. Data are presented as Mean ± SD of at least 3 independent experiments, each one done in triplicate.

CMC (Fig. 3.1G and H), being the LD_{50} for both MDCK II and Caco-2 cells 0.05 times CMC after 540 minutes exposure. However, despite the higher toxicity of C_{10}TAB when compared to the other surfactants tested, previous results from our laboratory showed that cationic surfactants are even more toxic to bacterial infectious agents than they are to columnar epithelial cells (Vieira *et al.*, 2008) and thus should be considered for development as bactericidal agents in the prophylaxis of STIs that have a bacterial etiology. On the contrary, despite their low toxicity, TX-100, DDPS and SDS were shown to have neither bactericidal nor spermicidal activity at concentrations that were not harmful to epithelial cells (Vieira *et al.*, 2008). The toxicity of the nonionic surfactant Monolaurin was also tested, since there are several studies that demonstrated its bactericidal efficacy (Ved *et al.*, 1990; Carpo *et al.*, 2007; Lin *et al.*, 2009). Up to a concentration of 10 times CMC Monolaurin was neither toxic to MDCK II nor to Caco-2 cells (Fig. 3.2A and B), which may justify more detailed studies of this surfactant in the future.

3.2.3. Surfactant toxicity towards human epithelial-like HeLa cells

The toxic effects of surfactants were also tested in confluent HeLa cell cultures as described for polarized epithelial cells. This cell line was chosen since it is a human cervical cell line. Despite the fact that these cells have epithelial origin, they are usually referred to as epithelial-like cells because they do not completely polarize and do not establish tight junctions between them. As observed with polarized columnar epithelial cells, the decay constants calculated for the exposure-time dependence of LD_{90}, LD_{50} and LD_{10} were similar for all the surfactants tested (Table 3.2). Moreover, the results show a similar trend as described for epithelial polarized cells, in which surfactant toxicity was dependent on the nature of the polar head. As in the case of polarized epithelial cells, TX-100, DDPS and SDS induced cell toxicity at concentrations close to CMC (Fig. 3.3). Although for short exposure times (20 and 60 minutes) these surfactants were more toxic to HeLa than to polarized epithelial cells, at longer exposure times the toxic concentrations are similar for all cell types. The effect of the nonionic Monolaurin was once again tested and, as described above for polarized epithelial cells, it did not induce cell toxicity at concentrations up to 10 times CMC (Fig. 3.2C). In the case of the cationic C_{10}TAB the difference in cell toxicity between polarized and non-polarized cells, as seen by the LD_{50}, was quite pronounced and persisted for longer exposure times (Fig. 3.1 and 3.3). The LD_{50} of C_{10}TAB after 540 minutes of incubation was 0.006 times CMC, corresponding to 10 times less than for MDCK II and Caco-2 cells. Surfactant toxicity is dependent on the ability to partition between the aqueous phase and the cell membrane and may also depend on its capacity to subsequently cross the membrane and enter the cytoplasm. The fact that amphiphile partition coefficients as well as

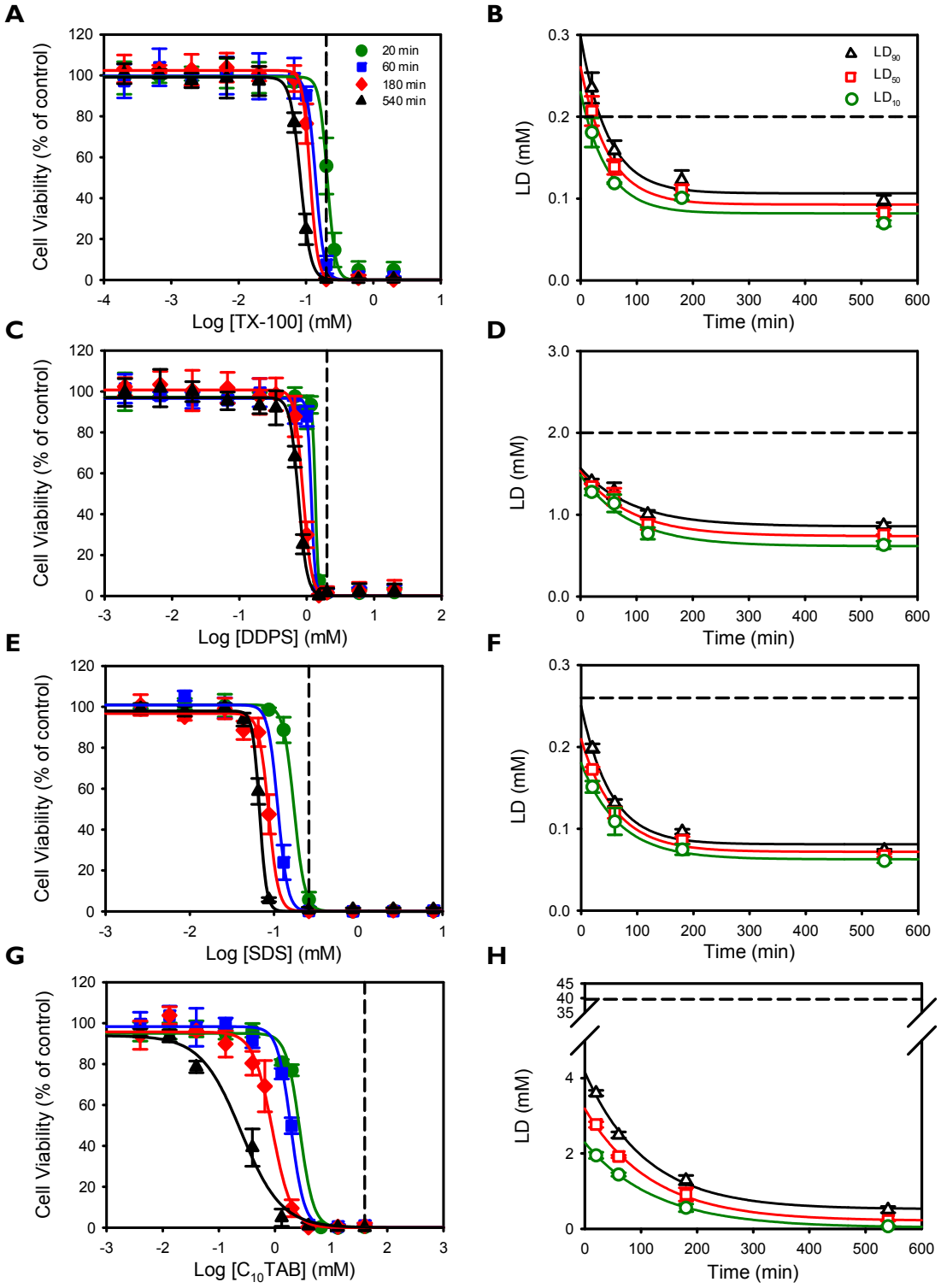

Figure 3.3. Effect of different surfactant classes on confluent HeLa cells viability. All data is as detailed in Figure 3.1.

the rate constants for surfactant insertion into and translocation across membranes are lower for more ordered membranes (Abreu *et al.*, 2004; Sampaio *et al.*, 2005; Moreno *et al.*, 2006; Estronca *et al.*, 2007; Apel-Paz *et al.*, 2008) explains why HeLa cells, which lack tight junctions and therefore the separation between apical (more ordered) and basolateral (less ordered) membrane domains, may be more susceptible to surfactant toxicity than fully polarized and confluent epithelial cells such as MDCK II and Caco-2 cell lines. Moreover, the apical membrane of polarized cells is more ordered than in HeLa cells and their total surface area is 8 times higher, due to the extensive microvillation of their apical membrane domain (Butor & Davoust, 1992).

3.2.4. Effect of surfactants on the viability of mammalian dendritic cells

The human cervicovaginal mucosa contains the full spectrum of cell types and immune modulators that comprise both the innate and adaptive immune system, which are necessary for an effective response against viral and bacterial infections. Among these, dendritic cells are of particular interest given their ability to sense and process pathogens and to present viral antigens, including HIV, to T cells (Masurier *et al.*, 1998; Hladik *et al.*, 2007; Liu *et al.*, 2009). An ideal microbicide should not induce mucosal inflammation nor interfere with the innate immune responses. Because of that, the toxic effect of surfactants towards a dendritic cell line (FSDC) was tested. Although FSDC cells were treated in the same way as described above for MDCK II, Caco-2 and HeLa cells, at the time of the exposure to the surfactants the cells were only 70-80% confluent. The results obtained (Fig. 3.4) were similar to the results for HeLa cells. However, FSDC were more sensitive to the effect of the nonionic TX-100 and Monolaurin surfactants. In these cells a monolaurin concentration of 10 times CMC reduced cell viability by almost 30% after 540 minutes exposure (Fig. 3.2D).

Rescigno and colleagues (2001) have demonstrated that dendritic cells can open the tight junctions between epithelial cells, send dendrites outside the epithelium and directly sample bacteria without leaving the *lamina propria*. Being so, it is possible that *in vivo* these cells are less exposed to the surfactants than in our *in vitro* model and the *in vivo* toxic effects may be lower than reported here.

3.2.5. Effect of cationic surfactant structure upon the viability of different types of mammalian cells

Despite the fact that clinical trials using surfactant-based gels have failed, it has been shown that several quaternary ammonium compounds, with various alkyl chain lengths and polar head groups, exert antibacterial activity against both Gram positive and Gram negative bacteria, as well

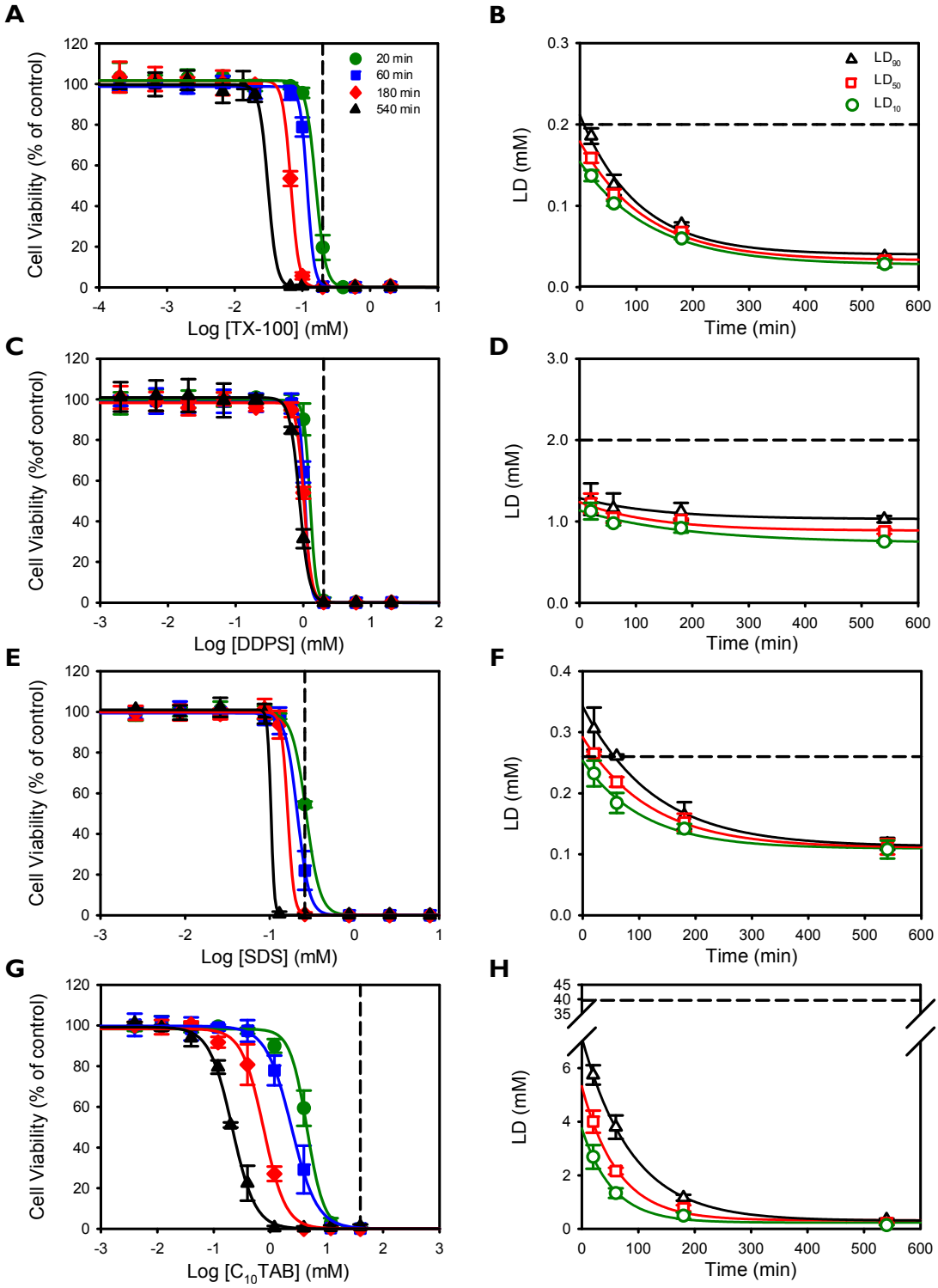

Figure 3.4. Effect of different surfactant classes on FSDC dendritic cells viability. All data is as detailed in Figure 3.1.

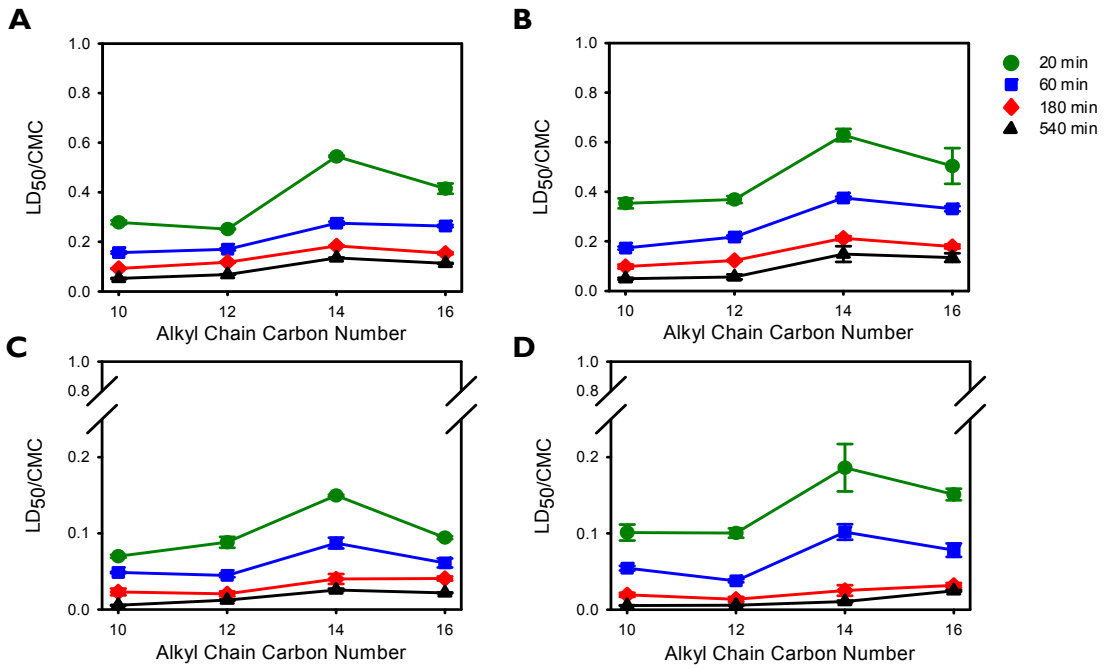

Figure 3.5. Effect of C_nTAB surfactants hydrophobic chain length upon cell viability. The graphs show the LD_{50} concentration of the surfactants $C_{10\text{-}16}$TAB for the polarized epithelial cells, MDCK II (**A**) and Caco-2 (**B**), epithelial-like HeLa cells (**C**) and FSDC dendritic cells (**D**) after exposure times of 20 (green closed circles), 60 (blue closed squares), 180 (red closed diamonds) and 540 (black closed triangles) minutes. LD_{50} concentrations of each surfactant are normalized with respect to the CMC. Data are presented as Mean ± SD of at least 3 independent experiments, each of which was done in triplicate.

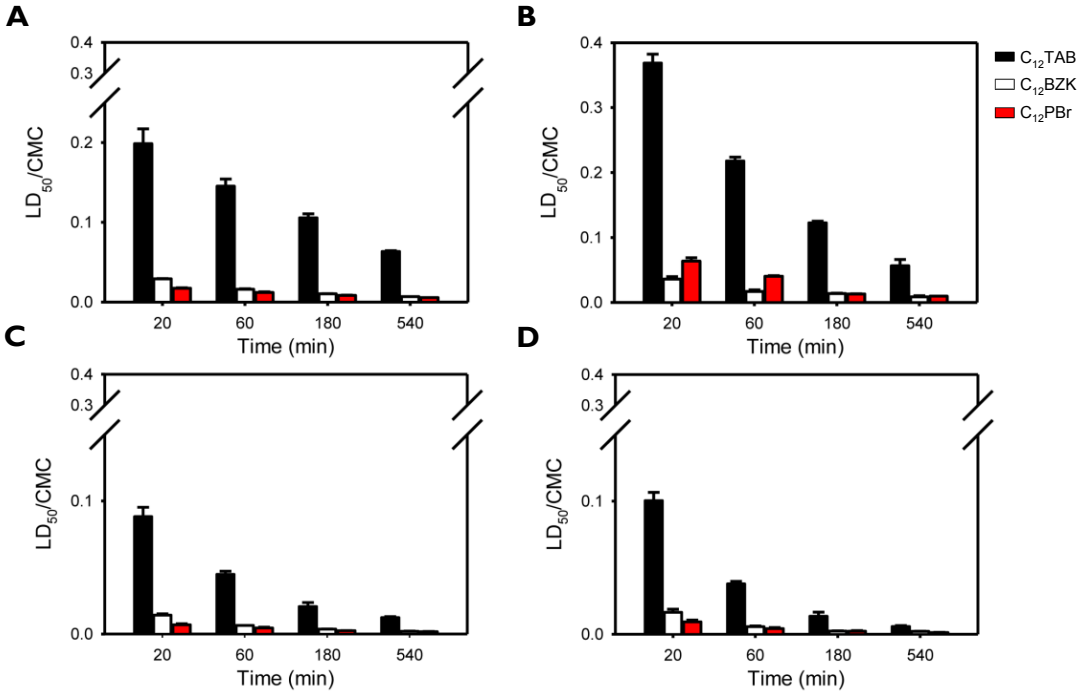

Figure 3.6. Effect of the polar head structure of cationic surfactants in cell viability. The LD_{50} concentration of the three cationic surfactants with similar hydrophobic chain length, but different polar head groups, was evaluated in polarized epithelial cells, MDCK II (**A**) and Caco-2 (**B**), epithelial-like HeLa cells (**C**) and FSDC dendritic cells (**D**). The surfactants tested were C_{12}TAB (black bars), C_{12}BZK (white bars) and C_{12}PB (red bars). LD_{50} concentrations of each surfactant are normalized with respect to the CMC. Data are presented as Mean ± SD of at least 3 independent experiments, each of which was done in triplicate.

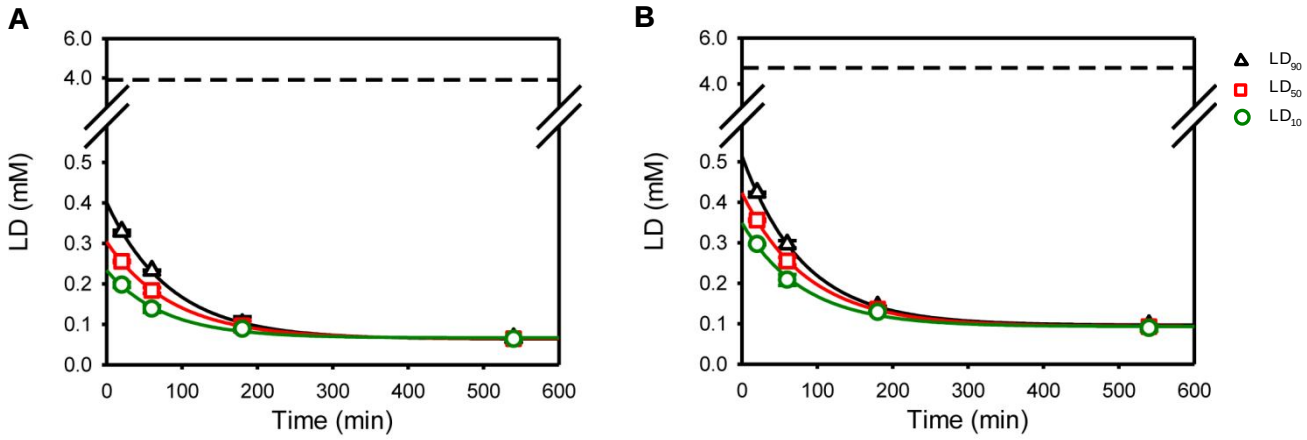

C

Surfactant		Lethal Dose/CMC after exposure time of			
		20 min	60 min	180 min	540 min
C_{12}PB	LD_{90}	(8.43 ± 0.09) X 10^{-2}	(5.96 ± 0.03) X 10^{-2}	(2.58 ± 0.47) X 10^{-2}	(1.68 ± 0.01) X 10^{-2}
	LD_{50}	(6.54 ± 0.09) X 10^{-2}	(4.67 ± 0.16) X 10^{-2}	(2.46 ± 0.31) X 10^{-2}	(1.65 ± 0.01) X 10^{-2}
	LD_{10}	(5.06 ± 0.16) X 10^{-2}	(3.53 ± 0.21) X 10^{-2}	(2.27 ± 0.08) X 10^{-2}	(1.62 ± 0.02) X 10^{-2}
C_{12}PC	LD_{90}	(8.64 ± 0.03) X 10^{-2}	(6.03 ± 0.18) X 10^{-2}	(2.91 ± 0.01) X 10^{-2}	(1.97 ± 0.02) X 10^{-2}
	LD_{50}	(7.25 ± 0.05) X 10^{-2}	(5.17 ± 0.16) X 10^{-2}	(2.78 ± 0.02) X 10^{-2}	(1.89 ± 0.10) X 10^{-2}
	LD_{10}	(6.04 ± 0.03) X 10^{-2}	(4.24 ± 0.27) X 10^{-2}	(2.62 ± 0.01) X 10^{-2}	(1.82 ± 0.15) X 10^{-2}

Figure 3.7. Effect of the counter-ion of cationic surfactants on polarized and confluent MDCK II cells viability. Since chloride ion is usually less toxic than bromide ions, the toxicity of C_{12}PB (**A**) and C_{12}PC (**B**) was evaluated. Cell viability was assessed by the MTT assay 24 hours after the cells had been exposed to different concentrations of surfactants for 20, 60, 180 and 540 minutes. The data of each independent experiment was fitted using a four parameter logistic equation and the LD_{10} (green open circles), LD_{50} (red open squares) and LD_{90} (black open triangles) concentrations determined for each time point (**A**, **B**). The CMC of each surfactant is represented by the black dashed line. For comparison purposes lethal doses are presented normalized with respect to the CMC (**C**). The CMC of the detergents used are: C_{12}PB, 3.9 X 10^{-3} M and C_{12}PC, 4.7 X 10^{-3} M. Data are presented as Mean ± SD of at least 3 independent experiments, each one done in triplicate.

as against some pathogenic species of fungi and protozoa, at concentrations that are not harmful to mammalian epithelial cells (Vieira & Carmona-Ribeiro, 2006; Vieira *et al.*, 2008).

The study of the relation between cationic surfactant structure and its toxic effects is crucial to understand the mechanisms involved in surfactant toxicity and make predictions of the impact that new surfactants will have in cell viability. To this end the effects of the hydrocarbon chain length and polar head group structure of the cationic surfactants upon cell viability were evaluated. To do so, the cells were treated with surfactants of a homologous series of cationic alkyl-N,N,N-trimethylammonium bromides ($C_{10\text{-}16}$TAB), C_{12}PB and C_{12}BZK.

The results in Figure 3.5 show that for the homologous series of cationic surfactants examined, the toxicity to mammalian cells was not linearly dependent upon the surfactant hydrophobic chain length. The toxicity ranking of the surfactants studied towards MDCK II, Caco-2 and HeLa cells, normalized with respect to CMC, was C_{10}TAB≥C_{12}TAB>C_{16}TAB>C_{14}TAB (see, e.g., Fig. 3.5). In the case of FSDC cells the ranking was similar for 20 and 60 minutes but for

longer exposures times C_{14}TAB was slightly more toxic than C_{16}TAB. The effect of the polar head group of the cationic surfactants was also evaluated by comparing the effects of three surfactants with a 12 carbon *n*-alkyl chain: C_{12}BZK and C_{12}PB are between 2 to 5 times more toxic (using the CMC-normalized concentration scale) than C_{12}TAB in all cell lines tested (Fig. 3.6). The reason for this difference is unclear but could be related to the larger polar head groups (C_{12}BZK and C_{12}PB) or to the more delocalized positive charge (C_{12}PB) and may merit further investigation.

All the cationic surfactants tested had bromide as a counter-ion. Since the bromide ion itself is known to be cytotoxic and the chloride ion is less so, the toxicity of C_{12}PB and C_{12}-pyridium chloride (C_{12}PC) to MDCK II cells was evaluated *in vitro*. As previously reported for C_nTAB compounds and their chloride analogues (Vieira *et al.*, 2008), no main differences were found between the two surfactants (Fig. 3.7). It is probable that at the concentrations used in this work the anion toxicity is not a relevant parameter.

3.2.6. Comparison of the MTT and the LDH leakage assays

In order to confirm the toxicity results obtained by the MTT assay, the activity of the cytoplasmic enzyme lactate dehydrogenase (LDH) was measured in the extracellular medium, an assay that evaluates plasma membrane integrity. HeLa cells were exposed for 540 minutes to C_nTAB surfactants, as described for the MTT assay. After that, the incubation medium was collected and replaced by fresh surfactant-free medium and the cells were kept in culture a further 24 hours. At the end of the experiment the culture medium was collected and the cells were lysed. The LDH activity of the incubation medium, cell culture medium and cell lysates was determined and expressed as percentage of the total activity for each condition. The cell viability results obtained with the MTT assay (Fig. 3.3) correlated well with the observed release of LDH from the cells (Fig. 3.8). However, in the case of C_{10}TAB and C_{12}TAB, the LD_{50} values obtained with the LDH leakage assay were significantly higher than with the MTT assay (Fig. 3.8E).

From the LDH results one can also observe that surfactant concentrations close to the critical micelle concentration cause acute toxicity while lower concentrations can lead to a persistent post-exposure toxicity (Fig. 3.9). This is stressed by the increase in LDH activity in the cell culture medium after surfactant removal (red bars, CMC/100 to CMC/30). Since in the majority of published papers concerning cell toxicity the tests were performed immediately after surfactant treatment, the toxic concentrations in those reports are probably underestimated.

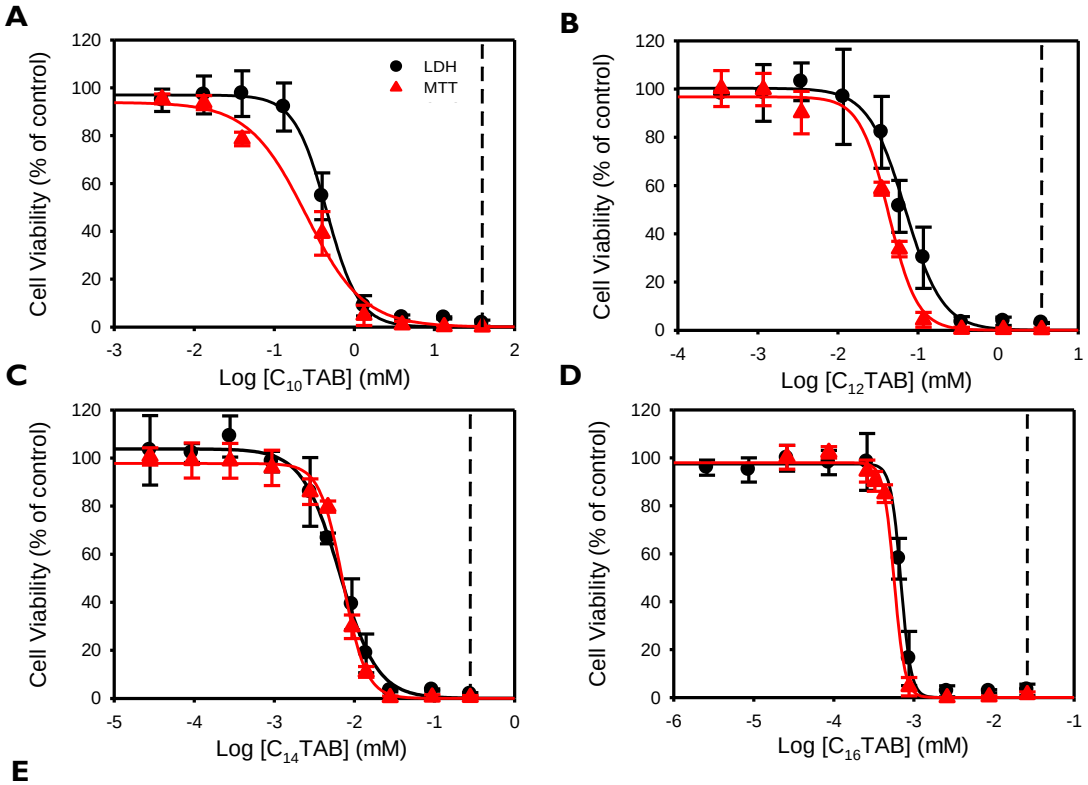

E

Surfactant		Lethal Dose (M) as determined by	
		MTT assay	LDH assay
C_{10}TAB	LD_{90}	(5.57 ± 0.13) X 10^{-4}	(6.37 ± 0.04) X 10^{-4}
	LD_{50}	(2.14 ± 0.14) X 10^{-4}	(4.26 ± 0.62) X 10^{-4} ***
	LD_{10}	(0.67 ± 0.21) X 10^{-4}	(2.59 ± 0.90) X 10^{-4} **
C_{12}TAB	LD_{90}	(6.34 ± 0.40) X 10^{-5}	(12.2 ± 2.87) X 10^{-5} **
	LD_{50}	(4.24 ± 0.17) X 10^{-5}	(8.19 ± 1.69) X 10^{-5} *
	LD_{10}	(2.33 ± 0.91) X 10^{-5}	(4.95 ± 1.99) X 10^{-5}
C_{14}TAB	LD_{90}	(0.98 ± 0.07) X 10^{-5}	(1.12 ± 0.21) X 10^{-5}
	LD_{50}	(7.13 ± 0.37) X 10^{-6}	(6.71 ± 1.22) X 10^{-6}
	LD_{10}	(4.92 ± 0.39) X 10^{-6}	(3.80 ± 1.41) X 10^{-6}
C_{16}TAB	LD_{90}	(6.53 ± 0.23) X 10^{-7}	(8.26 ± 1.44) X 10^{-7}
	LD_{50}	(5.65 ± 0.13) X 10^{-7}	(6.29 ± 1.01) X 10^{-7}
	LD_{10}	(4.84 ± 0.14) X 10^{-7}	(4.37 ± 1.70) X 10^{-7}

Figure 3.8. Comparison of LDH leakage assay and MTT assay in HeLa cells. The cells were exposed to C_{10}TAB (**A**), C_{12}TAB (**B**), C_{14}TAB (**C**) and C_{16}TAB (**D**) for 540 minutes. Cell viability was assessed by the MTT assay (red closed triangles) or LDH assay (black closed circles) 24 hours after the cells had been exposed to different concentrations of surfactants and cell viability is expressed as percentage of the viability of control cells or as percentage of the LDH intracellular activity of control, respectively. The CMC of each surfactant is represented by the black dashed line. The data of each independent experiment was fitted using a four parameter logistic equation and the LD_{10}, LD_{50} and LD_{90} concentrations were determined for each time point (**E**). Data are presented as Mean ± SD of at least 3 independent experiments, each one done in triplicate. Two-way ANOVA (Bonferroni's post-test): * $p < 0.05$, ** $p < 0.01$ and *** $p < 0.001$, significantly different from MTT results.

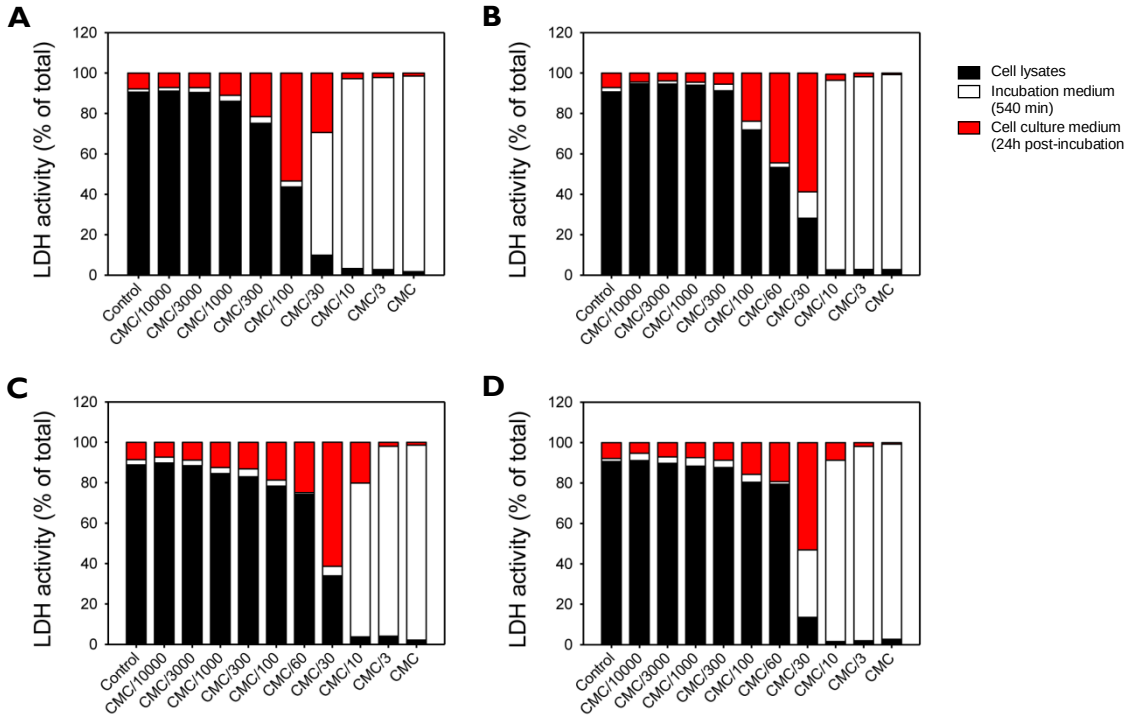

Figure 3.9. C_nTAB surfactants toxicity towards HeLa cells as evaluated by the LDH Leakage Assay. HeLa cells were exposed to different concentrations of C_{10}TAB (**A**), C_{12}TAB (**B**), C_{14}TAB (**C**) and C_{16}TAB (**D**) for 540 minutes. Afterwards, the incubation media was collected and replaced by fresh media and the cells were kept for more 24 hours. At the end of the experiment the culture media was collected and the cells were lysed. The LDH activity of the incubation media (white bars), cell culture media (red bars) and cell lysates (black bars) was determined and expressed as percentage of the total activity for each condition. Data are presented as Mean of at least 3 independent experiments, each of which was done in triplicate.

3.3. Discussion

There is an urgent need for cheap, safe, easy-to-use and easy-to-store woman-controlled topical vaginal microbicides that could be used by people in poor regions all over the world. Surfactants, if safe and effective, would be ideal candidates since they satisfy most of the remaining stipulated criteria (e.g. affordable, stable, easiness of storage, etc). The first criterion to be considered in the evaluation of the safety of topical vaginal microbicides is their toxicity to the cervicovaginal mucosa. On ethical grounds any such evaluation should begin with an *in vitro* screening before using animal models and human studies.

In the present study, a screening of the *in vitro* effects of concentration, exposure-time and surfactant structure on the viability of mammalian cells with characteristics mimicking the different cell types that exist in the human cervicovaginal mucosa was performed. Earlier studies identified vaginal columnar epithelial cells as the most critical site of damage caused by the surfactants Nonoxynol-9 (Fichorova *et al.*, 2001; Mesquita *et al.*, 2009) and C31G (Catalone *et al.*, 2005) in

humans. The present work was thus performed on two experimental models of mammalian columnar epithelial cells, namely, fully polarized MDCK II and Caco-2 cells grown to confluence. These cell cultures have well-formed tight junctions and are commonly used as models of "tight epithelia" in laboratory trans-epithelial drug transport studies. Non-polarized cells, in particular dendritic cells, have previously been identified as the primary sites of viral infection in the vagina (Masurier *et al.*, 1998; Hladik *et al.*, 2007; Hladik & Hope, 2009; Liu *et al.*, 2009). Therefore, the surfactant toxicity to dendritic cells, under non-confluent conditions, was also addressed. As a model for confluent but non-polarized cells, vaginal "epithelial-like" HeLa cells were also included in this study. A comparison of these two (fully-polarized and non-polarized) cell types is in itself instructive since the exposed cell surfaces are expected to be significantly different in membrane order (reviewed in Simons & Vaz, 2004) and, therefore, with regard to surfactant partition into (Abreu *et al.*, 2004; Sampaio *et al.*, 2005; Apel-Paz *et al.*, 2008) and translocation across membranes (Moreno *et al.*, 2006). The highly ordered apical membranes of fully polarized cells is the only membrane surface exposed to the surfactants in confluent polarized cell cultures and intact epithelia whereas non-polarized cells have significant amounts of less-ordered membrane domains exposed.

All surfactants used in this study revealed concentration and time-dependent toxic effects but exhibited different degrees of toxicity depending on the chemical nature of their polar head, which is in agreement with previous *in vitro* (Krebs *et al.*, 2000; Vieira *et al.*, 2008) and *in vivo* studies (Cone *et al.*, 2006). For Triton X-100, DDPS and SDS, cytotoxicity was not observed up to concentrations close to the critical micelle concentration (CMC), in both non-polarized (epithelial-like HeLa and dendritic FSDC) and polarized epithelial (MDCK II and Caco-2) cell lines, whereas the toxicity of cationic surfactants occurred at concentrations much lower than the surfactant CMC, being non-polarized cells around 10 times more sensitive to these surfactants than polarized epithelial cells. This result can be interpreted as meaning that TX-100, DDPS and SDS act mainly at the level of the plasma membrane of the cells, probably by causing structural changes at the level of the membrane or even its dissolution, as expected at concentrations close to surfactant CMC (Aranzazu Partearroyo *et al.*, 1990). On the other hand, the cationic surfactants most likely exert toxic effects through a more subtle mechanism, since toxicity occurs at concentrations that are not sufficient to significantly impair the physical integrity of the membranes. This toxicity could even result from effects at the intracellular level, conditioned by membrane partitioning and/or translocation across the membranes.

For the homologous series of cationic surfactants examined, the results show that the toxicity to mammalian cells was not linearly dependent upon the surfactant hydrophobic chain length. This observation may have complex reasons related to different affinities of the surfactant

for the different, possibly multiple, sites of action. The effect of the polar head group of the cationic surfactants was also evaluated; C_{12}BZK and C_{12}PB, which have the larger polar head groups and more delocalized charge, were between 2 to 5 times more toxic than C_{12}TAB in all cell lines studied. Delocalized charge on the surfactant head group makes its ionic radius considerably larger and reduces the work required for translocation of the polar group from one side of the membrane to the other (Honig *et al.*, 1986; Gennis, 1989).

Though there have been a large number of reports concerning the disinfectant properties of surfactants, their mechanism of action is still not fully understood. Attempts to use surfactants in STI prophylaxis relied upon their capacity to destroy viral and bacterial membranes, apparently without taking into account a fact that, in hindsight, appears all too obvious: by employing surfactant concentrations that owe its effectiveness on the disruption of bacterial and viral membranes, the membranes of vaginal epithelial cells would also be severely compromised. However, destruction of cell membranes is not the only mechanism of surfactant toxicity as is evidenced in the case of cationic surfactants. As argued above, their toxic effects probably do not involve gross disassembly of the cell membrane but rather more subtle effects. Candidate mechanisms that have been proposed in the literature include modulation of membrane curvature elastic stress and consequent reduction of membrane-bound protein activity (Dymond & Attard, 2008), alteration of the electrostatic surface potential of membranes (Vieira & Carmona-Ribeiro, 2006), or interaction with anionic polymers (DNA and RNA) in the cytoplasm or cell nucleus following translocation across the cell plasma membrane (Patrzykat *et al.*, 2002). Indeed, cationic surfactants are known to bind strongly to DNA and RNA (Spink & Chaires, 1997; Zhu & Evans, 2006) and induce drastic conformational changes in the structure of these polymers (Dias *et al.*, 2005).

The cell viability results obtained with the MTT assay correlate well with the observed release of LDH from cells. However, in the case of C_{10}TAB and C_{12}TAB, the LD_{50} values obtained with the LDH leakage assay were slightly but significantly higher than with the MTT assay. This can be explained by the nature of each assay: the LDH leakage assay, which evaluates the loss of intracellular LDH and its release into the culture medium, is an indicator of irreversible cell death either due to cell membrane damage directly caused by the surfactants or to loss of plasma membrane integrity posterior to cell death, whereas the MTT assay evaluates the metabolic capacity of the cell in reducing MTT to formazan. These results suggest that the molecular targets of the C_nTAB surfactants may be different depending on the length of their hydrophobic chain, since surfactants with shorter hydrophobic chain were found to affect cell metabolism prior to inducing cell membrane disruption. Amphiphiles with single short hydrocarbon chains insert faster into and translocate faster across lipid bilayers than amphiphiles with longer hydrocarbon chains

(Cardoso *et al.*, 2011). Furthermore, for amphiphiles with the same polar head groups, the longer the hydrocarbon chain the higher the partition coefficient between the membrane and the aqueous phase. Thus, the cationic surfactants with shorter hydrophobic chains are expected, at equilibrium, to be at a higher concentration within the cytoplasm than their analogues with longer hydrocarbon chains which are expected to be more concentrated in the cell membranes. From a kinetic perspective this also means that shorter hydrocarbon chain surfactants are expected to reach intracellular sites of metabolic activity, such as mitochondrial membranes, faster than their longer analogues.

The present results also show that surfactant concentrations close to the critical micelle concentration cause acute toxicity while lower concentrations can lead to a persistent post-exposure toxicity. This is evident when considering the high cell death that develops after surfactant removal, as in the case of lower surfactant concentrations (e.g. CMC/100 to CMC/30). It has been proposed that high concentrations of surfactants cause necrosis whereas low concentrations induce apoptosis (Perani *et al.*, 2001). Enomoto and co-workers (2007) demonstrated that some cationic surfactants, such as benzalkonium chloride, induce apoptosis at very low concentration (below CMC) by causing structural changes on the plasma membrane, for example, increasing phosphatidylserine translocation, while anionic and amphoteric surfactants were incapable of inducing apoptotic cell death.

In conclusion, the systematic study of structure-toxicity relationship in laboratory cell culture models is of utmost importance to understand the mechanisms underlying surfactant toxicity and its usefulness in prophylaxis against STIs. The detailed approach used in this work should be a mandatory first-line screening of possible microbicide candidates. Moreover, these results can be used to make predictions about the safety of these molecules, which would be helpful in the design of new, more effective and less harmful surfactants that could be used as broad-spectrum microbicides in vaginal gels. Among surfactants tested the results clearly show that only cationics have selective toxicity with respect to different mammalian cell types – they are significantly more toxic to non-polarized than they are to polarized cells. Similar selective toxicity was previously reported by other researchers in our laboratory (Vieira *et al.*, 2008) in a comparison of bacterial and yeast cells with polarized mammalian epithelial (MDCK II) cells. This feature should be taken into account in future endeavors of surfactant design. Finally, it should be wise to consider that a single "magic bullet" solution may never be found for prevention of STIs and that synergistic approaches, targeting simultaneously pathogens and host cells, must be sought.

Chapter IV

Mitochondrial dysfunction and cell apoptosis induced by monoalkyl quaternary ammonium surfactants: impact of surfactant structure on the mechanism of action

Summary

Mitochondrial dysfunction and cell apoptosis induced by monoalkyl quaternary ammonium surfactants: impact of surfactant structure on the mechanism of action

4.1. Introduction

The microbicidal action of surfactants is known since the mid 1930s, when Domagk synthesized and characterized the antibacterial activity of long-chain quaternary ammonium compounds (QACs) (Domagk, 1935). Since then, cationic surfactants have been extensively used as antiseptic and disinfectants for a variety of general hygiene and clinical purposes. Cetrimide (a mixture of alkyl-trimethylammmonium bromides), benzethonium chloride, benzalkonium chloride and cetylpiridinium bromide are some examples of broad-spectrum cationic surfactant microbicides (Gilbert & Al-taae, 1985; Belec *et al.*, 2000; Vieira & Carmona-Ribeiro, 2006; Vieira *et al.*, 2008; Lazzaro *et al.*, 2009) commonly found in skin disinfectant and cleansing products (reviewed in McDonnell & Russell, 1999; World Health Organization., 2009), oral disinfectants (Moran *et al.*, 2000; Witt *et al.*, 2005) and ophthalmologic products (reviewed in Baudouin *et al.*, 2010).

Antimicrobial and virucidal actions of surfactants have been attributed to their high affinity for biological membranes, which causes perturbation of membrane lipid bilayers and ultimately leads to cell lysis (reviewed in Gilbert & Moore, 2005). When used in high concentrations, to disrupt bacterial and viral membranes, surfactants have shown no selectivity, also destroying the membrane of mammalian cells (Aranzazu Partearroyo *et al.*, 1990). However, in the case of cationic surfactants, the microbicidal activity may also rely on the molecule charge (Gilbert & Moore, 2005; Kugler *et al.*, 2005) and alternative mechanisms other than cell membrane disruption have been proposed (Denyer & Hugo, 1977; Kopecka-Leitmanova *et al.*, 1989; Majtan & Majtanova, 1999; Vieira & Carmona-Ribeiro, 2006; Dymond & Attard, 2008).

Although, among surfactants, QACs have been proven to be the most useful antiseptic and disinfectants, the results from Chapter III show that these are also the most toxic for mammalian cells, limiting its use for systemic applications. Still, previous results from our group demonstrated that cationic surfactants exhibit some selectivity towards bacteria compared to mammalian polarized epithelial cells (Vieira *et al.*, 2008), thus justifying a more fundamental study about the

potential of those compounds for topical applications. Understanding the toxicity mechanisms, particularly at concentrations below surfactant CMC, and the sequence of events underlying surfactant-mediated epithelial cell death is crucial for the design and development of more effective and safer molecules. Moreover, data acquired through this approach may also prove relevant to the identification of appropriate safety biomarkers for the validation of new surfactant molecules in preclinical studies.

In recent years, several reports have demonstrated that low concentrations of cationic surfactants can induce apoptosis in different mammalian cell types (Debbasch *et al.*, 2001; Perani *et al.*, 2001; Yip *et al.*, 2006; Enomoto *et al.*, 2007; Pauly *et al.*, 2009; Nomura *et al.*, 2010), which is consistent with the results presented in the previous Chapter. The involvement of mitochondrial dysfunction in surfactant-induced apoptosis has also been suggested (Yip *et al.*, 2006; Levine *et al.*, 2007), nonetheless a detailed analysis of the mechanisms behind it has yet not been performed. In the present study, the effects of surfactant concentration and exposure time on the viability and mitochondrial function of fully polarized columnar epithelial cells (MDCK II) were evaluated. To elucidate the contribution of surfactant structure on the mechanisms mediating cell cytotoxicity, a homologous series of commercially available *n*-alkyl-N,N,N-trimethylammonium bromides (C_nTAB with *n* from 10 through 16), N-dodecylpyridinium bromide (C_{12}PB), and dodecyl-N-benzyl-N,N-dimethylammonium bromide (C_{12}BZK) were used.

4.2. Results

4.2.1. Caspase-mediated apoptosis in MDCK II cells promoted by low doses of C_{10}TAB

The ability of cationic surfactants to promote apoptosis at concentrations bellow CMC (Debbasch *et al.*, 2001; Perani *et al.*, 2001; Yip *et al.*, 2006; Enomoto *et al.*, 2007; Pauly *et al.*, 2009; Nomura *et al.*, 2010) suggests that at least part of the toxic effects described in the previous chapter can be a result of cell death through apoptosis. Therefore, in order to clarify the mechanisms underlying cationic surfactant toxicity, MDCK II epithelial cells were treated with different concentrations of the cationic surfactant C_{10}TAB and cell death was evaluated through different approaches. As already mentioned, MDCK II epithelial cells can be grown to a completely confluent and polarized state, with relatively non-leaky tight junctions, which makes this cell line a good *in vitro* model that closely resembles the characteristics of a columnar vaginal epithelium (Irvine *et al.*, 1999; Velarde *et al.*, 1999; Ekelund *et al.*, 2005; Vieira *et al.*, 2008). If used in topical applications, surfactants will be in direct contact with epithelial cells, hence, the study of the

toxicity towards this cell type is a crucial step in validating the safety of microbicide surfactant compounds.

In cell cultures the first morphologic changes and signs of activation of apoptotic pathways can become visible in less than two hours after the noxious stimulus (depending on the cell type and stimulus intensity and duration) (Kerr *et al.*, 1972; Messam & Pittman, 1998). Therefore, MDCK II cells were exposed to different concentrations of C_{10}TAB for 3 hours. At the end of incubation cell viability was measured using a commercial kit, which contains a cell-permeant fluorogenic viability reagent that is cleaved by live-cell proteases into a fluorescent product, a reaction that only takes place within cells with intact membrane. Cell viability results shown in Figure 4.1A are expressed as percentage of the viability of mock-treated control cells and the dose-toxicity curve was fitted with a five parameter logistic equation (Ricketts & Head, 1999; Van der Graaf & Schoemaker, 1999). Similar to what was observed 24 hours post-exposure (see Chapter III, Section 3.2.2), C_{10}TAB toxic effects herein described were dependent on surfactant concentration. Cell viability starts to decrease at concentrations between 1.33 (CMC/30) and 2 mM (CMC/20), showing a reduction of around 10%, to 90.12 ± 2.83% of control in the latter case. The surfactant concentration that reduces cell viability by 50% (LD_{50}) was determined from the dose-response curve as being 3.11 mM (95% CI, 2.93-3.30), approximately 13 times lower than C_{10}TAB CMC. The cytotoxic effect of C_{10}TAB was also evaluated by the LDH leakage assay, a measure of the plasma membrane integrity, which can be lost either due to cell membrane damage directly caused by the surfactants or posterior to cell death (e.g. latter stages of apoptosis). Hence, the release of the LDH enzyme to the cell culture medium is a reliable indicator of irreversible cell death. Results are presented in Figure 4.1C and expressed as percentage of total intracellular LDH activity from control (lysed mock-treated cells). C_{10}TAB cytotoxic effects were dose-dependent and data could be adjusted to a five parameter logistic equation. As can be seen, surfactant concentrations necessary to elicit membrane damage are higher than those necessary to cause loss of cell viability (Fig. 4.1A and C). Membrane damage was only detected at concentrations around 2.7 mM (CMC/15), inducing cell death by 14.40 ± 10.29% above control, and the LD_{50} is 3.84 mM (95% CI, 3.69-3.99). These results confirm that cationic surfactants with short hydrophobic chains affect cell metabolism prior to inducing cell membrane damage.

Programmed cell death is a highly regulated energy dependent process, characterized by several distinctive morphological and biochemical features such as: loss of mitochondrial membrane potential; changes in mitochondrial permeability; nuclear chromatin condensation and fragmentation; cell shrinkage; loss of plasma membrane asymmetry; membrane blebbing; and formation of apoptotic bodies (reviewed in Saraste, 1999; Fink & Cookson, 2005; Ward *et al.*,

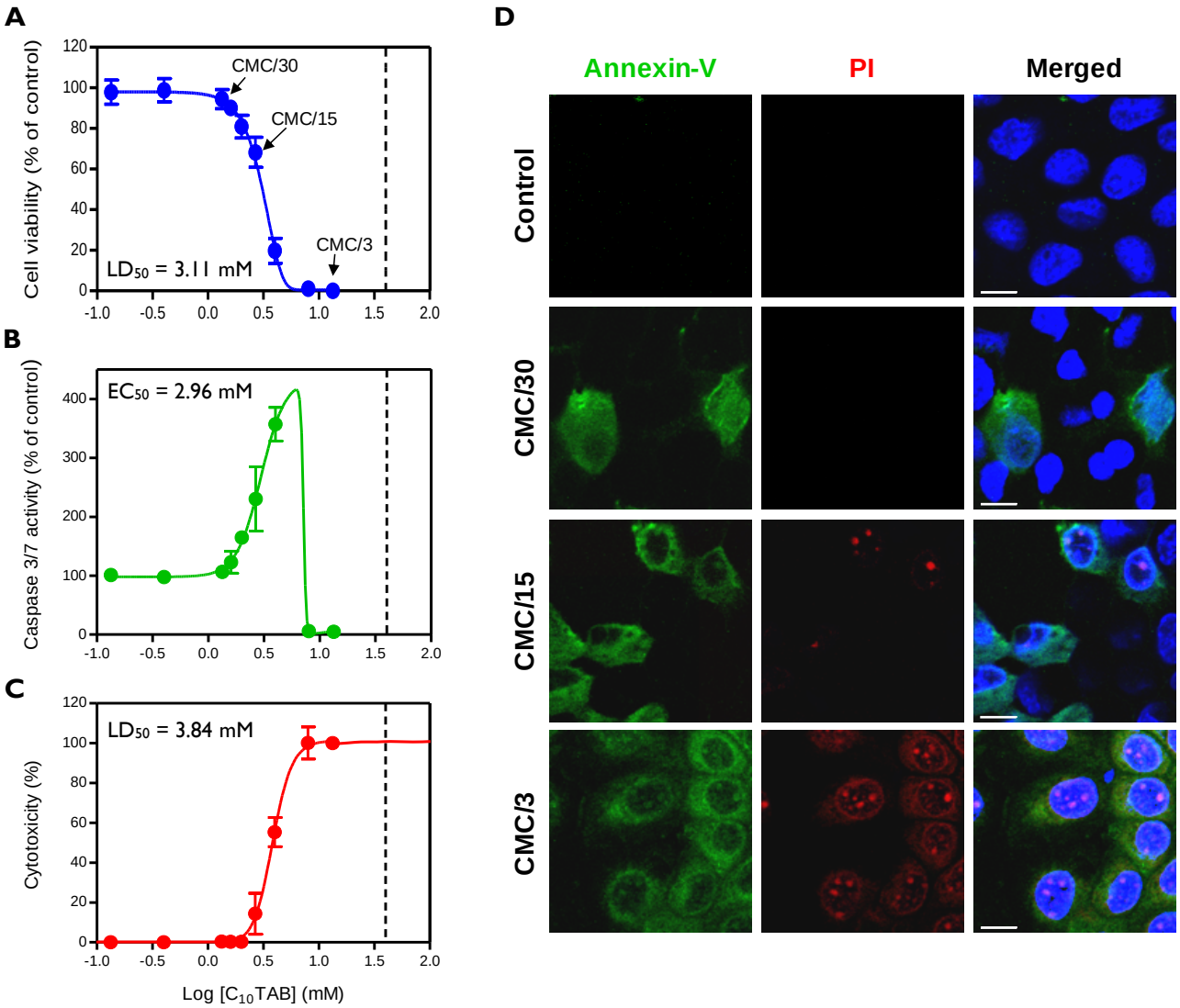

Figure 4.1. Concentration-dependent effects of C_{10}TAB on MDCK II cell viability, caspase activation and cytotoxicity after 3 hours exposure. Cell viability (**A**) and caspase 3/7 activity (**B**) were assessed immediately after exposing cells to different concentrations of C_{10}TAB, using a commercial kit (Caspase-Glo® 3/7 Assay). Data are expressed as percentage of control viability. To evaluate membrane integrity, the activity of LDH released to the cell culture medium was quantified (**C**). Results are presented as percentage of LDH activity from lysed mock-treated control cells. Data are presented as Mean ± SD of 4 independent experiments. LD_{50} concentrations with respect to cell viability and plasma membrane integrity were calculated from the dose-response curves and are 3.11 mM (95% CI, 2.93-3.30) and 3.84 mM (95% CI, 3.69-3.99) respectively. The concentration that increases caspase 3/7 activity by 50% (EC_{50}) was determined as being 2.96 mM (95% CI, 2.34-3.68).The CMC of C_{10}TAB is 4.0×10^{-2} M and is represented in the graphs by the black dashed line. Apoptotic and necrotic cells were imaged using live-confocal fluorescence microscopy (**D**). The apoptotic cells were visualized with annexin V staining (green) and necrotic cells with propidium iodide (PI, red). Nuclei were visualized by Hoechst 33342 staining (blue). Scale bars correspond to 10 µm.

2008). Contrary to apoptosis, necrotic cell death is characterized by the depletion of intracellular ATP stores, rapid cell swelling, disruption of cell organelles and loss of plasma membrane integrity without visible nuclei condensation (reviewed in Assunção Guimarães & Linden, 2004; Fink & Cookson, 2005; Zong & Thompson, 2006). Identification of the morphological and biochemical markers of apoptosis allows the distinction from other forms of cell death (reviewed in Krysko *et al.*, 2008; Ward *et al.*, 2008). In a first approach, the activation of the executioner caspases 3 and 7, a relatively early event in the apoptotic process (Budihardjo *et al.*, 1999; Slee *et al.*, 1999; Wolf &

Green, 1999; Wolf *et al.*, 1999), was assessed using a bioluminescent assay. As can be seen in Figure 4.1B, an increase of around 20% in caspase 3/7 activity, to 122.98 ± 18.63% of control, occurs simultaneously with the initial cell viability loss (Fig. 4.1A). Moreover, at concentrations between 2 (CMC/20) and 4 mM (CMC/10), caspase 3/7 activity increases proportionally to the reduction observed in MDCK II viability, reaching a maximum of activity close to the latter concentration (Fig. 4.1A and B). The surfactant dose that raises caspase 3/7 activity by 50% compared to control conditions (EC_{50}) was determined from the dose-response curve as being 2.96 mM (95% CI, 2.34-3.68), which is in the same range of concentrations of the LD_{50} obtained for the cell viability experiments. However, whereas low C_{10}TAB concentrations stimulated caspase 3/7 activity, high concentrations more close to the CMC evoked the opposite effect (Fig. 4.1B). At surfactant concentrations above 6.67 mM (CMC/6), the percentage of cytotoxicity peaked, reaching values above 90% (Fig. 4.1C), while no caspase 3/7 activation was detected (Fig. 4.1B). These results support the hypothesis that the decrease in MDCK II cell viability, resulting from exposure to low concentrations of C_{10}TAB, is an outcome of surfactant-induced apoptosis, whereas high concentrations of the same compound promptly lead to necrotic cell death.

To further explore the dual nature of cell death processes induced by cationic surfactants, annexin V and propidium iodide (PI) stainings were performed in MDCK II cells previously incubated with C_{10}TAB for 3 hours. One of the earliest hallmarks of apoptosis is the translocation of phosphatidylserine (PS) from the inner to the outer leaflet of the plasma membrane (Martin *et al.*, 1995). Annexin V, a Ca^{2+} dependent phospholipid-binding protein with high affinity for PS (Andree *et al.*, 1990), binds to the exposed PS on the membrane of apoptotic cells and can be used in combination with PI staining, a dye that only enters membrane-damaged injured cells (Macklis & Madison, 1990; Vitale *et al.*, 1993), to allow the identification of viable cells (annexin V and PI negative), early apoptotic cells (annexin V positive, PI negative) and late apoptotic and/or necrotic cells (annexin V and PI positive). Figure 4.1D shows that the number of annexin V positive cells increases proportionally to the surfactant dose and is accompanied by the appearance of pyknotic nuclei (as seen by the Hoechst 33342 staining). Moreover, the annexin V staining preceded the emergence of PI-positive cells, which were only visible at higher surfactant concentrations, confirming that cell death through necrosis is restricted to concentrations close to CMC.

4.2.2. Effect of C_{10}TAB on the energy state of epithelial cells

A distinctive physiological feature between apoptosis and necrosis is the amount of

intracellular ATP, which rapidly decreases during necrotic cell death but is only partially depleted in apoptotic dying cells (Eguchi *et al.*, 1997; Leist *et al.*, 1997; Tsujimoto, 1997; Feldenberg *et al.*, 1999; Izyumov *et al.*, 2004; Lyamzaev *et al.*, 2004). The intracellular ATP content is a crucial parameter in cellular homeostasis regulation: when ATP drops below a critical level for an amount of time sufficient to disrupt the normal functioning of the cell, the cell commits "suicide" by entering apoptosis. Given that the apoptotic signaling pathways contain several ATP-dependent stages (e.g. caspase 9 activation, DNA condensation/fragmentation) (Eguchi *et al.*, 1999), a drastic reduction in the intracellular ATP pool, beyond the reduction necessary to trigger apoptosis and below the ATP concentration required to fuel this process, will result in a switch to necrosis in spite of the nature of the noxious stimulus (Eguchi *et al.*, 1997; Feldenberg *et al.*, 1999). Since the energy state of the cell plays a central role in the fate of cell death, the effect of C_{10}TAB on the intracellular ATP levels was evaluated using the luciferin-luciferase bioluminescent assay. As a measurement of the cell energy charge, the ATP-to-ADP ratio was also determined (Smets *et al.*, 1994; Bradbury *et al.*, 2000). To correlate the events occurring during apoptosis, the normalized changes in intracellular ATP content and caspase 3/7 activity were plotted on a single graph (Fig. 4.2A). The results show that, although a 3 hours incubation with 1.33 mM (CMC/30) of C_{10}TAB did not significantly alter the intracellular ATP concentration (84.39 ± 16.10% of control), a significant reduction of 50% in the ATP/ADP ratio (2.88 ± 0.53 and 1.43 ± 0.28 for control and CMC/30, respectively; $p < 0.01$) was observed. At this concentration no loss of cell viability or increase in caspase 3/7 activity was detected, indicating that the cell energy status is affected prior to any sign of commitment to cell death. Furthermore, at concentrations between 2 (CMC/20) and 4 mM (CMC/10) the partial ATP depletion, ranging from 77.46% to 53.42% of control, resulted in a concentration-dependent induction of apoptosis, as evidenced by the simultaneous increase in caspase 3/7 activity (Fig. 4.2A). This was also accompanied by a gradual and significant decrease in the ATP/ADP ratio, from 2.88 ± 0.53 in mock-treated cells to a minimum value of 1.13 ± 0.37 at CMC/10 (Fig. 4.2B). As a positive control for apoptosis, cells were incubated with 1 µM staurosporine for 6 hours (Araki *et al.*, 2002; Bojarski *et al.*, 2004). Staurosporine, a microbial alkaloid, is a cell permeable protein kinase C inhibitor (Tamaoki *et al.*, 1986) and a potent inducer of apoptosis (Kabir *et al.*, 2002; Zhang *et al.*, 2004). The incubation with staurosporine led to a decrease of the intracellular ATP concentration by 35%, to 65.42 ± 10.94% of control, reduced cell viability to 88.88 ± 6.45% of control and increased caspase 3/7 activity to 225.36 ± 12.28% of control. This highlights the similarity between the molecular changes elicited by low concentrations of C_{10}TAB and the typical features of apoptosis.

In contrast, higher surfactant concentrations induced a distinctly different pattern of biochemical changes in MDCK II cells. Cell exposure to 13.33 mM of C_{10}TAB (CMC/3) caused

severe ATP depletion (0.76 ± 0.48% of control; $p < 0.001$) without detectable caspase 3/7 activation (Fig 4.2A).The ATP/ADP ratio also plummeted to 0.18 ± 0.32, reflecting the dissipation of the energy reservoirs that occurs during necrosis (Tsujimoto, 1997; Bradbury *et al.*, 2000).

A

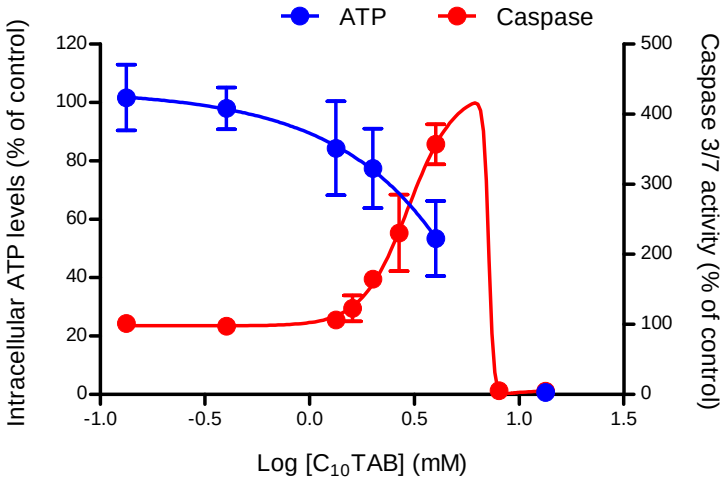

B

Treatment	Concentration (mM)		ATP (%)	ATP/ADP
Control			100.00 ± 10.31	2.88 ± 0.53
C_{10}TAB	CMC/300	0.13	101.70 ± 11.23	2.39 ± 0.26
	CMC/100	0.40	98.04 ± 7.15	2.24 ± 0.42
	CMC/30	1.33	84.39 ± 16.10	1.43 ± 0.28 **
	CMC/20	2.00	77.46 ± 13.59 *	1.35 ± 0.42 ***
	CMC/10	4.00	53.42 ± 12.85 ***	1.13 ± 0.37 ***
	CMC/3	13.33	0.76 ± 0.48 ***	0.18 ± 0.32 ***
Staurosporin		0.001	65.42 ± 10.94 **	ND

Figure 4.2. Effects of C_{10}TAB on intracellular ATP levels and ATP/ADP ratio in MDCK II cells. ATP intracellular levels were determined by the luciferin-luciferase assay after cells were incubated for 3 hours with different concentrations of C_{10}TAB (**A, B**). Results were normalized to protein content and expressed as percentage of mock-treated control cells (24.07 ± 2.48 nmol ATP/mg protein). For comparison purposes the results for caspase 3/7 activity are also shown (**A**). As a positive control for apoptosis cells were treated with staurosporin 1 µM for 6 hours. The ATP/ADP ratio was also analyzed by the luciferin-luciferase method. ADP levels were measured by converting it to ATP that was subsequently detected using the same reaction (**B**). Data are shown as Mean ± SD of at least 3 independent experiments. One-way ANOVA (Dunnet's post-test): * $p < 0.05$, ** $p < 0.01$ and *** $p < 0.001$, significantly different from the respective control. ND, not determined.

4.2.3. C_{10}TAB exposure results in loss of mitochondrial membrane potential ($\Delta\psi_m$) in epithelial cells

The ability of lipophilic cations to accumulate in negatively-charged cellular compartments, such as mitochondria, driven by the membrane potential is well known (Rottenberg, 1984; Murphy, 1997; Ross *et al.*, 2006; Ross *et al.*, 2008; Perry *et al.*, 2011). Despite their net positive charge, these compounds can easily cross phospholipid bilayers, due to their charge being delocalized over a large hydrophobic surface area and/or partially shielded by neutral groups (Ketterer *et al.*, 1971; Honig *et al.*, 1986; Gennis, 1989; reviwed in Ross *et al.*, 2005). Given the chemical properties of monoalkyl ammonium surfactants and the obtained results evidencing an

impairment of the cell energy status that precedes the commitment to cell death, mitochondria are a likely target for the harmful effects of this type of molecules. Indeed, the drop in intracellular ATP levels and ATP/ADP ratio observed in cells exposed to C_{10}TAB, at concentrations where no signs of cell viability loss were detectable, strongly suggests a compromise in the mitochondrial function and, possibly, mitochondrial-dependent apoptosis.

Mitochondrial membrane depolarization and loss of the electrochemical gradient during apoptosis have been extensively reported, both as a consequence of programmed cell death as well as its cause (reviewed in Bernardi *et al.*, 1999; Desagher & Martinou, 2000; Kroemer & Reed, 2000; Ly *et al.*, 2003; Kroemer *et al.*, 2007; Hand & Menze, 2008). To further elucidate the contribution of mitochondrial dysfunction to apoptosis induced by cationic surfactants, the effect of C_{10}TAB on the mitochondrial membrane potential ($\Delta\psi_m$) of MDCK II cells was evaluated. For that, after 3 hours of incubation with the surfactant, MDCK II cells were loaded with the mitochondrial membrane potential-sensitive probe Rhodamine 123 (Rh123), in parallel with PI to measure plasma membrane permeability. Rh123 is a cationic lipophilic dye that easily crosses the cell plasma membrane and distributes electrophoretically into the mitochondrial matrix in response to $\Delta\psi_m$, without passing through endocytotic vesicles or lysosomes (reviewed in Chen, 1988; Perry *et al.*, 2011). As a consequence of this, hyperpolarized mitochondria will accumulate more of the cationic dye whereas depolarized mitochondria will gather less. Polarized mitochondria were imaged as bright fluorescent large branched tubules, simple tubules and spheres.

As can be observed in Figure 4.3, cells exposed to concentrations above 1.33 mM (CMC/30) of C_{10}TAB display a steadily decrease in Rh123 mitochondrial accumulation, accompanied by the emergence of a faded and diffuse Rh123 staining in the cytoplasm, a feature compatible with a reduction in $\Delta\psi_m$. In addition, the mitochondrial structure also appears to be affected since the punctate pattern of the Rh123 staining reveals a reduction in the size of the labeled mitochondrial particles. These effects may account for the decrease in the intracellular ATP levels and ATP/ADP ratio, already visible at sub-lethal concentrations (i.e. CMC/30), and suggests that mitochondrial damage is an early event in cationic surfactant-mediated toxicity, preceding cell death. Accordingly, mitochondrial dysfunction should occur upstream to caspase 3/7 activation (Fig. 4.2A).

As the concentration of C_{10}TAB increases, Rh123 retention by the mitochondria of cells with intact membrane (PI-negative) is completely abolished (e.g. CMC/15). Nonetheless, high accumulation of Rh123 was observed in cells showing low PI fluorescence and condensed nuclei (blue staining). Similar features have been observed during fibroblast cell death prompted by serum deprivation (Simm *et al.*, 1997). Probably this cell population corresponds to cells that became

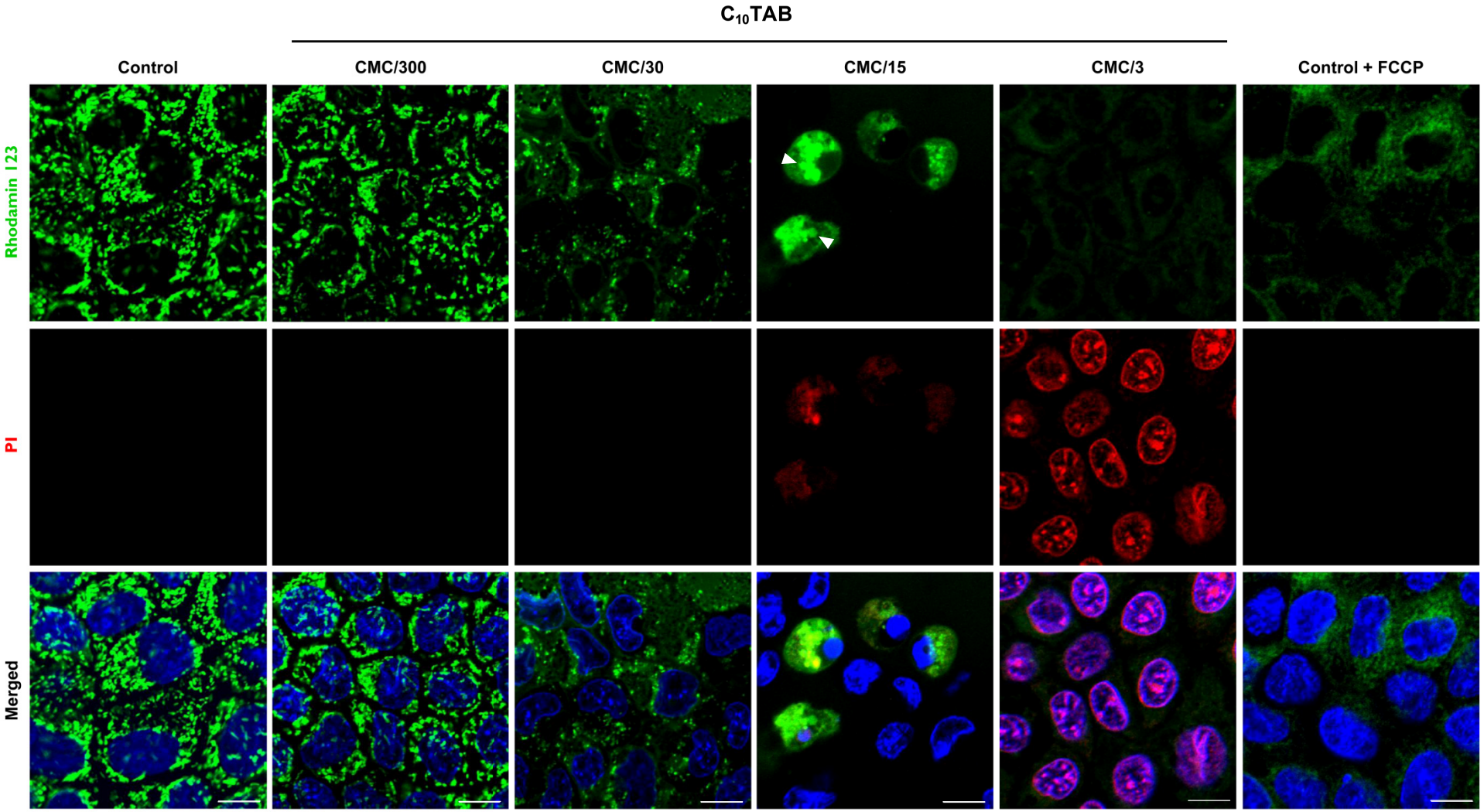

Figure 4.3. Changes on mitochondrial transmembrane potential ($\Delta\psi_m$) induced by C_{10}TAB. Representative live-cell confocal fluorescence microscopy images showing MDCK II cells stained with the mitochondrial membrane potential sensitive dye Rhodamine 123 (green) after 3 hours of incubation with different concentrations of C_{10}TAB. Necrotic cells were stained with propidium iodide (PI, red) and nuclei were visualized with Hoechst (blue). As a positive control, cells were incubated with 10 μM FCCP, a mitochondrial uncoupler. The loss of Rh123 fluorescence from the mitochondrial regions reflects the dissipation of the $\Delta\psi_m$. The bright round structures visible at CMC/15 (arrow heads) may correspond to swollen mitochondria. Scale bars correspond to 10 μm.

leaky but still possesses mitochondria that, although swollen, maintain their membrane potential. Another possible explanation is that Rh123 accumulation in these cells is unspecific and independent of the inner mitochondrial membrane potential, as it was only partially abolished after membrane depolarization by a protonophore. In fact, Rh123 unspecific accumulation in early necrotic cells has been previously mentioned by others (Nadakavukaren *et al.*, 1985; Lachowiez *et al.*, 1989; Metivier *et al.*, 1998). The cells exhibiting this morphology were not considered in further morphological analysis.

Exposure to higher surfactant concentrations, close to CMC (e.g. CMC/3), caused cell necrosis (Fig. 4.3). In fact, all cells exhibit PI-positivity and no Rh123 mitochondrial accumulation was visible, indicating a complete loss of the mitochondrial transmembrane potential.

To ascertain whether Rh123 accumulation in the mitochondria was correlated to $\Delta\psi_m$, the effect of mitochondrial depolarization caused by the mitochondrial uncoupler carbonyl cyanide 4-(trifluoromethoxy)phenylhydrazone (FCCP, 10 µM) on Rh123 staining was tested. As can be seen in Figure 4.3, after FCCP addition to control cells, Rh123 punctate distribution pattern is lost and the dye diffuses to the cytoplasm, showing a faded staining, very close to background levels. This supports the relation between $\Delta\psi_m$ dissipation and low Rh123 accumulation.

4.2.4. Sub-lethal concentrations of C_{10}TAB induce morphological changes in the mitochondrial network

Mitochondria are dynamic organelles, constantly undergoing fusion and fission, changing their overall shape and subcellular distribution, and thus forming complex networks ranging from interconnected large branched tubules to small individual organelles. Mitochondrial network dynamics and bioenergetics are intimately connected and it has been suggested that mitochondrial morphology reflects its functional status (reviewed in Karbowski & Youle, 2003; Arnoult, 2007; Sauvanet *et al.*, 2010). The relevant information provided by mitochondrial morphology regarding the cells physiological status, can also, conversely, address changes induced by noxious stimulus and its harmful potential. In addition, although mitochondrial fragmentation can occur without activation of programmed cell death, an increasing number of reports refer the occurrence of mitochondrial fragmentation at early stages of apoptosis (reviewed in Desagher & Martinou, 2000; Karbowski & Youle, 2003). Thus, in order to evaluate how mitochondrial morphology is affected by treatment with C_{10}TAB, MDCK II cells were stained with Rh123. After 1 or 3 hours of incubation with the surfactant, mitochondrial fragmentation and mitochondrial mass (i.e. number, area and volume) were estimated through confocal microscopy. Given that staurosporine-induced apoptosis comprises well described alterations in the mitochondrial inner membrane potential

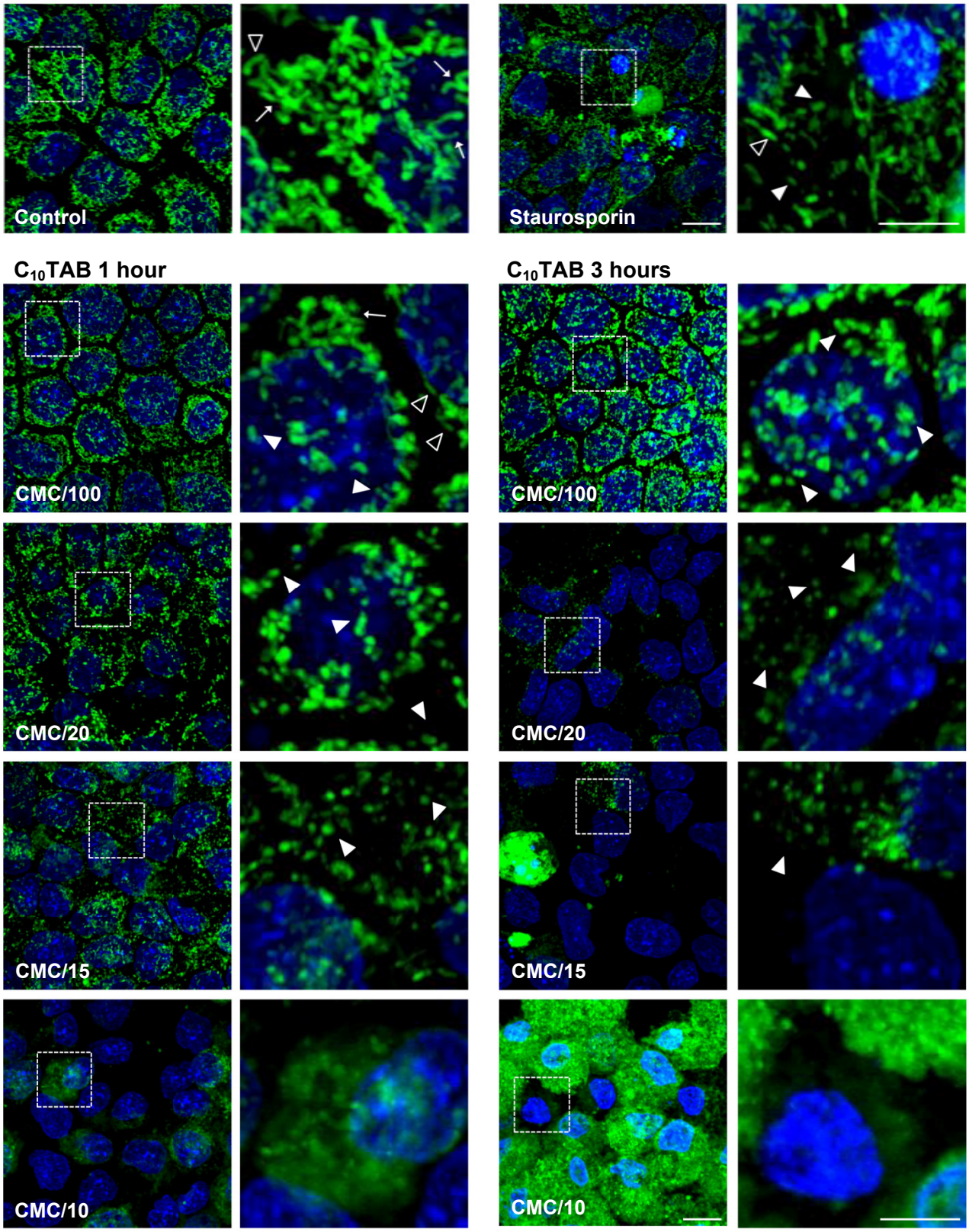

Figure 4.4. Morphological changes in the mitochondrial network of MDCK II cells after C_{10}TAB exposure. Representative maximum fluorescence intensity projection images obtained by live-cell confocal microscopy, showing the mitochondrial network of MDCK II cells after C_{10}TAB treatment for 1 and 3 hours. Mitochondrial structure was visualized with the mitochondrial membrane potential sensitive Rh123 dye (green). Control cells display reticulo-tubular mitochondrial morphology, mainly composed of large branched tubules (arrows) and simple tubules (open arrow heads). Exposure to C_{10}TAB gradually disintegrates the reticulo-tubular mitochondrial network into a punctiform phenotype, comprising numerous round fragments of varying sizes (arrow heads). As a positive control for alterations in mitochondrial morphology occurring during apoptosis, cells were incubated with 1 µM staurosporin for 6 hours. Nuclei were visualized with Hoechst (blue). The zoomed regions are indicated by the doted squares in the larger images. Scale bars correspond to 10 µm and 5 µm in larger and zoomed images, respectively.

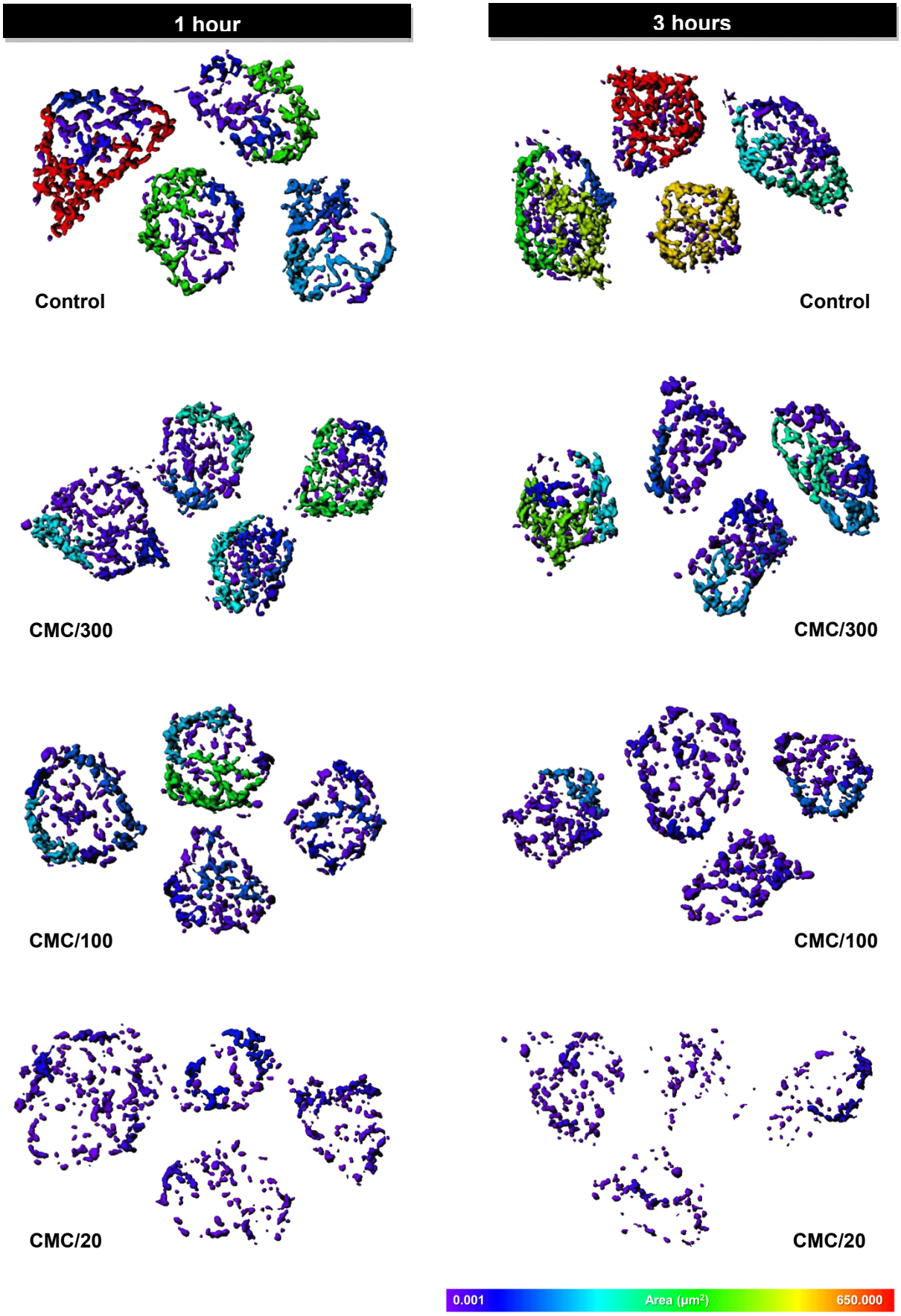

Figure 4.5. Mitochondria distribution and subtyping according to surface area in representative cells exposed to different concentrations of C_{10}TAB. Mitochondrial surfaces were rendered from confocal z-stacks using Imaris software and colour-coded based on their surface area. Hotter colours indicate larger contiguous surfaces. Control cells show larger masses of branched mitochondria whereas increasing concentrations of surfactant, as well as increased exposure duration, cause mitochondria fragmentation (dark blue/purple colour).

(Heiskanen *et al.*, 1999; Scarlett *et al.*, 2000) and fragmentation of the mitochondrial network (Frank *et al.*, 2001; Young *et al.*, 2010; Zhu *et al.*, 2012), cells were also incubated with 1 μM staurosporine for 6 hours as a positive control.

The results presented in Figures 4.4 and 4.5 show that the reticulo-tubular phenotype of healthy cells disintegrates into one characterized by numerous, small, rounded mitochondria after surfactant exposure, similar to what is observed after staurosporine induced-apoptosis. These morphological alterations occur gradually, and its severity depends on the surfactant concentration and the duration of exposure. Moreover, structural changes become visible after a short period of exposure to very low doses of C_{10}TAB (e.g. 1 hour exposure to CMC/300; see Fig. 4.5), prior to compromising the cell's energy status, as no changes in the intracellular ATP levels and ATP/ADP levels were detected (Fig. 4.2). Hence, reorganization of the mitochondrial network into small fragmented mitochondria seems to be the one of the first manifestations of the deleterious effect of cationic surfactants in epithelial cells but it does not necessarily culminate in apoptosis, given that increased concentrations were required to induced caspase activation (Fig. 4.1 and 4.2) and nuclear fragmentation (Fig. 4.3).

A more detailed analysis of the mitochondrial morphological changes revealed a progressive increase in the total number of individual mitochondria per cell, up to a concentration of 0.4 mM (CMC/100) of C_{10}TAB (Fig. 4.6A), and a simultaneous decrease of the total mitochondrial area (Fig. 4.6B) and volume (Fig. 4.6C) per cell. Conversely, surfactant concentrations higher than 0.4 mM evoked a reduction in the number of mitochondria per cell, which was more pronounced at longer exposure times. This reduction is probably related to the loss of $\Delta\psi_m$, and consequently a decrease in Rh123 accumulation inside the mitochondria (Fig. 4.6).

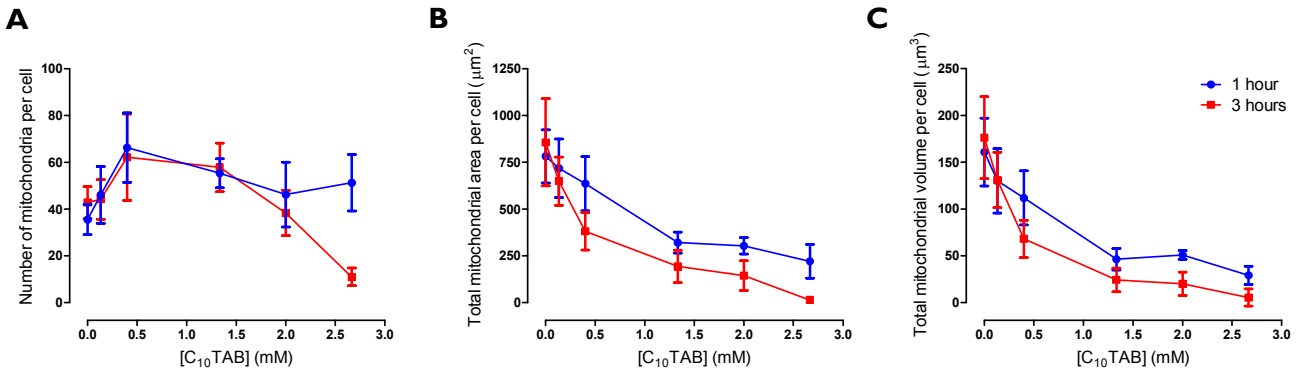

Figure 4.6. Effect of C_{10}TAB exposure on the number, area and volume of mitochondrial particles in individual cells. Mitochondrial morphometric analysis was carried out in confocal z-stacks of MDCK II cells probed with rhodamine 123, after 1 hour (blue circles) or 3 hours (red squares) of incubation with the surfactant. Volumetric reconstruction of mitochondrial surface was performed using Imaris software and the mitochondria number (**A**), total area (**B**) and total volume (**C**) per cell was determined. Data are shown as Means ± SD of at least 8 cells per each condition.

4.2.5. Cationic surfactants impair mitochondrial respiratory activity

The reorganization of the mitochondrial network after exposure to sub-lethal doses of C_{10}TAB strongly suggests that mitochondrial dysfunction might play a crucial role in cationic surfactant toxicity. Therefore, in order to study the direct interaction of cationic surfactants with mitochondria and clarify the toxicity mechanisms involved, basic bioenergetic parameters were evaluated in isolated mitochondria exposed to increasing concentrations of cationic surfactants. This was achieved by monitoring oxygen consumption dynamics with a Clark-type oxygen electrode, using a proper combination of substrates and inhibitors of the electron transfer and ADP phosporylation (see Fig. 4.7). This approach allowed the identification of specific sites of surfactant action in the redox chain and oxidative phosphorylation system.

After 5 minutes of incubation with different concentrations of C_{10}TAB, the respiration rates as well as the respiratory control ratio (RCR) and ADP-to-oxygen ratio (ADP/O) were measured in energized mitochondria with either glutamate/malate or succinate substrates. The effects of C_{10}TAB on mitochondrial respiratory State 2, State 3, State 4 and Uncoupled (FCCP-stimulated) State respiration rates are presented in Figure 4.8A-E. As can be observed, in a range of concentrations, from 6.67 μM (CMC/6000) up to 13.33 μM (CMC/3000), C_{10}TAB consistently and significantly decreases the FCCP-uncoupled respiration rate when mitochondria

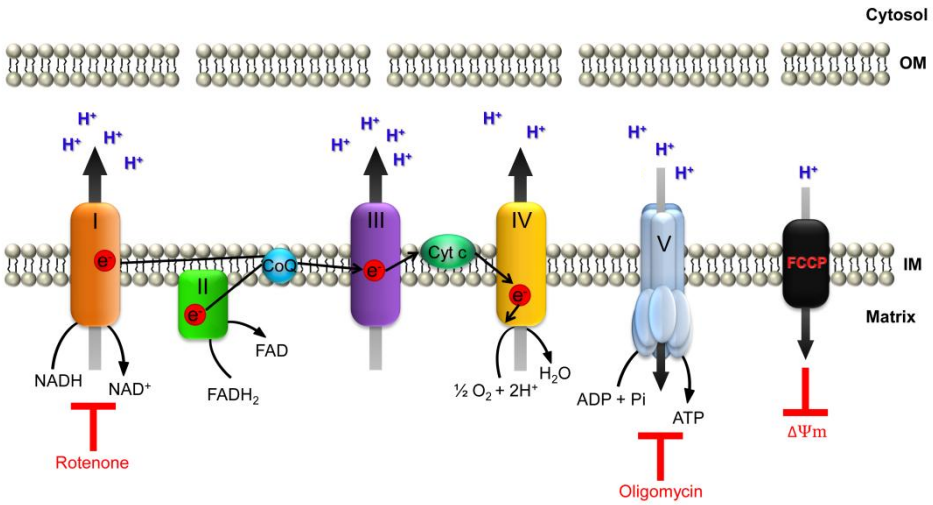

Figure 4.7. Schematic representation of the mitochondrial respiratory chain and the oxidative phosphorylation inhibitors used in the present work. The electron (e^-) transfer from NADH (Complex I, NADH-ubiquinone oxidoreductase) and $FADH_2$ (Complex II, succinate-ubiquinone oxidoreductase) to oxygen (Complex IV, cytocrome c oxidase) is accompanied by the outward translocation of protons from the mitochondrial matrix to the intermembrane space at Complex I, III and IV, generating an electrochemical proton gradient across the mitochondrial inner membrane (proton-motive force). This gradient provides the energy for ATP synthesis catalyzed by the membrane-located ATP synthase (Complex V). Glutamate and malate were used in order to generate NADH, the Complex I substrate, in the mitochondrial matrix, whereas succinate was employed as a Complex II substrate in rotenone-treated mitochondria. The oxidative phosphorylation inhibitors are indicated in the figure at their site of action: rotenone, Complex I inhibitor; oligomycin, Complex V inhibitor; FCCP, protonophore and uncoupler of oxidative phosphorylation (i.e. dissipates $\Delta\psi_m$). CoQ, ubiquinone (coenzyme Q_{10}); Cyt c, cytocrome c; OM, mitochondrial outer membrane; IM, mitochondrial inner membrane.

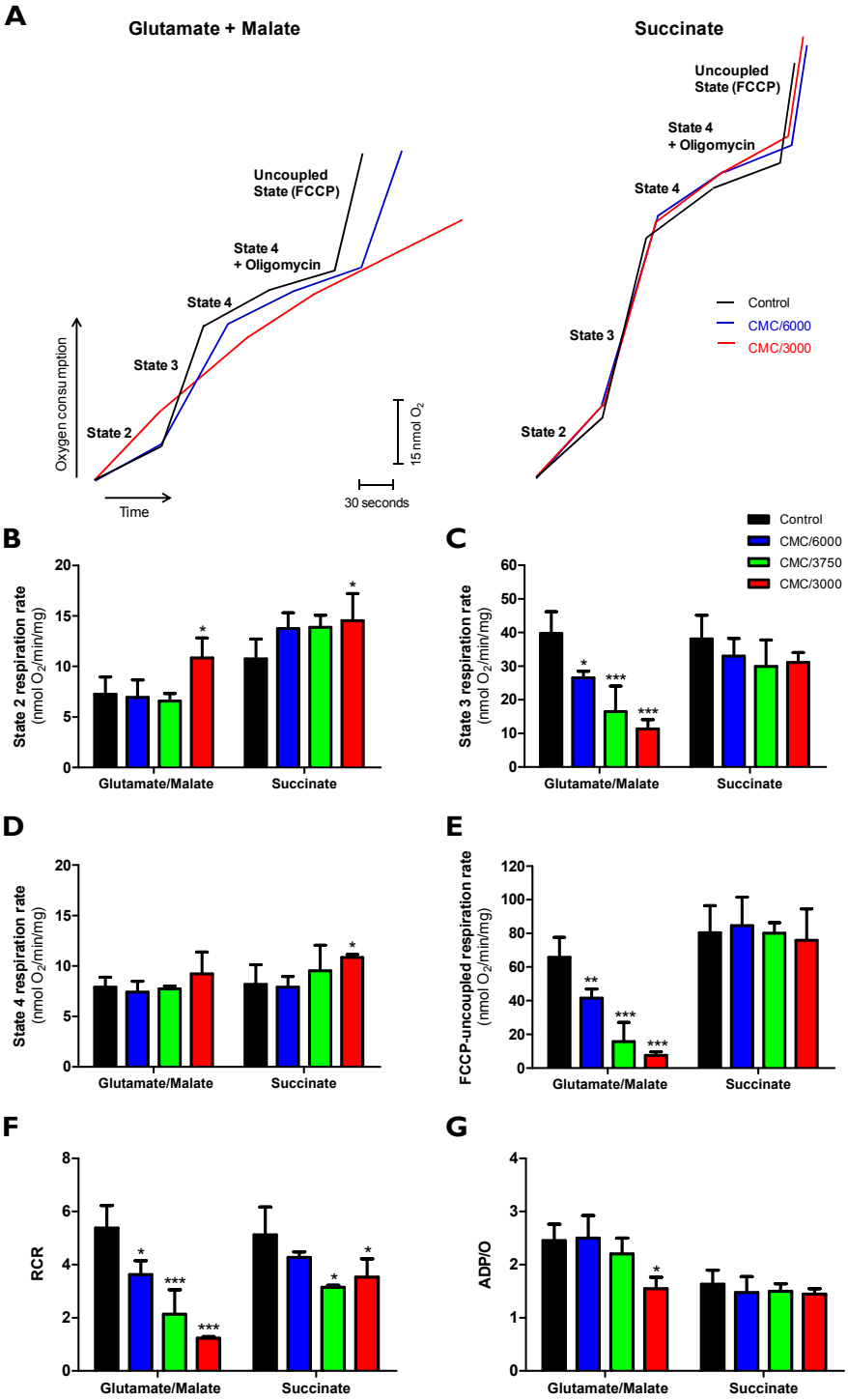

Figure 4.8. Effects of C_{10}TAB on mitochondrial oxygen consumption rates, RCR and ADP/O ratio. Schematic representation of the typical outcome of rat liver mitochondrial oxygen consumption after C_{10}TAB exposure (**A**). Freshly isolated rat liver mitochondria (1 mg/mL) were exposed to different concentrations of C_{10}TAB for 5 minutes prior to energization with 5 mM glutamate/2.5 mM malate or 5 mM succinate plus 2 µM rotenone (State 2 respiration). Respiratory State 3 was induced by addition of 125 nmol/mL of ADP. State 4 respiration rate was measured after complete phosphorylation of the added ADP. 1 µg/mL oligomycin was added to the system, in order to inhibit proton passive flux through the ATP synthase. Uncoupled State respiration was initiated by addition of 1 µM FCCP. The effect of C_{10}TAB on State 2 (**B**), State 3 (**C**), State 4 (**D**) and FCCP-uncoupled (**E**) respiration rates was determined. The respiratory control ratio (RCR), an indicator of mitochondrial membrane integrity, was calculated as the ratio between State 3 and State 4 respiration rates (**F**). The ADP/O, which is an index of oxidative phosphorylation efficiency, was calculated as the ratio between the amount of the amount of ADP phosphorylated and the amount of atomic oxygen consumed during ADP phosphorylation (State 3) (**G**). The CMC of C_{10}TAB is 4.0×10^{-2} M. Data are presented as Mean ± SD of at least 3 independent experiments. One-way ANOVA (Dunnet's post-test): * $p < 0.05$, ** $p < 0.01$ and *** $p < 0.001$, significantly different from the respective control.

were energized with a Complex I substrate (glutamate/malate which generates Complex I substrate, NADH, in the mitochondrial matrix; Fig. 4.8E). Concurrently, a decrease in the ADP-stimulated respiration (State 3) was noticed (Fig. 4.8C). On the other hand, when a substrate for Complex II (succinate) was used instead, the effect upon uncoupled respiration disappeared (Fig. 4.8.E.) and there was a less pronounced decrease in State 3 respiration rate (Fig. 4.8C). This indicates that at very low concentrations C_{10}TAB inhibits the electron transfer at the level of Complex I and, to a lesser extent, interferes with the overall mitochondrial phosphorylation system.

C_{10}TAB also stimulated Sate 2 (Fig. 4.8B) and state 4 respiration (Fig. 4.8D), although at higher concentrations than those needed to inhibit FCCP-stimulated respiration. The increase in State 2 and State 4 respiration rates observed at higher concentrations was more prominent when succinate was used as a substrate, since the severe inhibition of the respiratory chain, namely at Complex I level, may partially hide this outcome in mitochondria energized with glutamate/malate. Stimulation of oxygen consumption during respiratory State 2 and State 4 can be induced either by respiration uncouplers like FCCP, which dissipate the $\Delta\psi_m$ by transporting protons from the intermembrane space into the mitochondrial matrix, or by compounds that somehow diminish the intramitochondrial ATP levels and thus stimulate the phospholylation-coupled proton entry through the ATP synthase (Schonfeld *et al.*, 1988; Fromenty *et al.*, 1990). To distinguish between these two possibilities the proton flux through the F_0 of the ATP synthase was blocked with oligomycin. At the highest surfactant concentration (CMC/3000), oligomycin was not capable of preventing the increase in State 4 respiration rate (percentage of control, 117.83 ± 21.60% in the case of glutamate/malate and 139.83 ± 14.94% for succinate; see Fig. 4.8A), demonstrating that the observed effect is not dependent on the ATP synthase but possibly results from membrane permeabilization to protons and respiration uncoupling.

As expected from the effects on respiratory State 3, C_{10}TAB gradually decreases the RCR during both glutamate/malate and succinate oxidation (Fig 4.8F). However, this effect is more pronounced when a substrate for Complex I is used, a reduction of approximately 78% at the highest concentration in respect to control, versus only 31% in the case of succinate. In addition, even though the ADP/O ratio remained unchanged when mitochondria were energized by a Complex II substrate, 13.33 μM (CMC/3000) of C_{10}TAB produced a significant reduction in the ADP/O ratio comparatively to control, from 2.45 ± 0.31 to 1.55 ± 0.21 (* $p < 0.05$), indicating a compromise of the oxidative phosphorylation efficiency which is consistent with the inhibition of Complex I activity.

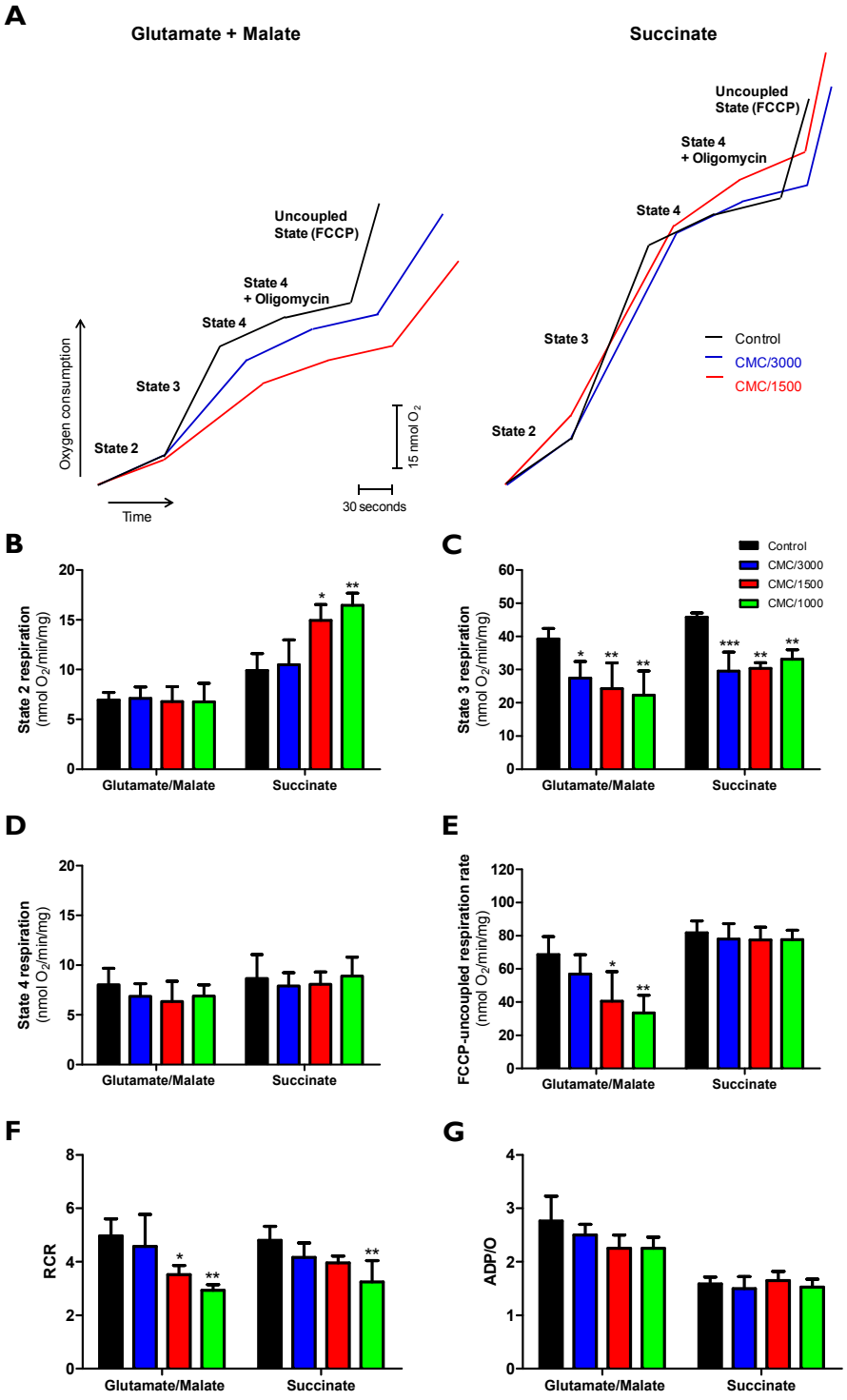

Figure 4.9. Oxygen consumption recording of mitochondria treated with C_{12}TAB. Schematic representation of rat liver mitochondrial oxygen consumption recordings after 5 minutes exposure (**A**). The traces are representative of at least 3 different mitochondrial preparations. The effect of C_{12}TAB on State 2 (**B**), State 3 (**C**), State 4 (**D**) and FCCP-uncoupled (**E**) respiration rates and RCR (**F**) and ADP/O (**G**) ratios was measured. The CMC of C_{12}TAB is 3.5 X 10^{-3} M. Data are presented as Mean ± SD of at least 3 independent experiments. One-way ANOVA (Dunnet's post-test): * $p < 0.05$, ** $p < 0.01$ and *** $p < 0.001$, significantly different from the respective control. For further details see Figure 4.7 legend.

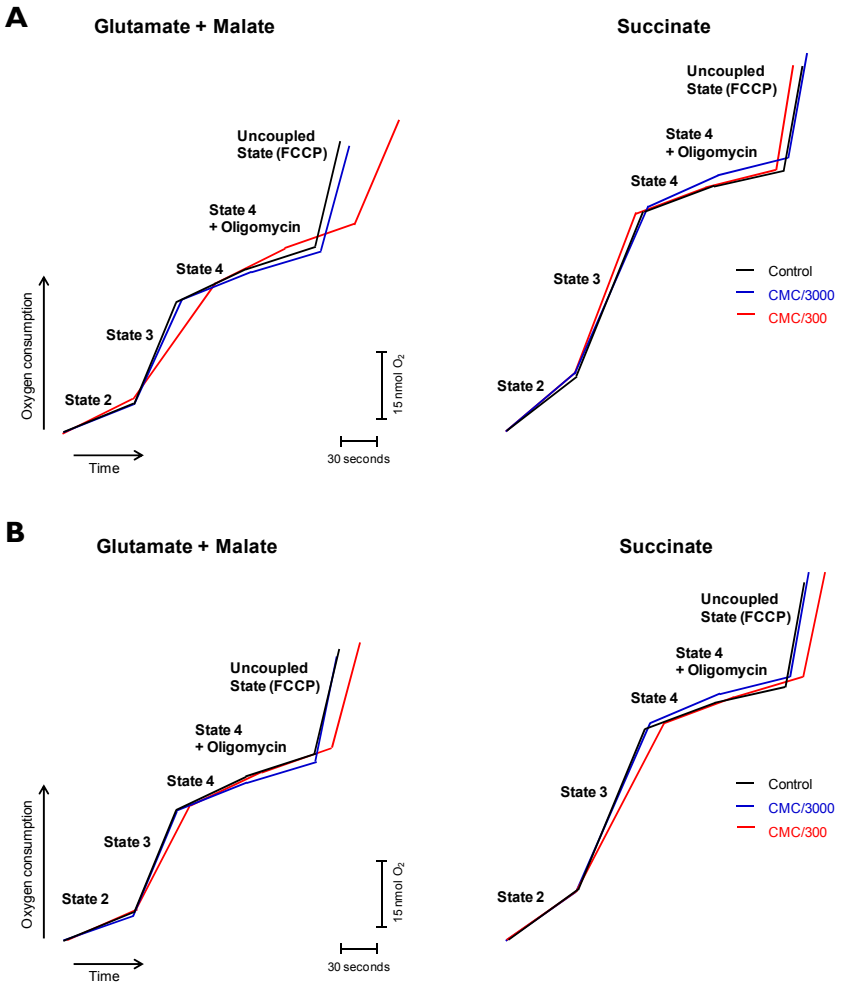

Figure 4.10. Mitochondrial oxygen consumption following C_{14}TAB and C_{16}TAB exposure. Representative oxygen consumption recordings of freshly isolated rat liver mitochondria after 5 minutes incubation with C_{14}TAB (**A**) or C_{16}TAB (**B**). The CMC of the detergents used are: C_{14}TAB, 2.9 X 10^{-4} M and C_{16}TAB, 2.6 X 10^{-5} M. For further details see Figure 4.7 legend.

As can be seen, the concentrations necessary to induce mitochondrial dysfunction in cells were around 10 times higher than those needed to affect respiration in isolated rat liver mitochondria. The simplest explanation for the observed difference between the concentration of C_{10}TAB required to induce toxicity in whole cells and the concentration required to disrupt mitochondrial respiration in isolated mitochondria is that the surfactant partitions equally into all membranes of the cell of which the mitochondrial membrane is only a small fraction. Thus, only a small fraction of the C_{10}TAB added to the whole cells actually gets to their mitochondria.

To elucidate the contribution of surfactant structure on the mechanisms mediating mitochondrial dysfunction, the impact of the hydrocarbon chain length and polar head group structure of the cationic surfactants upon mitochondrial bioenergetics were evaluated. For reasons discussed in Chapter III, Section 3.2.1, the surfactant effects were compared taking into account their respective critical micelle concentrations (CMC).

The effect of hydrocarbon chain length was evaluated using a homologous series of cationic alkyl-N,N,N-trimethylammonium bromides ($C_{10\text{-}16}$TAB). When the hydrophobic chain length was

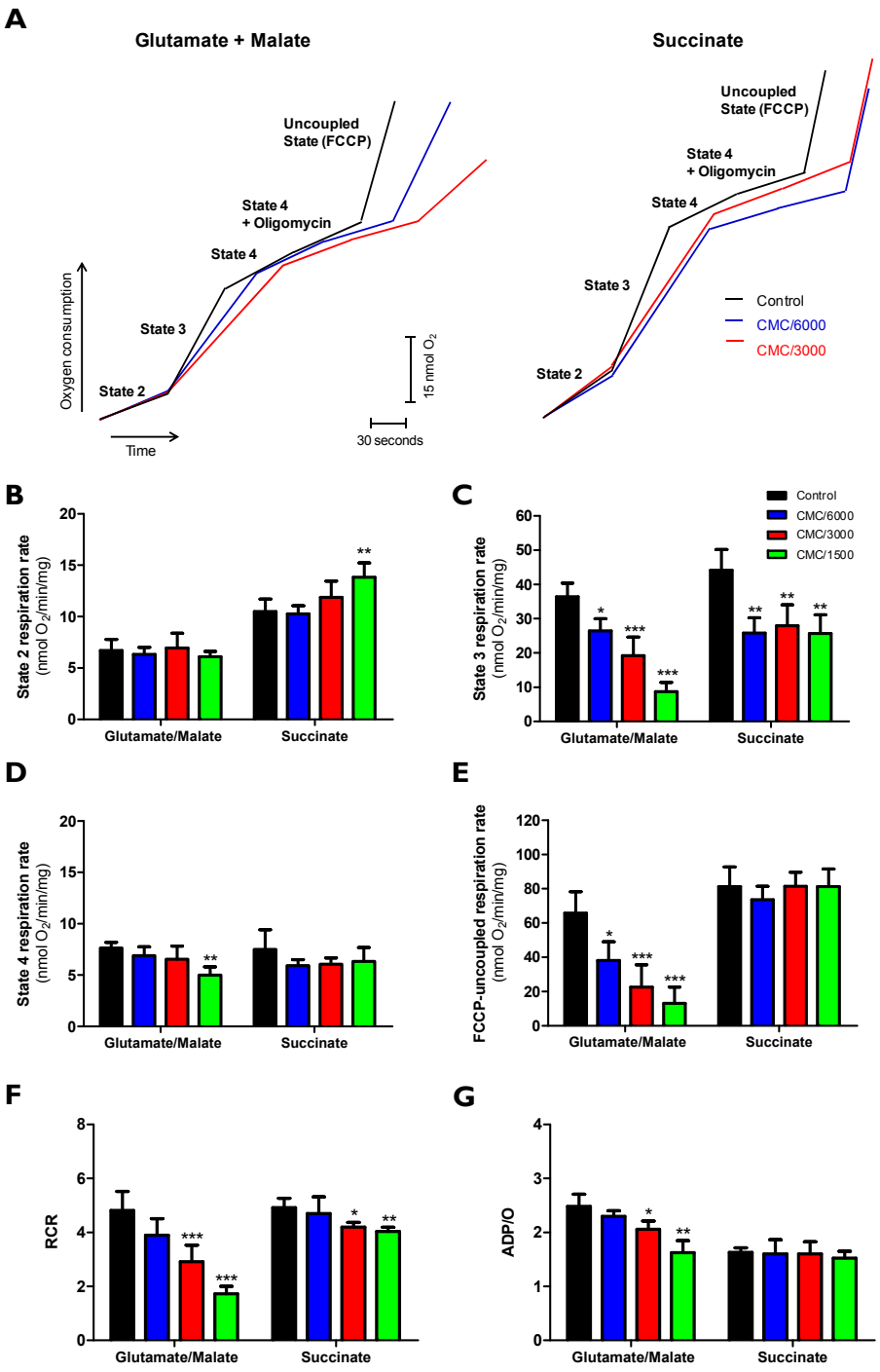

Figure 4.11. Mitochondrial respiratory rates, RCR and ADP/O ratios obtained from rat liver mitochondria incubated with C_{12}PB. Representative oxygen consumption recordings of freshly isolated rat liver mitochondria after 5 minutes incubation (**A**). The effect of C_{12}PB on State 2 (**B**), State 3 (**C**), State 4 (**D**) and FCCP-uncoupled (**E**) respiration rates and RCR (**F**) and ADP/O (**G**) ratios was measured. The CMC of C_{12}PB is 3.9 X 10^{-3} M. Data are presented as Mean ± SD of at least 3 independent experiments. One-way ANOVA (Dunnet's post-test): * $p < 0.05$, ** $p < 0.01$ and *** $p < 0.001$, significantly different from the respective control. For further details see Figure 4.7 legend.

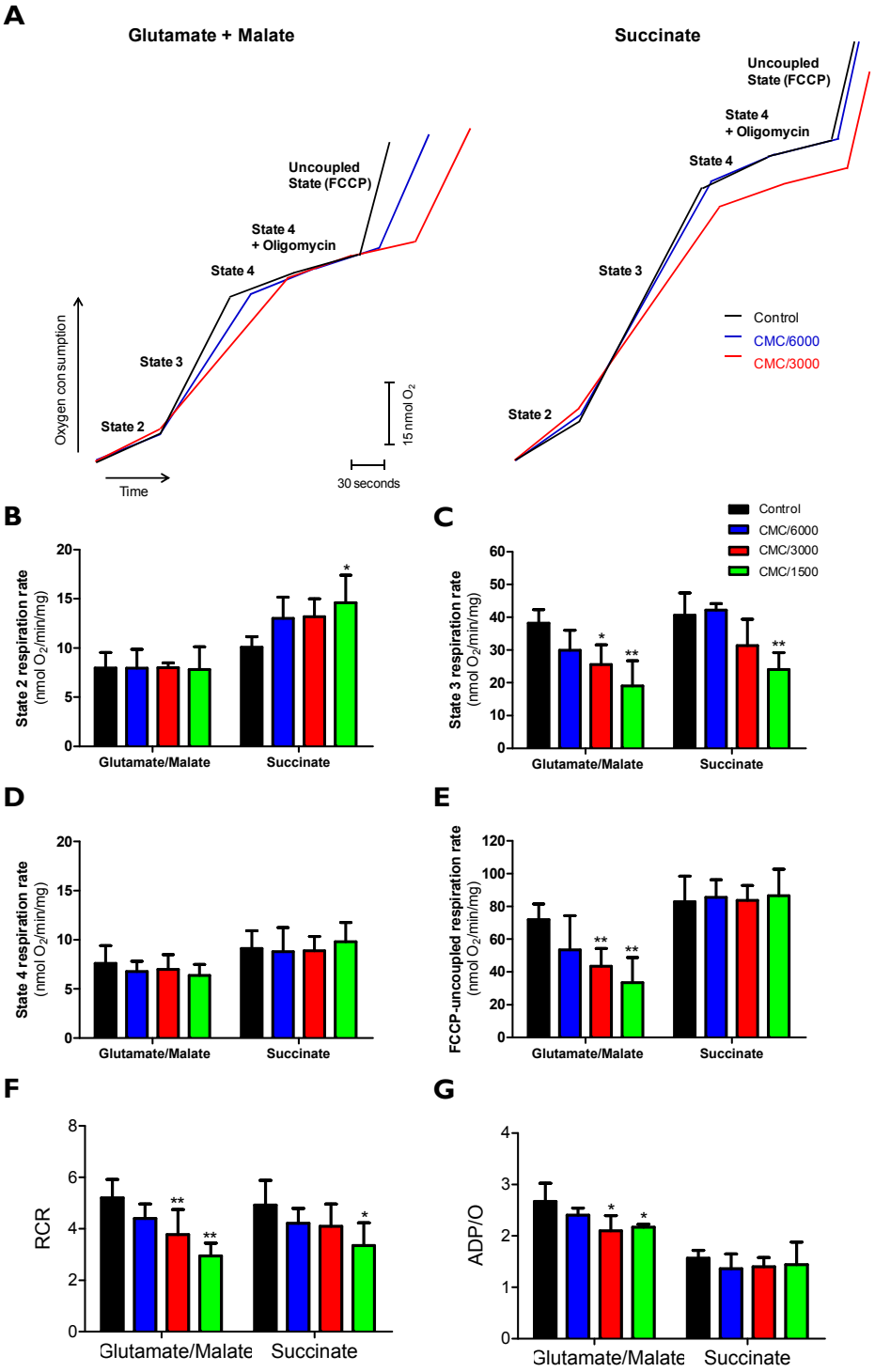

Figure 4.12. Effects of C_{12}BZK on mitochondrial oxygen consumption. Representative traces of rat liver mitochondrial oxygen consumption after C_{12}BKK exposure (**A**). The effect of C_{12}BZK on State 2 (**B**), State 3 (**C**), State 4 (**D**) and FCCP-uncoupled (**E**) respiration rates and RCR (**F**) and ADP/O (**G**) ratios was measured. Data are presented as Mean ± SD of at least 3 independent experiments. The CMC of C_{12}BZK is 1.7×10^{-3} M. One-way ANOVA (Dunnet's post-test): * $p < 0.05$, ** $p < 0.01$ and *** $p < 0.001$, significantly different from the respective control. For further details see Figure 4.7 legend.

two carbons longer than in the case for C_{10}TAB, that is, 12 instead of 10 carbons, the results obtained were quite similar (Fig. 4.9), although a greater amount of C_{12}TAB, with respect to CMC, was needed to produce a decrease in the RCR and ADP/O ratios. In addition, differing from the increase in respiratory State 4 observed at higher concentrations of C_{10}TAB, State 4 respiration rate remained unchanged after C_{12}TAB exposure, either during glutamate/malate or succinate oxidation. This suggest that similarly to C_{10}TAB, very low concentrations of C_{12}TAB inhibits the electron transfer at the level of Complex I and interfere with the mitochondrial phosphorylation system, while the uncoupling effect that occurs at higher concentrations, as noticed by an increase in State 2 respiration rate, was less pronounced. A further increase in hydrophobic chain length, to 14 (Fig. 4.10A) or 16 carbons (Fig. 4.10B), produced similar effects as those observed for C_{12}TAB, yet concentrations at least 10 times higher (relative to CMC) were needed to produce the same results. The simplest explanation for these quantitative differences is that the total concentration of cationic surfactant in the membrane is lower for the amphiphiles with longer hydrophobic chain. Within a given homologous series of surfactants the CMC is inversely proportional to the length of the hydrophobic chain, decreasing by around 10 times with the addition of every 2 carbons (Holmberg *et al.*, 2003; see Table 3.1, Chapter III, Section 3.2.1), so, for example, the absolute concentration of C_{12}TAB is 10 times lower than the absolute concentration of C_{10}TAB. Moreover, although the partitioning into the membranes is more favorable for C_{12}TAB than for C_{10}TAB, this does not totally compensate for the fact that the absolute concentration of C_{12}TAB is 10-fold lower. As a consequence, the concentration of C_{12}TAB in the mitochondrial membranes is lower than that for C_{10}TAB at the same CMC/χ concentration and the effects on the mitochondria will be quantitatively lower.

The impact of cationic surfactants' polar head group on mitochondrial bioenergetics was also evaluated by comparing the effects of different QACs with an identical *n*-alkyl chain of 12 carbons but differing in the size and charge delocalization of the polar head: C_{12}TAB, C_{12}PB and C_{12}BZK (Fig. 4.9, 4.10 and 4.11, respectively). Once again the results obtained were fairly similar only differing in the concentration (relative to CMC) needed to produce an effect. Regarding the reduction of the RCR and ADP/O ratios, the toxicity ranking, normalized with respect to CMC, was C_{12}PB>C_{12}BZK>C_{12}TAB.

Taken together, the described results show that at very low concentrations cationic surfactants act on mitochondrial bioenergetics through a common mechanism of action, which involves the inhibition of the NADH-ubiquinone oxidoreductase (Complex I) and the slowing-down of the mitochondrial phosphorylative system. Moreover, an uncoupling effect becomes relevant as the surfactant concentration increases. This strongly suggests that the positive charge is the major contributor for cationic surfactant-induced mitochondrial dysfunction

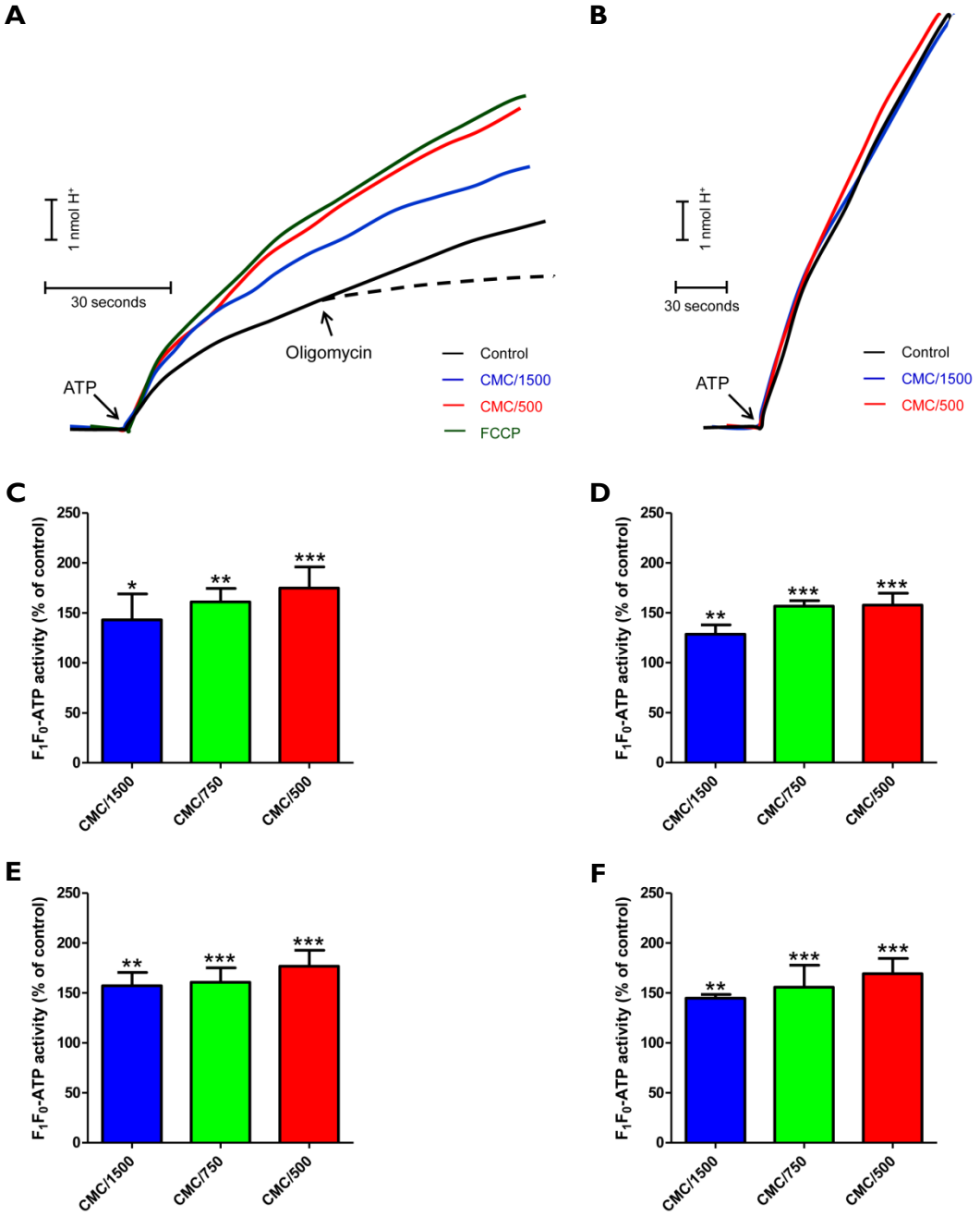

Figure 4.13. Effect of cationic surfactants on the F_1F_0-ATPase activity. Representative recording of the pH changes associated with ATP hydrolysis in freshly isolated rat liver mitochondria (**A**) and disrupted mitochondria (**B**), after 5 minutes of incubation with C_{10}TAB. The ATPase activity was evaluated at 30°C in 1 mL of respiration media (135 mM sucrose, 65 mM KCl, 2.5 mM $MgCl_2$, 2.5 mM KH_2PO_4, 0.5 mM HEPES, pH 7.0), supplemented with 2 µM rotenone. 1 mg of protein was used in each assay and reactions were started by adding 1 mM of Mg-ATP. A control assay was performed in the presence of 1 µM FCCP to induce membrane permeabilization to protons. The addition of 2 µg of oligomycin completely abolished the acidification of the respiration medium. KOH was added at the end of each assay as an internal control. Proton production by intact mitochondria exposed to C_{10}TAB (**C**), C_{12}TAB (**D**), C_{12}PB (**E**) or C_{12}BZK (**F**), was calculated 1.5 minutes after Mg-ATP addition. Control ATPase activity corresponded to 24.07 ± 2.48 nmol H^+/minute/mg protein. Data are expressed as percentage of control and are Mean ± SD of at least 3 independent experiments. One-way ANOVA (Dunnet's post-test): * $p < 0.05$, ** $p < 0.01$ and *** $p < 0.001$, significantly different from control.

and that the concentration of each surfactant necessary to produce similar effects s determined by the partition coefficient of the surfactant into membranes and the rate constants for its insertion into and desorption from membranes as well as its rate of translocation across them.

4.2.6. Exposure to cationic surfactants increases F_1F_0-ATPase activity in isolated mitochondria

The results from the previous Section, namely, the decrease in the ADP/O ratio on glutamate/malate-energized mitochondria, along with a reduction in State 3 respiration rate without changes in the Uncoupled State on the case of succinate-energized mitochondria, indicates that cationic surfactants may exert deleterious effects on the mitochondrial phosphorylation system (i.e. ATP synthase, ADP/ATP translocase, and phosphate translocase). To further explore this hypothesis, the effect of QACs on the F_1F_0-ATPase activity was evaluated by monitoring the pH changes occurring due to ATP hydrolysis[2]. Even though the F_1F_0-ATPase/ATP synthase (F-type ATPase, Complex V) is responsible for the ATP synthesis coupled to proton flux into the mitochondrial matrix, in the absence of an effective proton-motive force it can also operate in the reverse mode, as an ATP-driven proton pump (reviewed in Vinogradov, 1999). Hence, the F_1F_0-ATPase activity can provide an indirect yet reliable measure of the ATP synthase activity, with the additional benefit of, in our experimental conditions, being mostly independent of the electron transfer chain.

The results show that, after 5 minutes of incubation, all cationic surfactants tested increased F_1F_0-ATPase activity in the range of concentrations studied (Fig. 4.13A and C), similar to what is observed during membrane permeabilization to protons by FCCP (191.51 ± 43.71% of control). On the other hand, the ATPase activity in disrupted mitochondria (see Chapter II, Section 2.4.9) incubated with the same surfactant concentrations for 5 minutes shows no differences in terms of ATP hydrolysis compared to control (Fig. 4.13B), meaning that, for the concentrations tested, cationic surfactants do not inhibit the catalytic activity of the F_1F_0-ATPase/ATP synthase. These results are consistent with the increase in State 2 respiration rate observed in succinate-energized mitochondria, further supporting the conclusion that at the highest concentrations employed in the oxygen consumption assays, cationic surfactants may act as uncouplers of the oxidative phosphorylation by increasing membrane permeability to protons. The same uncoupling effect of surfactants may simultaneously favor the increase in the ATPase activity by dissipating the $\Delta\psi_m$.

[2] ATP hydrolysis is accompanied by the production of protons that are released into the respiration medium, causing a decrease in the pH that can be detected using a pH meter.

Another possible explanation for the observed reduction in State 3 respiration rate may be that the presence of the cationic surfactant in the membranes makes the electrostatic surface charge of the membranes more positive and, therefore, reduces the effective proton concentration in the Gouy-Chapman ionic cloud above the membrane surface (Vaz *et al.*, 1978). As a consequence, ATP synthase will be working at a lower basal rate. Furthermore, although it was not tested, there are other elements of the phosphorylative system, such as the adenine nucleotide translocase and the phosphate translocase, which can possibly be affected by cationic surfactants, since both transporters are dependent on the $\Delta\psi_m$ and, as already mentioned, cationic surfactants dissipate or otherwise reduce the trans-membrane electrical potential.

4.3. Discussion

The microbicidal activity of cationic surfactants has been recognized for many years and these molecules have been widely used as antiseptics and disinfectants. Despite the mechanisms mediating cationic surfactant toxicity not been fully understood, particularly at concentrations below the CMC, it is well established that beyond a threshold concentration surfactants can elicit cytotoxic effects. Therefore, the study of the relation between cationic surfactant structure and its toxic effects as well as an understanding of the sequence of events underlying surfactant-mediated cell death is essential for the advancement of research on potential therapeutic uses of surfactants. Regarding the use of surfactants for topical applications, epithelial cells are the first ones to be in contact with these molecules, thus, in the present study, a cell line that mimics a "tight epithelia" (MDCK II cells) was used as an *in vitro* model to study cationic surfactants toxicity mechanisms.

Several reports have already established how high concentrations of cationic surfactant (close to CMC) compromise plasma membrane integrity and induce cell necrosis, whereas lower concentrations can lead to cell death by apoptosis (Debbasch *et al.*, 2001; Perani *et al.*, 2001; Yip *et al.*, 2006; Enomoto *et al.*, 2007; Pauly *et al.*, 2009; Nomura *et al.*, 2010). The results presented here show that such a dual effect of cationic surfactants toxicity also occurs in polarized epithelial cells. Above a certain threshold concentration of C_{10}TAB, MDCK II cell viability starts to decrease and the cytotoxic effects become progressively more severe with increasing concentration. The initial loss of cell viability is strongly correlated with caspase 3/7 activation, a hallmark of apoptosis. Moreover, epithelial MDCK II cells undergoing cell death after exposure to cationic surfactants also exhibit morphological changes characteristic of apoptosis, including cell shrinkage, exposure of PS in the outer leaflet of the plasma membrane and nuclear DNA condensation and fragmentation. On the other hand, plasma membrane damage is only detectable after cell incubation with slightly

higher C_{10}TAB concentrations (CMC/15 to CMC/10), as a result of secondary necrosis since characteristic features of apoptosis were simultaneously observed (e.g. caspase 3/7 activation). Lastly, surfactant concentrations closer to CMC (above CMC/5) promptly lead to necrotic cell death without caspase activation.

A distinctive physiological feature between apoptosis and necrosis is the intracellular ATP content: whereas programmed cell death requires a minimal level of ATP to be carried out, necrosis is characterized by a severe disruption of bioenergetics and a consequent rapid ATP depletion (reviewed in Tsujimoto, 1997; Hand & Menze, 2008). Nonetheless, these two types of cell death can occur simultaneously in tissues or cell cultures exposed to the same stimulus, while the prevalence of either is determined by the intensity of the insult (Ankarcrona *et al.*, 1995; Bonfoco *et al.*, 1995; Shimizu *et al.*, 1996; Eguchi *et al.*, 1997; Leist *et al.*, 1997; Feldenberg *et al.*, 1999). In the present study, a gradual decrease in the intracellular ATP levels occurs after 3 hours of incubation with C_{10}TAB. A slight reduction in the intracellular ATP concentration was detected at a concentration of CMC/30, before the appearance of any sign of apoptotic signalling, which indicates that the cell energy status can be affected without commitment to cell death. Still, a further decrease in intracellular ATP below a critical level, sufficient to compromise the normal functioning of the cell, was observed for concentrations above CMC/25 and can be associated with apoptosis. In addition, the ATP-to-ADP ratio is also diminished, which is indicative of a lower ATP resynthesis and/or a higher ATP hydrolisis. Once again, this alteration in the ATP/ADP ratio was detectable prior to any visible sign of commitment to apoptosis. In fact, caspase 3/7 activation was only detectable at surfactant concentrations that that reduced the ATP/ADP ratio by more than 50%. Conversely, C_{10}TAB concentrations close to CMC (e.g. CMC/5 and CMC/3) cause severe ATP depletion and cell necrosis, without detectable morphological and biochemical markers of apoptosis (see Fig. 4.14). Since apoptosis takes place by a concerted action of well regulated processes, including several ATP-dependent reactions, the depletion in ATP may restrict the progression of apoptosis (Eguchi *et al.*, 1997; Leist *et al.*, 1997; Feldenberg *et al.*, 1999). Another possibility is that at concentrations very close to CMC, C_{10}TAB may interact with and denature some of the proteins involved in the apoptotic signalling (reviewed in Otzen, 2011) and/or directly cause membrane destabilization (Isomaa *et al.*, 1986; Bayerl *et al.*, 1989; Xia & Onyuksel, 2000), undercutting the entire apoptotic process in its genesis.

The reduction in the intracellular ATP content in the absence of apoptotic or necrotic features, suggests that mitochondria could be affected by cationic surfactants, given that in mammals this organelle contributes for the generation of 80 to 90% of the total intracellular ATP (reviewed in Szewczyk & Wojtczak, 2002). Moreover, since this decrease in the cellular ATP content precedes the loss of cell viability, mitochondrial dysfunction might be responsible for

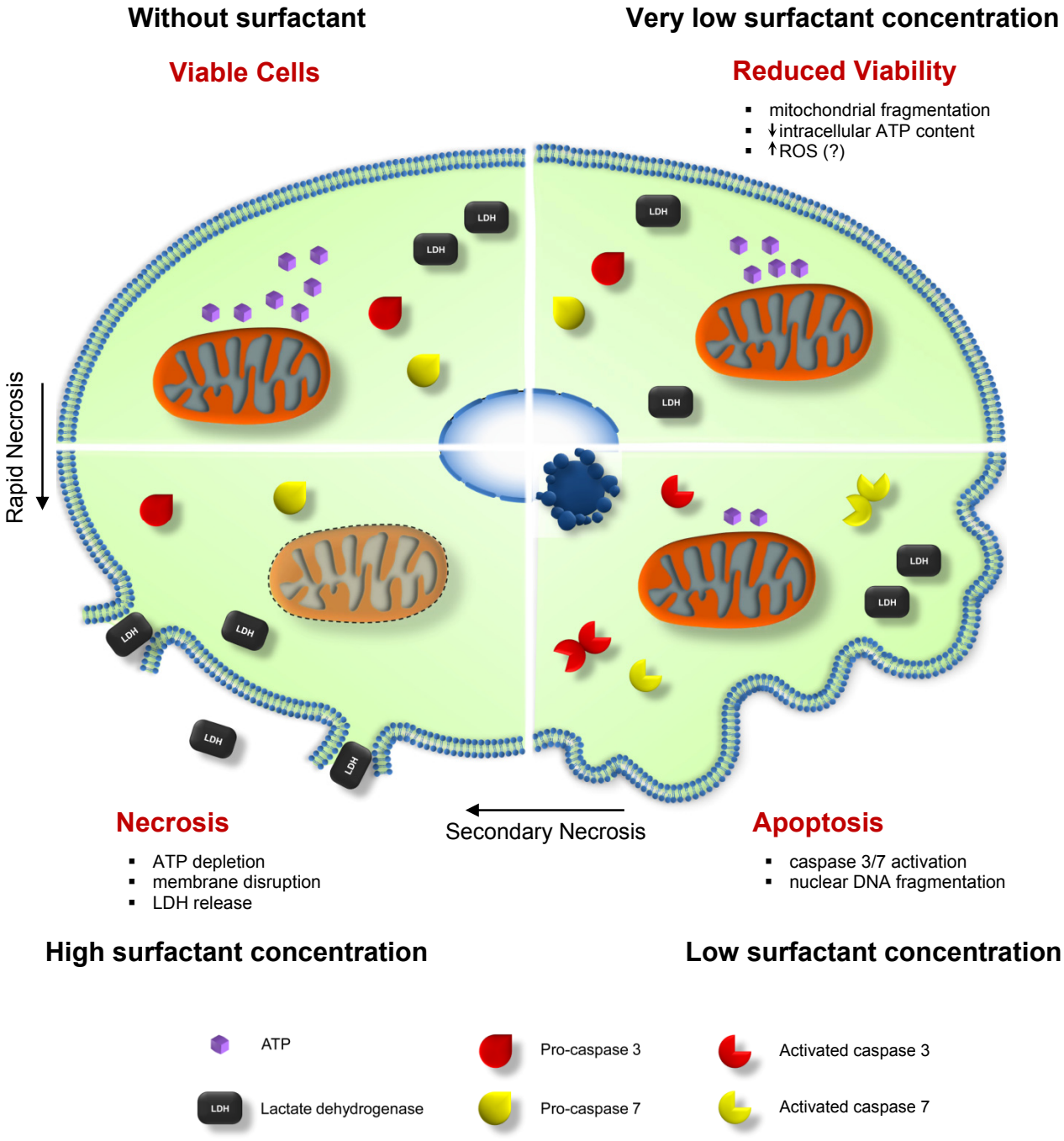

Figure 4.14. Schematic representation of the effects of cationic surfactants on epithelial cells. Cells incubated with very low concentrations of cationic surfactants undergo mitochondrial fragmentation, loss of mitochondrial inner membrane potential and a decrease in the intracellular ATP levels, which leads to a loss of cell viability. The inhibition of mitochondrial NADH-ubiquinone oxidoreductase (Complex I) that is also observed after exposure to very low concentrations of surfactants may induce an increase in ROS production. Increasing the surfactant concentration or the duration of exposure will culminate in cell apoptosis. On the other hand, high concentrations of surfactant, close to CMC, disrupt cell membranes directly causing necrosis.

triggering cell death. In fact, the cationic surfactants cetyltrimethylammonium bromide (C_{16}TAB) and nonyltrimethylammonium bromide have been shown to quickly accumulate in the matrix of isolated mitochondria (approximately 5 minutes), driven by the membrane potential (Bragadin & Dell'Antone, 1996), and several authors have suggested the involvement of mitochondrial dysfunction in surfactant-induced apoptosis (Yip *et al.*, 2006; Levine *et al.*, 2007). Bragadin and Dell'Antone (1996) have also shown that the accumulation of cationic surfactants in mitochondria dissipated the $\Delta\psi_m$ and led to a decline in ATP synthesis.

The functional status of mitochondria is dependent on the mitochondrial inner membrane potential, since most mitochondrial functions rely on the electrochemical gradient across the inner membrane (e.g. ATP synthesis and Ca^{2+} homeostasis; reviewed in Brookes *et al.*, 2004). This electrochemical gradient, also known as the proton-motive force, is generated by the ejection of protons from the mitochondrial matrix to the intermembrane space by the respiratory chain Complexes I, III and IV, a process that is made energetically possible by the large negative free energy change resulting from electron transfer to successive electron acceptors in the redox chain (reviewed in Papa *et al.*, 2012). The proton-motive force (Δp) has two components: the electrical potential across the membrane ($\Delta\psi_m$), which arises from the net movement of positive charge across the inner mitochondrial membrane, and the pH gradient (ΔpH). Under physiological conditions most of the proton-motive force generated in the mitochondria is in the form of a $\Delta\psi_m$ (reviewed in Chen, 1988). Accordingly, the $\Delta\psi_m$ can be used as an indicator of mitochondrial redox potential, which also reflects cell health. The results presented here show that a progressive decrease in the intracellular ATP levels was observed in tandem with a dissipation of $\Delta\psi_m$, already visible at sub-lethal concentrations (i.e. CMC/30) and prior to caspase 3/7 activation. Nonetheless, surfactant toxic effects possibly resulting from mitochondrial impairment only become evident at higher concentrations (i.e. around CMC/25), possibly a result of MDCK II cells having the basal glycolytic pathway stimulated, which may, thus, partially compensate for the failure in the mitochondrial phosphorylative system (Pampaloni *et al.*, 2010)[3].

Besides the decrease in $\Delta\psi_m$, surfactants also induced loss of mitochondrial connectivity and disintegration of the reticulo-tubular structures, giving rise to a wide spread reorganization into small and round mitochondria. Furthermore, fluorescence microscopy analysis revealed that mitochondrial fragmentation occurred after a short period of exposure to very low doses of C_{10}TAB (e.g. 1 hour exposure to CMC/300). After 1 or 3 hours of exposure to C_{10}TAB concentrations raging from CMC/300 to CMC/100, mitochondrial fragmentation was prominent

[3] Pampaloni and colleagues (2010) have shown that aerobic glycolysis is increased in MDCK II cells grown in flat 2-D uncoated plastic surfaces, similar to the culture conditions in the present work, when compared to cells grown in a 3-D collagen gel, which better mimics physiological conditions.

but neither a collapse of the mitochondrial membrane potential (i.e. treated cells still maintained Rh123 fluorescence) nor a compromise of the cells' energy status were observed. These results highlight mitochondrial fragmentation as one of the earliest manifestations of surfactant-induced toxicity. In addition, although mitochondrial fragmentation can occur without activation of programmed cell death, it has been reported that in the case of many apoptotic stimuli mitochondrial fragmentation works as an early triggering step in programmed cell death (reviewed in Karbowski & Youle, 2003; Kiefel *et al.*, 2006). For instance, proteins involved in the control of mitochondrial morphology appear to also participate in apoptosis and, conversely, proteins belonging to the apoptotic machinery also affect mitochondrial fusion and fission (Frank *et al.*, 2001; Karbowski *et al.*, 2004; Gomez-Lazaro *et al.*, 2008).

The mitochondrial morphological alterations observed after incubation with C_{10}TAB occur gradually, and its severity depends on the surfactant concentration and the duration of exposure. In all the concentrations tested, mitochondrial fragmentation was more severe after 3 hours of exposure compared to 1 hour. The shift from a highly branched to a fragmented mitochondrial network is mostly regulated by the rates of fission and fusion events. Indeed, mitochondrial fragmentation can result from both inhibition of fusion and/or an increase in the fission rate (Bleazard *et al.*, 1999; Sesaki & Jensen, 1999). The mechanisms that regulate mitochondrial morphology are not fully understood, yet there is strong evidence concerning the role of the lipid membrane environment (e.g. membrane curvature) in the modulation of the activity of some components of the machinery involved in the fusion process (reviewed in Soubannier & McBride, 2009). As previously reported by others, insertion of cationic surfactants into lipid bilayers may alter some of the membrane properties, such as, lateral packing and pressure, membrane curvature and membrane stored elastic stress (Balgavý *et al.*, 1984; Cirak *et al.*, 1988; Gallova *et al.*, 1990; Dymond & Attard, 2008; Heerklotz, 2008), interfering in this way with the activity of membrane-bound proteins (Cantor, 1997, 1999; Jensen & Mouritsen, 2004; Andersen & Koeppe, 2007). It is then possible that alterations in the mitochondrial membrane biophysical properties may result in the mitochondrial fragmentation observed after exposure to C_{10}TAB.

Changes in the mitochondrial network similar to the ones here described were observed after acute inhibition of Complex I with rotenone treatment (Koopman *et al.*, 2006; Benard *et al.*, 2007) and mitochondrial inner membrane depolarization by protonophores (Legros *et al.*, 2002). However, depending on the duration of the stimulus, after its removal mitochondria were able to reestablish the $\Delta\psi_m$, which was sufficient to allow a rapid recovery of the typical reticular arrangement of mitochondria of healthy cells. Even though the physiological significance of mitochondrial dynamics is not completely understood, growing evidence strongly suggests that the dynamics of mitochondrial morphology, regulated by fission and fusion events, reflects

mitochondrial energetic status (Benard *et al.*, 2007; Plecita-Hlavata *et al.*, 2008) and is crucial for key cellular functions (Brocard *et al.*, 2003; Chen & Chan, 2005; Chen *et al.*, 2005; Chan, 2006; Kiefel *et al.*, 2006). It is possible that, even if reversible, the mitochondrial morphological alterations induced by C_{10}TAB may impair epithelial cells physiology at sub-lethal concentrations, making cells more susceptible to other sources of stress.

Regarding the effects of cationic surfactants on standard respiratory parameters of isolated rat liver mitochondria, all the compounds tested inhibit electron flow from reduced substrates to oxygen due to inhibition of the NADH-ubiquinone oxidoreductase (Complex I), while also interfering with the mitochondrial phosphorylative system at very low concentrations (e.g. from CMC/6000 to CMC/1500 depending on the surfactant). Furthermore, as the concentration increases, up to CMC/1000, an uncoupling effect is also observed, as measured by a decrease in RCR ratios and by the increase in State 2 respiration rate, particularly evident when succinate was used for providing reducing equivalents directly to the succinate dehydrogenase (Complex II). These results are in agreement with a report by Rogers and Higgins (1973), who have also demonstrated that low concentrations of quaternary ammonium compounds inhibited electron transfer whereas high concentrations of the same compounds exerted an uncoupling effect. Moreover, these authors also detected a predominant effect on mitochondrial Complex I. This strongly suggests that the positive charge is the major contributor for cationic surfactant-induced mitochondrial dysfunction. Abnormalities in the properties of mitochondrial membranes have been reported to reduce electron flow from Complex I to Complex III, without affecting neither the electron transport from Complex II to Complex III nor the individual activity of mitochondrial Complex I, III or IV (Ellis *et al.*, 2005). As already mentioned, cationic surfactants insertion into biological membranes perturbs the membrane dynamics (Pantaler *et al.*, 2000; Dymond & Attard, 2008), which may justify the preferential effects of these compounds on Complex I.

In glutamate/malate-energized mitochondria, the mitochondrial phosphorylation efficiency is clearly affected in the presence of surfactants as inferred from either the decrease in the RCR and ADP/O ratios as from the inhibition of State 3 respiration rate. Although cationic surfactants appear to have more prominent effects on mitochondrial bioenergetics when Complex I substrates are used, succinate-sustained respiration is also inhibited (e.g. decrease in RCR and respiratory State 3), suggesting a broader range of targets in the respiratory chain. The observed reduction in intracellular ATP levels suggests that ATP synthase, the constituent of the phosphorylative system responsible for the production of ATP, might be affected by the surfactants. Notwithstanding, the ATPase activity in disrupted mitochondria was found to be unaffected by surfactants, indicating that at the concentrations tested these compounds do not directly impact the ATP synthase/ATPase. These results are in striking contrast with reports by

others showing that cationic surfactants inhibit the catalytic activity of the ATPase in an irreversible manner (Bârzu *et al.*, 1989; Datiles *et al.*, 2008; Ito *et al.*, 2009). However, it is important to state that the concentrations used in these works were very high, close or above the CMC, and which makes it likely that the observed effect was due to protein denaturation (reviewed in Otzen, 2011).

The ATPase activity in isolated intact mitochondria was stimulated in the presence of cationic surfactants, similarly to what is observed in the presence of the FCCP protonophore, reinforcing the hypothesis that at the higher concentrations tested surfactants increase the membrane permeability to protons by acting as uncouplers. Nonetheless, the positive charge of these compounds excludes the possibility that they may act as conventional protonophores, which are capable of accepting and discharging protons and, in this way, to work as lipophilic proton carriers. Hence, the uncoupling effect of surfactants probably results from structural or conformational alterations of the mitochondrial inner membrane. In fact, Pantaler and colleagues (2000) have demonstrate that at membranar threshold concentrations, well below CMC (at least 5 times below CMC in the case of C_{14}TAB to almost 40 times in the case of C_{10}TAB), C_nTAB surfactants (C_8-C_{14}) accelerate the flip-flop rate of NBD-labeled phosphatidylcoline from the outer to the inner membrane leaflet of red blood cells in a concentration-dependent manner, resulting in membrane expansion and increased membrane leak.

Complex I inhibition is often linked to an increase in the production of reactive oxygen species (ROS) (Li *et al.*, 2003; Benard *et al.*, 2007; Pereira *et al.*, 2007). Even though ROS production was not evaluated in the present work, the decrease in the ADP/O ratio observed when Complex I substrates were used, implies that cationic surfactants may stimulate the formation of ROS. Indeed, previous reports have shown that cationic surfactants, such as benzethonium chloride and benzalkonium chloride, are able to induce ROS production (Debbasch *et al.*, 2001; Enomoto *et al.*, 2007; Wu *et al.*, 2011). At the cellular level, ROS plays an important role in modulation of cell differentiation, cell cycle arrest and apoptosis (Allen & Tresini, 2000; Shackelford *et al.*, 2000; Wang *et al.*, 2008). Furthermore, a recent work by Geiger-Maor and colleagues (2012) demonstrated that normal healthy fibroblasts exposed to sub-lethal doses of oxidative stress release chemotactic signals that selectively attract monocytes and macrophages. Taking into account that in our experimental model mictochondrial dysfunction is already visible at sub-lethal doses, it is possible that a similar effect as that described by Geiger-Maor and colleagues may occur in recurrent exposures of epithelial cells to sub-lethal doses of cationic surfactants. Such considerations are of great importance concerning the possible application of these compounds in microbicide vaginal gels. For example, it is possible that excessive ROS production in addition to occasional cell death by necrosis may incite a pro-inflammatory response, which

could, among other ailments, increase the risk of infection by sexually transmitted pathogens. Specifically, a pro-inflammatory response may damage the vaginal mucosa and provide to HIV a direct access to the *lamina propria* where virus target cells are more abundant, increasing the risk of infection (Galen *et al.*, 2007).

In conclusion, the present work demonstrates that mitochondrial dysfunction is an early event in cationic surfactant-induced toxicity, already starting at sub-lethal concentrations, and characterized by mitochondrial fragmentation accompanied by decreased cellular energy charge at higher concentrations. Equally important, the results obtained on isolated mitochondrial fractions demonstrate that all the compounds tested acted by a common mechanism that involves the inhibition of the NADH-ubiquinone oxidoreductase (Complex I) and the hampering of the mitochondrial phosphorylative system. These results provide insights on the mechanism by which cationic surfactants interfere with epithelial cells viability and highlight the importance of including a rigorous assessment of mitochondrial function and cytotoxicity when evaluating new microbicide candidates.

Chapter V

Comparative antimicrobial activity of monoalkyl quaternary ammonium surfactants

Summary

Comparative antimicrobial activity of monoalkyl quaternary ammonium surfactants

5.1. Introduction

In recent years, the remarkable increase in multi-drug resistant pathogens, together with the lack of effective vaccines[4], makes the prevention of sexually transmitted infections (STIs) a challenge. Currently available options for prevention of STIs, including HIV, are essentially limited to condoms (Davis & Weller, 1999; Weller & Davis, 2002). However, gender power imbalances in sexual partnerships, particularly in developing countries, urges the development of prevention methods that can be used by women without requiring the partner's consent. Safe and effective topical microbicides, such as vaginal gels, represent one of the most promising prevention strategies.

Early research on potential vaginal microbicides was focused in broad-spectrum compounds such as surfactants. In the past two decades there have been a great number of reports concerning surfactants virucidal and bactericidal activity against sexually transmitted pathogens, such as *Chlamydia trachomatis* and *Neisseria gonorrhoeae*, and its utilization for prevention of STIs (to name a few: Bolch & Warren, 1973; Kelly *et al.*, 1985; Patton *et al.*, 1992; Wyrick *et al.*, 1997; Krebs *et al.*, 1999; Belec *et al.*, 2000). A recent work from our laboratory has demonstrated that although incapable of inhibiting viral infection at sub-lethal concentrations, cationic surfactants may function as bactericides at concentrations that are not harmful to polarized mammalian epithelial cells (Vieira et al., 2008). Since untreated STIs enhance both the acquisition and transmission of HIV by a factor of up to 10, effective prevention and treatment of bacterial and protozoal STIs can be an important HIV prevention strategy (reviewed in Fleming & Wasserheit, 1999; Mayaud & McCormick, 2001; Galvin & Cohen, 2004), justifying a more detailed study of the biological mechanisms responsible for both surfactant microbicidal activity as well as for its toxic effects, in order to improve their efficacy.

Given the amphiphilic nature of surfactants, their microbicidal activity is generally attributed to their interaction with biological membranes, altering their physical properties, such as lateral packing, surface hydration, membrane curvature and elasticity, surface charge, and ultimately

[4] Currently, the only STI vaccine available is for high-risk types of human papillomavirus.

membrane integrity (Hamilton, 1968; Tomlinson *et al.*, 1977; Vieira & Carmona-Ribeiro, 2006; Ioannou *et al.*, 2007; Dymond & Attard, 2008). Distinct chemical composition, physical properties and physiological functions of pathogens and host cells, as well as the total amount of membrane per cell, may result in different sensitivities to the harmful effects of surfactants at concentrations below CMC, which, consequently, can be exploited as a means of obtaining compounds with selective toxicity. Therefore, in the present study the effects of concentration, exposure time and chemical structure on the antibacterial activity of cationic surfactants were evaluated and compared with the toxic effects on epithelial polarized cell lines, in order to determine which surfactant properties favor the highest antibacterial efficacy without compromising mammalian cells integrity. Infections with *Chlamydia trachomatis* and *Neisseria gonorrhoeae*, both Gram-negative bacteria, are not only the two most common bacterial STIs, but also the most prevalent in co-infections with HIV (Creighton *et al.*, 2003; World Health Organization, 2007). To this end, *Escherichia coli*, a Gram-negative bacteria, was chosen as a model for evaluating the bactericidal activity of a homologous series of commercially available *n*-alkyl-N,N,N-trimethylammonium bromides - C_nTAB with *n* from 10 through 16 - and a series of quaternary ammonium compounds (QACs) of 12 carbons hydrophobic chain length with different chemical head groups - C_{12}TAB, N-dodecylpyridinium bromide (C_{12}PB), and dodecyl-N-benzyl-N,N-dimethylammonium bromide (C_{12}BZK). Given that *E. coli* is a well characterized and easy to grow bacteria, it provides a reliable model for studying the effects of cationic surfactants on Gram-negative bacteria.

5.2. Results

5.2.1. Antimicrobial activity of cationic surfactants

The minimal inhibitory concentration (MIC) corresponds to the lowest concentration of an antimicrobial agent that prevents visible growth of a microorganism under defined conditions. It is one of the simplest techniques of measuring the susceptibility of microorganisms to antimicrobial agents, requiring only a period of overnight incubation. For this reason, the effect of cationic surfactant chemical structure on the antibacterial activity against *E. coli* was first investigated by determining surfactant MIC using the broth macrodilution method (Wiegand *et al.*, 2008). The MIC results are summarized in Figure 5.1A. Concerning the absolute concentrations needed to inhibit *E. coli* cell growth, the results show that C_nTAB surfactants with longer hydrophobic chains (i.e. C_{14}TAB and C_{16}TAB) inhibit bacterial growth more efficiently than their shorter homologues, which is in accordance with previous reports (Domagk, 1935; Hoogerheide, 1945; Daoud *et al.*, 1983; Gilbert & Al-taae, 1985; Balgavy & Devensky, 1996). Similar toxicity patterns have been

A

Surfactant	MIC (mM) for an initial inoculum size of	
	1.5 X 10^5 CFU/mL	1.5 X 10^8 CFU/mL
C_{10}TAB	2.857	3.077
C_{12}TAB	0.318	0.350
C_{14}TAB	0.072	0.097
C_{16}TAB	0.052	0.078
C_{12}BZK	ND	0.013
C_{12}PB	ND	0.047

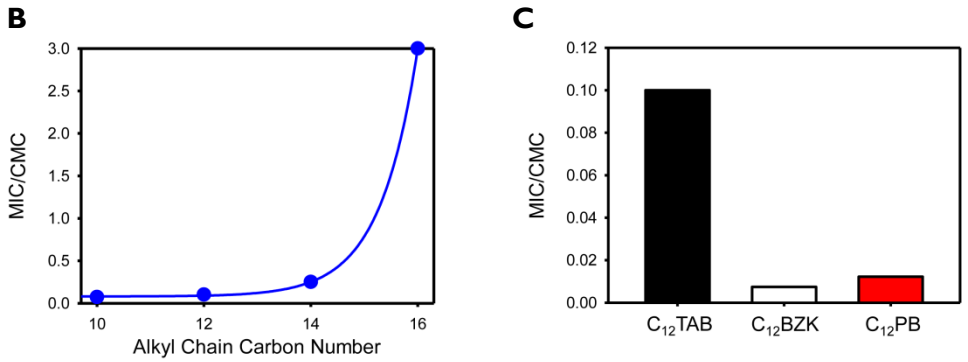

Figure 5.1. Minimal inhibitory concentration (MIC) of cationic surfactants against *E. coli*. Two inocula with different initial size were prepared from late logarithmic phase growing bacteria. The MICs were estimated by the broth macrodalution method and recorded as the lowest surfactant concentration at which no visible growth was observed after overnight incubation at 37°C (**A**). All experiments were repeated at least three times. In order to evaluate the effect of the hydrophobic chain length (**B**) and of the polar head structure (**C**) on the antibacterial efficacy of cationic surfactants, the MICs obtained for the highest initial inoculum size were normalized to the respective CMC (see details in the text). ND, not determined.

described regarding the antifungal activity of C_nTAB surfactants against *Candida albicans* (Ahlström et al., 1997), as well as for the fungicidal and bactericidal activity of other QACs homologous series, such as amphiphilic betaine esters with a chain length of C_{10}-C_{14} (Ahlström *et al.*, 1997; Ahlström *et al.*, 1999) or 1-alkyl-2-(4-pyridyl)pyridinium bromides (Denny *et al.*, 2005). Nonetheless, earlier studies showing the correlation between cationic amphiphiles hydrophobic chain length and its antibacterial activity have not taken into account the possible role played by the propensity of different surfactants to form micelles and in an indiscriminate way disrupt cell membranes above the the critical micelle concentration (CMC). Since within the homologous series of C_nTAB surfactants ranging from 10 to 16 carbons the CMC varies by a factor of as much as 1000 (see Table 3.1, Chapter III, Section 3.2.1), the contribution of the micelle formation to the bactericidal efficacy should not be overlooked. In view of the fact that the antimicrobial activity of surfactants is dependent on the thermodynamics of amphiphiles partitioning into the bacterial membranes, which is reflected in the CMC, the surfactant effects were once again compared taking into account their respective CMC (for further details see Chapter III, Section). As shown in Figure 5.1B, for the homologous series of cationic surfactants examined, the antimicrobial activity against *E. coli* exponentially decreases with the increase in surfactant hydrophobic chain

length. The toxicity ranking of the C_nTAB surfactants normalized with respect to CMC was C_{10}TAB>C_{12}TAB>C_{14}TAB>C_{16}TAB. It should be noted how when evaluating the antibacterial activity of cationic surfactants relative to its absolute concentration one would observe the opposite trend (a decrease in toxicity as one moves from C_{16}TAB to C_{10}TAB), highlighting the importance of normalizing the toxicity data relative to CMC in order to account for more specific mechanisms of toxicity and, therefore, of greater therapeutic relevance. As a matter of fact, although C_{16}TAB inhibits bacterial cell growth at very low concentrations, this antibacterial effect is observed at concentrations 2 or 3 times above the CMC (depending on the initial inoculum size), suggesting that it probably causes structural changes at the level of the membrane or even its dissolution, as expected at such concentrations. For this reason C_{16}TAB was not used in further assays. On the other hand, the remaining C_nTAB surfactants most likely exert toxic effects through one or several more subtle mechanisms, since their antibacterial activity occurs at concentrations below the CMC. Most important, this correlation is not observed in polarized mammalian epithelial cells (MDCK II and Caco-2 cell lines, see results from Chapter III), where all C_nTAB surfactants were toxic at concentrations below the CMC and the toxicity ranking with respect to CMC was C_{10}TAB≥C_{12}TAB>C_{16}TAB>C_{14}TAB. In what follows concentrations will always be expressed as concentrations normallized with respect to the CMC (i.e. [surfactant]/$CMC_{(surfactant)}$).

The effect of the polar head group of the cationic surfactants was also evaluated by comparing the antimicrobial activity of three surfactants with a 12 carbon *n*-alkyl chain: C_{12}TAB, C_{12}BZK and C_{12}PB. As in the case of mammalian cells, C_{12}BZK and C_{12}PB, which have larger polar head groups, are more toxic to *E. coli* than C_{12}TAB (Fig. 5.1C). While it may be true that qualitatively the susceptibility pattern was the same, in the case of mammalian polarized epithelial cells C_{12}BZK and C_{12}PB are between 2 to 5 times more toxic comparing to C_{12}TAB, whereas in the case of *E. coli* C_{12}PB and C_{12}BZK are around 8 and 15 times, respectively, more efficient in inhibiting bacterial cell growth than C_{12}TAB.

One of the critical factors that can affect the MIC is the inoculum size (Brown, 1988; Lambert, 2000; Wiegand *et al.*, 2008). For example, a 100-fold increase in the initial inoculum size has been reported to induce an eightfold or greater MIC increase when testing β-lactam antibiotics susceptibility in bacteria isolates that are able to produce β-lactamases which inactivate the tested antibiotics (Thomson & Moland, 2001). On the other hand, the use of a too small inoculum can lead to false susceptible results (Granier *et al.*, 2002). For this reason, in order to examine whether the inoculum size had an effect on the inhibition of bacterial cell growth, observed with respect to surfactant concentration, two inocula with a 1000-fold difference in their initial size were used. As can be seen in Figure 5.1A, a 1000-fold increase in the inoculum size had

a minor impact on the MIC. Further studies were performed using an initial inoculum size of 1.5 X 10^8 CFU/mL.

5.2.2. Effect of cationic surfactants structure on the bactericidal activity against *Escherichia coli*

Although the MIC is widely accepted as a measure of the antimicrobial activity of a drug, it does not give an indication whether the antimicrobial agent is exerting a bactericidal or bateriostatic action. Furthermore, if the cationic surfactants tested had a bateriostatic effect, bacteria may still be viable at the MIC and resume growth after surfactant removal. For that reason, a screening of the bactericidal activity of cationic surfactants against *E. coli* was carried out by cultivation and enumeration of colony forming units (CFU). To gain a deeper understanding of the bactericidal activity of cationic surfactants, a concentration dependent study was carried out by exposing bacterial cells to a wide range of surfactant concentrations for 10, 20, 60 and 120 minutes in LB medium.

Figure 5.2 shows the dose-response toxicity plots for C_{10}TAB-C_{14}TAB and C_{12}PB. A biphasic dose-toxicity curve was observed in *E. coli* exposed to C_nTAB surfactants, strongly suggesting that there are at least two distinct processes responsible for cationic surfactant bactericidal activity. For instance, in the case of C_{10}TAB, there is a clear difference between one toxicity process, which is visible at higher concentrations, and a second one, which occurs at lower concentrations, being both separated by a plateau at intermediate concentrations. Furthermore, with increasing duration of exposure to C_{10}TAB a shift occurs, and the second toxicity process becomes predominant over the first one, increasing from a fractional contribution of 0.33 at 20 minutes to 0.67 after 120 minutes of incubation (Fig. 5.2B). However, the separation between the two phases of the toxicity curve becomes less pronounced with the increase in the size of the hydrophobic chain, while the fractional contribution of the curve describing the toxicity observed at higher concentrations (Process 1) is still dominant even after 120 minutes of exposure. Moreover, in the case of C_{14}TAB the second toxicity process only appears for longer incubation periods (i.e. 60 and 120 minutes).

Given that the dose-response toxicity curves exhibit a biphasic sigmoid shape instead of a monotonic sigmoid profile, as in the case for mammalian cells (see Chapters III and IV), a combination of two logistic equations was adjusted to the data. From the analyses of the toxicity curves it was possible to calculate the lethal dose 90 (LD_{90}), lethal dose 50 (LD_{50}) and lethal dose 10 (LD_{10}), surfactant concentrations at which the viability of culturable bacteria was, respectively, 10%, 50% and 90% of the control for each time point (Table 5.1). The LD *vs.* exposure-time curves

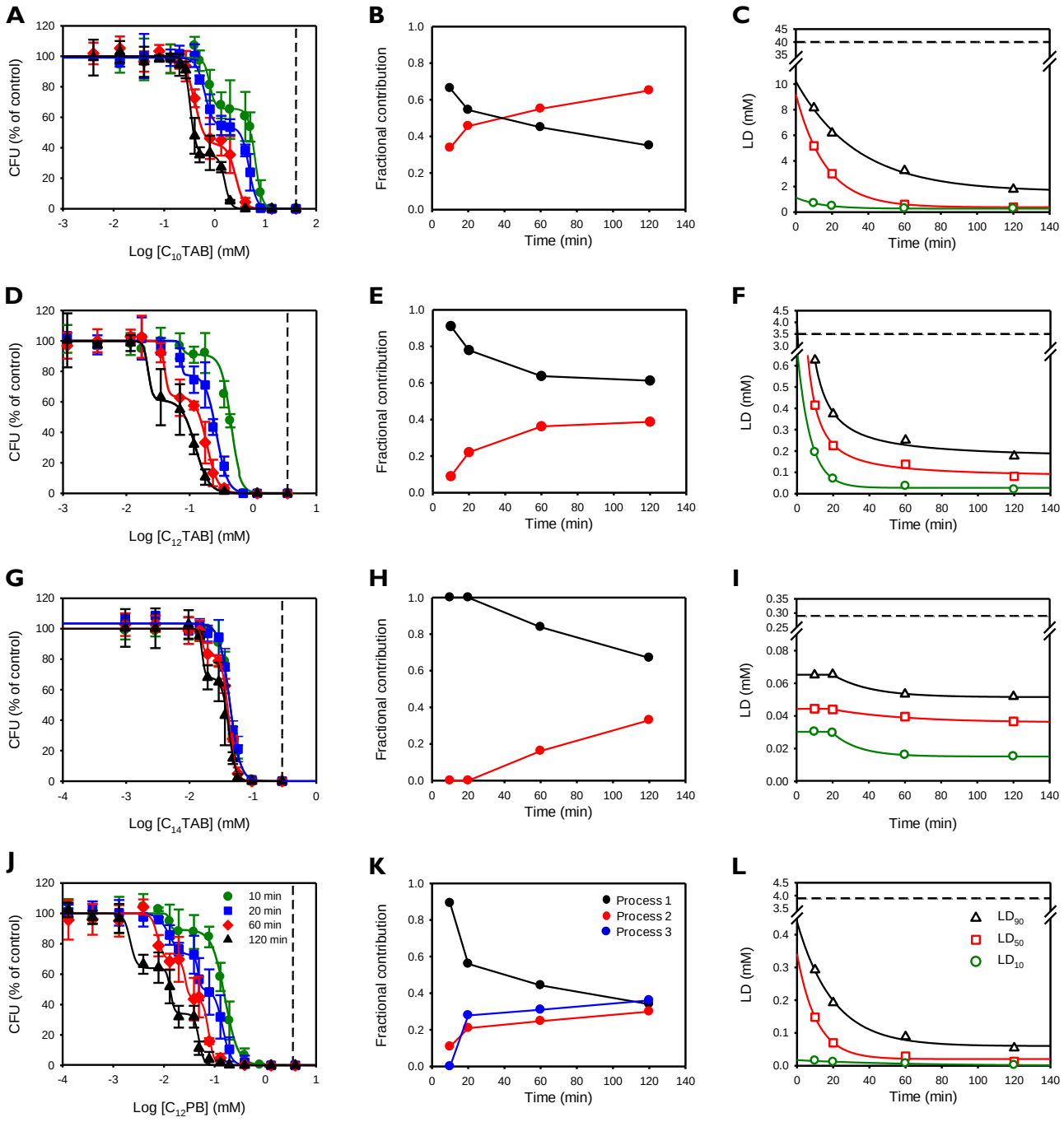

Figure 5.2. Cationic surfactants bactericidal activity against *E. coli*. Four cationic surfactants were evaluated: C_{10}TAB (**A-C**), C_{12}TAB (**D-F**), C_{14}TAB (**G-I**) and C_{12}PB (**J-L**). *E. coli* cell suspensions (1.5 X 10^8 CFU/mL) were incubated with the stipulated surfactant concentrations and grown for 10 (green closed circles), 20 (blue closed squares), 60 (red closed diamonds) and 120 (black closed triangles) minutes (left panels). At the end of the incubation an aliquot of each sample was serially diluted and spread in LB-agar plates which were incubated for 8-10 hours at 37°C. The survival of culturable bacteria was determined by counting the number of CFU/plate. Data are expressed as percentage of untreated control cultures and presented as Mean ± SD of at least 4 independent experiments. Given that the dose-response toxicity curves exhibit a biphasic sigmoid shape, a combination of two logistic equations was adjusted to the data. The fractional contribution of the equation that describes the toxicity process occurring at higher concentrations (Process 1, black circles) and of the equation that describes the toxicity process occurring at lower surfactant concentrations (Process 2, red circles) are shown in the middle panels. In the case of C_{12}PB after a third process became visible at even lower concentrations, after 20 minutes of incubation. In that case a combination of three logistic equations was adjusted to the data and the fractional contribution of the third process is also presented (Process 3, blue circles). From the toxicity curves it was possible to calculate the LD_{10} (green open circles), LD_{50} (red open squares) and LD_{90} (black open triangles) concentrations (right panels). A mono-exponential decay equation was fitted to the LD *vs.* exposure-time curves and for each surfactant tested the decay constants calculated for the LD_{90}, LD_{50} and LD_{10} curves were different. The CMC of each surfactant is represented by the black dashed line.

Table 5.1. Lethal doses of surfactant towards *E. coli* calculated from the toxicity curves presented in Figure 5.2.

Surfactant		Lethal Dose (mM) after exposure time of			
		10 min	20 min	60 min	120 min
C_{10}TAB	LD_{90}	8.130	6.167	3.236	1.780
	LD_{50}	5.176	2.992	0.603	0.388
	LD_{10}	0.692	0.474	0.282	0.268
C_{12}TAB	LD_{90}	0.626	0.374	0.251	0.176
	LD_{50}	0.415	0.225	0.138	0.081
	LD_{10}	0.194	0.070	0.036	0.019
C_{14}TAB	LD_{90}	0.065	0.065	0.053	0.052
	LD_{50}	0.044	0.044	0.040	0.037
	LD_{10}	0.030	0.030	0.016	0.015
C_{12}PB	LD_{90}	0.292	0.192	0.088	0.054
	LD_{50}	0.148	0.070	0.029	0.013
	LD_{10}	0.015	0.011	0.007	0.002

Table 5.2. Decay constants (min^{-1}) calculated for the exposure-time-dependence of the LD_{90}, LD_{50} and LD_{10} concentrations.

Surfactant	Decay constant (min^{-1})		
	LD_{10}	LD_{50}	LD_{90}
C_{10}TAB	7.21×10^{-2}	6.08×10^{-2}	2.95×10^{-2}
C_{12}TAB	1.37×10^{-1}	9.21×10^{-2}	8.96×10^{-2}
C_{14}TAB	6.89×10^{-2}	2.46×10^{-2}	4.76×10^{-2}
C_{12}PB	1.62×10^{-2}	9.24×10^{-2}	5.04×10^{-2}

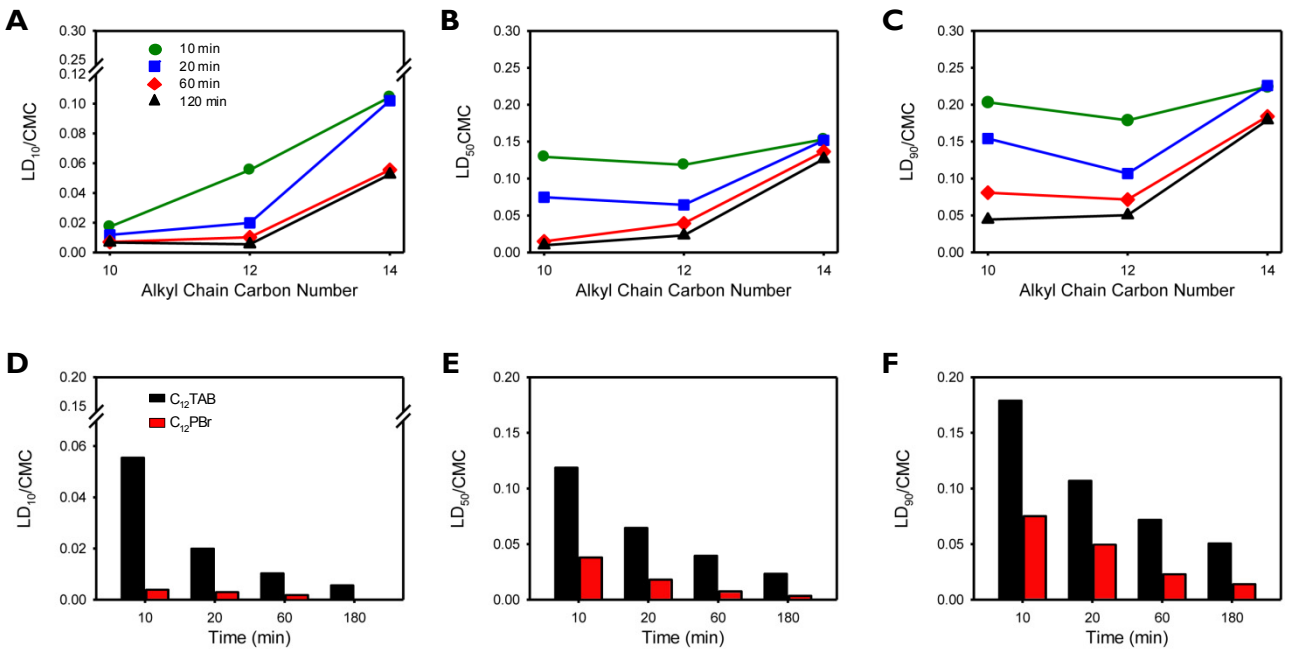

Figure 5.3. Effect of cationic surfactant structure on the bactericidal activity against *E. coli*. The graphs show the LD_{10}, LD_{50} and LD_{90} of C_nTAB surfactants (**A-C**) and of two cationic surfactants with similar hydrophobic chain but different polar head groups (**D-F**) after exposure times of 10, 20, 60 and 120 minutes. LD concentrations of each surfactant are normalized with respect to the CMC.

for each surfactant tested could be fitted using a mono-exponential decay equation (Fig. 5.1) and the decay constants obtained for the LD_{90}, LD_{50} and LD_{10} curves were different (Fig. 5.1 and Table 5.2), which indicates that distinct mechanisms are responsible for a reduction of 10%, 50% and 90% in the number of CFU. This observation is in agreement with the biphasic sigmoid shape of the toxicity curves. It is once again clear from Figure 5.3 that when evaluating the bactericidal activity of cationic surfactants in relation to CMC, the antibacterial potency of cationic surfactants decreases with the increase of the hydrophobic chain length. The toxicity ranking of the C_nTAB surfactants normalized with respect to CMC was C_{10}TAB≈C_{12}TAB>C_{14}TAB>C_{16}TAB.

When comparing the bactericidal activity of C_{12}TAB and C_{12}PB, which have the same *n*-alkyl chain of 12 carbons but differ in the structure of the polar head group, a third toxicity process, which occurs at very low concentrations, was detected after 20 minutes of incubation with C_{12}PB (Fig. 5.2). Contrary to C_{12}TAB, the curve describing the toxicity observed at higher concentrations does end up contributing to less than 50% of the observed toxicity (fractional contribution of 0.34) after 120 minutes of incubation, and while the two other remaining processes contribute less than 50% when taken separately (fractional contribution of 0.3 and 0.36 for the second and third processes, respectively, after 120 minutes of incubation), both combined contribute for almost 70% of the bactericidal effect. In fact, the third toxicity process increased in parallel with the second one, suggesting a common nature of the toxicity mechanism, although a more detailed analysis should be performed in the future in order to clarify this aspect. As in the case of the MIC, C_{12}PB, which has a larger polar head group and more delocalized positive charge, exhibited a more potent bactericidal activity than C_{12}TAB (Fig. 5.3).

5.2.3. Low concentrations of C_{10}TAB inhibit *E. coli* colony formation prior to reducing bacterial cell viability

Detection of viable bacteria is routinely performed by the classic colony count method, which is based in the ability of bacteria to grow and form colonies on solid agar medium, followed by CFU counts. However, the assessment of CFU counts is limited to culturable bacteria, meaning that if cationic surfactants somehow impaired and reduced cell growth or induced a quiescent state, commonly referred as viable but non-culturable (VBNC), bacteria can fail to reproduce on agar plates without necessarily implying that they are metabolic inactive and dead (Barer & Harwood, 1999; Nystrom, 2001). In order to ascertain if that was the case, particularly for the toxicity process detected at lower surfactant concentrations, bacterial viability was also evaluated using a cultivation-independent method. The relative proportion of live and dead bacteria was determined using a commercial bacterial viability kit (Live/Dead® BacLight™ Bacterial Viability kit),

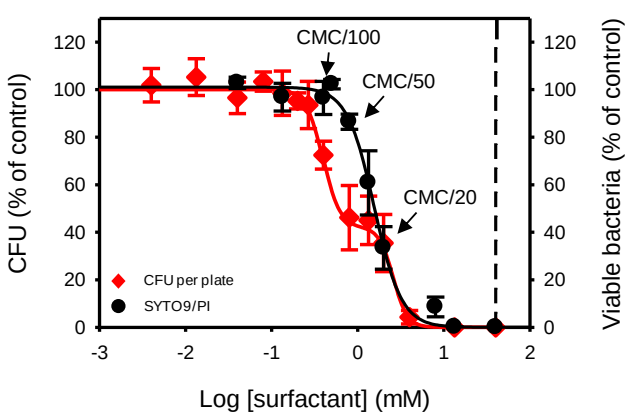

Figure 5.4. Bactericidal effect of C_{10}TAB against *Escherichia coli* as determined by culture-dependent and independent viability methods. *E. coli* viability was evaluated after 1 hour exposure to different concentrations of C_{10}TAB either by counting the number of CFU/plate (closed red diamonds) or using the BacLight™ bacterial viability kit (closed black circles). Data are expressed as percentage of untreated control cultures and presented as mean ± SD of at least 3 independent experiments. The CMC of C_{10}TAB is represented by the black dashed line.

which comprises two different fluorescent probes: SYTO 9, a green-fluorescent dye that stains the nucleic acids of both healthy and dead bacteria, and PI, a red-fluorescent nucleic acid probe that only penetrates in bacteria with damaged membranes. The detection of cell viability can then be performed using fluorescence spectroscopy analysis and calculating the ratio of integrated green fluorescence to integrated red fluorescence emission, which is proportional to the relative number of viable bacteria (Fig. 5.4). Alternatively, stained bacteria can be visualized under a fluorescence microscope (Fig. 5.5).

As can be seen in Figure 5.4, when bacterial viability was determined using the BacLight™ kit, the dose-response toxicity curve obtained after 1 hour of incubation with C_{10}TAB was monotonic instead of exhibiting a biphasic sigmoid profile as was the case when the colony count method was employed. In this case, the toxicity process that was visible at lower concentrations disappeared, and the toxicity curve was coincident with the one that corresponds to the toxicity process at higher concentrations. This result strongly suggests that the decrease in cell viability that is observed at lower concentrations actually corresponds to an impairment in cell division, possibly leading to cell cycle arrest and resulting in a diminished capacity of bacteria to form colonies. In fact, at C_{10}TAB concentrations as low as CMC/100, which resulted in a reduction of approximately 30% in the number of CFU, no signs of cell membrane damage were observable (undetectable PI staining) and long bacterial filaments could be found (Fig. 5.5). A more detail study will be necessary in order to clarify whether the reduction in the number of CFU is proportional to the number of bacteria presenting an elongated phenotype.

As an attempt to better understand the effect of cationic amphiphiles on the morphology of *E. coli* cells and to search for clues on why low surfactant concentrations result in the emergence of long bacteria filaments, transmission electron microscopy images of *E. coli* were taken after 1 hour of exposure to C_{10}TAB, C_{12}TAB and C_{12}PB at concentrations corresponding to the toxicity process most likely unrelated to direct membrane damage and cell death. Electron microscopy shows that the incubation of *E. coli* with cationic surfactants causes a significant change

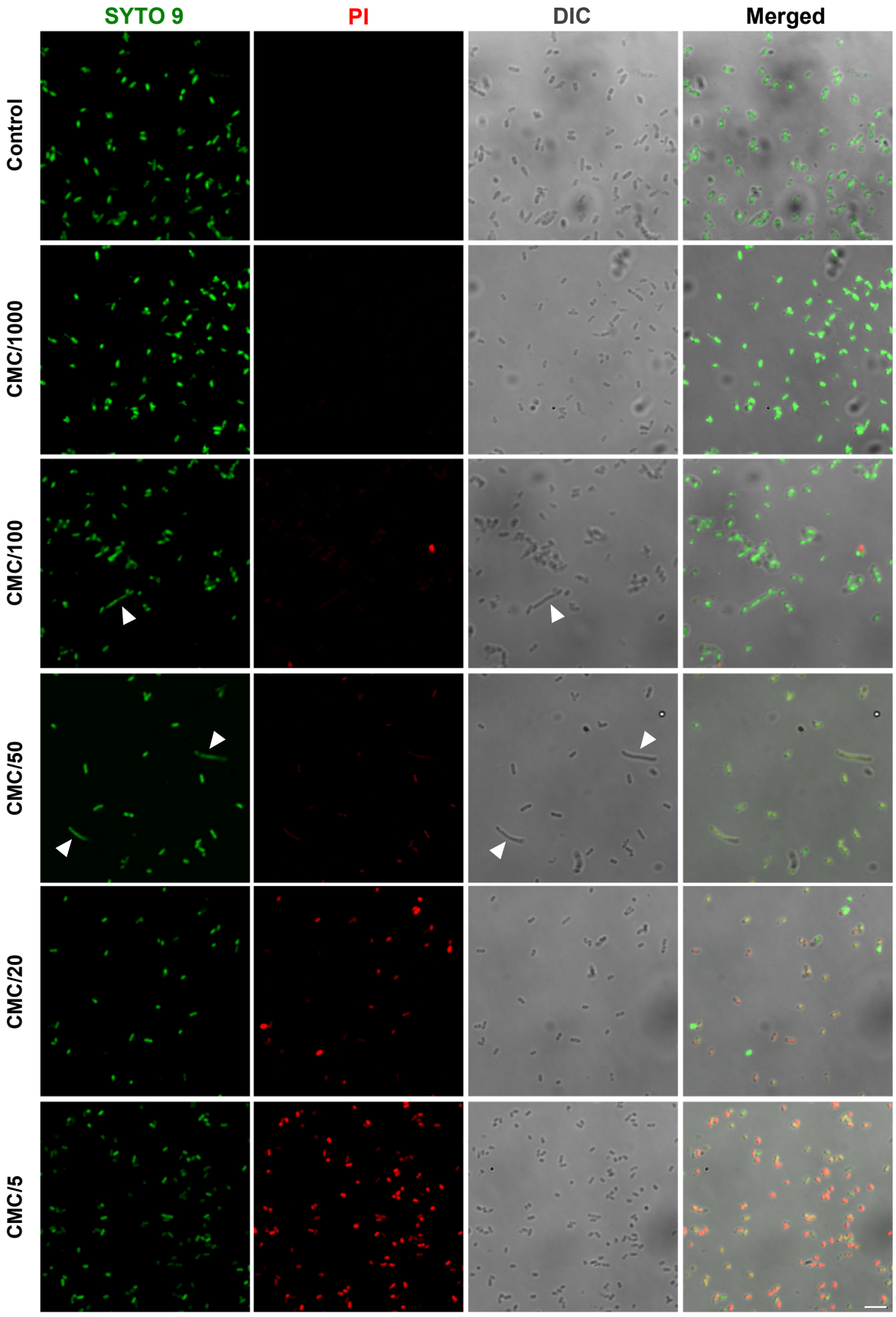

Figure 5.5. Effect of C_{10}TAB on *E. coli* cells viability. Representative confocal fluorescence images showing *E. coli* cells stained with the BacLight™ bacterial viability kit, after 1 hour of incubation with different concentrations of C_{10}TAB. Bacterial cells with intact membrane are green-fluorescent (SYTO 9 positive) whereas cells with damaged membranes are both green (with reduced fluorescence intensities) and red-fluorescent (SYTO 9 and PI positive). At CMC/100 and CMC/50 structures not observed in control conditions, identifiable as long bacterial filaments, are visible (arrow heads). Scale bar correspond to 5 μm.

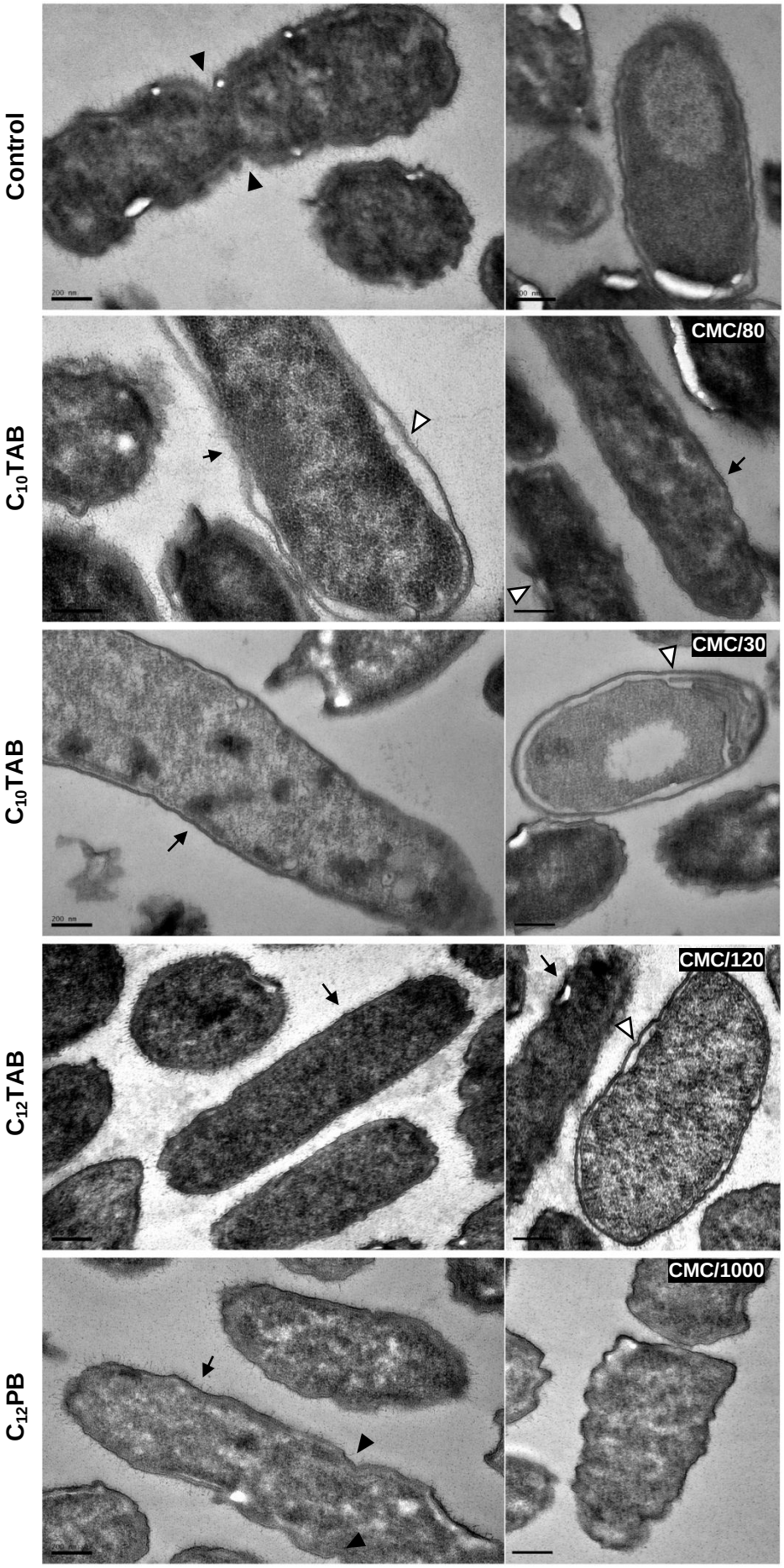

Figure 5.6. Morphological alterations in *E. coli* induced by cationic surfactants. Representative electron microscopy images showing the differences between the ultrastructure of mock-treated control bacteria and those incubated with C_{10}TAB, C_{12}TAB or C_{12}PB for 1 hour. Outer membrane detachment is visible as an electron-lucent gap between the inner and the outer membranes (open arrow heads). Morphological changes in the cytoplasmic membrane and failure in the formation of the septum (compare close arrow heads in C_{12}PB with control) leads to the emergence of elongated bacterial cells (arrows). Scale bar correspond to 200 nm.

in their cell morphology (Fig. 5.6). In the presence of low concentrations of the three compounds analyzed, bacteria seem unable to properly divide, as can be noticed by the anomalies in the septum formation and by the elongated morphology displayed by bacterial cells. In some cells, the outer membrane of *E. coli* appeared detached from the inner membrane, which would at first glance suggest that cationic surfactants alter the permeability properties of the bacterial cell envelope. However, the outer and inner membranes of bacteria exposed to low surfactant concentrations remained unbroken, with no observable leak of cytoplasm. For example, in the case of C_{10}TAB, only for higher concentrations such severity of cellular damage was reached (e.g. CMC/30). This was also corroborated by the results presented in Figure 5.4, which show that membrane damage only occurs at concentrations above CMC/80.

Another more subtle feature found in bacteria incubated with cationic surfactants was a prevalence of cells displaying a less electrodense cytoplasm with occasional emergence of highly electrodense clusters, suggesting that these surfactants may reach intracellular targets, such as anionic polymers following translocation across the cell plasma membrane. To be sure, cationic surfactants are known to bind strongly to DNA and RNA (Spink & Chaires, 1997; Zhu & Evans, 2006) and induce drastic conformational changes in the structure of these polymers (Dias *et al.*, 2005).

Taken together, the present results indicate that cationic surfactants affect bacterial cell growth and viability at different threshold concentrations and that there is a clear separation of the two effects, as seen by the biphasic toxicity curves obtained by CFU counting method. A previous study by Salt and Wiseman (1970) also found a similar pattern of toxicity when incubating *E. coli* with C_{16}TAB. The authors attributed such phenomenon to the existence of different thresholds of C_{16}TAB uptake necessary to first inhibit cell growth and then, for increasing concentrations, to cause cell lysis in an individual cell.

5.2.4. Evaluation of the selective toxicity of cationic surfactants towards bacterial cells and its therapeutic potential

The major concern in the development of clinically useful microbicides for the prophylaxis of STIs is their selective toxicity against the pathogenic agents. Ideally, a good microbicide should ensure a sound antimicrobial activity while also having minimal toxicity against the host cells. In the context of STIs prophylaxis, it is then imperative to directly compare both the bactericidal activity and the toxic effects towards mammalian polarized epithelial cells when evaluating the therapeutic potential of surfactants as microbicide candidate drugs. To this end, the dose-response toxicity curves obtained for MDCK II cells after 1 hour of exposure to C_{10}TAB, C_{12}TAB, C_{14}TAB and

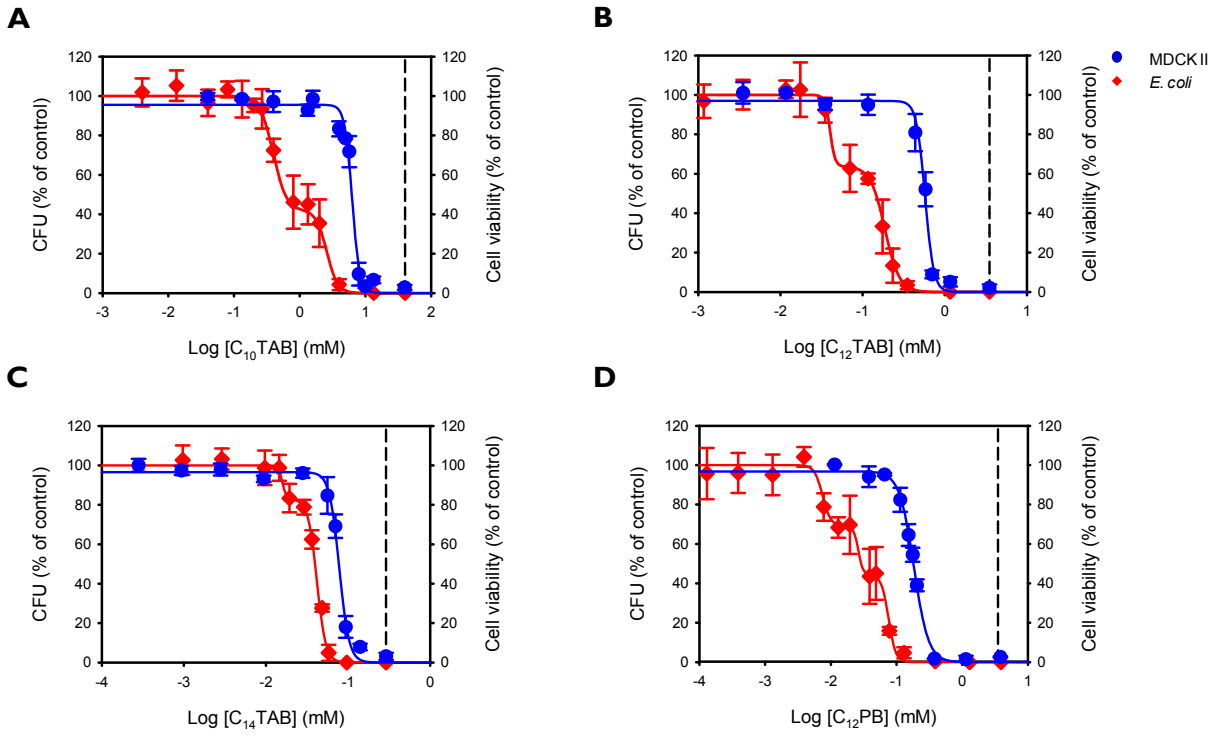

E

Surfactant	Therapeutic Index as determined by			
	LD_{50}(MDCK II)/LD_{50}(*E. coli*)		LD_{50}(Caco-2)/LD_{50}(*E. coli*)	
	20 min	60 min	20 min	60 min
C_{10}TAB	3.7	10.3	4.7	11.4
C_{12}TAB	3.9	4.3	5.7	5.5
C_{14}TAB	3.5	2.0	4.0	2.7
C_{12}PB	3.7	6.3	10.3	15.6

Figure 5.7. Comparison of the antimicrobial activity of cationic surfactants and its toxic effects towards polarized epithelial cells. C_{10}TAB (**A**), C_{12}TAB (**B**), C_{14}TAB (**C**) and C_{12}PB (**D**) toxicity towards MDCK II cells (blue closed circles) and *E. coli* (red closed diamonds) was evaluated, as previously described, after 60 minutes of incubation with different surfactant concentrations (for further details see Fig. 3.1 in Chapter III and Fig. 5.2 in the present Chapter, respectively). Data are expressed as percentage of untreated control cultures and presented as Mean ± SD of at least 3 independent experiments. The therapeutic indices calculated after 20 and 60 minutes of incubation are also shown (**E**).

C_{12}PB (Chapter III) were plotted together on a single graph with the correspondent toxicity curve obtained for *E. coli* by the colony-counting method (Fig. 5.7A-D). The results show that, compared to polarized epithelial cells, bacteria were more susceptible to all cationic surfactant tested and, as already mentioned, show biphasic (or triphasic in the case of C_{12}PB) dose-response toxicity curves contrasting with the monotonic sigmoid curves obtained for MDCK II cells.

The efficacy of the antibacterial activity depends on the balance between the concentration required for bacteriostatic and bactericidal functions and the concentration that causes damage to the vaginal epithelium, and this can be measured by a therapeutic index (i.e. the ratio between surfactant toxicity to bacterial cells and toxicity to the epithelial cells). The therapeutic indices

were calculated as the ratio of the LD_{50} value for polarized epithelial cells (MDCK II or Caco-2) to the LD_{50} value for *E. coli*, both treated with the same surfactant for the same exposure time, as describe elsewhere (Burns, 1999; Lard-Whiteford *et al.*, 2004). By this measurement, an enhanced antimicrobial activity in tandem with a high selectivity towards bacterial cells results in higher therapeutic indices. A desired therapeutic index (as defined above) should be ≥ 10. In agreement with the previous results, an increase in the number of carbons in the *n*-alkyl chain of C_nTAB surfactants resulted in a decrease of the therapeutic index (Fig. 5.7E). However, even though C_{10}TAB is demonstrably more effective than C_{12}TAB, evidenced by a higher therapeutic index after 1 hour of exposure (above 10 for C_{10}TAB and below 5 for C_{12}TAB), it is important to notice that the antimicrobial effect of C_{10}TAB is mainly comprised by a bacteriostatic action which occurs at low concentrations. In contrast, for C_{12}TAB the highest fractional contribution to its antimicrobial activity comes from a bactericidal action which occurs at higher surfactant concentrations.

The effect of the polar head structure on the therapeutic index was also evaluated by comparing C_{12}TAB with C_{12}PB. As can be seen by the results in Figure 5.7E, changing the structure of the polar head to a larger group with a more delocalized positive charge greatly enhanced the efficacy and selectivity towards bacteria over mammalian polarized epithelial cells. This was particularly evident when the therapeutic index was calculated as the ratio of the LD_{50} for Caco-2 cells to the LD_{50} for *E. coli*. Although the differences in the therapeutic indices as calculated using the toxicity data for MDCK II or Caco-2 may appear minor, with the exception of C_{12}PB, a better performance of cationic surfactants when evaluated with respect to Caco-2 toxicity is consistent among all the compounds tested for both exposure times. Surfactant toxicity is dependent on the ability to partition between the aqueous phase and the cell membrane and may also depend on its capacity to subsequently cross the membrane and enter the cytoplasm. Moreover, amphiphile partition coefficients as well as the rate constants for surfactant insertion into and translocation across membranes are lower for more ordered membranes (Abreu *et al.*, 2004; Sampaio *et al.*, 2005; Moreno *et al.*, 2006; Estronca *et al.*, 2007; Apel-Paz *et al.*, 2008). Since MDCK II display a lower transepithelial electrical resistance when compared with Caco-2 cells, which indicates the existence of less restrictive and more "leaky" tight junctions (Moore *et al.*, 2008; Van Itallie *et al.*, 2008; Dukes *et al.*, 2011), the access of surfactants to the basolateral (less ordered) membrane domains will be facilitated in MDCK II cells, leading to a increased susceptibility to surfactant toxic effects. One last observation must be made concerning the limitation of the *in vitro* cell line models used in the present work, particularly evident by the lack of mucus production, contrasting with conditions found *in vivo* (Le Ferrec *et al.*, 2001). It has been reported that the presence of a mucus gel, covering the epithelial cells surface, hence, mimicking physiological conditions, might limit

absorption, especially that of lipophilic drugs (Hilgendorf *et al.*, 2000). Thus, it is likely that *in vivo* the toxicity of cationic surfactants towards vaginal mucosa cells will be lower than reported here.

5.3. Discussion

The development of new microbicidal agents of broad-spectrum activity and with considerable biocompatibility regarding mammalian cells is of tremendous importance in the struggle to reduce the spread of STIs. Quaternary ammonium monoalkyl compounds have been proven to work as microbides against a wide range of Gram-positive and Gram-negative bacteria as well as against yeast (Domagk, 1935; Campanha *et al.*, 1999; Belec *et al.*, 2000; Vieira & Carmona-Ribeiro, 2006; Vieira *et al.*, 2008), however their toxic effects are also manifested towards mammalian cells. Therefore, the use of surfactants for STIs prophylaxis is not without its risks. An adequate strategy for finding suitable compounds for clinical applications is to study the mechanisms mediating both the microbicidal activity and the toxicity towards mammalian cells in order to better understand how surfactants exert toxic effects on each type of cell. This would make possible the design of new molecules capable of fulfilling specific tasks (e.g. inhibition of bacterial metabolism). With this in mind, the relation between cationic surfactant structure and its antimicrobial activity was evaluated. Since the most prevalent bacterial STIs are caused by Gram-negative bacteria, *Escherichia coli* was used as a Gram-negative bacteria cell model. The selectivity and safety of the tested compounds was also evaluated by directly comparing the dose-response toxicity curves obtained for the studied bacterial model and for mammalian polarized epithelial cells.

All the cationic surfactants used in the present study showed a potent antibacterial activity against *E. coli*. Nonetheless, the antimicrobial efficacy of the tested compounds was largely affected by the length of their alkyl chain. Comparing the different C_nTAB surfactants, taking into account their respective CMC, the antimicrobial activity of cationic surfactants decreased with the increase in the hydrophobic chain length. Furthermore, in the case of C_{16}TAB, although the absolute concentration required to inhibit bacterial cell growth was very low, the MIC was at least 2-fold higher than CMC, indicating that C_{16}TAB antibacterial effects results from structural changes at the level of the cytoplasmic membrane or even from its dissolution, in agreement with observations by others (Salton, 1951; Davies *et al.*, 1968; O'Neill *et al.*, 2004; Simoes *et al.*, 2006). In fact, Salton and colleagues (1951) reported that at bactericidal concentrations C_{16}TAB induced cytolytic damage and cell leakage in *Staphylococcus aureus*, *Streptococcus faecalis* and *Escherichia coli*, based on electron microscopy studies. The high threshold concentration required to produce an

antibacterial effect combined with the high toxicity of C_{16}TAB (below CMC) towards polarized epithelial cells, makes this compound unfit for STIs prophylaxis, despite this conclusion having been previously overlooked. In fact, it is commonly stated that the optimal cationic surfactant activity against Gram-negative bacteria is achieved for compounds with a chain length of 14-16 carbons, which is in contrast with the present results (reviewed in Balgavy & Devinsky, 1996; Gilbert & Moore, 2005). On the other hand, contrary to C_{16}TAB, all the other C_nTAB studied (C_{10}-C_{14}) exert their antibacterial activity at concentrations below CMC and lower than those that elicit cytotoxic effects in epithelial cells. Concerning the MIC, the toxicity ranking of the C_nTAB surfactants normalized with respect to CMC was C_{10}TAB>C_{12}TAB>C_{14}TAB>C_{16}TAB. A similar toxicity pattern was previously reported by our group, regarding the effects of C_nTAB surfactants (C_{10}-C_{14}) on the growth of several Gram-negative and Gram-positive bacteria, albeit different concentrations being required to produce a similar effect depending on the bacterial species (Vieira *et al.*, 2008). More important, the same study also showed that *Neisseria gonorrhoeae* (Gram-negative bacteria) was considerably more susceptible to cationic surfactants than *E. coli* and the other bacterial species examined.

The dependence of the antimicrobial activity of C_nTAB on the chain length may be related to the total amount of surfactant molecules that are able to reach the site(s) of action within a given time. As already stated, the CMC of surfactants within a homologous series is inversely proportional to the length of the hydrophobic chain, decreasing by around 10 times with the addition of every 2 carbons (Holmberg *et al.*, 2003; see Table 3.1, Chapter III, Section 3.2.1). As a result, for the same concentration expressed relatively to the CMC, the absolute concentration of C_{10}TAB will be 10-fold higher than that of C_{12}TAB, 100-fold higher than that of C_{14}TAB and about 1000-fold higher than that of C_{16}TAB. Furthermore, although the partitioning into the membranes is more favorable for compounds with longer hydrophobic chains, this does not totally compensate the fact that the absolute concentration of, for example, C_{14}TAB, is 10 times lower than that of C_{12}TAB. As a consequence, the concentration of C_{14}TAB in the bacterial membranes is lower than that for C_{12}TAB at the same concentration expressed relatively to CMC. If part of the surfactant antimicrobial activity is also dependent on it reaching intracellular targets (including the inner membrane of Gram-negative bacteria), the concentration at the site of action will be as well dependent on the ability of the compound to translocate across the membranes and partition into an aqueous phase, during the period of incubation. Therefore, the surfactant concentration at the site of action will be influenced by both the lipophilicity of the drug and of each compartment, as well as by the duration of exposure. Cationic surfactants with short hydrophobic chains would be less capable of inserting into the hydrophobic lipid bilayers, whereas long-chain compounds would not easily penetrate the hydrophilic aqueous compartments. Consequently, a compromise

between the capacity of surfactants to partition into both polar and apolar phases is required for the transport of the drug to their site(s) of action, in order to achieve maximal antimicrobial activity.

The antimicrobial efficiency of cationic surfactants was also dependent on the chemical nature of the polar head. The substitution of C_{12}TAB polar head structure by larger groups, such as in the case of C_{12}PB and C_{12}BZK, greatly enhances the antimicrobial activity, around 8 to 15 times, towards *E. coli*. Given that a delocalized charge on the surfactant head group makes its ionic radius considerably larger and reduces the work required for translocation of the polar group from one side of the membrane to the other (Honig *et al.*, 1986; Gennis, 1989), it is likely that the observed differences in the antimicrobial activity result from the fact that C_{12}PB and C_{12}BZK reach faster than C_{12}TAB the possible intracellular site(s) of action.

In order to gain a better understanding concerning the degree of cationic surfactant efficacy, the antimicrobial activity of the studied compounds was further compared regarding their ability to inhibit *E. coli* colony formation. All cationic surfactants used in this study displayed concentration and time-dependent toxic effects, although, as in the case for the MIC, surfactant efficacy was dependent on the hydrophobic chain length as well as on the polar head group. The dose-response toxicity curves showed a biphasic sigmoid shape, in which two distinct toxicity processes were observable. These processes were found to correspond to two distinct effects of cationic surfactants which occur at different threshold concentrations: a bacteriostatic action at low concentrations and a bactericidal activity at higher concentrations, a phenomenon previously suggested, yet since then unexplored, for the antimicrobial activity of C_{16}TAB (Salt & Wiseman, 1970). This dual action was revealed by comparing the results obtained by CFU counting and PI incorporation, a measure of the bacterial membrane integrity. The separation between the concentrations necessary to cause either effect becomes less sharp with increasing hydrophobic chain length. Moreover, the bacteriostatic effect became progressively smaller for the longer chain amphiphiles, consequently giving rise to an increment in the fractional contribution of the bactericidal effect to the global antimicrobial activity exerted by C_nTAB surfactants. When comparing the effect of the polar head group of the cationic surfactants on the dose-response toxicity curves, a third toxicity process, which occurs at very low concentrations (i.e. between CMC/500 and CMC/200 after 20 minutes of exposure), was visible for exposure durations equal or superior to 20 minutes of incubation with C_{12}PB. This third toxicity process increased in parallel with the second one, which in the case of C_{12}TAB most likely corresponds to a bacteriostatic effect, suggesting a common nature behind both mechanisms. It is possible that the two toxicity processes induce a VBNC state in *E. coli* cells, which, nonetheless, are manifest at different threshold concentrations, depending on the molecular target(s) involved. Whether those

bacteria cells are capable of recovering their capacity to divide or end up dying is not know and a more detailed analysis should be performed in the future in order to clarify this aspect.

Biological membranes act as selectively permeable barriers, allowing the formation and maintenance of essential ion gradients and also serving as an anchoring platform for transmembranar and peripheral proteins. The activity of membrane anchored proteins is strongly dependent on the molecular composition of the lipid bilayer in which they are placed (Cantor, 1997, 1999; Jensen & Mouritsen, 2004; Andersen & Koeppe, 2007). Modifications in the characteristics of the lipids which compose a membrane bilayer, such as head group type, length and saturations of the acyl chains or cholesterol addition, can all contribute to modulate membrane-spanning proteins function. Therefore, any interference with the properties of the lipid bilayers of biological membranes may result in a compromise of important physiological functions and concomitant cell death, without necessarily implying partial or full membrane disruption. For instance, mutant *E. coli* cells lacking the major membrane lipid phosphatidylethanolamine cannot properly divide, forming long multinucleoid filaments, probably due to a misassembly of cell division proteins, resulting in failure of cells to separate through constriction (Mileykovskaya *et al.*, 1998; Wikstrom *et al.*, 2004). Given the amphiphilic nature of surfactants, their microbicidal activity is generally attributed to their interaction with biological membranes, altering its physical properties, such as lateral packing, surface hydration, surface charge and ultimately membrane integrity (Hamilton, 1968; Tomlinson *et al.*, 1977; Vieira & Carmona-Ribeiro, 2006; Ioannou *et al.*, 2007; Dymond & Attard, 2008). In fact, it has been demonstrated that at concentrations below CMC, *n*-alkyl-N,N,N-trimethylammonium ions partition into model membranes and perturb the lipid bilayer by altering the lateral ordering of lipid hydrocarbon chains (Balgavý *et al.*, 1984; Cirak *et al.*, 1988; Gallova *et al.*, 1990).

In the present study, in bacterial cells exposed to low concentrations of C_{10}TAB, C_{12}TAB and C_{12}PB, significant morphological alterations, such as anomalies in the inner membrane structure and in the septum formation, emergence of elongated bacterial cells and, in some cases, detachment of the outer membrane, were visible after 1 hour of incubation. It should be stressed that at these concentrations the antimicrobial activity of cationic surfactants was mainly exerted through a bacteriostatic effect. Recently, Strahl and Hamoen (2010) have described a similar elongated phenotype in *E. coli* cells after membrane depolarization using the ionophore carbonyl cyanide m-chlorophenylhydrazone (CCCP). The authors concluded that the transmembrane potential directly modulates the spatial distribution and organization of several conserved cytoskeletal and cell division proteins and that membrane depolarization with CCCP affects the binding and correct assembling of the proteins responsible for the Z-ring formation, impeding proper septum formation and cell division. In light of the results obtained after incubation of

isolated mitochondria with cationic surfactants (Chapter IV, Section 4.2.5), it is possible that similar toxicity mechanism, which include inhibition of the respiratory chain and membrane depolarization, might also be responsible for the bacteriostatic action of cationic surfactants. To be sure, previous reports have demonstrated that cationic surfactants such as, alkyl-dimethyl-benzyl-ammonium chlorides, C_{12}PB and C_{16}TAB, inhibit respiration of different bacterial species even at sub-lethal concentrations (Miller & Baker, 1940; Baker *et al.*, 1941; Kopecka-Leitmanova *et al.*, 1989; Maillard, 2002; Simoes *et al.*, 2006). Moreover, in agreement with these observations, Ishikawa and colleagues (2002) have shown that bacterial sensitivity to cationic surfactants is affected by carbon source and anaerobiosis: *E. coli* cells grown in aerobic conditions, with succinate or acetate (substrates for the respiratory chain) as a carbon source, had a higher respiratory activity and were more susceptible to the effects of C_{16}TAB than those grown under anaerobic conditions with glucose as a carbon source. This supports the hypothesis that low surfactant concentrations may impair the activity of the respiratory chain, since bacteria dependent on respiration as a main source for ATP production are more affected by surfactants. On the other hand, even when grown under anaerobic conditions, in a situation of limited glucose availability, *E. coli* cells are still more susceptible to the toxic effects of cationic surfactants (Bjergbaek *et al.*, 2008).

Although most of the toxic effects of surfactants are likely related to its interaction with biological membranes, the interaction of these compounds with intracellular targets, such as anionic polymers like DNA and RNA, following translocation across the cell plasma membrane, is also a possibility that should not be overlooked. The insertion of surfactants with a single hydrophobic chain into membranes occurs at a rate that is almost diffusion-controlled and is, therefore, an extremely rapid process (Sampaio *et al.*, 2005; Cardoso *et al.*, 2011). After insertion, the surfactant can translocate across the membrane and establish equilibrium between the extracellular space and the cytoplasm. In fact, the electron microscopy images of bacteria incubated with cationic surfactants show a prevalence of cells displaying a more electrolucent cytoplasm with occasional emergence of highly electrodense clusters, suggesting that these surfactants may reach intracellular targets.

The specificity of cationic surfactants toxic effects was also addressed by comparing the toxicity curves obtained for both *E. coli* and mammalian polarized epithelial cells. With the exception of C_{16}TAB, bacteria were more susceptible to cationic surfactants than mammalian cells. Regarding the therapeutic indices, C_{10}TAB and C_{12}PB where the two surfactants that presented the strongest antimicrobial activity without having a major deleterious impact in mammalian cells. This cell selectivity may originate from the difference in the lipid composition as well as in the membrane potential between the target pathogen and host cell membranes. The adsorption and

translocation of lipid-soluble ions depends on the electrostatic interactions of the charged polar head with the charged groups at the membrane surface, and also on the hydrophobic interactions between the hydrophobic carbon chain and the apolar groups on the membrane lipids (Ketterer *et al.*, 1971; Heerklotz, 2008). The bacterial membranes are rich in negatively charged lipids, such as phosphatidylglycerol and lipopolysaccharide, whereas the mammalian cells are mostly composed of zwitterionic lipids, like phosphatidylcholine and sphingomyelin (Bretscher & Raff, 1975; Op den Kamp, 1979; Cronan, 2003; Hancock & Sahl, 2006; van Meer & de Kroon, 2011). Furthermore, the membrane potential across the plasma membrane of eukaryotic cells is more positive than in the case of prokaryotic cells (Op den Kamp, 1979; Stefani & Cereijido, 1983; Hancock & Sahl, 2006; Bot & Prodan, 2010). As a result, cationic surfactants will preferentially bind to the more negatively charged bacterial membrane. The cholesterol content in polarized epithelial cells, which is absent in the bacterial membrane, is also known to make membrane disruption more difficult (Schnitzer *et al.*, 2005). Lastly, the overall size and total membrane surface is higher in mammalian cells than in bacteria, thus the concentration of surfactant at its site(s) of action will be more diluted in the host cells, preventing from possible surfactant noxious effects.

Given that the fractional contribution of the bactericidal activity to the global antibacterial action is higher in the case of both C_{12}TAB and C_{14}TAB when compared to C_{10}TAB and C_{12}PB, which are predominantly bacteriostatic, it seems tempting to conclude that the former two cationic surfactants could make better microbicide candidates. However, the previously mentioned structural changes induced by cationic surfactants and a possible surfactant-induced metabolic stress - which probably underlie the bacteriostatic effect -, would make bacterial cells more prone to any response by the host immune system. Therefore, as suggested by the at least 2-fold higher therapeutic index, C_{10}TAB and C_{12}PB are likely the most efficient antimicrobial compounds among the tested surfactants.

Altogether, the results from the present work demonstrate that cationic surfactants with short hydrophobic chains (10 or 12 carbons), with larger polar head groups and more delocalized charge are the best candidates to be used for the prevention of bacterial STIs.

Chapter VI

General discussion

General discussion

Since the seminal work by Stein (1990), alerting to the need of women-controlled HIV prevention methods, the concept of microbicide use in STIs prevention gained substantial ground and intensive research on the field has been performed. The first generation of topical microbicides was primarily focused on broad-spectrum formulations, containing surfactants, such as Nonoxynol-9 and C31G, which disrupt viral and bacterial membranes (Krebs *et al.*, 1999; Krebs *et al.*, 2000; reviewed in Stone, 2002). The well known bacteriosctatic and bactericidal actions of surfactants, combined with their low price, high stability and undemanding storage conditions, make these compounds very attractive to be used in STIs prophylaxis. However, all the surfactant-based microbicide candidates that completed phase III clinical trials failed to prevent HIV infection (Stephenson, 2000; Fichorova *et al.*, 2001; Peterson *et al.*, 2007; Feldblum *et al.*, 2008) and their utility as general microbicides was also questioned. Faced with these difficulties, why should surfactants still elicit interest regarding their potential use as topical microbicides? First it should be acknowledged that the *in vitro* and *in vivo* pre-clinical studies, as well as the human clinical trials, have given scarce consideration to the fact that when the surfactant concentration in the aqueous phase is above CMC, these compounds form micelles which establish an equilibrium with the membranes. Since some proteins are also amphiphilic molecules they can, together with native membrane lipids, partition into the surfactant micelles, resulting in an indiscriminate and progressive concentration-dependent solubilization of the membranes. In Phase III trials, Nonoxynol-9 (CMC = 0.05 mg/mL) was tested at concentrations between 5 and 100 mg/mL (reviewed in Wilkinson *et al.*, 2002) and the surfactant mixture C31G (CMC = 0.005 mg/mL) was used at concentrations between 0.005 and 0.02 mg/mL (Peterson *et al.*, 2007; Feldblum *et al.*, 2008), which correspond to concentrations higher than the CMC, where the effects upon membranes are less specific. As a result, the outcomes of these clinical trials were deemed unsuccessful, since both compounds failed to prevent HIV transmission, due largely to a lack of selectivity – in the case of N-9 it has become well established that the causes of failure were related to damage dealt to the vaginal mucosa by the surfactant itself (Fichorova *et al.*, 2001; Catalone *et al.*, 2005; Cone *et al.*, 2006). In spite of the negative results obtained in clinical trials, a recent report by Vieira and colleagues (2008) has demonstrated that, contrary to the other surfactant families, cationic surfactants may work as bactericides at concentrations that are not

toxic to polarized mammalian epithelial cells, strongly suggesting that these compounds could be potentially useful in the prevention of, at least, bacterial STIs. For these reason, the negative results obtained in advanced clinical trials should not serve to put aside the potential therapeutic use of surfactants but to encourage the development of better *in vitro* models and surrogate toxicity makers for the pre-clinical evaluation of new microbicide candidates.

The present work shows how an integrated study of surfactants toxicity towards models of host cells and pathogens is useful for the identification of selective and potent bacteriostatic and bactericidal agents. A major concern in the development of clinically useful microbicides for the prophylaxis of STIs is their selective toxicity against the pathogenic agents. Ideally, a good microbicide should ensure a sound antimicrobial activity while also having minimal toxicity against the host cells. Using *in vitro* cell models mimicking different cell types from the vaginal mucosa in combination with bacterial cell cultures, it is possible to overcome the shortcomings of using animal models, while at the same time allowing the screening of an extensive range of compounds. One of the crucial steps in correctly evaluating and comparing the efficacy of different surfactants is to analyze the data taking into account the respective critical micelle concentration (CMC). Since these compounds are amphiphilic molecules, the site of interaction with any kind of cells are cell membranes. This interaction is dependent on the partition coefficient between the aqueous and membrane phases, which in turn is related with the CMC of the surfactant. Through this methodology it was possible to identify a group of cationic surfactant with great potential to be used as microbicide agents in the prophylaxis of bacterial STIs. Contrary to what is frequently stated in the current literature, C_nTAB surfactants with shorter hydrophobic chains (10 or 12 carbons) were found to be the most efficient and selective with regards to its antimicrobial activity. In contrast, C_{16}TAB which is often referred among C_nTAB surfactants to have the highest bactericidal activity against Gram-negative bacteria (reviewed in Balgavy & Devinsky, 1996; Gilbert & Moore, 2005), was more toxic to mammalian epithelial cells than to *Escherichia coli*, only exerting its antibacterial effect at concentrations above the CMC. It is then likely that C_{16}TAB may produce effects similar to those of N-9 when administered *in vivo* and should not be considered in further studies. The efficiency of cationic surfactants was greatly improved by changing the polar head structure of C_nTAB compounds to larger polar groups, as in the case of C_{12}PB and C_{12}BZK, thus suggesting that the design of new molecules should include compounds with short alkyl-chains, probably with 10 carbons, and large polar head group with delocalized positive charge.

Even though the present study focused only on the surfactant bactericidal effects, its relevance is still carried over to situations of viral infections, since bacterial STIs are intimately related with increased risk of HIV transmission (reviewed in Wasserheit, 1992; Galvin & Cohen, 2004; Celum, 2010). In fact, a growing body of evidence has been gathered supporting the notion

that an effective STIs treatment and prevention reduces HIV transmission and largely contributes to the control of the HIV/AIDS epidemic (reviewed in Mayaud & McCormick, 2001; Dallabetta & Neilson, 2004; White *et al.*, 2008; Steen *et al.*, 2009). An analysis of the cost-effectiveness of controlling HIV transmission by treating curable STIs, performed in four populations in East and West Africa, has shown that at least 50% of the new HIV infections could be attributed to STIs co-infection (White *et al.*, 2008). Moreover, the same study also revealed that an effective management of curable STIs, not only contributes to the control of HIV transmission, but also brings about cost-savings in the treatment of STIs and AIDS afflicted patients. A similar study performed in the United States has come to similar conclusions (Chesson & Pinkerton, 2000). Equally important, by protecting women from bacterial STIs, microbicides could also play a critical role, albeit indirectly, in reducing STIs transmission from mother to infant during childbirth, having in this way a positive impact on the associated morbidity and mortality as well as in direct costs of treatment, which is important, particularly in developing countries.

A previous work from our laboratory has shown that C_nTAB surfactants (C_{10}-C_{14}) are not capable of preventing polarized epithelial cells infection by adenovirus (non-enveloped virus) or lentivirus (an enveloped retrovirus) at sub-toxic concentrations for the mammalian cells (Vieira *et al.*, 2008). Since membrane fusion is a critical process in viral infection, which is dependent on a very high membrane negative curvature, the future development of surfactant molecules to prevent viral infections may benefit from focusing on the synthesis of compounds that once inserted into biological membranes affect the membrane-lipid critical packing in a way that inhibits membrane fusion (Israelachvili *et al.*, 1977; Chernomordik & Kozlov, 2003; Jahn, 2008). This concept has been shown to work in model membranes (reviewed in Chernomordik & Kozlov, 2003) but has yet to be explored on biological models.

In view of the fact that women will conceivably use a microbide gel frequently and over long periods of time during their sexually active years, it is crucial that microbicides are not harmful to the reproductive tract epithelium. After the failure of N-9, the first microbicide to be tested in clinical trials, combined efforts have been made in order to identify new, highly reproducible, predictive safety biomarkers, as well as to establish good experimental models in order to correctly evaluate microbicide-induced changes in the vaginal mucosa (Doncel *et al.*, 2004; Fichorova *et al.*, 2004; Lard-Whiteford *et al.*, 2004; Trifonova *et al.*, 2007; Cummins & Doncel, 2009; Keller & Herold, 2009; Doncel & Clark, 2010; Stone, 2010). The results from the present work have demonstrated that even at sub-lethal concentrations cationic surfactants are capable of interfering with the mitochondrial network, affecting its morphology and function, which stresses the importance of including a rigorous assessment of mitochondrial function when evaluating new microbicide candidates belonging to this family of compounds. Other safety aspects

that should be addressed for the most promising compounds include: Determination of the effects on mucosal inflammation and immunity; Possible compromise of the structure of the tight junction in epithelial cells; Impact on the natural microflora; Outcomes of chronic mucosal exposure to microbicides. Concerning the vaginal microflora, a special consideration should be made with respect to the effect of cationic surfactants on the *Lactobacillus* species which comprises an important role in the prevention of STIs, by avoiding the colonization of the urogenital tract by pathogenic bacteria, being crucial for women's reproductive and general health (Schwebke, 2001; Valore *et al.*, 2002; Reid & Bocking, 2003; Mijac *et al.*, 2006; Zarate & Nader-Macias, 2006; Graver & Wade, 2011). Cationic amphiphiles have been proven to work as antibacterial agents, despite the fact that different concentrations are required to produce the expected effect depending on the bacterial species (Soike *et al.*, 1952; Vieira *et al.*, 2008). In general, the antimicrobial activity of QACs is less pronounced at an acidic pH, an effect that has been attributed to a decrease ionization of the phosphate groups of the phospholipids and lipopolysaccharide in the bacterial membranes, which in consequence decreases the electrostatic interactions with the cationic surfactants (Matsumura *et al.*, 1986; Lindstedt *et al.*, 1990). However, the effect of pH acidification on the antimicrobial activity of QACs is not as straight forward as it may seem and is mainly dependent on the differences in membrane composition between different bacterial species (Soike *et al.*, 1952). Therefore, it will be important to address the effect pH changes exert over the antibacterial effects of QACs on either *Lactobacillus* species as well as in pathogenic Gram-negative bacteria, in order to evaluate whether the microbicidal compound is compatible with the normal vaginal flora.

Overall, the main conclusions of this study are:

1) Among the surfactant families studied, only cationic amphiphiles are toxic at concentrations below their CMC. QACs toxicity exhibit a non-linear dependence of their toxicity on the alkyl chain length and is also dependent on the chemical structure of the polar head group, being surfactants with larger polar head groups and more delocalized positive charge the most toxic
2) Of the surfactant families studied, cationic surfactants are the only ones that show selectivity towards different cell types.
3) Exposure of polarized epithelial cells to QACs induces mitochondrial fragmentation accompanied by a decrease in the cellular energy charge at higher concentrations. All the cationic surfactants were found to inhibit the NADH-ubiquinone oxidoreductase (Complex I) and impair the mitochondrial phosphorylative system. At low concentrations,

cationic surfactants-induced mitochondrial dysfunction leads to the apoptotic cell death of epithelial cells, whereas at high concentrations there is a prevalence of necrosis.

4) Mitochondrial fragmentation is an early event in cationic surfactant-induced toxicity, which starts at sub-lethal concentrations emphasizing the importance of a rigorous assessment of mitochondrial function when evaluating new cationic surfactants microbicide candidates.
5) With the exception of C_{16}TAB, all cationic surfactants were more toxic to *E. coli* than to mammalian epithelial polarized cells. Cationic surfactants exert their antimicrobial activity by two distinct mechanisms: a bacteriostatic action at low concentrations and a bactericidal activity at higher concentrations. With the increase in the alkyl chain length, the contribution of the bacteriostatic effect to the global antimicrobial activity of QACs also decreases, giving rise to a predominant bactericidal action. As in the case of mammalian cells, surfactants with larger polar head groups and more delocalized positive charge were more toxic.
6) Exposure of bacterial cells to low concentrations of QACs induces significant morphological alterations, such as, anomalies in the inner membrane structure and in the septum formation, emergence of elongated bacterial cells and, in some cases, detachment of the outer membrane.
7) Cationic surfactants with short hydrophobic chains (10 or 12 carbons), larger polar head groups and more delocalized charge display the highest therapeutic indices and are the best candidates for use in the prevention of bacterial STIs.

In conclusion, the results presented in this thesis shed some light into the mechanisms involved in surfactants antimicrobial activity as well as the mechanisms mediating its toxic effects in mammalian cells. Moreover, the present analysis also offer predictive power with regards to their safety, which may be useful in the design of more effective and less harmful surfactants for the use in topical applications for STI prophylaxis. Therefore, the detailed approach used in this work should be a mandatory first-line screening of possible microbicide candidates. Finally, it should be stressed how a single molecule which combines in itself the capacity of inhibiting the transmission of all STIs may never be found and, therefore, the future of microbicides development may reside in combining different molecules with more than one mechanism of action in order to provide protection against a broader range of pathogens and reduce the risk of drug-resistance development. Lastly, but equally as important, education of health providers and general public is essential for the successful implementation of any microbicide.

Appendix A

Appendix A

Surfactant dose-response toxicity curves

A.1. Overview

Dose-response toxicity curves describe the correlation between changes in cell viability caused by exposure to a range of concentrations of a given drug or compound, after a certain exposure time. They are typically graphed with the dose or dose function (e.g. $\log_{10}$ dose) on the x-axis and the measured effect on the y-axis. The analysis of the shape and slope of these curves is useful to predict compound toxicity and to understand its mechanism of action. When plotted as semi-logarithmic graphs, concentration-toxicity curves typically have a sigmoid-shape that can be defined by four parameters: The upper limit, which corresponds to a range of low concentrations that have no effect in cell viability; The lower limit, corresponding to the maximum toxicity; The curve slope, which measures the change in response per unit dose (steep curves have large slope values whereas shallow curves have small slope values); The drug concentration that induces an effect half way between the upper and lower limits (IC_{50}, inhibitory concentration 50). The mathematical model most commonly used to describe this type of toxicity curves is the logistic form of the Hill equation (Seefeldt *et al.*, 1995; Knezevic *et al.*, 2007; Goutelle *et al.*, 2008; Sebaugh, 2011), also referred in the literature as logistic equation or four-parameter logistic equation due to its similarity to the original logistic equation that described population growth and auto-catalytic chemical processes as functions of time (Neubig *et al.*, 2003; Goutelle *et al.*, 2008). The reverse modified Hill equation (Equation 1A) can be represented in its logistic form (Equation 1B) as follows:

$$y = C + \frac{D - C}{1 + \left(\frac{x}{IC_{50}}\right)^{b}} \qquad \textit{Equation 1A}$$

$$y = C + \frac{D - C}{1 + 10^{\left(\left(\log(x) - \log(IC_{50})\right) \times b\right)}} \qquad \textit{Equation 1B}$$

Where C is the curve lower limit; D is the upper limit, x is the drug concentration; IC_{50} is the inhibitory concentration 50; b is the curve slope (Hill coefficient[5]). When *y* values decrease in function of *x* the Hill coefficient has a negative value. This mathematical model assumes that the

[5] The Hill coefficient is indicative of the cooperativity of the process.

curve is symmetrical around the IC_{50}, i.e. the inflection point. However, some dose-response curves are not symmetrical. In these cases the use of an alternative model, described by the Richards equation, is recommended (Ricketts & Head, 1999; Van der Graaf & Schoemaker, 1999). This model, also called the five-parameter logistic equation, adds a new parameter to the logistic Hill equation, S, which quantifies the curve symmetry. The Richards equation is given by Equation 2:

$$y = C + \frac{D - C}{\left[1 + 10^{\left(\left(\log(x) - \log(IC_{50})\right) \times b\right)}\right]^{S}} \qquad \textit{Equation 2}$$

Where C is the curve lower limit; D is the upper limit; x is the drug concentration; IC_{50} is the inhibitory concentration 50; b is the curve slope (Hill coefficient); S is the Richards coefficient. When S = 1, the Richards equation is equal to the logistic Hill equation and the curve is symmetrical. One example of asymmetrical dose-response curves is the data obtained for MDCK II cell viability after exposure to C_{10}TAB presented in Chapter IV, Figure 4.1A. In this case the concentration-response toxicity curve was adjusted to the five-parameter logistic equation (Equation 2).

In other cases, dose-response curves do not have a sigmoid profile but exhibit a bell-shaped appearance, where low concentrations of the drug induce a stimulatory or inhibitory effect but high concentrations of the same compound evoke the opposite response. One way of fitting this kind of curves is to adjust the data using a combination of two sigmoidal shaped curves, one describing the stimulatory response and the other the inhibitory effect (Tucek *et al.*, 2002). The data obtained for caspase 3/7 activity in Chapter IV, Figure 4.1B, follows this behavior and the dose-response curve was fitted using the following equation:

$$y = C + \frac{D1 - C}{1 + 10^{\left(\left(\log(x) - \log(EC_{50}1)\right) \times b1\right)}} + \frac{D2 - C}{1 + 10^{\left(\left(\log(x) - \log(IC_{50}2)\right) \times b2\right)}} \qquad \textit{Equation 3}$$

Where x is the drug concentration; $D1$ is the plateau of the first curve; $D2$ is the plateau of the second curve, C is the point where the curve shape turns over from one tendency (e.g. stimulatory effect) to the other (e.g. inhibitory effect); $EC_{50}1$ is the stimulatory concentration 50 of the first curve; $IC_{50}2$ is the inhibitory concentration 50 of the second curve; $b1$ is the slope of curve one (Hill coefficient); and $b2$ is the slope of the second curve. In this model the Hill

coefficient has a positive value in one equation (ascending curve) and a negative value in the other (descending curve).

Another deviation from the standard monotonic sigmoid dose-response curves was observed in the case of toxicity results obtained for *Escherichia coli* in Chapter V, which exhibit a biphasic sigmoid shape. To analyze this data the following equation was used:

$$y = C + \frac{(D-C)\times Frac.}{1+10^{\left(\left(\log(x)-\log(IC_{50}1)\right)\times b1\right)}} + \frac{(D-C)\times(1-Frac.)}{1+10^{\left(\left(\log(x)-\log(IC_{50}2)\right)\times b2\right)}} \qquad \textit{Equation 4}$$

Where C and D are the minimal (lower limit) and maximal (upper limit) responses, respectively; $IC_{50}1$ is the inhibitory concentration 50 of the first curve; $IC_{50}2$ is the inhibitory concentration 50 of the second curve; $b1$ and $b2$ are the slopes of each equation; $Frac.$ is the fraction of the curve corresponding to the first equation; x is the drug concentration. In this case both Hill coefficients have negative values, since both phases of the concentration-toxicity curve are descendent, meaning the *y* values decrease in function of *x.* Moreover, were a curve to have three different phases instead of only two, a mathematical model similar to Equation 4 but combining three sigmoidal shaped curves could be used. In both cases the sum of the fraction corresponding to the contribution of each equation to the toxicity-curve should be equal to 1.

A.2. Surfactant toxicity towards mammalian cells

In the present work, the cell viability concentration-response curves in Chapter III were adjusted using Equation 1B. From this analysis, it was possible to calculate the LD_{90}, LD_{50} and LD_{10} concentrations, as described in Materials and methods (Chapter II, Section 2.3.5). The results obtained for each cell line are presented in Table A.1-A.4.

Table A.1. Lethal doses of surfactant towards polarized and confluent MDCK II cells.

Surfactant			Lethal Dose (M) after exposure time of			
Family	**Name**		**20 min**	**60 min**	**180 min**	**540 min**
Non-ionic	TX-100	LD_{90}	(3.18 ± 0.11) X 10^{-4}	(2.14 ± 0.17) X 10^{-4}	(1.58 ± 0.07) X 10^{-4}	(9.95 ± 0.37) X 10^{-5}
		LD_{50}	(2.88 ± 0.10) X 10^{-4}	(1.98 ± 0.16) X 10^{-4}	(1.50 ± 0.07) X 10^{-4}	(9.53 ± 0.35) X 10^{-5}
		LD_{10}	(2.63 ± 0.09) X 10^{-4}	(1.87 ± 0.15) X 10^{-4}	(1.41 ± 0.07) X 10^{-4}	(9.13 ± 0.34) X 10^{-5}
Zwiterionic	DDPS	LD_{90}	(2.50 ± 0.08) X 10^{-3}	(2.25 ± 0.05) X 10^{-3}	(1.86 ± 0.02) X 10^{-3}	(1.56 ± 0.01) X 10^{-3}
		LD_{50}	(2.34 ± 0.07) X 10^{-3}	(2.12 ± 0.02) X 10^{-3}	(1.71 ± 0.03) X 10^{-3}	(1.41 ± 0.01) X 10^{-3}
		LD_{10}	(2.18 ± 0.07) X 10^{-3}	(1.99 ± 0.03) X 10^{-3}	(1.56 ± 0.04) X 10^{-3}	(1.26 ± 0.02) X 10^{-3}
Anionic	SDS	LD_{90}	(6.68 ± 0.23) X 10^{-4}	(2.80 ± 0.26) X 10^{-4}	(1.79 ± 0.02) X 10^{-4}	(1.18 ± 0.03) X 10^{-4}
		LD_{50}	(5.57 ± 0.19) X 10^{-4}	(2.51 ± 0.23) X 10^{-4}	(1.69 ± 0.02) X 10^{-4}	(1.14 ± 0.03) X 10^{-4}
		LD_{10}	(4.69 ± 0.16) X 10^{-4}	(2.27 ± 0.21) X 10^{-4}	(1.60 ± 0.02) X 10^{-4}	(1.11 ± 0.02) X 10^{-4}
Cationic	C_{10}TAB	LD_{90}	(1.19 ± 0.03) X 10^{-2}	(7.04 ± 0.21) X 10^{-3}	(4.03 ± 0.02) X 10^{-3}	(2.30 ± 0.11) X 10^{-3}
		LD_{50}	(1.10 ± 0.03) X 10^{-2}	(6.20 ± 0.18) X 10^{-3}	(3.64 ± 0.02) X 10^{-3}	(2.05 ± 0.10) X 10^{-3}
		LD_{10}	(1.03 ± 0.03) X 10^{-2}	(5.39 ± 0.16) X 10^{-3}	(3.15 ± 0.02) X 10^{-3}	(1.67 ± 0.08) X 10^{-3}
	C_{12}TAB	LD_{90}	(1.01 ± 0.04) X 10^{-3}	(6.39 ± 0.09) X 10^{-4}	(4.27 ± 0.08) X 10^{-4}	(2.47 ± 0.02) X 10^{-4}
		LD_{50}	(8.71 ± 0.03) X 10^{-4}	(5.92 ± 0.16) X 10^{-4}	(4.11 ± 0.08) X 10^{-4}	(2.38 ± 0.02) X 10^{-4}
		LD_{10}	(6.95 ± 0.64) X 10^{-4}	(5.08 ± 0.31) X 10^{-4}	(3.69 ± 0.18) X 10^{-4}	(2.22 ± 0.04) X 10^{-4}
	C_{14}TAB	LD_{90}	(1.94 ± 0.01) X 10^{-4}	(8.89 ± 0.21) X 10^{-5}	(5.44 ± 0.04) X 10^{-5}	(3.89 ± 0.02) X 10^{-5}
		LD_{50}	(1.52 ± 0.01) X 10^{-4}	(7.74 ± 0.18) X 10^{-5}	(5.14 ± 0.04) X 10^{-5}	(3.73 ± 0.01) X 10^{-5}
		LD_{10}	(1.07 ± 0.01) X 10^{-4}	(6.91 ± 0.16) X 10^{-5}	(4.89 ± 0.04) X 10^{-5}	(3.64 ± 0.01) X 10^{-5}
	C_{16}TAB	LD_{90}	(1.33 ± 0.07) X 10^{-5}	(8.10 ± 0.15) X 10^{-6}	(5.14 ± 0.16) X 10^{-6}	(3.43 ± 0.11) X 10^{-6}
		LD_{50}	(1.20 ± 0.06) X 10^{-5}	(6.86 ± 0.13) X 10^{-6}	(4.02 ± 0.13) X 10^{-6}	(2.94 ± 0.05) X 10^{-6}
		LD_{10}	(8.54 ± 0.43) X 10^{-6}	(5.83 ± 0.11) X 10^{-6}	(3.18 ± 0.10) X 10^{-6}	(2.54 ± 0.03) X 10^{-6}
	C_{12}PBr	LD_{90}	(3.29 ± 0.03) X 10^{-4}	(2.33 ± 0.01) X 10^{-4}	(1.01 ± 0.18) X 10^{-4}	(6.55 ± 0.05) X 10^{-5}
		LD_{50}	(2.55 ± 0.03) X 10^{-4}	(1.82 ± 0.07) X 10^{-4}	(9.58 ± 1.21) X 10^{-5}	(6.43 ± 0.06) X 10^{-5}
		LD_{10}	(1.97 ± 0.06) X 10^{-4}	(1.38 ± 0.08) X 10^{-4}	(8.85 ± 0.31) X 10^{-5}	(6.32 ± 0.06) X 10^{-5}
	C_{12}BZK	LD_{90}	(1.55 ± 0.02) X 10^{-4}	(8.73 ± 0.64) X 10^{-5}	(5.41 ± 0.08) X 10^{-5}	(3.65 ± 0.09) X 10^{-5}
		LD_{50}	(1.45 ± 0.02) X 10^{-4}	(8.00 ± 0.33) X 10^{-5}	(5.18 ± 0.07) X 10^{-5}	(3.45 ± 0.03) X 10^{-5}
		LD_{10}	(1.37 ± 0.03) X 10^{-4}	(7.28 ± 0.30) X 10^{-5}	(4.94 ± 0.07) X 10^{-5}	(3.25 ± 0.00) X 10^{-5}

Data are shown as Mean ± SD of at least 3 independent experiments. LD_{90} – lethal dose 90; LD_{50} – lethal dose 50; LD_{10} – lethal dose 10.

Table A.2. Lethal doses of surfactant towards polarized and confluent Caco-2 cells.

Surfactant		Lethal Dose (M) after exposure time of				
Family	**Name**		**20 min**	**60 min**	**180 min**	**540 min**
Non-ionic	TX-100	LD_{90}	(2.01 ± 0.33) X 10^{-4}	(9,80 ± 0.16) X 10^{-5}	(8.19 ± 0.56) X 10^{-5}	(7.29 ± 0.13) X 10^{-5}
		LD_{50}	(1.70 ± 0.31) X 10^{-4}	(9.16 ± 0.54) X 10^{-5}	(7.77 ± 0.45) X 10^{-5}	(7.12 ± 0.14) X 10^{-5}
		LD_{10}	(1.57 ± 0.42) X 10^{-4}	(8.56 ± 0.92) X 10^{-5}	(7.38 ± 0.41) X 10^{-5}	(6.96 ± 0.15) X 10^{-5}
Zwiterionic	DDPS	LD_{90}	(2.40 ± 0.10) X 10^{-3}	(2.38 ± 0.03) X 10^{-3}	(1.94 ± 0.20) X 10^{-3}	(1.23 ± 0.07) X 10^{-3}
		LD_{50}	(2.22 ± 0.03) X 10^{-3}	(2.14 ± 0.02) X 10^{-3}	(1.47 ± 0.21) X 10^{-3}	(1.06 ± 0.05) X 10^{-3}
		LD_{10}	(2.00 ± 0.03) X 10^{-3}	(1.90 ± 0.02) X 10^{-3}	(1.09 ± 0.16) X 10^{-3}	(9.17 ± 0.45) X 10^{-4}
Anionic	SDS	LD_{90}	(8.78 ± 0.44) X 10^{-3}	(5.26 ± 0.06) X 10^{-4}	(1.81 ± 0.11) X 10^{-4}	(1.28 ± 0.11) X 10^{-4}
		LD_{50}	(7.38 ± 0.82) X 10^{-4}	(3.89 ± 0.10) X 10^{-4}	(1.49 ± 0.09) X 10^{-4}	(1.15 ± 0.07) X 10^{-4}
		LD_{10}	(6.2 ± 1.08) X 10^{-4}	(2.89 ± 0.10) X 10^{-4}	(1.23 ± 0.07) X 10^{-4}	(1.03 ± 0.04) X 10^{-4}
Cationic	$C_{10}TAB$	LD_{90}	(1.59 ± 0.21) X 10^{-2}	(8.23 ± 0.52) X 10^{-3}	(4.74 ± 0.42) X 10^{-3}	(2.15 ± 0.19) X 10^{-3}
		LD_{50}	(1.40 ± 0.08) X 10^{-2}	(6.85 ± 0.25) X 10^{-3}	(3.89 ± 0.33) X 10^{-3}	(1.95 ± 0.14) X 10^{-3}
		LD_{10}	(1.24 ± 0.04) X 10^{-2}	(5.75 ± 0.41) X 10^{-3}	(3.19 ± 0.34) X 10^{-3}	(1.77 ± 0.17) X 10^{-3}
	$C_{12}TAB$	LD_{90}	(1.43 ± 0.08) X 10^{-3}	(8.69 ± 0.23) X 10^{-4}	(4.70 ± 0.20) X 10^{-4}	(2.07 ± 0.28) X 10^{-4}
		LD_{50}	(1.29 ± 0.05) X 10^{-3}	(7.61 ± 0.20) X 10^{-4}	(4.30 ± 0.09) X 10^{-4}	(1.97 ± 0.34) X 10^{-4}
		LD_{10}	(1.16 ± 0.03) X 10^{-3}	(6.63 ± 0.21) X 10^{-4}	(3.93 ± 0.03) X 10^{-4}	(1.87 ± 0.39) X 10^{-4}
	$C_{14}TAB$	LD_{90}	(2.07 ± 0.07) X 10^{-4}	(1.16 ± 0.04) X 10^{-4}	(6.69 ± 0.09) X 10^{-5}	(4.79 ± 1.28) X 10^{-5}
		LD_{50}	(1.76 ± 0.07) X 10^{-4}	(1.05 ± 0.02) X 10^{-4}	(5.95 ± 0.24) X 10^{-5}	(4.17 ± 0.88) X 10^{-5}
		LD_{10}	(1.48 ± 0.11) X 10^{-4}	(9.59 ± 0.10) X 10^{-5}	(5.30 ± 0.41) X 10^{-5}	(3.64 ± 0.59) X 10^{-5}
	$C_{16}TAB$	LD_{90}	(1.56 ± 0.07) X 10^{-5}	(9.87 ± 0.51) X 10^{-6}	(5.21 ± 0.15) X 10^{-6}	(3.81 ± 0.61) X 10^{-6}
		LD_{50}	(1.31 ± 0.19) X 10^{-5}	(8.60 ± 0.26) X 10^{-6}	(4.65 ± 0.21) X 10^{-6}	(3.49 ± 0.44) X 10^{-6}
		LD_{10}	(1.10 ± 0.16) X 10^{-5}	(7.49 ± 0.50) X 10^{-6}	(4.16 ± 0.40) X 10^{-6}	(3.18 ± 0.30) X 10^{-6}
	$C_{12}PBr$	LD_{90}	(8.97 ± 0.39) X 10^{-4}	(5.74 ± 0.01) X 10^{-4}	(1.85 ± 0.08) X 10^{-4}	(1.13 ± 0.02) X 10^{-4}
		LD_{50}	(7.19 ± 0.58) X 10^{-4}	(4.52 ± 0.15) X 10^{-4}	(1.48 ± 0.04) X 10^{-4}	(1.08 ± 0.02) X 10^{-4}
		LD_{10}	(5.53 ± 0.78) X 10^{-4}	(3.11 ± 0.63) X 10^{-4}	(1.07 ± 0.14) X 10^{-4}	(1.03 ± 0.02) X 10^{-4}
	$C_{12}BZK$	LD_{90}	(2.82 ± 0.14) X 10^{-4}	(1.23 ± 0.14) X 10^{-4}	(8.93 ± 0.35) X 10^{-5}	(5.22 ± 0.19) X 10^{-5}
		LD_{50}	(1.79 ± 0.19) X 10^{-4}	(8.39 ± 1.16) X 10^{-5}	(6.75 ± 0.21) X 10^{-5}	(4.21 ± 0.96) X 10^{-5}
		LD_{10}	(1.20 ± 0.28) X 10^{-4}	(5.88 ± 1.76) X 10^{-5}	(4.87 ± 0.34) X 10^{-5}	(3.49 ± 1.62) X 10^{-5}

Data are shown as Mean ± SD of at least 3 independent experiments. LD_{90} – lethal dose 90; LD_{50} – lethal dose 50; LD_{10} – lethal dose 10.

Table A.3. Lethal doses of surfactant towards confluent HeLa cells.

Surfactant		Lethal Dose (M) after exposure time of				
Family	**Name**		**20 min**	**60 min**	**180 min**	**540 min**
Non-ionic	TX-100	LD_{90}	(2.35 ± 0.19) X 10^{-4}	(1.59 ± 0.12) X 10^{-4}	(1.23 ± 0.12) X 10^{-4}	(9.75 ± 0.64) X 10^{-5}
		LD_{50}	(2.07 ± 0.18) X 10^{-4}	(1.38 ± 0.09) X 10^{-4}	(1.11 ± 0.06) X 10^{-4}	(8.26 ± 0.42) X 10^{-5}
		LD_{10}	(1.81 ± 0.18) X 10^{-4}	(1.19 ± 0.01) X 10^{-4}	(1.01 ± 0.03) X 10^{-4}	(6.97 ± 0.37) X 10^{-5}
Zwiterionic	DDPS	LD_{90}	(1.41 ± 0.03) X 10^{-3}	(1.29 ± 0.10) X 10^{-3}	(1.01 ± 0.04) X 10^{-3}	(8.70 ± 0.34) X 10^{-4}
		LD_{50}	(1.34 ± 0.03) X 10^{-3}	(1.22 ± 0.10) X 10^{-3}	(8.81 ± 0.64) X 10^{-4}	(7.50 ± 0.07) X 10^{-4}
		LD_{10}	(1.28 ± 0.04) X 10^{-3}	(1.14 ± 0.11) X 10^{-3}	(7.72 ± 0.72) X 10^{-4}	(6.30 ± 0.47) X 10^{-4}
Anionic	SDS	LD_{90}	(1.99 ± 0.05) X 10^{-4}	(1.32 ± 0.04) X 10^{-4}	(9.65 ± 0.29) X 10^{-5}	(7.38 ± 0.12) X 10^{-5}
		LD_{50}	(1.73 ± 0.03) X 10^{-4}	(1.19 ± 0.02) X 10^{-4}	(8.57 ± 0.44) X 10^{-5}	(6.72 ± 0.20) X 10^{-5}
		LD_{10}	(1.51 ± 0.07) X 10^{-4}	(1.09 ± 0.16) X 10^{-4}	(7.46 ± 0.64) X 10^{-5}	(6.07 ± 0.25) X 10^{-5}
Cationic	C_{10}TAB	LD_{90}	(3.60 ± 0.07) X 10^{-3}	(2.49 ± 0.08) X 10^{-3}	(1.29 ± 0.12) X 10^{-3}	(5.10 ± 0.83) X 10^{-4}
		LD_{50}	(2.74 ± 0.07) X 10^{-3}	(1.91 ± 0.04) X 10^{-3}	(9.02 ± 1.65) X 10^{-4}	(2.14 ± 0.14) X 10^{-4}
		LD_{10}	(1.95 ± 0.08) X 10^{-3}	(1.44 ± 0.05) X 10^{-3}	(5.60 ± 1.01) X 10^{-4}	(6.68 ± 2.07) X 10^{-5}
	C_{12}TAB	LD_{90}	(4.30 ± 0.37) X 10^{-4}	(2.13 ± 0.17) X 10^{-4}	(1.17 ± 0.12) X 10^{-4}	(6.34 ± 0.40) X 10^{-5}
		LD_{50}	(3.03 ± 0.21) X 10^{-4}	(1.55 ± 0.08) X 10^{-4}	(7.08 ± 1.09) X 10^{-5}	(4.24 ± 0.17) X 10^{-5}
		LD_{10}	(1.71 ± 0.27) X 10^{-4}	(1.03 ± 0.12) X 10^{-4}	(4.04 ± 0.82) X 10^{-5}	(2.33 ± 0.91) X 10^{-5}
	C_{14}TAB	LD_{90}	(6.02 ± 0.31) X 10^{-5}	(3.54 ± 0.20) X 10^{-5}	(1.76 ± 0.21) X 10^{-5}	(9.82 ± 0.74) X 10^{-6}
		LD_{50}	(4.17 ± 0.07) X 10^{-5}	(2.42 ± 0.18) X 10^{-5}	(1.13 ± 0.16) X 10^{-5}	(7.13 ± 0.37) X 10^{-6}
		LD_{10}	(2.83 ± 0.05) X 10^{-5}	(1.61 ± 0.09) X 10^{-5}	(7.39 ± 0.87) X 10^{-6}	(4.92 ± 0.38) X 10^{-6}
	C_{16}TAB	LD_{90}	(3.60 ± 0.08) X 10^{-6}	(2.22 ± 0.17) X 10^{-5}	(1.31 ± 0.02) X 10^{-6}	(6.53 ± 0.23) X 10^{-7}
		LD_{50}	(2.45 ± 0.03) X 10^{-6}	(1.59 ± 0.13) X 10^{-6}	(1.05 ± 0.07) X 10^{-6}	(5.65 ± 0.13) X 10^{-7}
		LD_{10}	(1.65 ± 0.03) X 10^{-6}	(1.13 ± 0.07) X 10^{-6}	(8.18 ± 1.53) X 10^{-7}	(4.84 ± 0.14) X 10^{-7}
	C_{12}PBr	LD_{90}	(1.30 ± 0.03) X 10^{-4}	(7.28 ± 0.66) X 10^{-5}	(4.39 ± 0.32) X 10^{-5}	(2.74 ± 0.15) X 10^{-5}
		LD_{50}	(7.78 ± 0.87) X 10^{-5}	(5.03 ± 0.57) X 10^{-5}	(2.79 ± 0.07) X 10^{-5}	(1.94 ± 0.22) X 10^{-5}
		LD_{10}	(4.43 ± 0.87) X 10^{-5}	(2.72 ± 0.62) X 10^{-5}	(1.67 ± 0.09) X 10^{-5}	(1.29 ± 0.12) X 10^{-5}
	C_{12}BZK	LD_{90}	(8.90 ± 0.69) X 10^{-5}	(3.95 ± 0.21) X 10^{-5}	(2.31 ± 0.08) X 10^{-5}	(1.24 ± 0.08) X 10^{-5}
		LD_{50}	(6.91 ± 0.47) X 10^{-5}	(3.17 ± 0.03) X 10^{-5}	(1.81 ± 0.06) X 10^{-5}	(9.99 ± 0.05) X 10^{-6}
		LD_{10}	(3.64 ± 0.99) X 10^{-5}	(2.34 ± 0.09) X 10^{-5}	(1.13 ± 0.30) X 10^{-5}	(7.22 ± 0.62) X 10^{-6}

Data are shown as Mean ± SD of at least 3 independent experiments. LD_{90} – lethal dose 90; LD_{50} – lethal dose 50; LD_{10} – lethal dose 10.

Table A.4. Lethal doses of surfactant towards confluent FSDC cells.

Surfactant		Lethal Dose (M) after exposure time of				
Family	**Name**		**20 min**	**60 min**	**180 min**	**540 min**
Non-ionic	TX-100	LD_{90}	(1.86 ± 0.09) X 10^{-4}	(1.26 ± 0.12) X 10^{-4}	(7.73 ± 0.23) X 10^{-5}	(3.76 ± 0.28) X 10^{-5}
		LD_{50}	(1.59 ± 0.06) X 10^{-4}	(1.14 ± 0.06) X 10^{-4}	(6.79 ± 0.15) X 10^{-5}	(3.27 ± 0.35) X 10^{-5}
		LD_{10}	(1.37 ± 0.07) X 10^{-4}	(1.03 ± 0.03) X 10^{-4}	(5.98 ± 0.10) X 10^{-5}	(2.84 ± 0.42) X 10^{-5}
Zwiterionic	DDPS	LD_{90}	(1.27 ± 0.19) X 10^{-3}	(1.16 ± 0.18) X 10^{-3}	(1.12 ± 0.10) X 10^{-3}	(1.03 ± 0.04) X 10^{-3}
		LD_{50}	(1.22 ± 0.19) X 10^{-3}	(1.04 ± 0.06) X 10^{-3}	(1.02 ± 0.02) X 10^{-3}	(8.79 ± 0.29) X 10^{-4}
		LD_{10}	(1.13 ± 0.10) X 10^{-3}	(9.77 ± 0.27) X 10^{-4}	(9.20 ± 0.57) X 10^{-4}	(7.53 ± 0.14) X 10^{-4}
Anionic	SDS	LD_{90}	(3.06 ± 0.34) X 10^{-4}	(2.61 ± 0.03) X 10^{-4}	(1.63 ± 0.22) X 10^{-4}	(1.17 ± 0.10) X 10^{-4}
		LD_{50}	(2.65 ± 0.03) X 10^{-4}	(2.19 ± 0.08) X 10^{-4}	(1.52 ± 0.14) X 10^{-4}	(1.12 ± 0.12) X 10^{-4}
		LD_{10}	(2.32 ± 0.02) X 10^{-4}	(1.84 ± 0.16) X 10^{-4}	(1.42 ± 0.08) X 10^{-4}	(1.08 ± 0.15) X 10^{-4}
Cationic	$C_{10}TAB$	LD_{90}	(5.74 ± 0.36) X 10^{-3}	(3.80 ± 0.44) X 10^{-3}	(1.16 ± 0.11) X 10^{-3}	(3.35 ± 0.48) X 10^{-4}
		LD_{50}	(3.98 ± 0.42) X 10^{-3}	(2.16 ± 0.12) X 10^{-3}	(7.64 ± 1.11) X 10^{-4}	(2.14 ± 0.18) X 10^{-4}
		LD_{10}	(2.69 ± 0.44) X 10^{-3}	(1.34 ± 0.18) X 10^{-3}	(4.94 ± 1.14) X 10^{-4}	(1.35 ± 0.04) X 10^{-4}
	$C_{12}TAB$	LD_{90}	(4.90 ± 0.45) X 10^{-4}	(1.94 ± 0.30) X 10^{-4}	(7.77 ± 0.91) X 10^{-5}	(2.96 ± 0.24) X 10^{-5}
		LD_{50}	(3.50 ± 0.23) X 10^{-4}	(1.33 ± 0.06) X 10^{-4}	(4.73 ± 1.03) X 10^{-5}	(2.03 ± 0.19) X 10^{-5}
		LD_{10}	(2.48 ± 0.47) X 10^{-4}	(9.18 ± 0.67) X 10^{-5}	(2.96 ± 0.97) X 10^{-5}	(1.38 ± 0.12) X 10^{-5}
	$C_{14}TAB$	LD_{90}	(8.58 ± 1.14) X 10^{-5}	(3.62 ± 0.54) X 10^{-5}	(9.92 ± 2.51) X 10^{-6}	(4.44 ± 0.48) X 10^{-6}
		LD_{50}	(5.21 ± 0.87) X 10^{-5}	(2.84 ± 0.29) X 10^{-5}	(7.01 ± 1.93) X 10^{-6}	(2.99 ± 0.36) X 10^{-6}
		LD_{10}	(3.47 ± 0.57) X 10^{-5}	(2.24 ± 0.31) X 10^{-5}	(4.95 ± 1.64) X 10^{-6}	(2.04 ± 0.25) X 10^{-6}
	$C_{16}TAB$	LD_{90}	(5.82 ± 0.20) X 10^{-6}	(2.73 ± 0.50) X 10^{-6}	(1.07 ± 0.07) X 10^{-6}	(4.23 ± 0.29) X 10^{-7}
		LD_{50}	(3.89 ± 0.19) X 10^{-6}	(2.02 ± 0.21) X 10^{-6}	(8.30 ± 0.78) X 10^{-7}	(3.63 ± 0.15) X 10^{-7}
		LD_{10}	(2.51 ± 0.23) X 10^{-6}	(1.49 ± 0.12) X 10^{-6}	(6.51 ± 1.18) X 10^{-7}	(3.04 ± 0.13) X 10^{-7}
	$C_{12}PBr$	LD_{90}	(1.89 ± 0.09) X 10^{-4}	(8.60 ± 0.89) X 10^{-5}	(4.42 ± 1.00) X 10^{-7}	(1.85 ± 0.03) X 10^{-5}
		LD_{50}	(1.05 ± 0.14) X 10^{-4}	(4.85 ± 0.66) X 10^{-5}	(2.56 ± 0.50) X 10^{-5}	(1.47 ± 0.05) X 10^{-5}
		LD_{10}	(5.43 ± 1.04) X 10^{-5}	(2.59 ± 0.57) X 10^{-5}	(1.49 ± 0.27) X 10^{-5}	(1.17 ± 0.09) X 10^{-5}
	$C_{12}BZK$	LD_{90}	(1.23 ± 0.22) X 10^{-4}	(4.53 ± 0.80) X 10^{-5}	(1.36 ± 0.04) X 10^{-5}	(1.13 ± 0.10) X 10^{-5}
		LD_{50}	(8.17 ± 1.04) X 10^{-5}	(2.85 ± 0.24) X 10^{-5}	(1.20 ± 0.06) X 10^{-5}	(1.07 ± 0.05) X 10^{-5}
		LD_{10}	(5.23 ± 0.45) X 10^{-5}	(1.78 ± 0.18) X 10^{-5}	(1.07 ± 0.07) X 10^{-5}	(1.02 ± 0.01) X 10^{-5}

Data are shown as Mean ± SD of at least 3 independent experiments. LD_{90} – lethal dose 90; LD_{50} – lethal dose 50; LD_{10} – lethal dose 10.

Appendix B

Appendix B

Characterization of the Escherichia coli isolate

B.1. Overview

In Chapter V, *Escherichia coli* isolated from human necropsies by Dr Célia Nogueira, at the Microbiology Institute of the Faculty of Medicine from the University of Coimbra (Coimbra, Portugal), was used as a Gram negative bacterial cell model to test the microbicidal activity of cationic surfactants. In order to confirm the bacterial identity and to characterize its biochemical profile, the *E. coli* isolate was subjected to a standardized API 20E V4.1 test strip (from bioMérieux, Inc.). This system allows the rapid identification of enteric bacteria and other non-fastidious Gram-negative rods according to their analytical profile index (API) (Janin, 1976; Holmes *et al.*, 1978). The antibiotic resistance profile was also determined by disk diffusion method (Jorgensen & Turnidge, 2007). Both procedures were kindly performed by Dr Luísa Jordão at Instituto Nacional de Saúde Doutor Ricardo Jorge (INSA), DDI Laboratório de Micobactérias (Lisbon, Portugal).

B.2. Biochemical characterization of the *E. coli* isolate

The analytical profile index is a classification system based on a few conventional biochemical tests which allows the rapid identification of closely related bacterial species. Particularly, the API 20E strip is a standardized identification system used for Enterobacteriaceae and other non-fastidious Gram-negative rods. The API 20E strip uses 21 miniaturized biochemical tests that come in 20 separated compartments (Table B.1), containing dehydrated media to which bacterial suspensions are added. In result of bacterial metabolism some of the wells will undergo a colour change (e.g. due to pH changes). The result of each reaction is read as positive or negative according to the colour modification (Table B.1). In the result sheet the tests come separated into groups of three and a value of 1, 2 or 4 is attributed to each test (Fig. B.1). The 21st test is the oxidase reaction and has a value of 4 if the reaction is positive. By adding together the values corresponding to positive reactions within each group, as indicated in Figure B.1, a 7-digit profile number is obtained and can be entered into the API 20E V4.1 identification software containing the reference bacterial taxa. Bacteria are classified according to the percentage of identification accuracy (% ID), an estimation of how closely related are the taxon of the bacterial sample with

respect to all other taxa in the database, and also to the T index (T), an estimate of similarity between the sample's biochemical profile and the most typical set of reactions for the reference taxon (ranging from 0 to 1 and inversely proportional to the number of atypical tests). According to this procedure, the identification result can be categorized as excellent (% ID ≥ 99.9, T ≥ 0.75), very good (% ID ≥ 99.0, T ≥ 0.5), good (% ID ≥ 90.0, T ≥ 0.25) and acceptable (% ID ≥ 80.0, T ≥ 0).

The results obtained for the *Escherichia coli* used in the present work gave a biochemical profile number of 5144572 (Table B.2). The bacteria isolate was recognized as *E. coli* (colony type 1), with a very good identification (99.5% ID).

Table B.1. API 20E strip reading table.

Test	Substrate	Reaction tested	Result	
			Positive	Negative
ONPG	*o*-nitrophenyl-β-D-galactopyranoside	beta-galactosidase	colorless	yellow
ADH	arginine	arginine dihydrolase	yellow	red/orange
LDC	lysine	lysine descarboxylase	yellow	red/orange
ODC	ornithine	ornithine descarboxylase	yellow	red/orange
CIT	citrate	citrate utilization	pale green/ yellow	blue-green/blue
H_2S	sodium thiosulfate	H_2S production	colorless/grey	black deposit
URE	urea	urea hydrolysis	yellow	red/orange
TDA	tryptophan	deaminase	yellow	brown-red
IND	tryptophan	indole production	yellow	red (2 min)
VP	sodim pyruvate	acetoin production	colorless	pink/red (10 min)
GEL	charcoal gelatin	gelatinase	no diffusion of black	black diffuse
GLU	glucose	fermentation/oxidation	blue/blue-green	yellow
MAN	mannitol	fermentation/oxidation	blue/blue-green	yellow
INO	inositol	fermentation/oxidation	blue/blue-green	yellow
SOR	sorbitol	fermentation/oxidation	blue/blue-green	yellow
RHA	rhamnose	fermentation/oxidation	blue/blue-green	yellow
SAC	sucrose	fermentation/oxidation	blue/blue-green	yellow
MEL	melibiose	fermentation/oxidation	blue/blue-green	yellow
AMY	amygdalin	fermentation/oxidation	blue/blue-green	yellow
ARA	arabinose	fermentation/oxidation	blue/blue-green	yellow
OX	oxidase	oxidase	colorless/yellow	violet

Adapted from the API 20E product information datasheet provided by the manufacturer (bioMérieux, Inc.)

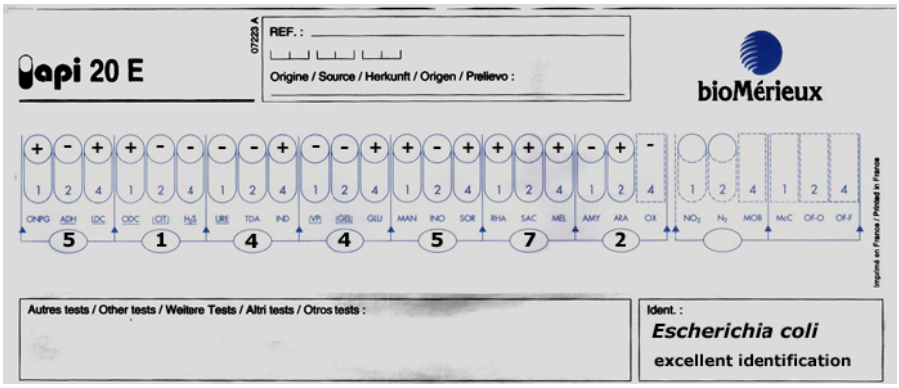

Figure B.1. API 20E strip score sheet. The tests come separated into groups of three and a value of 1, 2 or 4 is attributed to each one, as indicated. By adding together the values corresponding to positive reactions within each group, a profile number with 7 digits is obtained. The bacteria identification is performed using the V4.1 database. Adapted from the API 20E product information provided by the manufacturer (bioMérieux, Inc.)

Test	Result	Numerical profile
ONPG	positive (+)	
ADH	negative (-)	**5** (1+0+4)
LDC	positive (+)	
ODC	positive (+)	
CIT	negative (-)	**1** (1+0+0)
H_2S	negative (-)	
URE	negative (-)	
TDA	negative (-)	**4** (0+0+4)
IND	positive (+)	
VP	negative (-)	
GEL	negative (-)	**4** (0+0+4)
GLU	positive (+)	
MAN	positive (+)	
INO	negative (-)	**5** (1+0+4)
SOR	positive (+)	
RHA	positive (+)	
SAC	positive (+)	**7** (1+2+4)
MEL	positive (+)	
AMY	negative (-)	
ARA	positive (+)	**2** (0+2+0)
OX	negative (-)	

Table B.2. Biochemical characterization of the *E. coli* isolate using the API 20E strip. The numerical profile obtained was 5144572. Bacteria identification was performed using the V4.1 database. According to the analytical profile index the bacteria isolate was recognized as *E. coli* (colony type1), with a very good identification (99.5% ID).

B.3. Determination of the *E. coli* isolate's antibiotic resistance profile

The antibiotic resistance profile (antibiogram) of the isolated bacteria was determined by the standardized Kirby-Bauer disk diffusion susceptibility test (Jorgensen & Turnidge, 2007). In this method, bacteria are grown on Müller-Hinton agar plates and antimicrobial impregnated filter paper disks are placed on the inoculated agar plates. The absence of bacteria around the disks (zone of inhibition) is an indirect measure of the ability of the tested compound to inhibit the growth of that organism and the results are interpreted as resistant, intermediate (the inhibition that occurs is not sufficient to eradicate the bacteria) or susceptible according to diameter of the inhibition zone (Table B.3), using standard guidelines of the Clinical Laboratory Standards Institute (CLSI, 2006). The results obtained are presented in Table B.4.

Table B.3. Inhibition zone diameter standards for *Escherichia coli* and other enteric Gram-negative rods.

Antibiotic	Zone of inhibition (mm)		
	Resistant	Intermediate	Susceptible
Ampicillin	≤ 13	14-15	≥ 16
Amoxillin+Clavulanic acid	≤ 13	14-17	≥ 18
Cefuroxime	≤ 14	≤ 14	≥ 18
Trimethoprim	≤ 10	11-15	≥ 16
Ofloxacin	≤ 12	13-15	≥ 16
Nitrofurantoin	≤ 14	15-16	≥ 17
Fosfomycin	≤ 12	13-15	≥ 16
Norfloxacin	≤ 12	13-16	≥ 17
Ciprofloxacin	≤ 15	16-20	≥ 21
Gentamicin	≤ 12	14-15	≥ 16
Cefotaxime	≤ 14	15-22	≥ 23
Ceftazidime	≤ 14	15-17	≥ 18
Ceftriaxone	≤ 13	14-20	≥ 21
Amikacin	≤ 14	15-16	≥ 17
Aztreonan	≤ 15	16-21	≥ 22
Netilmicin	≤ 12	13-14	≥ 15
Imipenem	≤ 13	14-15	≥ 16
Piperacillin-Tazobactam	≤ 17	18-20	≥ 21

Adapted from the CLSI document M2-A9 (CLSI, 2006).

Table B.4. Antibiogram of the *Escherichia coli* isolate.

Antibiotic	Result	
	Zone of inhibition (mm)	Susceptibility
Ampicillin	0	R
Amoxillin+Clavulanic acid	18	S
Cefuroxime	25	S
Trimethoprim	0	R
Ofloxacin	0	R
Nitrofurantoin	24	S
Fosfomycin	35	S
Norfloxacin	0	R
Ciprofloxacin	0	R
Gentamicin	19	S
Cefotaxime	28	S
Ceftazidime	26	S
Ceftriaxone	29	S
Amikacin	20	S
Aztreonan	32	S
Netilmicin	22	S
Imipenem	31	S
Piperacillin-Tazobactam	25	S

R – resistant; S – susceptible

References

References

Abdool Karim, Q., Abdool Karim, S.S., Frohlich, J.A., Grobler, A.C., Baxter, C., Mansoor, L.E., Kharsany, A.B., Sibeko, S., Mlisana, K.P., Omar, Z., Gengiah, T.N., Maarschalk, S., Arulappan, N., Mlotshwa, M., Morris, L. & Taylor, D. (2010) Effectiveness and safety of tenofovir gel, an antiretroviral microbicide, for the prevention of HIV infection in women. *Science*, **329**, 1168-1174.

Abraham, J.J. (1948) Some account of the history of the treatment of syphilis. *Br J Vener Dis*, **24**, 153-161.

Abreu, M.S., Moreno, M.J. & Vaz, W.L. (2004) Kinetics and thermodynamics of association of a phospholipid derivative with lipid bilayers in liquid-disordered and liquid-ordered phases. *Biophys J*, **87**, 353-365.

Abu-Raddad, L.J., Magaret, A.S., Celum, C., Wald, A., Longini, I.M., Jr., Self, S.G. & Corey, L. (2008) Genital herpes has played a more important role than any other sexually transmitted infection in driving HIV prevalence in Africa. *PloS ONE*, **3**, e2230.

Ackermann, L. & de Klerk, G.W. (2002) Social factors that make South African women vulnerable to HIV infection. *Health Care Women Int*, **23**, 163-172.

Ahlström, B., Chelminska-Bertilsson, M., Thompson, R.A. & Edebo, L. (1997) Submicellar complexes may initiate the fungicidal effects of cationic amphiphilic compounds on *Candida albicans*. *Antimicrob Agents and Chemother*, **41**, 544-550.

Ahlström, B., Thompson, R.A. & Edebo, L. (1999) The effect of hydrocarbon chain length, pH, and temperature on the binding and bactericidal effect of amphiphilic betaine esters on *Salmonella typhimurium*. *APMIS*, **107**, 318-324.

Ahyayauch, H., Larijani, B., Alonso, A. & Goni, F.M. (2006) Detergent solubilization of phosphatidylcholine bilayers in the fluid state: influence of the acyl chain structure. *Biochim Biophys Acta*, **1758**, 190-196.

Allen, R.G. & Tresini, M. (2000) Oxidative stress and gene regulation. *Free Radic Biol Med*, **28**, 463-499.

Andersen, O.S. & Koeppe, R.E. 2nd (2007) Bilayer thickness and membrane protein function: an energetic perspective. *Annu Rev Biophys Biomol Struct*, **36**, 107-130.

Andree, H.A., Reutelingsperger, C.P., Hauptmann, R., Hemker, H.C., Hermens, W.T. & Willems, G.M. (1990) Binding of vascular anticoagulant alpha (VAC alpha) to planar phospholipid bilayers. *J Biol Chem*, **265**, 4923-4928.

Andres, M.T. & Fierro, J.F. (2010) Antimicrobial mechanism of action of transferrins: selective inhibition of H^+-ATPase. *Antimicrobl Agents Chemother*, **54**, 4335-4342.

Ankarcrona, M., Dypbukt, J.M., Bonfoco, E., Zhivotovsky, B., Orrenius, S., Lipton, S.A. & Nicotera, P. (1995) Glutamate-induced neuronal death: a succession of necrosis or apoptosis depending on mitochondrial function. *Neuron*, **15**, 961-973.

Apel-Paz, M., Doncel, G.F. & Vanderlick, T.K. (2008) Surfactants as microbicidal contraceptives: a calorimetric study of partitioning and translocation in model membrane systems. *Ind. Eng. Chem. Res.*, **47**, 3554-3561.

Araki, T., Hayashi, M., Watanabe, N., Kanuka, H., Yoshino, J., Miura, M. & Saruta, T. (2002) Down-regulation of Mcl-1 by inhibition of the PI3-K/Akt pathway is required for cell shrinkage-dependent cell death. *Biochem Biophys Res Commun*, **290**, 1275-1281.

Aranzazu Partearroyo, M., Ostolaza, H., Goni, F.M. & Barbera-Guillem, E. (1990) Surfactant-induced cell toxicity and cell lysis. A study using B16 melanoma cells. *Biochem Pharmacol*, **40**, 1323-1328.

Arnoult, D. (2007) Mitochondrial fragmentation in apoptosis. *Trends Cell Biol*, **17**, 6-12.

Assunção Guimarães, C. & Linden, R. (2004) Programmed cell death. Apoptosis and alternative deathstyles. *Eur J Biochem*, **271**, 1638-1650.

Autran, B., Carcelain, G., Li, T.S., Blanc, C., Mathez, D., Tubiana, R., Katlama, C., Debre, P. & Leibowitch, J. (1997) Positive effects of combined antiretroviral therapy on $CD4^+$ T cell homeostasis and function in advanced HIV disease. *Science*, **277**, 112-116.

Ayotte, N. & Colin, P. (2002) Spermicidal activity of a new contraceptive sponge. *Adv Ther*, **19**, 219-228.

Baker, Z., Harrison, R.W. & Miller, B.F. (1941) The bactericidal action of synthetic detergents. *J Exp Med*, **74**, 611-620.

Balgavý, P. & Devinsky, F. (1996) Cut-off effects in biological activities of surfactants. *Adv Colloid Interface Sci*, **66**, 23-63.

Balgavý, P., Gawrisch, K. & Frischleder, H. (1984) Effect of N-alkyl-N,N,N-trimethylammonium ions on phosphatidylcholine model membrane structure as studied by ^{31}P NMR. Biochim. *Biophys. Acta* **772**, 58-64.

Bar, W., Bade-Schumann, U., Krebs, A. & Cromme, L. (2009) Rapid method for detection of minimal bactericidal concentration of antibiotics. *J Microbiol Methods*, **77**, 85-89.

Baracca, A., Sgarbi, G., Solaini, G. & Lenaz, G. (2003) Rhodamine 123 as a probe of mitochondrial membrane potential: evaluation of proton flux through F_0 during ATP synthesis. *Biochim Biophys Acta*, **1606**, 137-146.

Barer, M.R. & Harwood, C.R. (1999) Bacterial viability and culturability. *Adv Microb Physiol*, **41**, 93-137.

Bârzu, O., Guerrieri, F., Scarfo, R., Capozza, G. & Papa, S. (1989) Effect of cetyltrimethylammonium on ATP hydrolysis and proton translocation in the F_0-F_1 H^+-ATP synthase of mitochondria. *J Bioenerg Biomembr*, **21**, 403-414.

Baudouin, C., Labbe, A., Liang, H., Pauly, A. & Brignole-Baudouin, F. (2010) Preservatives in eyedrops: the good, the bad and the ugly. *Prog Retin Eye Res*, **29**, 312-334.

Bayerl, T.M., Werner, G.D. & Sackmann, E. (1989) Solubilization of DMPC and DPPC vesicles by detergents below their critical micellization concentration: high-sensitivity differential scanning calorimetry, Fourier transform infrared spectroscopy and freeze-fracture electron microscopy reveal two interaction sites of detergents in vesicles. *Biochim Biophys Acta*, **984**, 214-224.

Belec, L., Tevi-Benissan, C., Bianchi, A., Cotigny, S., Beumont-Mauviel, M., Si-Mohamed, A. & Malkin, J.E. (2000) *In vitro* inactivation of Chlamydia trachomatis and of a panel of DNA (HSV-2, CMV, adenovirus, BK virus) and RNA (RSV, enterovirus) viruses by the spermicide benzalkonium chloride. *J Antimicrob Chemother*, **46**, 685-693.

Belland, R.J., Morrison, S.G., Ison, C. & Huang, W.M. (1994) *Neisseria gonorrhoeae* acquires mutations in analogous regions of gyrA and parC in fluoroquinolone-resistant isolates. *Mol Microbiol*, **14**, 371-380.

Benard, G., Bellance, N., James, D., Parrone, P., Fernandez, H., Letellier, T. & Rossignol, R. (2007) Mitochondrial bioenergetics and structural network organization. *J Cell Sci*, **120**, 838-848.

Bereiter-Hahn, J. & Voth, M. (1994) Dynamics of mitochondria in living cells: shape changes, dislocations, fusion, and fission of mitochondria. *Microsc Res Tech*, **27**, 198-219.

Bernardi, P., Scorrano, L., Colonna, R., Petronilli, V. & Di Lisa, F. (1999) Mitochondria and cell death. Mechanistic aspects and methodological issues. *Eur J Biochem*, **264**, 687-701.

Bjergbaek, L.A., Haagensen, J.A., Molin, S. & Roslev, P. (2008) Effect of oxygen limitation and starvation on the benzalkonium chloride susceptibility of *Escherichia coli*. *J Appl Microbiol*, **105**, 1310-1317.

Bleazard, W., McCaffery, J.M., King, E.J., Bale, S., Mozdy, A., Tieu, Q., Nunnari, J. & Shaw, J.M. (1999) The dynamin-related GTPase Dnm1 regulates mitochondrial fission in yeast. *Nat Cell Biol*, **1**, 298-304.

Bojarski, C., Weiske, J., Schoneberg, T., Schroder, W., Mankertz, J., Schulzke, J.D., Florian, P., Fromm, M., Tauber, R. & Huber, O. (2004) The specific fates of tight junction proteins in apoptotic epithelial cells. *J Cell Sci*, **117**, 2097-2107.

Bolch, O.H., Jr. & Warren, J.C. (1973) *In vitro* effects of Emko on *Neisseria gonorrhoeae* and *Trichomonas vaginalis*. *Am J Obstet Gynecol*, **115**, 1145-1148.

Bonfoco, E., Krainc, D., Ankarcrona, M., Nicotera, P. & Lipton, S.A. (1995) Apoptosis and necrosis: two distinct events induced, respectively, by mild and intense insults with N-methyl-D-aspartate or nitric oxide/superoxide in cortical cell cultures. *Proc Natl Acad Sci U S A*, **92**, 7162-7166.

Bot, C.T. & Prodan, C. (2010) Quantifying the membrane potential during *E. coli* growth stages. *Biophys Chem*, **146**, 133-137.

Boulos, L., Prevost, M., Barbeau, B., Coallier, J. & Desjardins, R. (1999) LIVE/DEAD BacLight : application of a new rapid staining method for direct enumeration of viable and total bacteria in drinking water. *J Microbiol Methods*, **37**, 77-86.

Bradbury, D.A., Simmons, T.D., Slater, K.J. & Crouch, S.P. (2000) Measurement of the ADP:ATP ratio in human leukaemic cell lines can be used as an indicator of cell viability, necrosis and apoptosis. *J Immunol Methods*, **240**, 79-92.

Bragadin, M. & Dell'Antone, P. (1996) Mitochondrial bioenergetics as affected by cationic detergents. *Arch Environ Contam Toxicol*, **30**, 280-284.

Bretscher, M.S. & Raff, M.C. (1975) Mammalian plasma membranes. *Nature*, **258**, 43-49.

Brito, R.M. & Vaz, W.L. (1986) Determination of the critical micelle concentration of surfactants using the fluorescent probe N-phenyl-1-naphthylamine. *Analytical Biochemistry*, **152**, 250-255.

Brocard, J.B., Rintoul, G.L. & Reynolds, I.J. (2003) New perspectives on mitochondrial morphology in cell function. *Biol Cell*, **95**, 239-242.

Brookes, P.S., Yoon, Y., Robotham, J.L., Anders, M.W. & Sheu, S.S. (2004) Calcium, ATP, and ROS: a mitochondrial love-hate triangle. *Am J Physiol Cell Physiol*, **287**, C817-833.

Brown, W.J. (1988) National Committee for Clinical Laboratory Standards agar dilution susceptibility testing of anaerobic gram-negative bacteria. *Antimicrob Agents Chemother*, 32, 385-390.

Buchbinder, S.P., Mehrotra, D.V., Duerr, A., Fitzgerald, D.W., Mogg, R., Li, D., Gilbert, P.B., Lama, J.R., Marmor, M., Del Rio, C., McElrath, M.J., Casimiro, D.R., Gottesdiener, K.M., Chodakewitz, J.A., Corey, L. & Robertson, M.N. (2008) Efficacy assessment of a cell-mediated immunity HIV-1 vaccine (the Step Study): a double-blind, randomised, placebo-controlled, test-of-concept trial. *Lancet*, **372**, 1881-1893.

Budihardjo, I., Oliver, H., Lutter, M., Luo, X. & Wang, X. (1999) Biochemical pathways of caspase activation during apoptosis. *Annu Rev Cell Dev Biol*, **15**, 269-290.

Burns, M. (1999) Management of narrow therapeutic index drugs. *J Thromb Thrombolysis*, **7**, 137-143.

Campanhã, M.T., Mamizuka, E.M. & Carmona-Ribeiro, A.M. (1999) Interactions between cationic liposomes and bacteria: the physical-chemistry of the bactericidal action. *J Lipid Res*, **40**, 1495-1500.

Cantor, R.S. (1997) Lateral pressures in cell membranes: a mechanism for modulation of protein function. *J. Phys. Chem. B*, **101**, 1723-1725.

Cantor, R.S. (1999) The influence of membrane lateral pressures on simple geometric models of protein conformational equilibria. *Chem Phys Lipids*, **101**, 45-56.

Cardoso, R.M., Martins, P.A., Gomes, F., Doktorovova, S., Vaz, W.L. & Moreno, M.J. (2011) Chain-length dependence of insertion, desorption, and translocation of a homologous series of 7-nitrobenz-2-oxa-1,3-diazol-4-yl-labeled aliphatic amines in membranes. *J Phys Chem B*, **115**, 10098-10108.

Carpo, B.G., Verallo-Rowell, V.M. & Kabara, J. (2007) Novel antibacterial activity of monolaurin compared with conventional antibiotics against organisms from skin infections: an *in vitro* study. *J Drugs Dermatol*, **6**, 991-998.

Catalone, B.J., Kish-Catalone, T.M., Neely, E.B., Budgeon, L.R., Ferguson, M.L., Stiller, C., Miller, S.R., Malamud, D., Krebs, F.C., Howett, M.K. & Wigdahl, B. (2005) Comparative safety evaluation of the candidate vaginal microbicide C31G. *Antimicrob Agents Chemother*, **49**, 1509-1520.

Celum, C.L. (2010) Sexually transmitted infections and HIV: epidemiology and interventions. *Top HIV Med*, **18**, 138-142.

Chan, D.C. (2006) Mitochondria: dynamic organelles in disease, aging, and development. *Cell*, **125**, 1241-1252.

Chance, B. & Williams, G.R. (1956) The respiratory chain and oxidative phosphorylation. *Adv Enzymol Relat Subj Biochem*, **17**, 65-134.

Chen, H. & Chan, D.C. (2005) Emerging functions of mammalian mitochondrial fusion and fission. *Hum Mol Genet*, **14 Spec No. 2**, R283-289.

Chen, H., Chomyn, A. & Chan, D.C. (2005) Disruption of fusion results in mitochondrial heterogeneity and dysfunction. *J Biol Chem*, **280**, 26185-26192.

Chen, L.B. (1988) Mitochondrial membrane potential in living cells. *Annu Rev Cell Biol*, **4**, 155-181.

Chernomordik, L.V. & Kozlov, M.M. (2003) Protein-lipid interplay in fusion and fission of biological membranes. *Annu Rev Biochem*, 72, 175-207.

Chesson, H.W. & Pinkerton, S.D. (2000) Sexually transmitted diseases and the increased risk for HIV transmission: implications for cost-effectiveness analyses of sexually transmitted disease prevention interventions. *J Acquir Immune Defic Syndr*, **24**, 48-56.

Cirak, J., Balgavý, P. & Devinsky, F. (1988) The lateral order of dipalmitoylphosphatidylcholine model membranes in the presence of N-alkyl-N,N,N-trimethylammonium ions as studied by Raman spectroscopy. *Gen Physiol Biophys*, **7**, 633-642.

CLSI (2006) *Clinical and Laboratory Standards Institute: performance standards for antimicrobial disk susceptibility testing. Approved Standard - 9th ed. Document M2-A9.* Clinical and Laboratory Standards Institute, Wayne, USA.

CLSI (2009) *Methods for dilution antimicrobial susceptibility tests for bacteria that grow aerobically; Approved Standard—8th ed. Document M07-A8.* Clinical and Laboratory Standards Institute, Wayne, USA.

Cohen, M.S., Chen, Y.Q., McCauley, M., Gamble, T., Hosseinipour, M.C., Kumarasamy, N., Hakim, J.G., Kumwenda, J., Grinsztejn, B., Pilotto, J.H., Godbole, S.V., Mehendale, S., Chariyalertsak, S., Santos, B.R., Mayer, K.H., Hoffman, I.F., Eshleman, S.H., Piwowar-Manning, E., Wang, L., Makhema, J., Mills, L.A., de Bruyn, G., Sanne, I., Eron, J., Gallant, J., Havlir, D., Swindells, S., Ribaudo, H., Elharrar, V., Burns, D., Taha, T.E., Nielsen-Saines, K., Celentano, D., Essex, M. & Fleming, T.R. (2011) Prevention of HIV-1 infection with early antiretroviral therapy. *N Engl J Med*, **365**, 493-505.

Cone, R.A., Hoen, T., Wong, X., Abusuwwa, R., Anderson, D.J. & Moench, T.R. (2006) Vaginal microbicides: detecting toxicities *in vivo* that paradoxically increase pathogen transmission. *BMC Infect Dis*, **6**, 90.

Corey, L., Wald, A., Celum, C.L. & Quinn, T.C. (2004) The effects of Herpes Simplex Virus-2 on HIV-1 acquisition and transmission: a review of two overlapping epidemics. *J Acquir Immune Defic Syndr*, **35**, 435-445.

Creighton, S., Tenant-Flowers, M., Taylor, C.B., Miller, R. & Low, N. (2003) Co-infection with gonorrhoea and chlamydia: how much is there and what does it mean? *Int J STD AIDS*, **14**, 109-113.

Cronan, J.E. (2003) Bacterial membrane lipids: where do we stand? *Annu Rev Microbiol*, **57**, 203-224.

Cummins, J.E., Jr. & Doncel, G.F. (2009) Biomarkers of cervicovaginal inflammation for the assessment of microbicide safety. *Sex Transm Dis*, **36**, S84-91.

Cutler, B. & Justman, J. (2008) Vaginal microbicides and the prevention of HIV transmission. *Lancet Infect Dis*, **8**, 685-697.

Dallabetta, G. & Neilson, G. (2004) Efforts to control sexually transmitted infections as a means to limit HIV transmission: what is the evidence? *Curr HIV/AIDS Rep*, **1**, 166-171.

Datiles, M.J., Johnson, E.A. & McCarty, R.E. (2008) Inhibition of the ATPase activity of the catalytic portion of ATP synthases by cationic amphiphiles. *Biochim Biophys Acta*, **1777**, 362-368.

Davies, A., Bentley, M. & Field, B.S. (1968) Comparison of the action of vantocil, cetrimide and chlorhexidine on *Escherichia coli* and its spheroplasts and the protoplasts of Gram positive bacteria. *J Appl Bacteriol*, **31**, 448-461.

Davis, K.R. & Weller, S.C. (1999) The effectiveness of condoms in reducing heterosexual transmission of HIV. *Fam Plann Perspect*, **31**, 272-279.

Debbasch, C., Brignole, F., Pisella, P.J., Warnet, J.M., Rat, P. & Baudouin, C. (2001) Quaternary ammoniums and other preservatives' contribution in oxidative stress and apoptosis on Chang conjunctival cells. *Invest Ophthalmol Vis Sci*, **42**, 642-652.

DeGruttola, V., Seage, G.R. 3rd, Mayer, K.H. & Horsburgh, C.R., Jr. (1989) Infectiousness of HIV between male homosexual partners. *J Clin Epidemiol*, **42**, 849-856.

Denny, B.J., Novotny, L., West, P.W., Blesova, M. & Zamocka, J. (2005) Antimicrobial activity of a series of 1-alkyl-2-(4-pyridyl)pyridinium bromides against Gram-positive and Gram-negative bacteria. *Med Princ Pract*, **14**, 377-381.

Denyer, S.P. & Hugo, W.B. (1977) The mode of action of tetradecyltrimethyl ammonium bromide (CTAB) on *Staphylococcus aureus* [proceedings]. *J Pharm Pharmacol*, **29 Suppl**, 66P.

Desagher, S. & Martinou, J.C. (2000) Mitochondria as the central control point of apoptosis. *Trends Cell Biol*, **10**, 369-377.

Dias, R.S., Innerlohinger, J., Glatter, O., Miguel, M.G. & Lindman, B. (2005) Coil-globule transition of DNA molecules induced by cationic surfactants: a dynamic light scattering study. *J Phys Chem B*, **109**, 10458-10463.

Domagk, G. (1935) A new class of disinfectant. *Deut Med Wochenschr*, 61, 829-832.

Doncel, G.F., Chandra, N. & Fichorova, R.N. (2004) Preclinical assessment of the proinflammatory potential of microbicide candidates. *J Acquir Immune Defic Syndr*, **37 Suppl 3**, S174-180.

Doncel, G.F. & Clark, M.R. (2010) Preclinical evaluation of anti-HIV microbicide products: New models and biomarkers. *Antiviral Res*, **88 Suppl 1**, S10-18.

Dukes, J.D., Whitley, P. & Chalmers, A.D. (2011) The MDCK variety pack: choosing the right strain. *BMC Cell Biol*, **12**, 43.

Dymond, M.K. & Attard, G.S. (2008) Cationic type I amphiphiles as modulators of membrane curvature elastic stress *in vivo*. *Langmuir*, **24**, 11743-11751.

Eguchi, Y., Shimizu, S. & Tsujimoto, Y. (1997) Intracellular ATP levels determine cell death fate by apoptosis or necrosis. *Cancer Res*, **57**, 1835-1840.

Eguchi, Y., Srinivasan, A., Tomaselli, K.J., Shimizu, S. & Tsujimoto, Y. (1999) ATP-dependent steps in apoptotic signal transduction. *Cancer Res*, **59**, 2174-2181.

Ekelund, K., Osth, K., Pahlstorp, C., Bjork, E., Ulvenlund, S. & Johansson, F. (2005) Correlation between epithelial toxicity and surfactant structure as derived from the effects of polyethyleneoxide surfactants on Caco-2 cell monolayers and pig nasal mucosa. *J Pharm Sci*, **94**, 730-744.

Ellis, C.E., Murphy, E.J., Mitchell, D.C., Golovko, M.Y., Scaglia, F., Barcelo-Coblijn, G.C. & Nussbaum, R.L. (2005) Mitochondrial lipid abnormality and electron transport chain impairment in mice lacking alpha-synuclein. *Mol Cell Biol*, **25**, 10190-10201.

Emaus, R.K., Grunwald, R. & Lemasters, J.J. (1986) Rhodamine 123 as a probe of transmembrane potential in isolated rat-liver mitochondria: spectral and metabolic properties. *Biochim Biophys Acta*, **850**, 436-448.

Enomoto, R., Suzuki, C., Ohno, M., Ohasi, T., Futagami, R., Ishikawa, K., Komae, M., Nishino, T., Konishi, Y. & Lee, E. (2007) Cationic surfactants induce apoptosis in normal and cancer cells. *Ann N Y Acad Sci*, **1095**, 1-6.

Estabrook, R.W. (1967) Mitochondrial respiratory control and the polarographic measurement of ADP/O ratios. *Methods Enzymol*, **10**, 41-47.

Feldblum, P.J., Adeiga, A., Bakare, R., Wevill, S., Lendvay, A., Obadaki, F., Olayemi, M.O., Wang, L., Nanda, K. & Rountree, W. (2008) SAVVY vaginal gel (C31G) for prevention of HIV infection: a randomized controlled trial in Nigeria. *PloS ONE*, **3**, e1474.

Feldenberg, L.R., Thevananther, S., del Rio, M., de Leon, M. & Devarajan, P. (1999) Partial ATP depletion induces Fas- and caspase-mediated apoptosis in MDCK cells. *Am J Physiol*, **276**, F837-846.

Fichorova, R.N., Tucker, L.D. & Anderson, D.J. (2001) The molecular basis of Nonoxynol-9-induced vaginal inflammation and its possible relevance to human immunodeficiency virus type 1 transmission. *J Infect Dis*, **184**, 418-428.

Fichorova, R.N., Bajpai, M., Chandra, N., Hsiu, J.G., Spangler, M., Ratnam, V. & Doncel, G.F. (2004) Interleukin (IL)-1, IL-6, and IL-8 predict mucosal toxicity of vaginal microbicidal contraceptives. *Biol Reprod*, **71**, 761-769.

Fink, S.L. & Cookson, B.T. (2005) Apoptosis, pyroptosis, and necrosis: mechanistic description of dead and dying eukaryotic cells. *Infect Immun*, **73**, 1907-1916.

Fleming, D.T. & Wasserheit, J.N. (1999) From epidemiological synergy to public health policy and practice: the contribution of other sexually transmitted diseases to sexual transmission of HIV infection. *Sex Transm Infect*, **75**, 3-17.

Flynn, N.M., Forthal, D.N., Harro, C.D., Judson, F.N., Mayer, K.H. & Para, M.F. (2005) Placebo-controlled phase 3 trial of a recombinant glycoprotein 120 vaccine to prevent HIV-1 infection. *J Infect Dis*, **191**, 654-665.

Frank, S., Gaume, B., Bergmann-Leitner, E.S., Leitner, W.W., Robert, E.G., Catez, F., Smith, C.L. & Youle, R.J. (2001) The role of dynamin-related protein 1, a mediator of mitochondrial fission, in apoptosis. *Dev Cell*, **1**, 515-525.

Frezza, C., Cipolat, S. & Scorrano, L. (2007) Measuring mitochondrial shape changes and their consequences on mitochondrial involvement during apoptosis. *Methods Mol Biol*, **372**, 405-420.

Fromenty, B., Fisch, C., Berson, A., Letteron, P., Larrey, D. & Pessayre, D. (1990) Dual effect of amiodarone on mitochondrial respiration. Initial protonophoric uncoupling effect followed by inhibition of the respiratory chain at the levels of Complex I and Complex II. *J Pharmacol Exp Ther*, **255**, 1377-1384.

Galen, B.T., Martin, A.P., Hazrati, E., Garin, A., Guzman, E., Wilson, S.S., Porter, D.D., Lira, S.A., Keller, M.J. & Herold, B.C. (2007) A comprehensive murine model to evaluate topical vaginal microbicides: mucosal inflammation and susceptibility to genital Herpes as surrogate markers of safety. *J Infect Dis*, **195**, 1332-1339.

Gallo, R.C. & Montagnier, L. (2003) The discovery of HIV as the cause of AIDS. *N Engl J Med*, **349**, 2283-2285.

Gallova, J., Devinsky, F. & Balgavý, P. (1990) Interaction of surfactants with model and biological membranes. II. Effect of N-alkyl-N,N,N-trimethylammonium ions on phosphatidylcholine bilayers as studied by spin probe ESR. *Chem Phys Lipids*, **53**, 231-241.

Galvin, S.R. & Cohen, M.S. (2004) The role of sexually transmitted diseases in HIV transmission. *Nat Rev Microbiol*, **2**, 33-42.

Geiger-Maor, A., Levi, I., Even-Ram, S., Smith, Y., Bowdish, D.M., Nussbaum, G. & Rachmilewitz, J. (2012) Cells exposed to sublethal oxidative stress selectively attract monocytes/macrophages via scavenger receptors and MyD88-mediated signaling. *J Immunol*, 188, 1234-1244.

Gennis, R.B. (1989) *Biomembranes: Molecular Structure and Function*. Springer-Verlag, New York, USA.

Gerbase, A.C., Rowley, J.T., Heymann, D.H., Berkley, S.F. & Piot, P. (1998) Global prevalence and incidence estimates of selected curable STDs. *Sex Transm Infect*, **74 Suppl 1**, S12-16.

Gilbert, P. & Al-taae, A. (1985) Antimicrobial activity of some alkyltrimethylammonium bromides. *Lett Appl Microbiol*, **1**, 101-105.

Gilbert, P. & Moore, L.E. (2005) Cationic antiseptics: diversity of action under a common epithet. *J Appl Microbiol*, **99**, 703-715.

Girolomoni, G., Lutz, M.B., Pastore, S., Assmann, C.U., Cavani, A. & Ricciardi-Castagnoli, P. (1995) Establishment of a cell line with features of early dendritic cell precursors from fetal mouse skin. *Eur J Immunol*, **25**, 2163-2169.

Gomez-Lazaro, M., Bonekamp, N.A., Galindo, M.F., Jordan, J. & Schrader, M. (2008) 6-Hydroxydopamine (6-OHDA) induces Drp1-dependent mitochondrial fragmentation in SH-SY5Y cells. *Free Radic Biol Med*, **44**, 1960-1969.

Gornall, A.G., Bardawill, C.J. & David, M.M. (1949) Determination of serum proteins by means of the biuret reaction. *J Biol Chem*, **177**, 751-766.

Goutelle, S., Maurin, M., Rougier, F., Barbaut, X., Bourguignon, L., Ducher, M. & Maire, P. (2008) The Hill equation: a review of its capabilities in pharmacological modelling. *Fundam Clin Pharmacol*, **22**, 633-648.

Granier, S.A., Nicolas-Chanoine, M.H., Nguyen Van, J.C., Leflon-Guibout, V., Kitzis, M.D. & Goldstein, F.W. (2002) False susceptibility of *Klebsiella oxytoca* to some extended-spectrum cephalosporins. *J Antimicrob Chemother*, **50**, 303-304.

Grant, R.M., Lama, J.R., Anderson, P.L., McMahan, V., Liu, A.Y., Vargas, L., Goicochea, P., Casapia, M., Guanira-Carranza, J.V., Ramirez-Cardich, M.E., Montoya-Herrera, O., Fernandez, T., Veloso, V.G., Buchbinder, S.P., Chariyalertsak, S., Schechter, M., Bekker, L.G., Mayer, K.H., Kallas, E.G., Amico, K.R., Mulligan, K., Bushman, L.R., Hance, R.J., Ganoza, C., Defechereux, P., Postle, B., Wang, F., McConnell, J.J., Zheng, J.H., Lee, J., Rooney, J.F., Jaffe, H.S., Martinez, A.I., Burns, D.N. & Glidden, D.V. (2010) Preexposure chemoprophylaxis for HIV prevention in men who have sex with men. *N Engl J Med*, **363**, 2587-2599.

Graver, M.A. & Wade, J.J. (2011) The role of acidification in the inhibition of *Neisseria gonorrhoeae* by vaginal lactobacilli during anaerobic growth. *Ann Clin Microbiol Antimicrob*, **10**, 8.

Gray, G.E., Allen, M., Moodie, Z., Churchyard, G., Bekker, L.G., Nchabeleng, M., Mlisana, K., Metch, B., de Bruyn, G., Latka, M.H., Roux, S., Mathebula, M., Naicker, N., Ducar, C., Carter, D.K., Puren, A., Eaton, N., McElrath, M.J., Robertson, M., Corey, L. & Kublin, J.G. (2011) Safety and efficacy of the HVTN 503/Phambili study of a clade-B-based HIV-1 vaccine in South Africa: a double-blind, randomised, placebo-controlled test-of-concept phase 2b study. *Lancet Infect Dis*, **11**, 507-515.

Gray, R.H., Wawer, M.J., Brookmeyer, R., Sewankambo, N.K., Serwadda, D., Wabwire-Mangen, F., Lutalo, T., Li, X., vanCott, T. & Quinn, T.C. (2001) Probability of HIV-1 transmission per coital act in monogamous, heterosexual, HIV-1-discordant couples in Rakai, Uganda. *Lancet*, **357**, 1149-1153.

Hamilton, W.A. (1968) The mechanism of the bacteriostatic action of tetrachlorosalicylanilide: A membrane-active antibacterial compound. *J Gen Microbiol*, **50**, 441-458.

Hancock, R.E. & Sahl, H.G. (2006) Antimicrobial and host-defense peptides as new anti-infective therapeutic strategies. *Nat Biotechnol*, **24**, 1551-1557.

Hand, S.C. & Menze, M.A. (2008) Mitochondria in energy-limited states: mechanisms that blunt the signaling of cell death. *J Exp Biol*, **211**, 1829-1840.

Hartman, G.W. (1915) Combined treatment of Syphilis with mercury and Salvarsan. *Cal State J Med*, **13**, 115-117.

Hawkes, S. (2008) Addressing sexually transmitted infections (STIs), including HIV/AIDS, in the context of sexual health. *International Journal of Sexual Health*, **20**, 91-108.

Heerklotz, H. (2008) Interactions of surfactants with lipid membranes. *Q Rev Biophys*, **41**, 205-264.

Heise, L.L. & Elias, C. (1995) Transforming AIDS prevention to meet women's needs: a focus on developing countries. *Soc Sci Med*, **40**, 931-943.

Heiskanen, K.M., Bhat, M.B., Wang, H.W., Ma, J. & Nieminen, A.L. (1999) Mitochondrial depolarization accompanies cytochrome c release during apoptosis in PC6 cells. *J Biol Chem*, **274**, 5654-5658.

Hendrix, C.W., Cao, Y.J. & Fuchs, E.J. (2009) Topical microbicides to prevent HIV: clinical drug development challenges. *Annu Rev Pharmacol Toxicol*, **49**, 349-375.

Hicks, D.R., Martin, L.S., Getchell, J.P., Heath, J.L., Francis, D.P., McDougal, J.S., Curran, J.W. & Voeller, B. (1985) Inactivation of HTLV-III/LAV-infected cultures of normal human lymphocytes by Nonoxynol-9 *in vitro*. *Lancet*, **2**, 1422-1423.

Hilgendorf, C., Spahn-Langguth, H., Regardh, C.G., Lipka, E., Amidon, G.L. & Langguth, P. (2000) Caco-2 versus Caco-2/HT29-MTX co-cultured cell lines: permeabilities via diffusion, inside- and outside-directed carrier-mediated transport. *J Pharm Sci*, **89**, 63-75.

Hitchcock, P.J. (2000) Topical Microbicides. In Stanberry, L.R., Bernstein, D.I. (eds) *Sexually transmitted diseases: vaccines, prevention and control*. Academic Press, San Diego, California, pp. 149-166.

Hladik, F. & Hope, T.J. (2009) HIV infection of the genital mucosa in women. *Curr HIV/AIDS Rep*, **6**, 20-28.

Hladik, F., Sakchalathorn, P., Ballweber, L., Lentz, G., Fialkow, M., Eschenbach, D. & McElrath, M.J. (2007) Initial events in establishing vaginal entry and infection by Human Immunodeficiency Virus type-1. *Immunity*, **26**, 257-270.

Hladik, F. & Doncel, G.F. (2010) Preventing mucosal HIV transmission with topical microbicides: challenges and opportunities. *Antiviral Res*, **88 Suppl 1**, S3-9.

Hoffer, K.M. & Robles, G. (2002) Microbicides: prevention tool of the future. *Posit Aware*, **13**, 56-57.

Holmberg, K., Jönsson, B., Kronberg, B. & Lindman, B. (eds) (2003) *Surfactants and polymers in aqueous solution.* John Wiley & Sons, Ltd., Chichester, England, pp. 3-23.

Holmes, B., Willcox, W.R. & Lapage, S.P. (1978) Identification of Enterobacteriaceae by the API 20E system. *J Clin Pathol*, **31**, 22-30.

Honig, B.H., Hubbell, W.L. & Flewelling, R.F. (1986) Electrostatic interactions in membranes and proteins. *Annu Rev Biophys Biophys Chem*, **15**, 163-193.

Hoogerheide, J.C. (1945) The germicidal properties of certain quarternary ammonium salts with special reference to cetyl-trimethyl-ammonium bromide. *J Bacteriol*, **49**, 277-289.

Hymes, K.B., Green, J.B. & Mann, J.M. (1989) AIDS: a worldwide pandemic. In Gottlieb, M.S., Jeffries, D.J., Mildvan, D., Pinching, A.J., Quinn, T.C. (eds) *Current topics in AIDS (Vol. 2)*. John Wiley & Sons, London, England.

Ioannou, C.J., Hanlon, G.W. & Denyer, S.P. (2007) Action of disinfectant quaternary ammonium compounds against *Staphylococcus aureus*. *Antimicrob Agents Chemother*, **51**, 296-306.

Irvine, J.D., Takahashi, L., Lockhart, K., Cheong, J., Tolan, J.W., Selick, H.E. & Grove, J.R. (1999) MDCK (Madin-Darby canine kidney) cells: A tool for membrane permeability screening. *J Pharm Sci*, **88**, 28-33.

Ishikawa, S., Matsumura, Y., Katoh-Kubo, K. & Tsuchido, T. (2002) Antibacterial activity of surfactants against *Escherichia coli* cells is influenced by carbon source and anaerobiosis. *J Appl Microbiol*, **93**, 302-309.

Isomaa, B., Hagerstrand, H., Paatero, G. & Engblom, A.C. (1986) Permeability alterations and antihaemolysis induced by amphiphiles in human erythrocytes. *Biochim Biophys Acta*, **860**, 510-524.

Israelachvili, J.N., Mitchell, D.J. & Ninham, B.W. (1977) Theory of self-assembly of lipid bilayers and vesicles. *Biochim Biophys Acta*, **470**, 185-201.

Ito, E., Yip, K.W., Katz, D., Fonseca, S.B., Hedley, D.W., Chow, S., Xu, G.W., Wood, T.E., Bastianutto, C., Schimmer, A.D., Kelley, S.O. & Liu, F.F. (2009) Potential use of cetrimonium bromide as an apoptosis-promoting anticancer agent for head and neck cancer. *Mol Pharmacol*, **76**, 969-983.

Izyumov, D.S., Avetisyan, A.V., Pletjushkina, O.Y., Sakharov, D.V., Wirtz, K.W., Chernyak, B.V. & Skulachev, V.P. (2004) "Wages of fear": transient threefold decrease in intracellular ATP level imposes apoptosis. *Biochim Biophys Acta*, **1658**, 141-147.

Jahn, R. (2008) Some classic papers in the field of membrane fusion--a personal view. *Nat Struct Mol Biol*, 15, 655-657.

Janin, R.R. (1976) Development of a bacteriological identification system: theory and practice. In Johnston, H.H., Newsom, S.W.B. (eds) *Rapid methods and automation in microbiology*. Learned Information (Europe) Ltd., Oxford, England, pp. 155-162.

Jensen, M.O. & Mouritsen, O.G. (2004) Lipids do influence protein function-the hydrophobic matching hypothesis revisited. *Biochim Biophys Acta*, **1666**, 205-226.

Johnson, L.V., Walsh, M.L., Bockus, B.J. & Chen, L.B. (1981) Monitoring of relative mitochondrial membrane potential in living cells by fluorescence microscopy. *J Cell Biol*, **88**, 526-535.

Jorgensen, J.H. & Turnidge, J.D. (2007) Susceptibility test methods: dilution and disk diffusion methods. In Murray, P.R., Baron, E.J., Jorgensen, J.H., Landry, M.L., Pfaller, M.A. (eds) *Manual of clinical microbiology*. ASM Press, Washington,D.C., USA, pp. 1152–1172.

Kabir, J., Lobo, M. & Zachary, I. (2002) Staurosporine induces endothelial cell apoptosis via focal adhesion kinase dephosphorylation and focal adhesion disassembly independent of focal adhesion kinase proteolysis. *Biochem J*, **367**, 145-155.

Karbowski, M. & Youle, R.J. (2003) Dynamics of mitochondrial morphology in healthy cells and during apoptosis. *Cell Death Differ*, **10**, 870-880.

Karbowski, M., Arnoult, D., Chen, H., Chan, D.C., Smith, C.L. & Youle, R.J. (2004) Quantitation of mitochondrial dynamics by photolabeling of individual organelles shows that mitochondrial fusion is blocked during the Bax activation phase of apoptosis. *J Cell Biol*, **164**, 493-499.

Karim, S.S.A. Microbicides for the prevention of HIV Infection. Reviews 2006; Available from: http://www.hiv.lanl.gov/content/sequence/HIV/COMPENDIUM/2005/partl/karim.pdf.

Keller, M.J. & Herold, B.C. (2009) Understanding basic mechanisms and optimizing assays to evaluate the efficacy of vaginal microbicides. *Sex Transm Dis*, **36**, S92-95.

Kelly, J.P., Reynolds, R.B., Stagno, S., Louv, W.C. & Alexander, W.J. (1985) *In vitro* activity of the spermicide nonoxynol-9 against *Chlamydia trachomatis*. *Antimicrob Agents Chemother*, **27**, 760-762.

Kerr, J.F., Wyllie, A.H. & Currie, A.R. (1972) Apoptosis: a basic biological phenomenon with wide-ranging implications in tissue kinetics. *Br J Cancer*, **26**, 239-257.

Ketterer, B., Neumcke, B. & Läuger, P. (1971) Transport mechanism of hydrophobic ions through lipid bilayer membranes. *Journal of Membrane Biology*, **5**, 225-245.

Kiefel, B.R., Gilson, P.R. & Beech, P.L. (2006) Cell biology of mitochondrial dynamics. *Int Rev Cytol*, **254**, 151-213.

Knapp, J.S. (1998) *Neisseria gonorrhoeae* resistant to ciprofloxacin and ofloxacin. *Sex Transm Dis*, **25**, 425-426.

Knezevic, S.Z., Streibig, J.C. & Ritz, C. (2007) Utilizing R Software Package for dose-response studies: The concept and data analysis. *Weed Technology,* **21**, 840–848.

Koopman, W.J., Visch, H.J., Verkaart, S., van den Heuvel, L.W., Smeitink, J.A. & Willems, P.H. (2005) Mitochondrial network complexity and pathological decrease in Complex I activity are tightly correlated in isolated human complex I deficiency. *Am J Physiol Cell Physiol*, **289**, C881-890.

Koopman, W.J., Visch, H.J., Smeitink, J.A. & Willems, P.H. (2006) Simultaneous quantitative measurement and automated analysis of mitochondrial morphology, mass, potential, and motility in living human skin fibroblasts. *Cytometry A*, **69**, 1-12.

Kopecka-Leitmanova, A., Devinsky, F., Mlynarcik, D. & Lacko, I. (1989) Interaction of amine oxides and quaternary ammonium salts with membrane and membrane-associated processes in *E. coli* cells: mode of action. *Drug Metabol Drug Interact*, **7**, 29-51.

Kopecky, F. (1996) Micellization and other associations of amphiphilic antimicrobial quaternary ammonium salts in aqueous solutions. *Pharmazie*, **51**, 135-144.

Krebs, F.C., Miller, S.R., Malamud, D., Howett, M.K. & Wigdahl, B. (1999) Inactivation of Human Immunodeficiency Virus type 1 by nonoxynol-9, C31G, or an alkyl sulfate, sodium dodecyl sulfate. *Antiviral Res*, **43**, 157-173.

Krebs, F.C., Miller, S.R., Catalone, B.J., Welsh, P.A., Malamud, D., Howett, M.K. & Wigdahl, B. (2000) Sodium dodecyl sulfate and C31G as microbicidal alternatives to nonoxynol 9: comparative sensitivity of primary human vaginal keratinocytes. *Antimicrob Agents Chemother*, **44**, 1954-1960.

Kroemer, G. & Reed, J.C. (2000) Mitochondrial control of cell death. *Nat Med*, **6**, 513-519.

Kroemer, G., Galluzzi, L. & Brenner, C. (2007) Mitochondrial membrane permeabilization in cell death. *Physiol Rev*, **87**, 99-163.

Krysko, D.V., Vanden Berghe, T., D'Herde, K. & Vandenabeele, P. (2008) Apoptosis and necrosis: detection, discrimination and phagocytosis. *Methods*, **44**, 205-221.

Kugler, R., Bouloussa, O. & Rondelez, F. (2005) Evidence of a charge-density threshold for optimum efficiency of biocidal cationic surfaces. *Microbiology*, **151**, 1341-1348.

Lachowiez, R.M., Clayton, B., Thallman, K., Dix, J.A. & Van Buskirk, R.G. (1989) Rhodamine 123 as a probe of *in vitro* toxicity in MDCK cells. *Cytotechnology*, **2**, 203-211.

Lambert, R.J. (2000) Susceptibility testing: inoculum size dependency of inhibition using the Colworth MIC technique. *J Appl Microbiol*, **89**, 275-279.

Lard-Whiteford, S.L., Matecka, D., O'Rear, J.J., Yuen, I.S., Litterst, C. & Reichelderfer, P. (2004) Recommendations for the nonclinical development of topical microbicides for prevention of HIV transmission: an update. *J Acquir Immune Defic Syndr*, **36**, 541-552.

Lazzaro, D.R., Abulawi, K. & Hajee, M.E. (2009) In vitro cytotoxic effects of benzalkonium chloride on adenovirus. *Eye Contact Lens*, **35**, 329-332.

Le Ferrec, E., Chesne, C., Artusson, P., Brayden, D., Fabre, G., Gires, P., Guillou, F., Rousset, M., Rubas, W. & Scarino, M.L. (2001) *In vitro* models of the intestinal barrier. The report and recommendations of ECVAM Workshop 46. European Centre for the Validation of Alternative methods. *Altern Lab Anim*, **29**, 649-668.

Lederman, M.M., Connick, E., Landay, A., Kuritzkes, D.R., Spritzler, J., St Clair, M., Kotzin, B.L., Fox, L., Chiozzi, M.H., Leonard, J.M., Rousseau, F., Wade, M., Roe, J.D., Martinez, A. & Kessler, H. (1998) Immunologic responses associated with 12 weeks of combination antiretroviral therapy consisting of zidovudine, lamivudine, and ritonavir: results of AIDS Clinical Trials Group Protocol 315. *J Infect Dis*, 178, 70-79.

Lederman, M.M., Offord, R.E. & Hartley, O. (2006) Microbicides and other topical strategies to prevent vaginal transmission of HIV. *Nat Rev Immunol*, **6**, 371-382.

Legros, F., Lombes, A., Frachon, P. & Rojo, M. (2002) Mitochondrial fusion in human cells is efficient, requires the inner membrane potential, and is mediated by mitofusins. *Mol Biol Cell*, **13**, 4343-4354.

Leist, M., Single, B., Castoldi, A.F., Kuhnle, S. & Nicotera, P. (1997) Intracellular adenosine triphosphate (ATP) concentration: a switch in the decision between apoptosis and necrosis. *J Exp Med*, **185**, 1481-1486.

Levine, S.L., Han, Z., Liu, J., Farmer, D.R. & Papadopoulos, V. (2007) Disrupting mitochondrial function with surfactants inhibits MA-10 Leydig cell steroidogenesis. *Cell Biol Toxicol*, **23**, 385-400.

Lewis, D.A. & Lukehart, S.A. (2011) Antimicrobial resistance in *Neisseria gonorrhoeae* and *Treponema pallidum*: Evolution, therapeutic challenges and the need to strengthen global surveillance. *Sex Transm Infect*, **87 Suppl 2**, ii39-43.

Li, N., Ragheb, K., Lawler, G., Sturgis, J., Rajwa, B., Melendez, J.A. & Robinson, J.P. (2003) Mitochondrial Complex I inhibitor rotenone induces apoptosis through enhancing mitochondrial reactive oxygen species production. *J Biol Chem*, **278**, 8516-8525.

Lin, Y.C., Schlievert, P.M., Anderson, M.J., Fair, C.L., Schaefers, M.M., Muthyala, R. & Peterson, M.L. (2009) Glycerol monolaurate and dodecylglycerol effects on *Staphylococcus aureus* and toxic shock syndrome toxin-1 *in vitro* and *in vivo*. *PloS ONE*, **4**, e7499.

Lindstedt, M., Allenmark, S., Thompson, R.A. & Edebo, L. (1990) Antimicrobial activity of betaine esters, quaternary ammonium amphiphiles which spontaneously hydrolyze into nontoxic components. *Antimicrobial agents and chemotherapy*, **34**, 1949-1954.

Little, S.J., Holte, S., Routy, J.P., Daar, E.S., Markowitz, M., Collier, A.C., Koup, R.A., Mellors, J.W., Connick, E., Conway, B., Kilby, M., Wang, L., Whitcomb, J.M., Hellmann, N.S. & Richman, D.D. (2002) Antiretroviral-drug resistance among patients recently infected with HIV. *N Engl J Med*, **347**, 385-394.

Liu, B., Woltman, A.M., Janssen, H.L. & Boonstra, A. (2009) Modulation of dendritic cell function by persistent viruses. *Journal of Leukocyte Biology*, **85**, 205-214.

Liu, Y.Q., Zhang, Y.Z. & Gao, P.J. (2004) Novel concentration-killing curve method for estimation of bactericidal potency of antibiotics in an in vitro dynamic model. *Antimicrob Agents Chemother*, **48**, 3884-3891.

Looker, K.J., Garnett, G.P. & Schmid, G.P. (2008) An estimate of the global prevalence and incidence of Herpes Simplex Virus type 2 infection. *Bull World Health Organ*, **86**, 805-812, A.

Ly, J.D., Grubb, D.R. & Lawen, A. (2003) The mitochondrial membrane potential $\Delta\psi_m$ in apoptosis; an update. *Apoptosis*, **8**, 115-128.

Lyamzaev, K.G., Izyumov, D.S., Avetisyan, A.V., Yang, F., Pletjushkina, O.Y. & Chernyak, B.V. (2004) Inhibition of mitochondrial bioenergetics: the effects on structure of mitochondria in the cell and on apoptosis. *Acta Biochim Pol*, **51**, 553-562.

Macklis, J.D. & Madison, R.D. (1990) Progressive incorporation of propidium iodide in cultured mouse neurons correlates with declining electrophysiological status: a fluorescence scale of membrane integrity. *J Neurosci Methods*, **31**, 43-46.

Madeira, V.M., Antunes-Madeira, M.C. & Carvalho, A.P. (1974) Activation energies of the ATPase activity of sarcoplasmic reticulum. *Biochem Biophys Res Commun*, **58**, 897-904.

Maillard, J.Y. (2002) Bacterial target sites for biocide action. *Symp Ser Soc Appl Microbiol*, 16S-27S.

Majtan, V. & Majtanova, L. (1999) The effect of new disinfectant substances on the metabolism of *Enterobacter cloacae*. *Int J Antimicrob Agents*, **11**, 59-64.

Malkovsky, M., Newell, A. & Dalgleish, A.G. (1988) Inactivation of HIV by Nonoxynol-9. *Lancet*, **1**, 645.

Martin, H.L., Jr., Stevens, C.E., Richardson, B.A., Rugamba, D., Nyange, P.M., Mandaliya, K., Ndinya-Achola, J. & Kreiss, J.K. (1997) Safety of a nonoxynol-9 vaginal gel in Kenyan prostitutes. A randomized clinical trial. *Sex Transm Dis*, **24**, 279-283.

Martin, S.J., Reutelingsperger, C.P., McGahon, A.J., Rader, J.A., van Schie, R.C., LaFace, D.M. & Green, D.R. (1995) Early redistribution of plasma membrane phosphatidylserine is a general feature of apoptosis regardless of the initiating stimulus: inhibition by overexpression of Bcl-2 and Abl. *J Exp Med*, **182**, 1545-1556.

Masurier, C., Salomon, B., Guettari, N., Pioche, C., Lachapelle, F., Guigon, M. & Klatzmann, D. (1998) Dendritic cells route human immunodeficiency virus to lymph nodes after vaginal or intravenous administration to mice. *J Virol*, **72**, 7822-7829.

Matsumura, H., Ivamoto, M. & Furusawa, K. (1986) Adsorp- tion of cationic surfactants on phospholipid membranes and its contributions to membrane-surface potential. *Bull. Chem. Soc. Jpn.*, **59**, 1533-1537.

Mayaud, P. & McCormick, D. (2001) Interventions against sexually transmitted infections (STI) to prevent HIV infection. *Br Med Bull*, **58**, 129-153.

Mayaud, P. & Mabey, D. (2004) Approaches to the control of sexually transmitted infections in developing countries: old problems and modern challenges. *Sex Transm Infect*, **80**, 174-182.

McCormack, S., Ramjee, G., Kamali, A., Rees, H., Crook, A.M., Gafos, M., Jentsch, U., Pool, R., Chisembele, M., Kapiga, S., Mutemwa, R., Vallely, A., Palanee, T., Sookrajh, Y., Lacey, C.J., Darbyshire, J., Grosskurth, H., Profy, A., Nunn, A., Hayes, R. & Weber, J. (2010) PRO2000 vaginal gel for prevention of HIV-1 infection (Microbicides Development Programme 301): a phase 3, randomised, double-blind, parallel-group trial. *Lancet*, **376**, 1329-1337.

McDonnell, G. & Russell, A.D. (1999) Antiseptics and disinfectants: activity, action, and resistance. *Clin Microbiol Rev*, **12**, 147-179.

McGowan, I. (2006) Microbicides: a new frontier in HIV prevention. *Biologicals*, **34**, 241-255.

Mesquita, P.M., Cheshenko, N., Wilson, S.S., Mhatre, M., Guzman, E., Fakioglu, E., Keller, M.J. & Herold, B.C. (2009) Disruption of tight junctions by cellulose sulfate facilitates HIV infection: model of microbicide safety. *J Infect Dis*, **200**, 599-608.

Messam, C.A. & Pittman, R.N. (1998) Asynchrony and commitment to die during apoptosis. *Exp Cell Res*, **238**, 389-398.

Metivier, D., Dallaporta, B., Zamzami, N., Larochette, N., Susin, S.A., Marzo, I. & Kroemer, G. (1998) Cytofluorometric detection of mitochondrial alterations in early CD95/Fas/APO-1-triggered apoptosis of Jurkat T lymphoma cells. Comparison of seven mitochondrion-specific fluorochromes. *Immunol Lett*, **61**, 157-163.

Mijac, V.D., Dukic, S.V., Opavski, N.Z., Dukic, M.K. & Ranin, L.T. (2006) Hydrogen peroxide producing lactobacilli in women with vaginal infections. *Eur J Obstet Gynecol Reprod Biol*, **129**, 69-76.

Miles, A.A., Misra, S.S. & Irwin, J.O. (1938) The estimation of the bactericidal power of the blood. *J Hyg (Lond)*, **38**, 732-749.

Mileykovskaya, E., Sun, Q., Margolin, W. & Dowhan, W. (1998) Localization and function of early cell division proteins in filamentous *Escherichia coli* cells lacking phosphatidylethanolamine. *J Bacteriol*, **180**, 4252-4257.

Miller, B.F. & Baker, Z. (1940) Inhibition of bacterial metabolism by synthetic detergents. *Science*, **91**, 624-625.

Miller, C.J. & Shattock, R.J. (2003) Target cells in vaginal HIV transmission. *Microbes Infect*, **5**, 59-67.

Miller, V., de Bethune, M.P., Kober, A., Sturmer, M., Hertogs, K., Pauwels, R., Stoffels, P. & Staszewski, S. (1998) Patterns of resistance and cross-resistance to human immunodeficiency virus type 1 reverse transcriptase inhibitors in patients treated with the nonnucleoside reverse transcriptase inhibitor loviride. *Antimicrob Agents Chemother*, **42**, 3123-3129.

Moore, E.R., Fischer, E.R., Mead, D.J. & Hackstadt, T. (2008) The chlamydial inclusion preferentially intercepts basolaterally directed sphingomyelin-containing exocytic vacuoles. *Traffic*, **9**, 2130-2140.

Moore, J.P. (2005) Topical microbicides become topical. *N Engl J Med*, **352**, 298-300.

Moran, J., Addy, M., Jackson, R. & Newcombe, R.G. (2000) Comparative effects of quaternary ammonium mouthrinses on 4-day plaque regrowth. *J Clin Periodontol*, **27**, 37-40.

Moreno, A.J. & Madeira, V.M. (1991) Mitochondrial bioenergetics as affected by DDT. *Biochim Biophys Acta*, **1060**, 166-174.

Moreno, M.J., Estronca, L.M. & Vaz, W.L. (2006) Translocation of phospholipids and dithionite permeability in liquid-ordered and liquid-disordered membranes. *Biophys J*, **91**, 873-881.

Mosmann, T. (1983) Rapid colorimetric assay for cellular growth and survival: application to proliferation and cytotoxicity assays. *J Immunol Methods*, **65**, 55-63.

Murphy, E.L., Collier, A.C., Kalish, L.A., Assmann, S.F., Para, M.F., Flanigan, T.P., Kumar, P.N., Mintz, L., Wallach, F.R. & Nemo, G.J. (2001) Highly active antiretroviral therapy decreases mortality and morbidity in patients with advanced HIV disease. *Ann Intern Med*, **135**, 17-26.

Murphy, M.P. (1997) Selective targeting of bioactive compounds to mitochondria. *Trends Biotechnol*, **15**, 326-330.

Nadakavukaren, K.K., Nadakavukaren, J.J. & Chen, L.B. (1985) Increased Rhodamine 123 uptake by carcinoma cells. *Cancer Res*, **45**, 6093-6099.

Neubig, R.R., Spedding, M., Kenakin, T. & Christopoulos, A. (2003) International Union of Pharmacology Committee on Receptor Nomenclature and Drug Classification. XXXVIII. Update on terms and symbols in quantitative pharmacology. *Pharmacol Rev*, **55**, 597-606.

Neves, B.M., Cruz, M.T., Francisco, V., Goncalo, M., Figueiredo, A., Duarte, C.B. & Lopes, M.C. (2008) Differential modulation of CXCR4 and CD40 protein levels by skin sensitizers and irritants in the FSDC cell line. *Toxicol Lett*, **177**, 74-82.

Nicholls, D.G. & Ferguson, S.J. (2002) *Bioenergetics 3*. Academic Press, San Diego, California, USA. pp. 69-73.

Nomura, Y., Bhawal, U.K., Nishikiori, R., Sawajiri, M., Maeda, T. & Okazaki, M. (2010) Effects of high-dose major components in oral disinfectants on the cell cycle and apoptosis in primary human gingival fibroblasts *in vitro*. *Dent Mater J*, **29**, 75-83.

Nuttall, J. (2010) Microbicides in the prevention of HIV infection: current status and future directions. *Drugs*, **70**, 1231-1243.

Nystrom, T. (2001) Not quite dead enough: on bacterial life, culturability, senescence, and death. *Arch Microbiol*, **176**, 159-164.

O'Neill, A.J., Miller, K., Oliva, B. & Chopra, I. (2004) Comparison of assays for detection of agents causing membrane damage in *Staphylococcus aureus*. *J Antimicrob Chemother*, **54**, 1127-1129.

Obiero, J., Mwethera, P.G. & Wiysonge, C.S. (2012) Topical microbicides for prevention of sexually transmitted infections. *Cochrane Database Syst Rev*, **6**, CD007961.

Op den Kamp, J.A. (1979) Lipid asymmetry in membranes. *Annu Rev Biochem*, **48**, 47-71.

Oriel, J.D. (1994) *The scars of Venus : a history of venereology*. Springer-Verlag, London, England.

Otzen, D. (2011) Protein-surfactant interactions: a tale of many states. *Biochim Biophys Acta*, **1814**, 562-591.

Padian, N.S., Shiboski, S.C., Glass, S.O. & Vittinghoff, E. (1997) Heterosexual transmission of Human Immunodeficiency Virus (HIV) in northern California: results from a ten-year study. *Am J Epidemiol*, **146**, 350-357.

Palella, F.J., Jr., Delaney, K.M., Moorman, A.C., Loveless, M.O., Fuhrer, J., Satten, G.A., Aschman, D.J. & Holmberg, S.D. (1998) Declining morbidity and mortality among patients with advanced human immunodeficiency virus infection. HIV Outpatient Study Investigators. *N Engl J Med*, **338**, 853-860.

Pampaloni, F., Stelzer, E.H., Leicht, S. & Marcello, M. (2010) Madin-Darby canine kidney cells are increased in aerobic glycolysis when cultured on flat and stiff collagen-coated surfaces rather than in physiological 3-D cultures. *Proteomics*, **10**, 3394-3413.

Pantaler, E., Kamp, D. & Haest, C.W. (2000) Acceleration of phospholipid flip-flop in the erythrocyte membrane by detergents differing in polar head group and alkyl chain length. *Biochim Biophys Acta*, **1509**, 397-408.

Pao, D., Fisher, M., Hue, S., Dean, G., Murphy, G., Cane, P.A., Sabin, C.A. & Pillay, D. (2005) Transmission of HIV-1 during primary infection: relationship to sexual risk and sexually transmitted infections. *AIDS*, **19**, 85-90.

Papa, S., Martino, P.L., Capitanio, G., Gaballo, A., De Rasmo, D., Signorile, A. & Petruzzella, V. (2012) The oxidative phosphorylation system in mammalian mitochondria. *Adv Exp Med Biol*, **942**, 3-37.

Patrzykat, A., Friedrich, C.L., Zhang, L., Mendoza, V. & Hancock, R.E. (2002) Sublethal concentrations of pleurocidin-derived antimicrobial peptides inhibit macromolecular synthesis in *Escherichia coli*. *Antimicrob Agents Chemother*, **46**, 605-614.

Patton, D.L., Wang, S.K. & Kuo, C.C. (1992) In vitro activity of nonoxynol 9 on HeLa 229 cells and primary monkey cervical epithelial cells infected with *Chlamydia trachomatis*. *Antimicrob Agents Chemother*, **36**, 1478-1482.

Pauly, A., Meloni, M., Brignole-Baudouin, F., Warnet, J.M. & Baudouin, C. (2009) Multiple endpoint analysis of the 3D-reconstituted corneal epithelium after treatment with benzalkonium chloride: early detection of toxic damage. *Invest Ophthalmol Vis Sci*, **50**, 1644-1652.

Perani, A., Gerardin, C., Stacey, G., Infante, M.R., Vinardell, P., Rodehuser, L., Selve, C. & Maugras, M. (2001) Interactions of surfactants with living cells. Induction of apoptosis by detergents containing a beta-lactam moiety. *Amino Acids*, **21**, 185-194.

Pereira, G.C., Branco, A.F., Matos, J.A., Pereira, S.L., Parke, D., Perkins, E.L., Serafim, T.L., Sardão, V.A., Santos, M.S., Moreno, A.J., Holy, J. & Oliveira, P.J. (2007) Mitochondrially targeted effects of berberine [Natural Yellow 18, 5,6-dihydro-9,10-dimethoxybenzo(g)-1,3-benzodioxolo(5,6-a) quinolizinium] on K1735-M2 mouse melanoma cells: comparison with direct effects on isolated mitochondrial fractions. *J Pharmacol Exp Ther*, **323**, 636-649.

Perez Bercoff, D., Trinqueneaux, P., Lambert, C., Oumar, A.A., Ternes, A.M., Dao, S., Goubau, P., Schmit, J.C. & Ruelle, J. (2010) Polymorphisms of HIV-2 integrase and selection of resistance to raltegravir. *Retrovirology*, **7**, 98.

Perine, P.L., Handsfield, H.H., Holmes, K.K. & Blount, J.H. (1985) Epidemiology of the sexually transmitted diseases. *Annu Rev Public Health*, **6**, 85-106.

Perry, S.W., Norman, J.P., Barbieri, J., Brown, E.B. & Gelbard, H.A. (2011) Mitochondrial membrane potential probes and the proton gradient: a practical usage guide. *Biotechniques*, **50**, 98-115.

Peterman, T.A. & Curran, J.W. (1986) Sexual transmission of Human Immunodeficiency Virus. *JAMA*, **256**, 2222-2226.

Peterson, L., Nanda, K., Opoku, B.K., Ampofo, W.K., Owusu-Amoako, M., Boakye, A.Y., Rountree, W., Troxler, A., Dominik, R., Roddy, R. & Dorflinger, L. (2007) SAVVY (C31G) gel for prevention of HIV infection in women: a Phase 3, double-blind, randomized, placebo-controlled trial in Ghana. *PloS ONE*, **2**, e1312.

Piao, J., Kishi, S. & Adachi, S. (2006) Surface tensions of aqueous solutions of 1-O-monoacyl sugar alcohols. *Colloid Surface A*, **277**, 15-19.

Pilcher, C.D., Tien, H.C., Eron, J.J., Jr., Vernazza, P.L., Leu, S.Y., Stewart, P.W., Goh, L.E. & Cohen, M.S. (2004) Brief but efficient: acute HIV infection and the sexual transmission of HIV. *J Infect Dis*, **189**, 1785-1792.

Pitisuttithum, P., Gilbert, P., Gurwith, M., Heyward, W., Martin, M., van Griensven, F., Hu, D., Tappero, J.W. & Choopanya, K. (2006) Randomized, double-blind, placebo-controlled efficacy trial of a bivalent recombinant glycoprotein 120 HIV-1 vaccine among injection drug users in Bangkok, Thailand. *J Infect Dis*, **194**, 1661-1671.

Plecita-Hlavata, L., Lessard, M., Santorova, J., Bewersdorf, J. & Jezek, P. (2008) Mitochondrial oxidative phosphorylation and energetic status are reflected by morphology of mitochondrial network in INS-1E and HEP-G2 cells viewed by 4Pi microscopy. *Biochim Biophys Acta*, **1777**, 834-846.

Powers, K.A., Poole, C., Pettifor, A.E. & Cohen, M.S. (2008) Rethinking the heterosexual infectivity of HIV-1: a systematic review and meta-analysis. *Lancet Infect Dis*, **8**, 553-563.

Rebbapragada, A., Wachihi, C., Pettengell, C., Sunderji, S., Huibner, S., Jaoko, W., Ball, B., Fowke, K., Mazzulli, T., Plummer, F.A. & Kaul, R. (2007) Negative mucosal synergy between Herpes Simplex type 2 and HIV in the female genital tract. *AIDS*, **21**, 589-598.

Reid, G. & Bocking, A. (2003) The potential for probiotics to prevent bacterial vaginosis and preterm labor. *Am J Obstet Gynecol*, **189**, 1202-1208.

Rerks-Ngarm, S., Pitisuttithum, P., Nitayaphan, S., Kaewkungwal, J., Chiu, J., Paris, R., Premsri, N., Namwat, C., de Souza, M., Adams, E., Benenson, M., Gurunathan, S., Tartaglia, J., McNeil, J.G., Francis, D.P., Stablein, D., Birx, D.L., Chunsuttiwat, S., Khamboonruang, C., Thongcharoen, P., Robb, M.L., Michael, N.L., Kunasol, P. & Kim, J.H. (2009) Vaccination with ALVAC and AIDSVAX to prevent HIV-1 infection in Thailand. *N Engl J Med*, **361**, 2209-2220.

Rescigno, M., Urbano, M., Valzasina, B., Francolini, M., Rotta, G., Bonasio, R., Granucci, F., Kraehenbuhl, J.P. & Ricciardi-Castagnoli, P. (2001) Dendritic cells express tight junction proteins and penetrate gut epithelial monolayers to sample bacteria. *Nature Immunology*, **2**, 361-367.

Ricketts, J.H. & Head, G.A. (1999) A five-parameter logistic equation for investigating asymmetry of curvature in baroreflex studies. *Am J Physiol*, **277**, R441-454.

Rogers, K.S. & Higgins, E.S. (1973) Lipophilic interactions of organic cations with mitochondrial inner membranes during respiratory control. *J Biol Chem*, **248**, 7142-7148.

Rosenberg, Z.F., Nel, A., Heyward, W. & Mitchnick, M. (2006) Microbicides for the prevention of HIV infection in women: an overview of recent trials. *Curr Opin HIV AIDS*, **1**, 514-519.

Ross, M.F., Kelso, G.F., Blaikie, F.H., James, A.M., Cocheme, H.M., Filipovska, A., Da Ros, T., Hurd, T.R., Smith, R.A. & Murphy, M.P. (2005) Lipophilic triphenylphosphonium cations as tools in mitochondrial bioenergetics and free radical biology. *Biochemistry (Mosc)*, **70**, 222-230.

Ross, M.F., Da Ros, T., Blaikie, F.H., Prime, T.A., Porteous, C.M., Severina, II, Skulachev, V.P., Kjaergaard, H.G., Smith, R.A. & Murphy, M.P. (2006) Accumulation of lipophilic dications by mitochondria and cells. *Biochem J*, **400**, 199-208.

Ross, M.F., Prime, T.A., Abakumova, I., James, A.M., Porteous, C.M., Smith, R.A. & Murphy, M.P. (2008) Rapid and extensive uptake and activation of hydrophobic triphenylphosphonium cations within cells. *Biochem J*, **411**, 633-645.

Rothschild, B.M. (2005) History of Syphilis. *Clin Infect Dis*, **40**, 1454-1463.

Rottenberg, H. (1984) Membrane potential and surface potential in mitochondria: uptake and binding of lipophilic cations. *J Membr Biol*, **81**, 127-138.

Ruiz, M. (2010) Fallen women and the London Lock Hospital laws and by-laws of 1840 (revised 1848). *Journal of English Studies*, **8**, 141-158.

Salt, W.G. & Wiseman, D. (1970) The relation between the uptake of cetyltrimethylammonium bromide by *Escherichia coli* and its effects on cell growth and viability. *J Pharm Pharmacol*, **22**, 261-264.

Salton, M.R. (1951) The adsorption of cetyltrimethylammonium bromide by bacteria, its action in releasing cellular constituents and its bactericidal effects. *J Gen Microbiol*, **5**, 391-404.

Salton, M.R., Horne, R.W. & Cosslett, V.E. (1951) Electron microscopy of bacteria treated with cetyltrimethylammonium bromide. *J Gen Microbiol*, **5**, 405-407.

Sampaio, J.L., Moreno, M.J. & Vaz, W.L. (2005) Kinetics and thermodynamics of association of a fluorescent lysophospholipid derivative with lipid bilayers in liquid-ordered and liquid-disordered phases. *Biophys J*, **88**, 4064-4071.

Sandoz, K.M. & Rockey, D.D. (2010) Antibiotic resistance in Chlamydiae. *Future Microbiol*, **5**, 1427-1442.

Santos, P.F., Caramelo, O.L., Carvalho, A.P. & Duarte, C.B. (1999) Characterization of ATP release from cultures enriched in cholinergic amacrine-like neurons. *J Neurobiol*, **41**, 340-348.

Saraste, A. (1999) Morphologic criteria and detection of apoptosis. *Herz*, **24**, 189-195.

Sauvanet, C., Duvezin-Caubet, S., di Rago, J.P. & Rojo, M. (2010) Energetic requirements and bioenergetic modulation of mitochondrial morphology and dynamics. *Semin Cell Dev Biol*, **21**, 558-565.

Scarlett, J.L., Sheard, P.W., Hughes, G., Ledgerwood, E.C., Ku, H.H. & Murphy, M.P. (2000) Changes in mitochondrial membrane potential during staurosporine-induced apoptosis in Jurkat cells. *FEBS Lett*, **475**, 267-272.

Schnitzer, E., Kozlov, M.M. & Lichtenberg, D. (2005) The effect of cholesterol on the solubilization of phosphatidylcholine bilayers by the non-ionic surfactant Triton X-100. *Chem Phys Lipids*, **135**, 69-82.

Schonfeld, P., Wojtczak, A.B., Geelen, M.J., Kunz, W. & Wojtczak, L. (1988) On the mechanism of the so-called uncoupling effect of medium- and short-chain fatty acids. *Biochim Biophys Acta*, **936**, 280-288.

Schwebke, J.R. (2001) Role of vaginal flora as a barrier to HIV acquisition. *Curr Infect Dis Rep*, **3**, 152-155.

Schwebke, J.R. & Vermund, S.H. (2001) Antimicrobial resistance among *Neisseria gonorrhoeae* isolates from Ulaanbaatar, Mongolia. *Sex Transm Infect*, **77**, 463.

Sebaugh, J.L. (2011) Guidelines for accurate EC_{50}/IC_{50} estimation. *Pharm Stat*, **10**, 128-134.

Seefeldt, S.S., Jensen, J.E. & Fuerst, E.P. (1995) Log-Logistic analysis of herbicide dose-response relationships. *Weed Technology*, **9**, 218-227.

Sesaki, H. & Jensen, R.E. (1999) Division versus fusion: Dnm1p and Fzo1p antagonistically regulate mitochondrial shape. *J Cell Biol*, **147**, 699-706.

Shackelford, R.E., Kaufmann, W.K. & Paules, R.S. (2000) Oxidative stress and cell cycle checkpoint function. *Free Radic Biol Med*, **28**, 1387-1404.

Shafir, S.C., Sorvillo, F.J. & Smith, L. (2009) Current issues and considerations regarding trichomoniasis and Human Immunodeficiency Virus in African-Americans. *Clin Microbiol Rev*, **22**, 37-45, Table of Contents.

Shattock, R.J., Griffin, G.E. & Gorodeski, G.I. (2000) *In vitro* models of mucosal HIV transmission. *Nat Med*, **6**, 607-608.

Shattock, R.J. & Moore, J.P. (2003) Inhibiting sexual transmission of HIV-1 infection. *Nat Rev Microbiol*, **1**, 25-34.

Shimizu, S., Eguchi, Y., Kamiike, W., Itoh, Y., Hasegawa, J., Yamabe, K., Otsuki, Y., Matsuda, H. & Tsujimoto, Y. (1996) Induction of apoptosis as well as necrosis by hypoxia and predominant prevention of apoptosis by Bcl-2 and Bcl-XL. *Cancer Res*, **56**, 2161-2166.

Silva, A.M. & Oliveira, P.J. (2012) Evaluation of respiration with Clark-type electrode in isolated mitochondria and permeabilized animal cells. *Methods Mol Biol*, **810**, 7-24.

Silva, M.T., Appelberg, R., Silva, M.N. & Macedo, P.M. (1987) *In vivo* killing and degradation of *Mycobacterium aurum* within mouse peritoneal macrophages. *Infect Immun*, **55**, 2006-2016.

Simm, A., Bertsch, G., Frank, H., Zimmermann, U. & Hoppe, J. (1997) Cell death of AKR-2B fibroblasts after serum removal: a process between apoptosis and necrosis. *J Cell Sci*, **110 (Pt 7)**, 819-828.

Simões, M., Pereira, M.O., Machado, I., Simões, L.C. & Vieira, M.J. (2006) Comparative antibacterial potential of selected aldehyde-based biocides and surfactants against planktonic *Pseudomonas fluorescens*. *J Ind Microbiol Biotechnol*, **33**, 741-749.

Simoncic, B. & Span, J. (1998) Thermodynamics of micellization of n-alkylpyridinium chlorides: a potentiometric study. *Acta Chimica Slovenica*, **45**, 143-152.

Simons, K. & Vaz, W.L. (2004) Model systems, lipid rafts, and cell membranes. *Annu Rev Biophys Biomol Struct*, **33**, 269-295.

Skerjanc, J., Kogej, K. & Cerar, J. (1999) Equilibrium and transport properties of alkylpyridinium bromides. *Langmuir*, **15**, 5023-5028.

Skoler-Karpoff, S., Ramjee, G., Ahmed, K., Altini, L., Plagianos, M.G., Friedland, B., Govender, S., De Kock, A., Cassim, N., Palanee, T., Dozier, G., Maguire, R. & Lahteenmaki, P. (2008) Efficacy of Carraguard for prevention of HIV infection in women in South Africa: a randomised, double-blind, placebo-controlled trial. *Lancet*, **372**, 1977-1987.

Slee, E.A., Harte, M.T., Kluck, R.M., Wolf, B.B., Casiano, C.A., Newmeyer, D.D., Wang, H.G., Reed, J.C., Nicholson, D.W., Alnemri, E.S., Green, D.R. & Martin, S.J. (1999) Ordering the cytochrome c-initiated caspase cascade: hierarchical activation of caspases-2, -3, -6, -7, -8, and -10 in a caspase-9-dependent manner. *J Cell Biol*, **144**, 281-292.

Smets, L.A., Van den Berg, J., Acton, D., Top, B., Van Rooij, H. & Verwijs-Janssen, M. (1994) BCL-2 expression and mitochondrial activity in leukemic cells with different sensitivity to glucocorticoid-induced apoptosis. *Blood*, **84**, 1613-1619.

Smith-McCune, K.K., Shiboski, S., Chirenje, M.Z., Magure, T., Tuveson, J., Ma, Y., Da Costa, M., Moscicki, A.B., Palefsky, J.M., Makunike-Mutasa, R., Chipato, T., van der Straten, A. & Sawaya, G.F. (2010) Type-specific cervico-vaginal human papillomavirus infection increases risk of HIV acquisition independent of other sexually transmitted infections. *PloS ONE*, **5**, e10094.

Smith, J.C. (1990) Potential-sensitive molecular probes in membranes of bioenergetic relevance. *Biochim Biophys Acta*, **1016**, 1-28.

Soike, K.F., Miller, D.D. & Elliker, P.R. (1952) Effect of pH of solution on germicidal activity of quaternary ammonium compounds. *Journal of Dairy Science*, **35**, 764-711.

Solaini, G., Sgarbi, G., Lenaz, G. & Baracca, A. (2007) Evaluating mitochondrial membrane potential in cells. *Biosci Rep*, **27**, 11-21.

Somani, J., Bhullar, V.B., Workowski, K.A., Farshy, C.E. & Black, C.M. (2000) Multiple drug-resistant *Chlamydia trachomatis* associated with clinical treatment failure. *J Infect Dis*, **181**, 1421-1427.

Soubannier, V. & McBride, H.M. (2009) Positioning mitochondrial plasticity within cellular signaling cascades. *Biochim Biophys Acta*, **1793**, 154-170.

Spink, C.H. & Chaires, J.B. (1997) Thermodynamics of the binding of a cationic lipid to DNA. *J Am Chem Soc*, **119**, 10920-10928.

Stamm, L.V. (2010) Global challenge of antibiotic-resistant *Treponema pallidum*. *Antimicrob Agents Chemother*, **54**, 583-589.

Steen, R., Wi, T.E., Kamali, A. & Ndowa, F. (2009) Control of sexually transmitted infections and prevention of HIV transmission: mending a fractured paradigm. *Bull World Health Organ*, **87**, 858-865.

Stefani, E. & Cereijido, M. (1983) Electrical properties of cultured epithelioid cells (MDCK). *J Membr Biol*, **73**, 177-184.

Stein, Z.A. (1990) HIV prevention: the need for methods women can use. *Am J Public Health*, **80**, 460-462.

Stephenson, J. (2000) Widely used spermicide may increase, not decrease, risk of HIV transmission. *JAMA*, **284**, 949.

Stone, A. (2002) Microbicides: a new approach to preventing HIV and other sexually transmitted infections. *Nat Rev Drug Discov*, **1**, 977-985.

Stone, A. & Jiang, S. (2006) Microbicides: stopping HIV at the gate. *Lancet*, **368**, 431-433.

Stone, A. (2010) *Regulatory issues in microbicide development.* WHO Press, Geneva, Switzerland.

Strahl, H. & Hamoen, L.W. (2010) Membrane potential is important for bacterial cell division. *Proc Natl Acad Sci USA*, **107**, 12281-12286.

Szewczyk, A. & Wojtczak, L. (2002) Mitochondria as a pharmacological target. *Pharmacol Rev*, **54**, 101-127.

Tamaoki, T., Nomoto, H., Takahashi, I., Kato, Y., Morimoto, M. & Tomita, F. (1986) Staurosporine, a potent inhibitor of phospholipid/Ca^{++}dependent protein kinase. *Biochem Biophys Res Commun*, **135**, 397-402.

Tanford, C. (1991) *The Hydrophobic Effect: Formation of Micelles and Biological Membranes.* . Krieger Publishing Company ed., Malabar, Fl., pp. 233.

Terris-Prestholt, F., Vyas, S., Kumaranayake, L., Mayaud, P. & Watts, C. (2006) The costs of treating curable sexually transmitted infections in low- and middle-income countries: a systematic review. *Sex Transm Dis*, **33**, S153-166.

Thomson, K.S. & Moland, E.S. (2001) Cefepime, piperacillin-tazobactam, and the inoculum effect in tests with extended-spectrum beta-lactamase-producing Enterobacteriaceae. *Antimicrobial agents and chemotherapy*, **45**, 3548-3554.

Thurman, A.R. & Doncel, G.F. (2011) Innate immunity and inflammatory response to *Trichomonas vaginalis* and bacterial vaginosis: relationship to HIV acquisition. *Am J Reprod Immunol*, **65**, 89-98.

Tomlinson, E., Brown, M.R. & Davis, S.S. (1977) Effect of colloidal association on the measured activity of alkylbenzyldimethylammonium chlorides against *Pseudomonas aeruginosa*. *J Med Chem*, **20**, 1277-1282.

Trifonova, R.T., Bajpai, M., Pasicznyk, J.M., Chandra, N., Doncel, G.F. & Fichorova, R.N. (2007) Biomarkers of leukocyte traffic and activation in the vaginal mucosa. *Biomarkers*, **12**, 608-622.

Tsujimoto, Y. (1997) Apoptosis and necrosis: intracellular ATP level as a determinant for cell death modes. *Cell Death Differ*, **4**, 429-434.

Tucek, S., Michal, P. & Vlachova, V. (2002) Modelling the consequences of receptor-G-protein promiscuity. *Trends Pharmacol Sci*, **23**, 171-176.

UNAIDS (2010) *Report on the global AIDS epidemic 2010.* . Joint United Nations Programme on HIV/AIDS., Geneva, Switzerland.

Unemo, M. & Shafer, W.M. (2011) Antibiotic resistance in Neisseria gonorrhoeae: origin, evolution, and lessons learned for the future. *Ann N Y Acad Sci*, **1230**, E19-28.

Valore, E.V., Park, C.H., Igreti, S.L. & Ganz, T. (2002) Antimicrobial components of vaginal fluid. *Am J Obstet Gynecol*, **187**, 561-568.

van de Wijgert, J.H., Morrison, C.S., Cornelisse, P.G., Munjoma, M., Moncada, J., Awio, P., Wang, J., Van der Pol, B., Chipato, T., Salata, R.A. & Padian, N.S. (2008) Bacterial vaginosis and vaginal yeast, but not vaginal cleansing, increase HIV-1 acquisition in African women. *J Acquir Immune Defic Syndr*, **48**, 203-210.

van der Graaf, P.H. & Schoemaker, R.C. (1999) Analysis of asymmetry of agonist concentration-effect curves. *J Pharmacol Toxicol Methods*, **41**, 107-115.

van der Pol, B., Kwok, C., Pierre-Louis, B., Rinaldi, A., Salata, R.A., Chen, P.L., van de Wijgert, J., Mmiro, F., Mugerwa, R., Chipato, T. & Morrison, C.S. (2008) *Trichomonas vaginalis* infection and Human Immunodeficiency Virus acquisition in African women. *J Infect Dis*, **197**, 548-554.

van Itallie, C.M., Holmes, J., Bridges, A., Gookin, J.L., Coccaro, M.R., Proctor, W., Colegio, O.R. & Anderson, J.M. (2008) The density of small tight junction pores varies among cell types and is increased by expression of Claudin-2. *J Cell Sci*, **121**, 298-305.

van Meer, G. & de Kroon, A.I. (2011) Lipid map of the mammalian cell. *J Cell Sci*, **124**, 5-8.

Vaz, W.L., Nisksch, A. & Jahnig, F. (1978) Electrostatic interactions at charged lipid membranes. Measurement of surface pH with fluorescent lipoid pH indicators. *Eur J Biochem*, **83**, 299-305.

Ved, H.S., Gustow, E. & Pieringer, R.A. (1990) Synergism between penicillin G and the antimicrobial ether lipid, rac-1-dodecylglycerol, acting below its critical micelle concentration. *Lipids*, **25**, 119-121.

Velarde, G., Ait-Aissa, S., Gillet, C., Rogerieux, F., Lambre, C., Vindimian, E. & Porcher, J.M. (1999) Use of the caco-2 model in the screening of polluting substance toxicity. *Toxicol In Vitro*, **13**, 719-722.

Vieira, B. & Carmona-Ribeiro, A.M. (2006) Cationic lipids and surfactants as antifungal agents: mode of action. *J Antimicrob Chemother.*, **58**, 760-767.

Vieira, O.V., Hartmann, D.O., Cardoso, C.M., Oberdoerfer, D., Baptista, M., Santos, M.A., Almeida, L., Ramalho-Santos, J. & Vaz, W.L. (2008) Surfactants as microbicides and contraceptive agents: A systematic in *vitro study*. *PloS ONE*, **3**, e2913.

Vinogradov, A.D. (1999) Mitochondrial ATP synthase: fifteen years later. *Biochemistry (Mosc)*, **64**, 1219-1229.

Vitale, M., Zamai, L., Mazzotti, G., Cataldi, A. & Falcieri, E. (1993) Differential kinetics of propidium iodide uptake in apoptotic and necrotic thymocytes. *Histochemistry*, **100**, 223-229.

Vittinghoff, E., Douglas, J., Judson, F., McKirnan, D., MacQueen, K. & Buchbinder, S.P. (1999) Per-contact risk of Human Immunodeficiency Virus transmission between male sexual partners. *Am J Epidemiol*, **150**, 306-311.

Wainberg, M.A. & Friedland, G. (1998) Public health implications of antiretroviral therapy and HIV drug resistance. *JAMA*, **279**, 1977-1983.

Wald, A. & Link, K. (2002) Risk of Human Immunodeficiency Virus infection in Herpes Simplex virus type 2-seropositive persons: a meta-analysis. *J Infect Dis*, **185**, 45-52.

Wang, L., Azad, N., Kongkaneramit, L., Chen, F., Lu, Y., Jiang, B.H. & Rojanasakul, Y. (2008) The Fas death signaling pathway connecting reactive oxygen species generation and FLICE inhibitory protein down-regulation. *J Immunol*, **180**, 3072-3080.

Ward, T.H., Cummings, J., Dean, E., Greystoke, A., Hou, J.M., Backen, A., Ranson, M. & Dive, C. (2008) Biomarkers of apoptosis. *Br J Cancer*, 99, 841-846.

Wasserheit, J.N. (1992) Epidemiological synergy. Interrelationships between Human Immunodeficiency Virus infection and other sexually transmitted diseases. *Sex Transm Dis*, **19**, 61-77.

Weller, S. & Davis, K. (2002) Condom effectiveness in reducing heterosexual HIV transmission. *Cochrane Database Syst Rev*, CD003255.

West, B., Changalucha, J., Grosskurth, H., Mayaud, P., Gabone, R.M., Ka-Gina, G. & Mabey, D. (1995) Antimicrobial susceptibility, auxotype and plasmid content of *Neisseria gonorrhoeae* in northern Tanzania: emergence of high level plasmid mediated tetracycline resistance. *Genitourin Med*, **71**, 9-12.

White, R.G., Orroth, K.K., Glynn, J.R., Freeman, E.E., Bakker, R., Habbema, J.D., Terris-Prestholt, F., Kumaranayake, L., Buve, A. & Hayes, R.J. (2008) Treating curable sexually transmitted infections to prevent HIV in Africa: still an effective control strategy? *J Acquir Immune Defic Syndr*, **47**, 346-353.

Wiegand, I., Hilpert, K. & Hancock, R.E. (2008) Agar and broth dilution methods to determine the minimal inhibitory concentration (MIC) of antimicrobial substances. *Nat Protoc*, **3**, 163-175.

Wikstrom, M., Xie, J., Bogdanov, M., Mileykovskaya, E., Heacock, P., Wieslander, A. & Dowhan, W. (2004) Monoglucosyldiacylglycerol, a foreign lipid, can substitute for phosphatidylethanolamine in essential membrane-associated functions in *Escherichia coli*. *J Biol Chem*, **279**, 10484-10493.

Wilkinson, D., Tholandi, M., Ramjee, G. & Rutherford, G.W. (2002) Nonoxynol-9 spermicide for prevention of vaginally acquired HIV and other sexually transmitted infections: systematic review and meta-analysis of randomised controlled trials including more than 5000 women. *Lancet Infect Dis*, **2**, 613-617.

Williams, K.J. (2009) The introduction of 'chemotherapy' using arsphenamine - the first magic bullet. *J R Soc Med*, **102**, 343-348.

Wilson, D.P., Coplan, P.M., Wainberg, M.A. & Blower, S.M. (2008) The paradoxical effects of using antiretroviral-based microbicides to control HIV epidemics. *Proc Natl Acad Sci U S A*, **105**, 9835-9840.

Witt, J., Ramji, N., Gibb, R., Dunavent, J., Flood, J. & Barnes, J. (2005) Antibacterial and antiplaque effects of a novel, alcohol-free oral rinse with cetylpyridinium chloride. *J Contemp Dent Pract*, **6**, 1-9.

Wolf, B.B. & Green, D.R. (1999) Suicidal tendencies: apoptotic cell death by caspase family proteinases. *J Biol Chem*, **274**, 20049-20052.

Wolf, B.B., Schuler, M., Echeverri, F. & Green, D.R. (1999) Caspase-3 is the primary activator of apoptotic DNA fragmentation via DNA fragmentation factor-45/inhibitor of caspase-activated DNase inactivation. *J Biol Chem*, **274**, 30651-30656.

World Health Organization (2002) *Gender and HIV/AIDS*. WHO Press, Geneva, Switzerland.

World Health Organization (2007) *Global stratergy for the prevention and control of sexually transmitted infections: 2006-2015. Breaking the chain of transmission.* WHO Press, Geneva, Switzerland.

World Health Organization. (2009) *WHO guidelines on hand hygiene in health care : first global patient safety challenge : clean care is safer care*. World Health Organization, Patient Safety, Geneva, Switzerland.

Wu, H., Zhang, H., Wang, C., Wu, Y., Xie, J., Jin, X., Yang, J. & Ye, J. (2011) Genoprotective effect of hyaluronic acid against benzalkonium chloride-induced DNA damage in human corneal epithelial cells. *Mol Vis*, **17**, 3364-3370.

Wyrick, P.B., Knight, S.T., Gerbig, D.G., Jr., Raulston, J.E., Davis, C.H., Paul, T.R. & Malamud, D. (1997) The microbicidal agent C31G inhibits *Chlamydia trachomatis* infectivity *in vitro*. *Antimicrob Agents Chemother*, **41**, 1335-1344.

Xia, W.J. & Onyuksel, H. (2000) Mechanistic studies on surfactant-induced membrane permeability enhancement. *Pharm Res*, **17**, 612-618.

Yip, K.W., Mao, X., Au, P.Y., Hedley, D.W., Chow, S., Dalili, S., Mocanu, J.D., Bastianutto, C., Schimmer, A. & Liu, F.F. (2006) Benzethonium chloride: a novel anticancer agent identified by using a cell-based small-molecule screen. *Clin Cancer Res*, **12**, 5557-5569.

Young, K.W., Pinon, L.G., Bampton, E.T. & Nicotera, P. (2010) Different pathways lead to mitochondrial fragmentation during apoptotic and excitotoxic cell death in primary neurons. *J Biochem Mol Toxicol*, **24**, 335-341.

Zarate, G. & Nader-Macias, M.E. (2006) Influence of probiotic vaginal lactobacilli on *in vitro* adhesion of urogenital pathogens to vaginal epithelial cells. *Lett Appl Microbiol*, **43**, 174-180.

Zhang, X.D., Gillespie, S.K. & Hersey, P. (2004) Staurosporine induces apoptosis of melanoma by both caspase-dependent and -independent apoptotic pathways. *Mol Cancer Ther*, **3**, 187-197.

Zhu, D.M. & Evans, R.K. (2006) Molecular mechanism and thermodynamics study of plasmid DNA and cationic surfactants interactions. *Langmuir*, **22**, 3735-3743.

Zhu, Y., Li, M., Wang, X., Jin, H., Liu, S., Xu, J. & Chen, Q. (2012) Caspase cleavage of cytochrome c1 disrupts mitochondrial function and enhances cytochrome c release. *Cell Res*, **22**, 127-141.

Zong, W.X. & Thompson, C.B. (2006) Necrotic death as a cell fate. *Genes Dev*, **20**, 1-15.